Proceedings of Connecticut Area Medical Physics Society (CAMPS) 2013 Annual Conferences

Contents

Preface

Confucius once said, “One can gain new insights through reviewing old knowledge”. That’s exactly what we are hoping for when compiling this first annual CAMPS proceedings. The idea is to offer our members a chance to reflect on what has been discussed by our distinguished invited speakers during the three conferences held in 2013. As a result, some innovative ideas may be sparked and fruitful collaborations may be initiated.

Connecticut Area Medical Physics Society (CAMPS) 2013 Spring Conference

March 14, 2013

Yale Harkness Lounge
New Haven, CT

Cancer Risks from CT Scans: Now We Have Data… What Next?

David J. Brenner, PhD, DSc
Center for Radiological Research
Columbia University Medical Center

djb3@columbia.edu

There is no question that CT has revolutionized medical practice

- ✓ *More effective surgical treatment*
- ✓ *Shorter hospital stays*
- ✓ *Elimination of exploratory surgeries*
- ✓ *Better diagnosis and treatment of cancer*
- ✓ *More efficient treatment after injury*
- ✓ *Better treatment of stroke*
- ✓ *Better treatment of cardiac conditions*

Why are we particularly interested in CT?

Examination	Relevant organ	Relevant organ dose (mGy)
Dental x ray	Brain	0.005
PA Chest x ray	Lung	0.01
Lateral chest x ray	Lung	0.15
Screening mammogram	Breast	3
Adult abdominal CT	Stomach	11
Adult head CT	Brain	13
Child abdominal CT	Stomach	10-25
Child head CT	Brain	20-25
Adult ^{18}F-FDG PET	Bladder	18

Why are we particularly interested in CT?

Conventional Radiograph

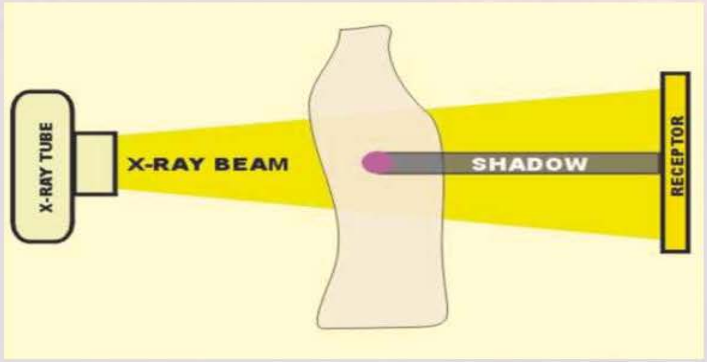

CT

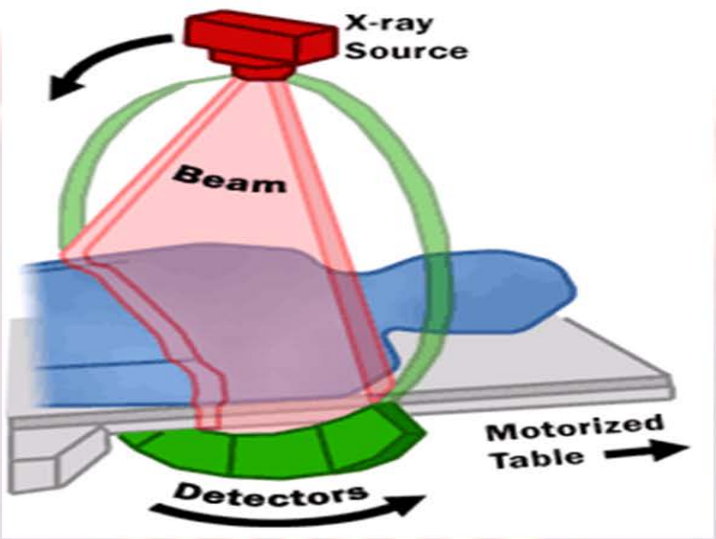

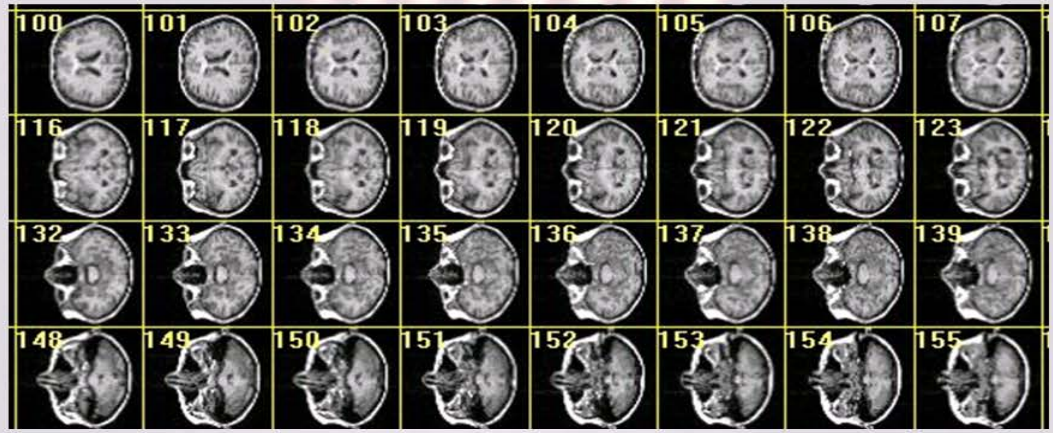

Why are we particularly interested in CT?

Frequency of CT scans per year

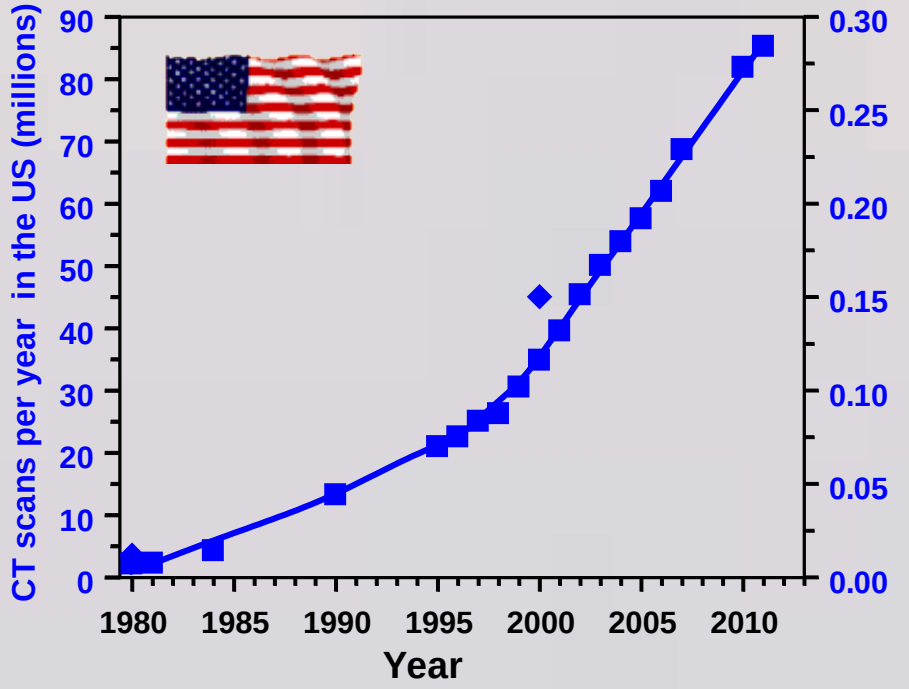

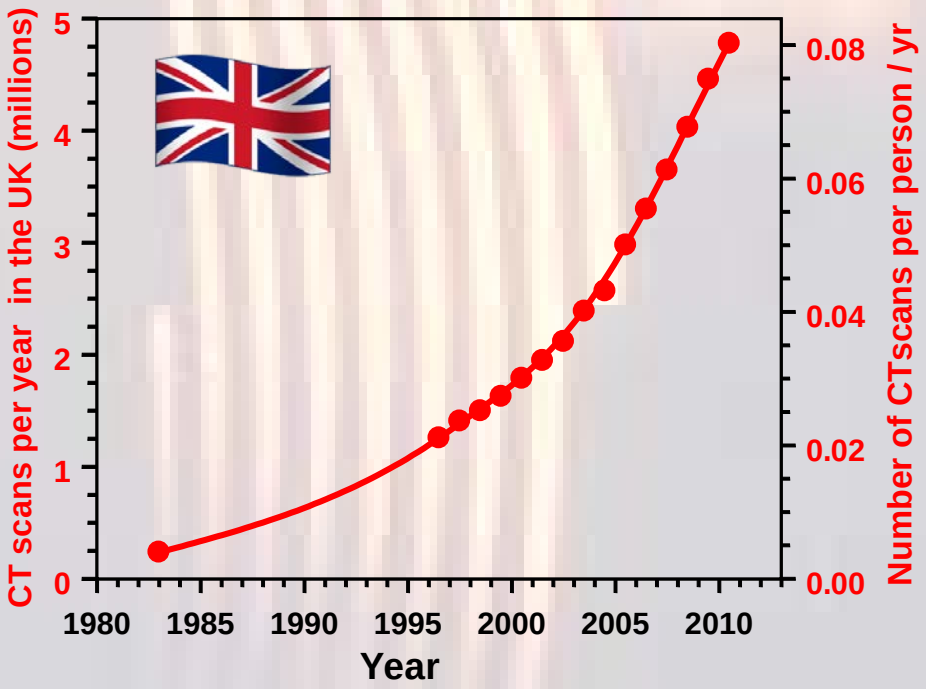

Mean individual total radiation dose in the US: 1980 vs. 2011

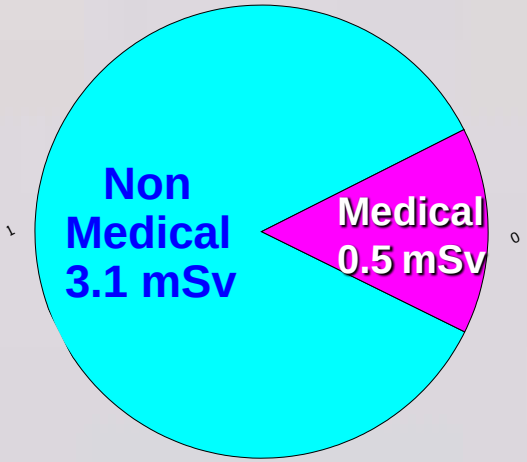

1980: 3.6 mSv

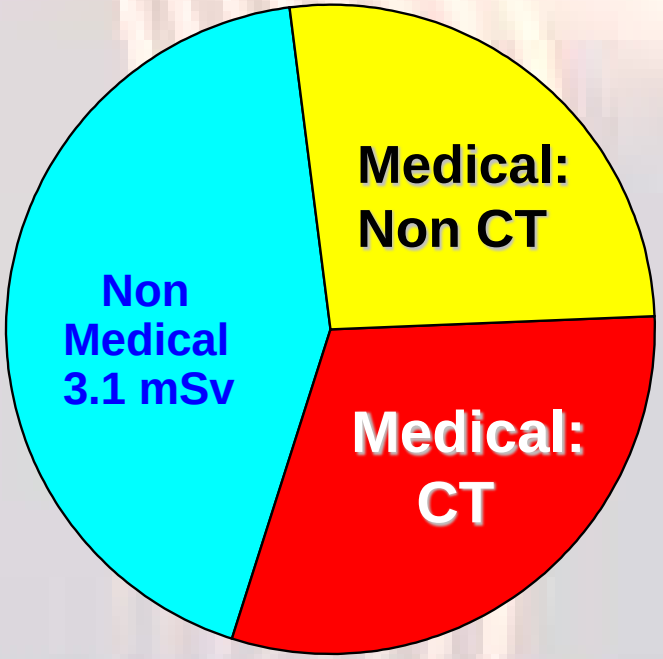

2011: 7.2 mSv

Average individual dose from medical imaging
USA: 1980 vs. 2011

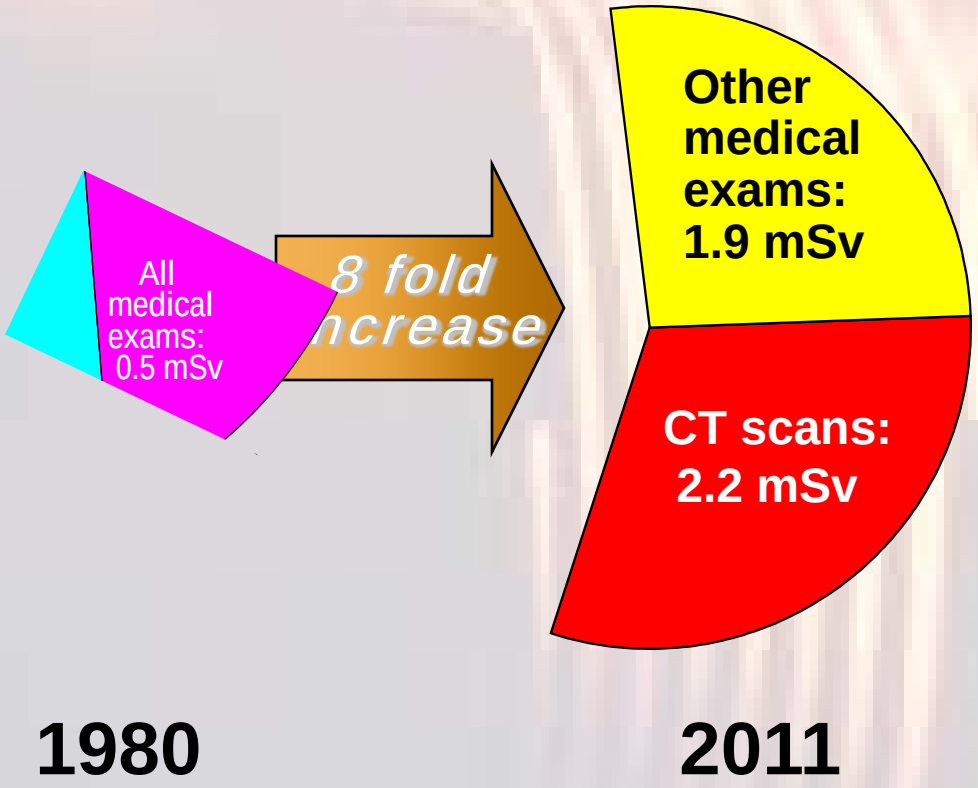

The key organ-dose ranges of relevance for CT

Taking into account

* **Machine variability,**
* **Usage variability,**
* **Age variability,**
* **Scans done with and without contrast**
* **Multiple scans**

Relevant organ dose ranges for CT are

5 - 100 mSv for a single series of scans

Atomic bomb survivor locations by dose

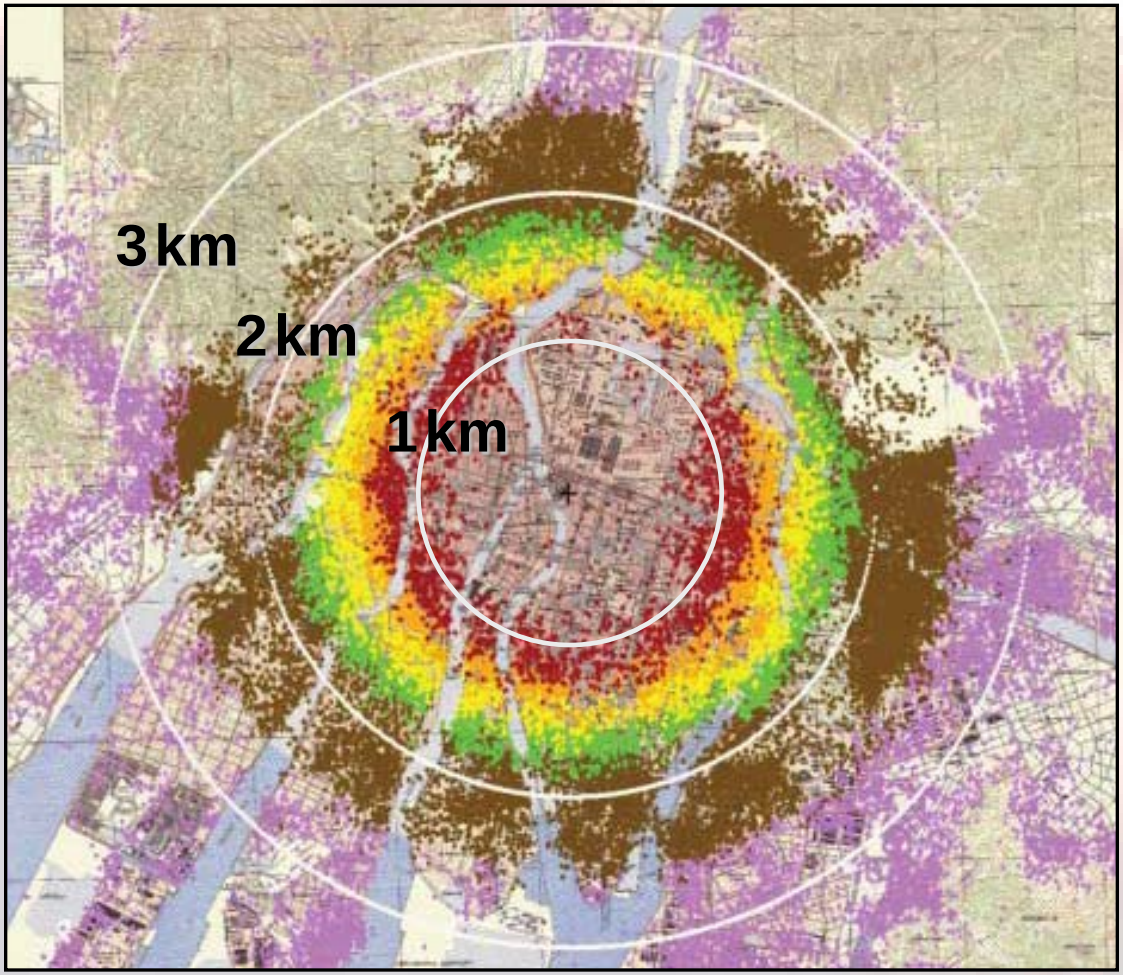

Green dots: Individuals exposed to between 100 and 200 mGy

Brown dots: Individuals exposed to between 5 and 100 mGy (~25,000)

Douple *et al* 2011

Number of solid cancers in A-bomb survivors exposed to doses between 5 and 100 mSv

Small but statistically significant increase in risk

	Cancer incidence (1958-98)
Study population (5-100 mSv)	27,789
Total solid cancers observed	4,406
Solid cancers expected (controls)	4,325
Radiation-related excess solid cancers	81

Preston *et al* 2007

Estimating the radiation-induced cancer risks from CT exams

- Direct epidemiology on people who received CT scans
- Risk estimation based on organ doses and A-bomb survivor data

Risk estimation based on organ doses and A-bomb survivor data

1. **Estimate the dose to each organ, as a function of age, gender, and type of CT exam**

2. **Apply estimates of age-, gender-, and organ-specific risks-per-unit dose**

   (low-dose risks from A-bomb survivors, "transferred" to a Western population)

3. **Sum the estimated risks for all organs**

Risk estimates based on organ doses and A-bomb survivor data - 2001

AJR American Journal of Roentgenology
Diagnostic Imaging and Related Sciences

Estimated Risks of Radiation-Induced Fatal Cancer from Pediatric CT

David J. Brenner[1]
Carl D. Elliston[1]
Eric J. Hall[1]
Walter E. Berdon[2]

OBJECTIVE. In light of the rapidly increasing frequency of pediatric CT examinations, the purpose of our study was to assess the lifetime cancer mortality risks attributable to radiation from pediatric CT.

MATERIALS AND METHODS. Organ doses as a function of age-at-diagnosis were estimated for common CT examinations, and estimated attributable lifetime cancer mortality risks (per unit dose) for different organ sites were applied. Standard models that assume a linear extrapolation of risks from intermediate to low doses were applied. On the basis of current standard practice, the same exposures (milliampere-seconds) were assumed, independent of age.

RESULTS. The larger doses and increased lifetime radiation risks in children produce a sharp increase, relative to adults, in estimated risk from CT. Estimated lifetime cancer mortality risks attributable to the radiation exposure from a CT in a 1-year-old are 0.18% (abdominal) and 0.07% (head)—an order of magnitude higher than for adults—although those figures still represent a small increase in cancer mortality over the natural background rate. In the United States, of approximately 600,000 abdominal and head CT examinations annually performed in children under the age of 15 years, a rough estimate is that 500 of these individuals might ultimately die from cancer attributable to the CT radiation.

CONCLUSION. The best available risk estimates suggest that pediatric CT will result in significantly increased lifetime radiation risk over adult CT, both because of the increased dose per milliampere-second, and the increased lifetime risk per unit dose. Lower milliampere-second settings can be used for children without significant loss of information. Although the risk–benefit balance is still strongly tilted toward benefit, because the frequency of pediatric CT examinations is rapidly increasing, estimates that quantitative lifetime radiation risks for children undergoing CT are not negligible may stimulate more active reduction of CT exposure settings in pediatric patients.

The use of CT has increased rapidly in the past two decades, fueled in part by the development of helical CT [1]. For example, the estimated annual number of CT examinations in the United States rose approximately sevenfold from 2.8 million in 1981 [2] to 20 million in 1995 [3]. By their nature, CT examinations contribute disproportionately to the collective diagnostic radiation dose to the population; for example, in Britain it has been estimated that approximately 4% of diagnostic radiology procedures are CT examinations, but their contribution to the collective dose is approximately 40% [4].

Figure 1 shows a breakdown of the number of CT examinations by age at examination, based on the results of a 1980 British survey [5]; in this survey, approximately 4% of CT examinations (which corresponds to about 10^6/year in the United States) were performed on children under the age of 15 years. The proportion of childhood CT examinations is rapidly increasing (indeed, an average value of 9% was estimated in 1993 [6]); for example, Coren et al. [7] reported a 63% increase in requests for pediatric CT between 1991 and 1994.

The recent increase in pediatric CT examinations is particularly marked in the United States. Figure 2 shows the number of abdominal and pelvic CT examinations of children under a given age at a major American children's hospital for 1996 through 1999. This figure shows, for example, a 92% increase between 1998 and 1999 in abdominal and pelvic CT examinations on children less

Received March 2, 2000; accepted after revision July 12, 2000.

Supported in part by grant DE-FG02-98ER62686 from the United States Department of Energy and by grant CA-77285 from the National Cancer Institute.

[1]Center for Radiological Research, Columbia University, 630 W. 168th St., New York, NY 10032. Address correspondence to D. J. Brenner.

[2]Department of Radiology, Division of Pediatric Radiology, Columbia-Presbyterian Medical Center, 630 W. 168th St., New York, NY 10032.

AJR 2001;176:289–296

0361–803X/01/1762–289

www.usatoday.com THE NATION'S NEWSPAPER 50 CENTS

FINAL SPORTS

Super Bowl

Let the hype begin

Clock is ticking toward Sunday. Full report, 1-4C
▸ 10 years ago, war was on our minds, 1C
▸ Coming Friday: Bonus Section

USA TODAY

NO. 1 IN THE USA

The Golden Globes

'Gladiator' wins best drama film

Julia Roberts, Tom Hanks honored for drama roles; *Almost Famous* named best comedy film ■ 1-2D
▸ The red carpet, 5D

By Robert Hanashiro, USA TODAY

Roberts: Smiles for *Erin Brockovich*.

Monday, January 22, 2001

Newsline

News ■ Money ■ Sports ■ Life

usatoday.com's new look

USA TODAY .com

Get the latest news, stocks, scores and more right now at USA TODAY's 24-hour online news site, all with a clean new interface. Plus, a stand-alone Tech section.

■ Asia stocks mixed overnight

Japan's Nikkei average is down 137 points, 1.0%, to 13,852 early today. Hong Kong's Hang Seng index is up 136 points, 0.9%, to 16,069.

CT scans in children linked to cancer later

By Steve Sternberg
USA TODAY

Each year, about 1.6 million children in the USA get CT scans to the head and abdomen — and about 1,500 of those will die later in life of radiation-induced cancer, according to research out today.

What's more, CT or computed tomography scans given to kids are typically calibrated for adults, so children absorb two to six times the radiation needed to produce clear images, a second study shows. These doses are "way bigger than the sorts of doses that people at Three Mile Island were getting," David Brenner of Columbia University says. "Most people got a tenth or a hundredth of the dose of a CT."

Both studies appear in February's *American Journal of Roentgenology*, the nation's leading radiology journal. The first, by Brenner and colleagues, is the first to estimate the risks of "radiation-induced fatal cancer" from pediatric CT scans. Until a decade ago, CT scans took too long to perform on children without giving them anesthesia to keep them still. Today's scanners spiral around the patient in seconds, providing cross sections, or "slices," of anatomy.

Doctors use CT scans on children to search for cancers and ailments such as appendicitis and kidney stones.

"There's a huge number of people who don't just receive one scan," says Fred Mettler of the University of New Mexico, noting that CT scans are used for diagnosis and to plan and evaluate treatment. "The breast dose from a CT scan of the chest is somewhere between 10 and 20 mammograms. You'd want to think long and hard about giving your young daughter 10 to 20 mammograms unless she really needs it."

Mettler recently published a study showing that 11% of the CT scans at his center are done on children younger than 15, and they get 70% of the total radiation dose given to patients. Children have more rapidly dividing cells than adults, which are more susceptible to radiation damage. Children also will live long enough for cancers to develop.

Researchers led by Lane Donnelly at Cincinnati's Children's Hospital found that children often get radiation doses six times higher than necessary. Cutting the adult dose in half would yield a clear image and cut the risk a like amount, Brenner says. "Radiologists genuinely believe the risks are small," he says. "I suspect they've never been confronted with numbers like this."

Not everyone was convinced…

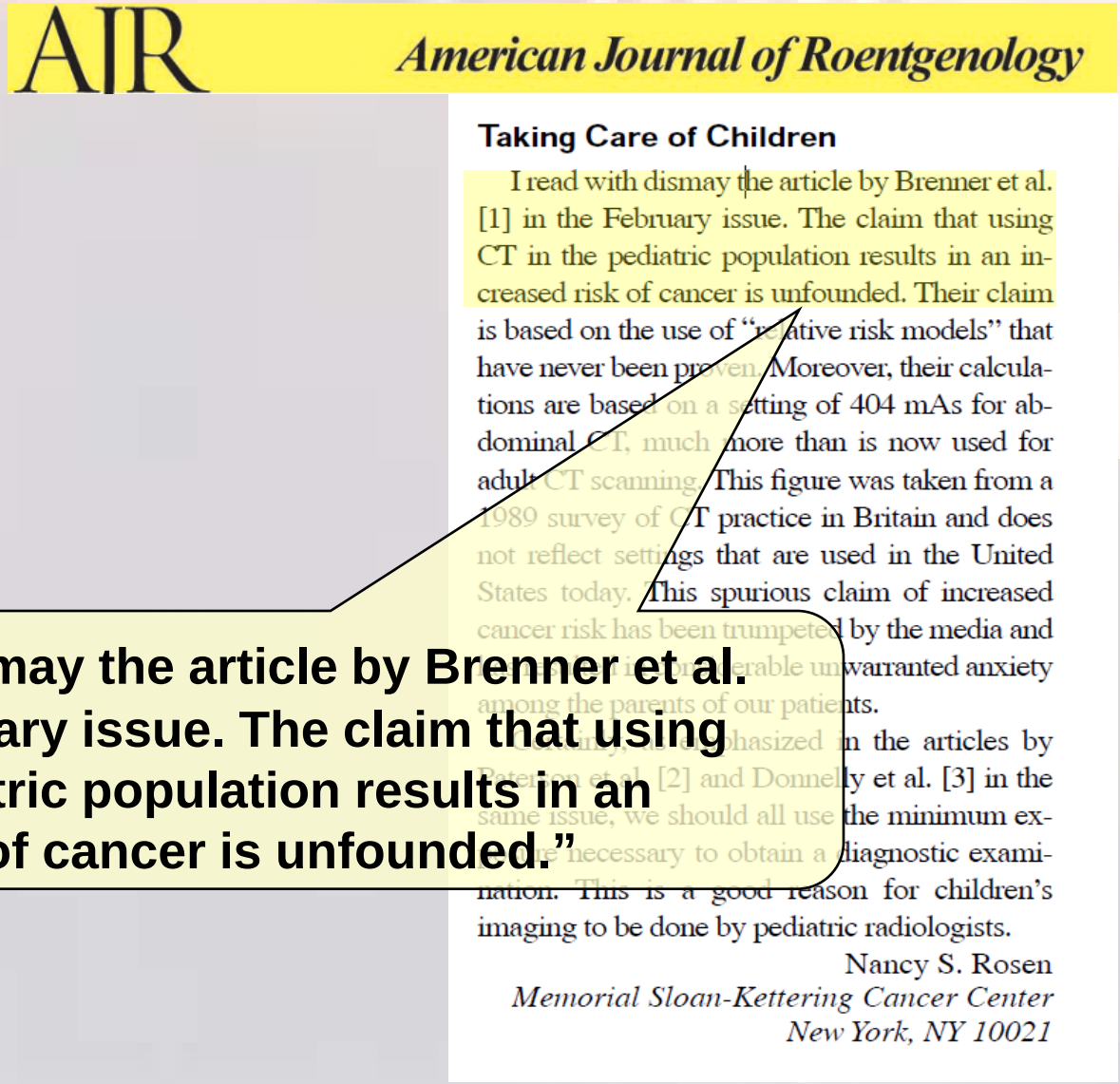

AJR American Journal of Roentgenology

Taking Care of Children

I read with dismay the article by Brenner et al. [1] in the February issue. The claim that using CT in the pediatric population results in an increased risk of cancer is unfounded. Their claim is based on the use of "relative risk models" that have never been proven. Moreover, their calculations are based on a setting of 404 mAs for abdominal CT, much more than is now used for adult CT scanning. This figure was taken from a 1989 survey of CT practice in Britain and does not reflect settings that are used in the United States today. This spurious claim of increased cancer risk has been trumpeted by the media and [illegible] unwarranted anxiety among the parents of our patients.

As emphasized in the articles by Paterson et al. [2] and Donnelly et al. [3] in the same issue, we should all use the minimum exposure necessary to obtain a diagnostic examination. This is a good reason for children's imaging to be done by pediatric radiologists.

Nancy S. Rosen
Memorial Sloan-Kettering Cancer Center
New York, NY 10021

"I read with dismay the article by Brenner et al. [1] in the February issue. The claim that using CT in the pediatric population results in an increased risk of cancer is unfounded."

Not everyone was convinced…

"Risks of medical imaging at effective doses below 50 mSv for single procedures or 100 mSv for multiple procedures over short time periods are too low to be detectable and may be non-existent"

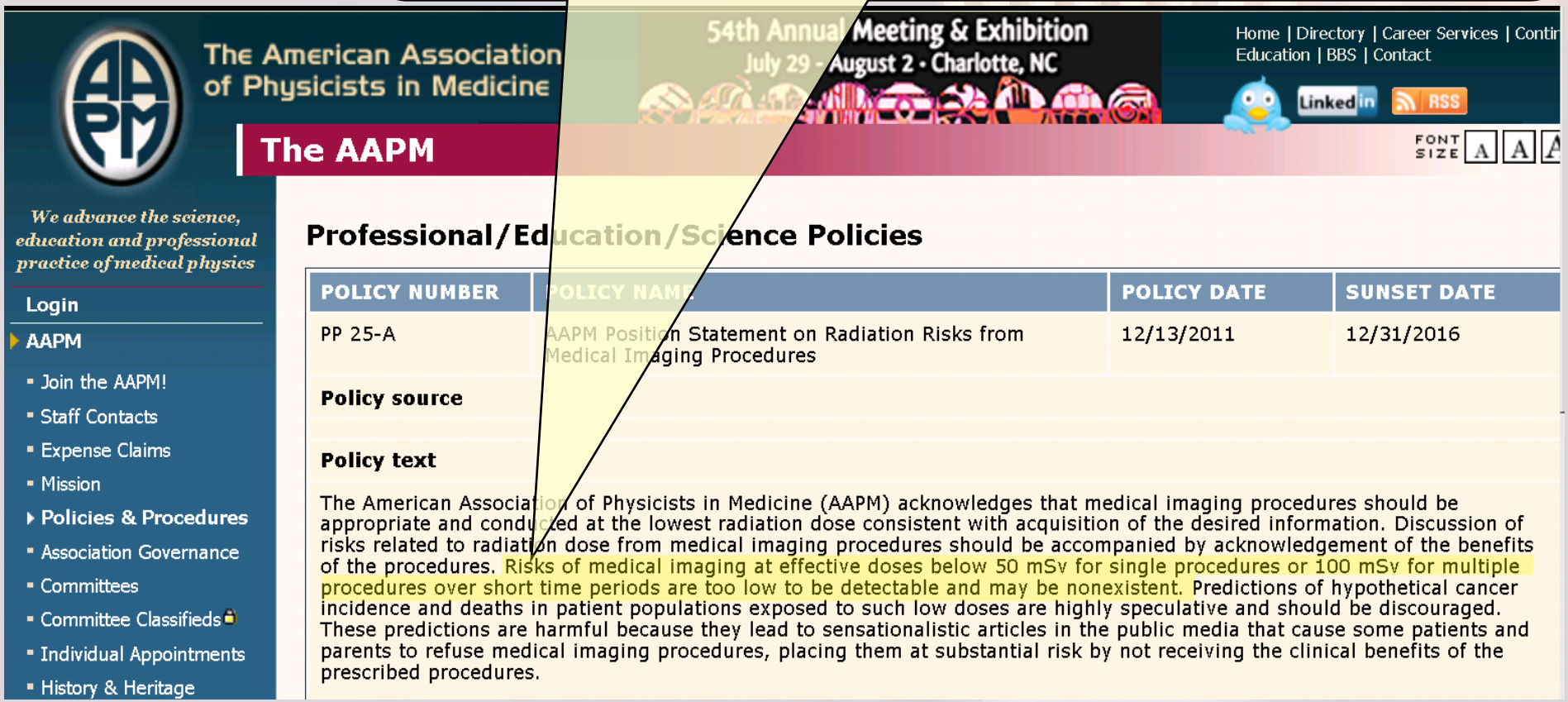

Could we design an epidemiological study of CT risks in the US?

The 2012 UK CT Study

Radiation exposure from CT scans in childhood and subsequent risk of leukaemia and brain tumours: a retrospective cohort study

Mark S Pearce, Jane A Salotti, Mark P Little, Kieran McHugh, Choonsik Lee, Kwang Pyo Kim, Nicola L Howe, Cecile M Ronckers, Preetha Rajaraman, Sir Alan W Craft, Louise Parker, Amy Berrington de González

www.thelancet.com **Published online June 7, 2012** **DOI:10.1016/S0140-6736(12)60815-0**

~10 year follow-up of 175,000 patients who received CT scans in the UK, age <22, between 1985 and 2002

- **Statistically significant linear associations were seen between brain dose and brain tumor risk ($p<0.0001$), and between bone-marrow dose and leukemia risk ($p=0.01$)**

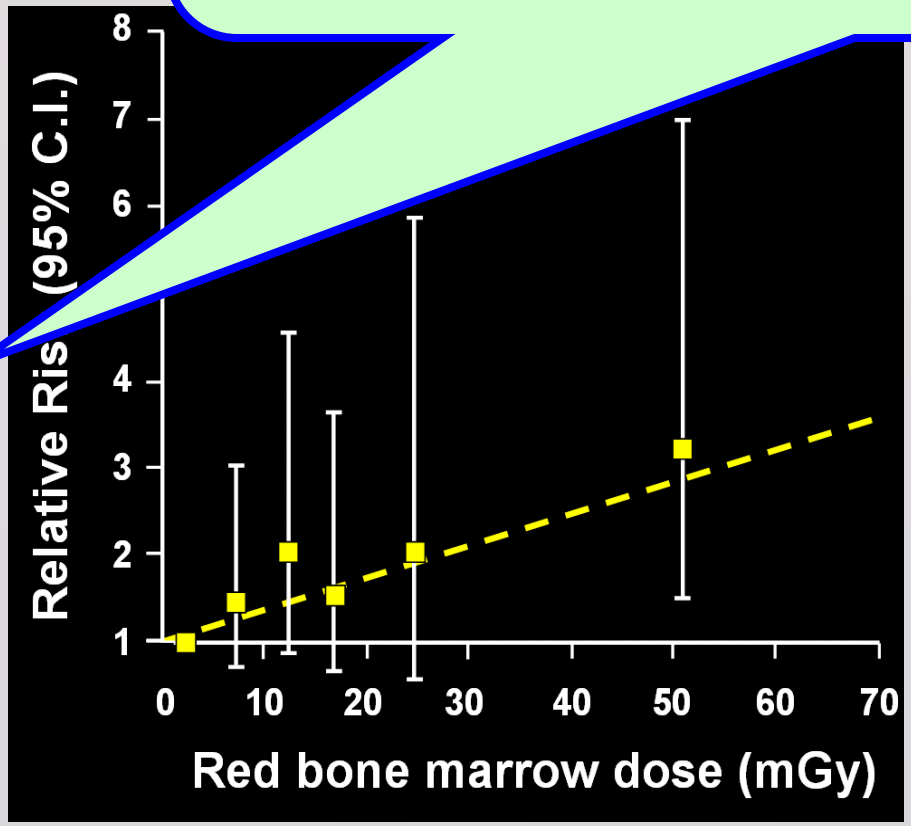

Leukemia

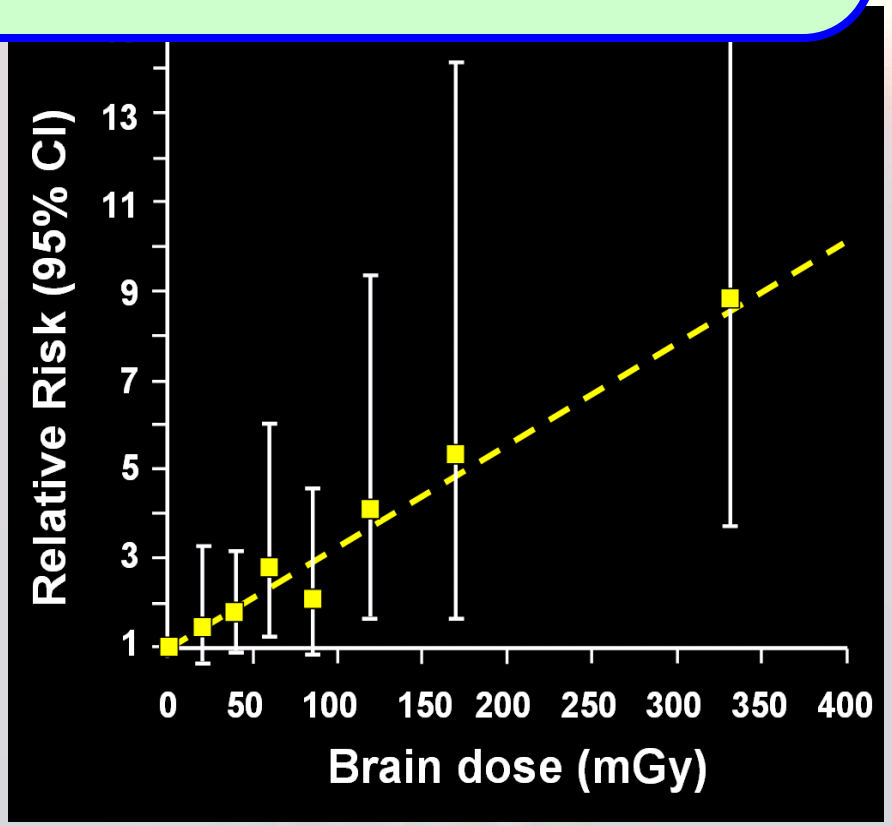

Brain tumors

Could the reason for the CT also be a cause of cancer?

- Reverse causation….
- For example does head trauma causes cancer?

Cancer Causes Control. 2001 Oct;12(8):733-7.

Primary brain tumors following traumatic brain injury--a population-based cohort study in Sweden.

Nygren C, Adami J, Ye W, Bellocco R, af Geijerstam JL, Borg J, Nyrén O.

Department of Rehabilitation Medicine, Karolinska Institute, Danderyd Hospital, Stockholm, Sweden. catharina.nygren@mbox304.swipnet.se

Abstract

OBJECTIVES: The aim of this study was to explore the association between traumatic brain injury and brain tumor development.

METHODS: A cohort of patients hospitalized for traumatic brain injury during 1965-1994 was compiled using the Swedish Inpatient Register. Complete follow-up through 1995 was attained through record linkage with the Swedish Cancer Register, the Cause of Death Register, and the Emigration Register. Standardized incidence ratios (SIRs), defined as the ratios of the observed to the expected numbers of brain tumors, were used as the measure of relative risk. The expected number of brain tumors was calculated by multiplying the observed person-time by age-, gender- and calendar year-specific incidence-rates derived from the general Swedish population.

RESULTS: The cohort included 311,006 patients contributing 3,225,317 person-years. A total of 281 cases of brain tumors were diagnosed during follow-up. No associations were found between traumatic brain injury and the risk of primary brain tumors, neither overall (SIR: 1.0; 95% confidence interval (CI): 0.9-1.2), nor in analyses broken down by main groups of brain tumors. Stratified analyses according to age at entry into the cohort, year of follow-up, and severity of the brain injury all showed essentially the same null results.

CONCLUSION: No association between traumatic head injury and primary brain tumors has been found.

- Statistically significant linear associations were seen between brain dose and brain tumor risk ($p<0.0001$), and between bone-marrow dose and leukemia risk ($p=0.01$)
- Small risks, but almost certainly real

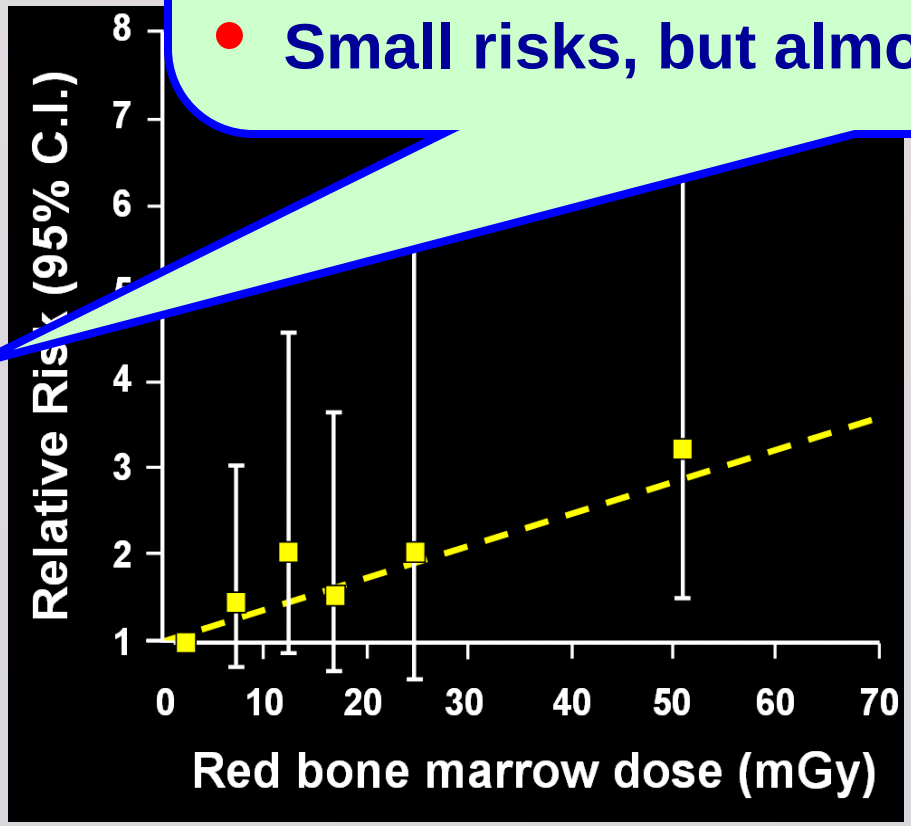

Leukemia

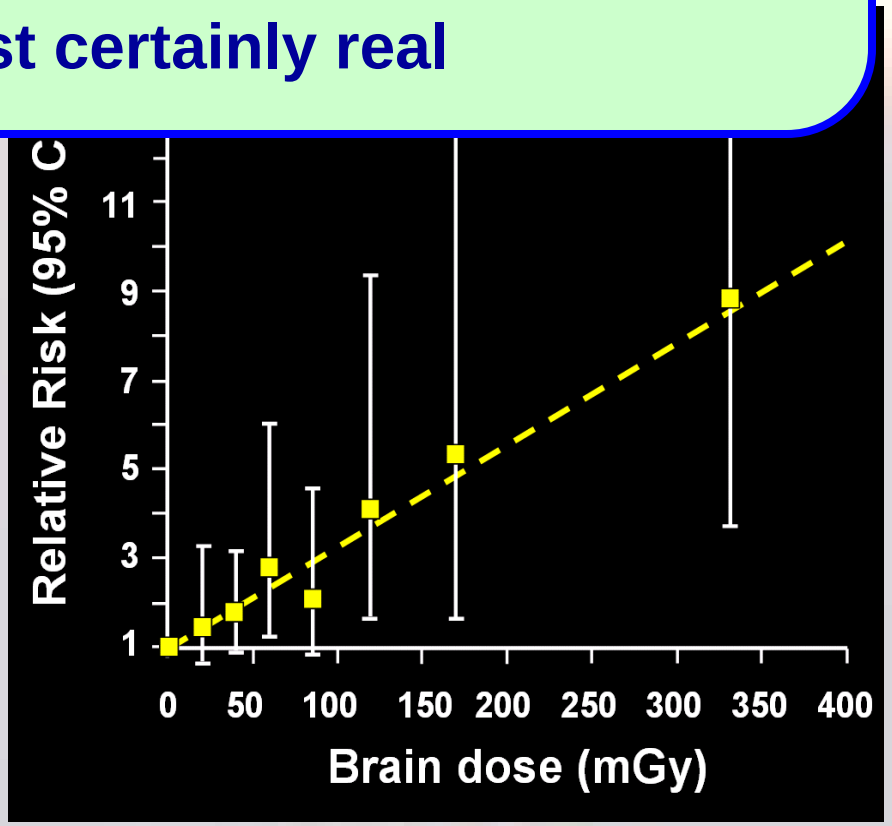

Brain tumors

The UK CT Study:
A pretty important event in our field

- **We have now passed a watershed in the field, where it is no longer reasonable to suggest that CT risks are "*too low to be detectable and may be non-existent*"**

The UK CT Study
Absolute risk estimates

- **Pearce *at al* estimated absolute risks of about 1 in 10,000 per head CT scan, both for leukemia and for brain tumors**

The UK CT Study:
CT Risks are real but small

- **So the results of the study imply that if a CT exam is clinically justified, its benefits by far exceed its risks**
  - ***No real need for any complicated benefit-risk calculations***

The UK CT Study
Absolute risk estimates

- Pearce *at al* estimated absolute risks of about 1 in 10,000 per head CT scan, both for leukemia and for brain tumors

- How does this compare with lifetime risk estimates based on organ doses and A-bomb survivor data?

AJR American Journal of Roentgenology

Diagnostic Imaging and Related Sciences

Estimated Risks of Radiation-Induced Fatal Cancer from Pediatric CT

David J. Brenner[1]
Carl D. Elliston[1]
Eric J. Hall[1]
Walter E. Berdon[2]

OBJECTIVE. In light of the rapidly increasing frequency of pediatric CT examinations, the purpose of our study was to assess the lifetime cancer mortality risks attributable to radiation from pediatric CT.

MATERIALS AND METHODS. Organ doses as a function of age at diagnostic CT were assessed for common CT examinations, and estimated attributable lifetime cancer mortality risks (per scan dose) for different organ sites were applied. Standard models that assume a linear extrapolation of risks from intermediate to low doses were applied. On the basis of current standard practice, the many exposures (milliroentgen-per-month) were assumed, independent of age.

RESULTS. The larger doses and associated lifetime radiation risks in children produce a sharp increase, relative to adults, in estimated risk from CT. Estimated lifetime cancer mortality risks attributable to the radiation exposure from a CT at a 1-year-old are 0.18% (abdomen) and 0.07% (brain)—an order of magnitude higher than for adults—although these figures still represent a small increase in cancer mortality over the normal background rate. In the United States, of approximately 600,000 abdominal and head CT examinations annually performed in children under the age of 15 years, a rough estimate is that 500 of these individuals might ultimately die from cancer attributable to the CT radiation.

CONCLUSION. The best available risk estimates suggest that pediatric CT will result in significantly increased lifetime radiation risk over adult CT, both because of the increased dose per milliroentgen-meter-second, and the increased lifetime risk per rad dose. Lower milliampere-second settings can be used for children without significant loss of information. Although the risk–benefit balance is still strongly tilted toward benefit, because the frequency of pediatric CT examinations is rapidly increasing, estimates that quantitative lifetime radiation risks for children undergoing CT are not negligible may stimulate more active reduction of CT exposure settings in pediatric patients.

The use of CT has increased rapidly in the past two decades, fueled in part by the development of helical CT [1]. For example, the estimated number of CT examinations in the United States rose approximately sevenfold from 2.8 million in 1981 [2] to 20 million in 1995 [3]. By these means, CT examinations contribute disproportionately to the collective diagnostic radiation dose to the population; for example, in Britain it has been estimated that approximately 4% of diagnostic radiology procedures are CT examinations, but these contribution to the collective dose is approximately 40% [4].

Figure 1 shows a breakdown of the number of CT examinations by age at examination, based on the results of a 1992 British survey [3]. In this survey, approximately 4% of CT examinations (which corresponds to about 10^6/year in the United States) were performed on children under the age of 15 years. The proportion of childhood CT examinations is rapidly increasing; indeed, an average value of 6% was estimated in 1993 [5]. For example, Coons et al. [7] reported a 154% increase in requests for pediatric CT between 1991 and 1994.

The recent increase in pediatric CT examinations is particularly marked in the United States. Figure 2 shows the number of abdominal and pelvic CT examinations of children under a given age at a major American children's hospital for 1980 through 1989. This figure shows, for example, a 95% increase between 1980 and 1989 in abdominal and pelvic CT examinations on children less

Received March 6, 2000; accepted after revision July 31, 2000.

Supported in part by grant DE-FG02-98ER62626 from the United States Department of Energy and by grant CA 81200 from the National Cancer Institute.

[1]Center for Radiological Research, Columbia University, 630 W. 168th St., New York, NY 10032. Address correspondence to D. J. Brenner.

[2]Department of Radiology, Division of Pediatric Radiology, Columbia–Presbyterian Medical Center, 630 W. 168th St., New York, NY 10032.

AJR 2001;176:289–296

0361–803X/01/1762–289

The UK CT Study
Absolute risk estimates

- **The mean follow-up time in the Pearce study was less than 10 years**
  - **From studies of other irradiated populations, we expect that not all the radiation-induced cancers that are going to appear, have actually yet appeared**

Cancer Incidence in Atomic Bomb Survivors. Part III: Leukemia, Lymphoma and Multiple Myeloma, 1950-1987

Preston et al. 1994

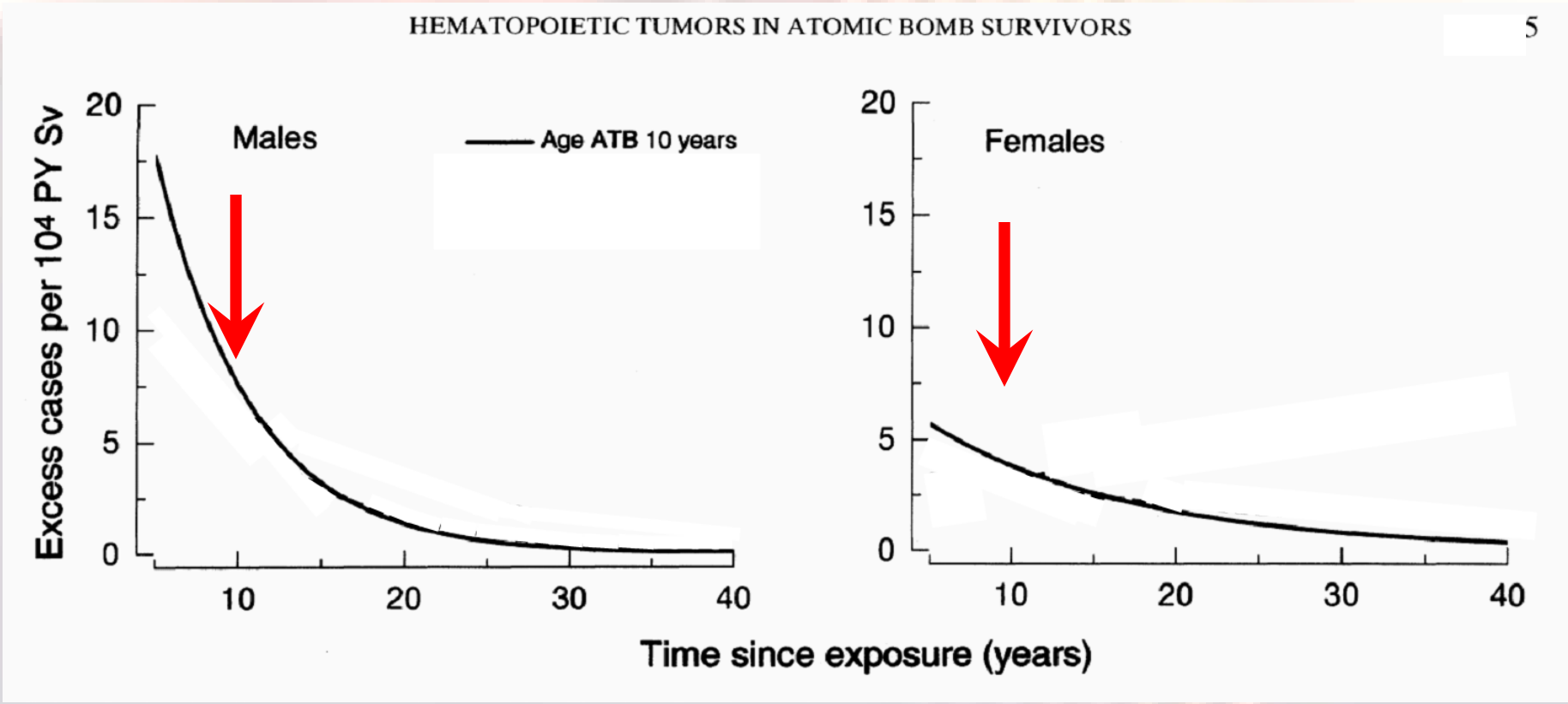

Percent of total radiation induced leukemias after 10 years follow up: 73%

Tumors of the Brain and Nervous System after Radiotherapy in Childhood

Ron et al NEJM 1988

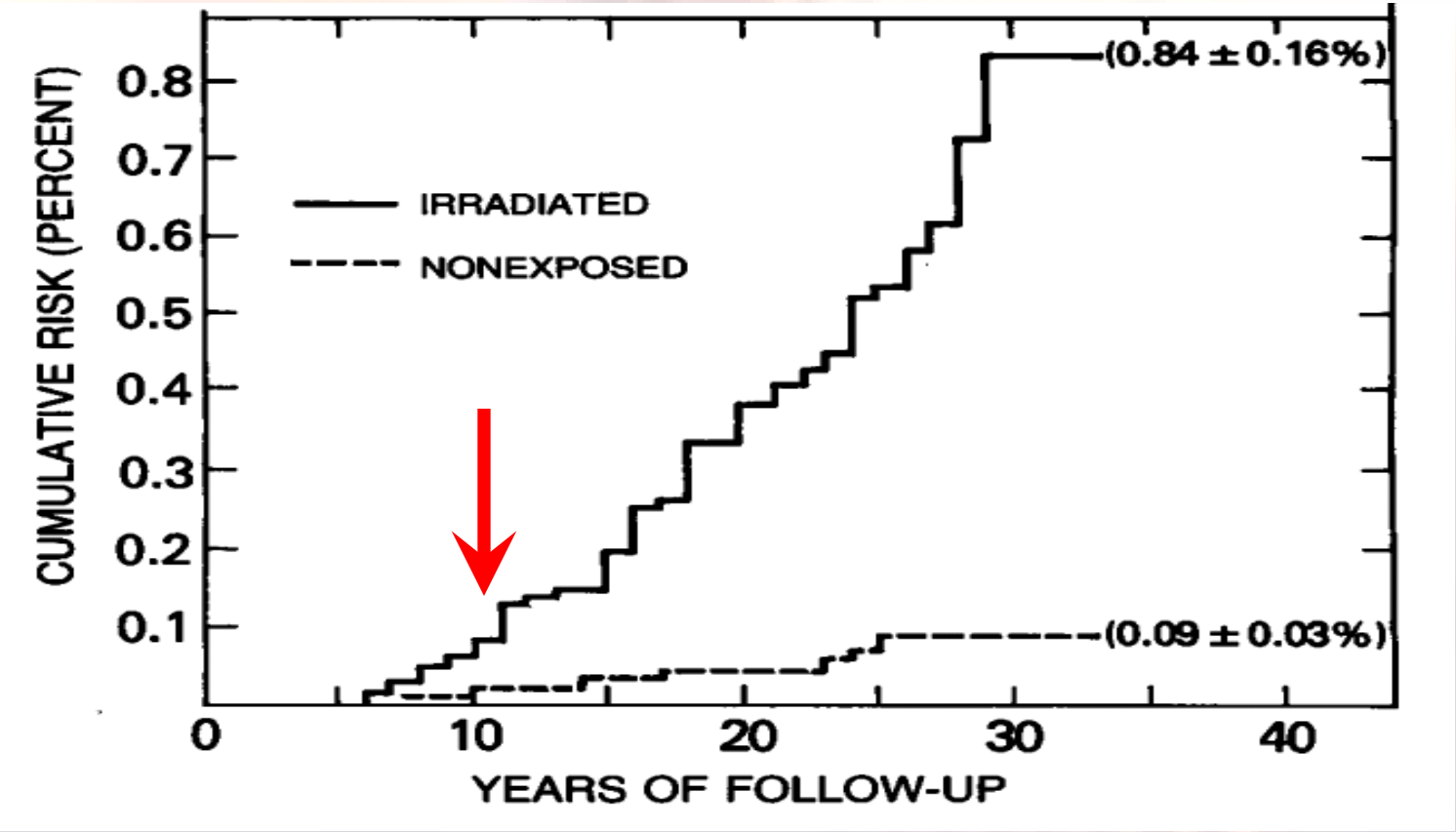

Percent of total radiation induced brain tumors after 10 years follow up: 8%

UK CT study: Absolute risks *vs.* A-bomb based estimates

For a pediatric head CT scan, done around 1995

	UK CT study (10 yrs follow-up)	*UK CT study (corrected to lifetime follow-up)*	*A-bomb estimates, (corrected to lifetime follow-up)*
Leukemia	**1 in 10,000**	**1 in 7,500**	**1 in 10,000**
Brain tumor	**1 in 10,000**	**1 in 1,000**	**1 in 2,000**

Based on Pearce et al 2012

Based on Brenner et al 2001

The UK CT Study
Absolute risk estimates

- The various risk estimates for CT that have appeared in the past decade seem to have been pretty near the mark
- So the standard methodology of estimating low-dose radiological risks from A-bomb survivor data and physical dosimetry is probably not unreasonable
- … which is just as well, because we are going to have to wait a long time for the full epidemiological-based story
  - Other cancers
  - Lifetime risks
  - Adult CT

How long would a CT epi study need to be to estimate lifetime risks?

Median latency time: The time required to accumulate 50% of the predicted total lifetime radiation-induced absolute cancer risk

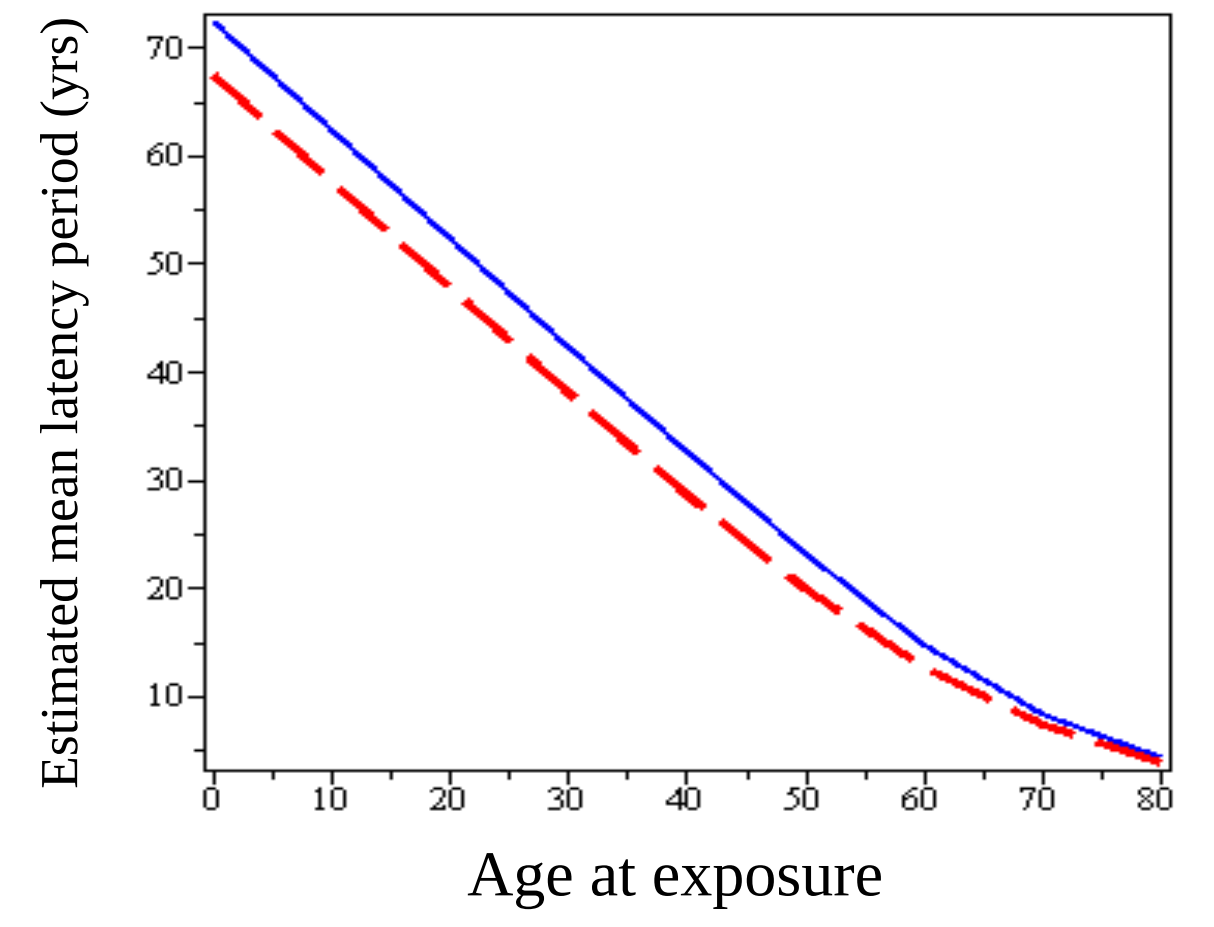

We are going to be reliant for quite a while on dosimetrically-based methods to estimate CT risks

1. **Estimate the dose to each organ, as a function of age, gender, and type of CT exam**

2. **Apply estimates of age-, gender-, and organ-specific risks-per-unit dose**

   (low-dose risks from A-bomb survivors, "transferred" to a Western population)

3. **Sum the estimated risks for all organs**

Should we be primarily concerned about children and young adults?

Estimated radiation-induced lifetime cancer risks as a function of age at exposure, from BEIR-VII

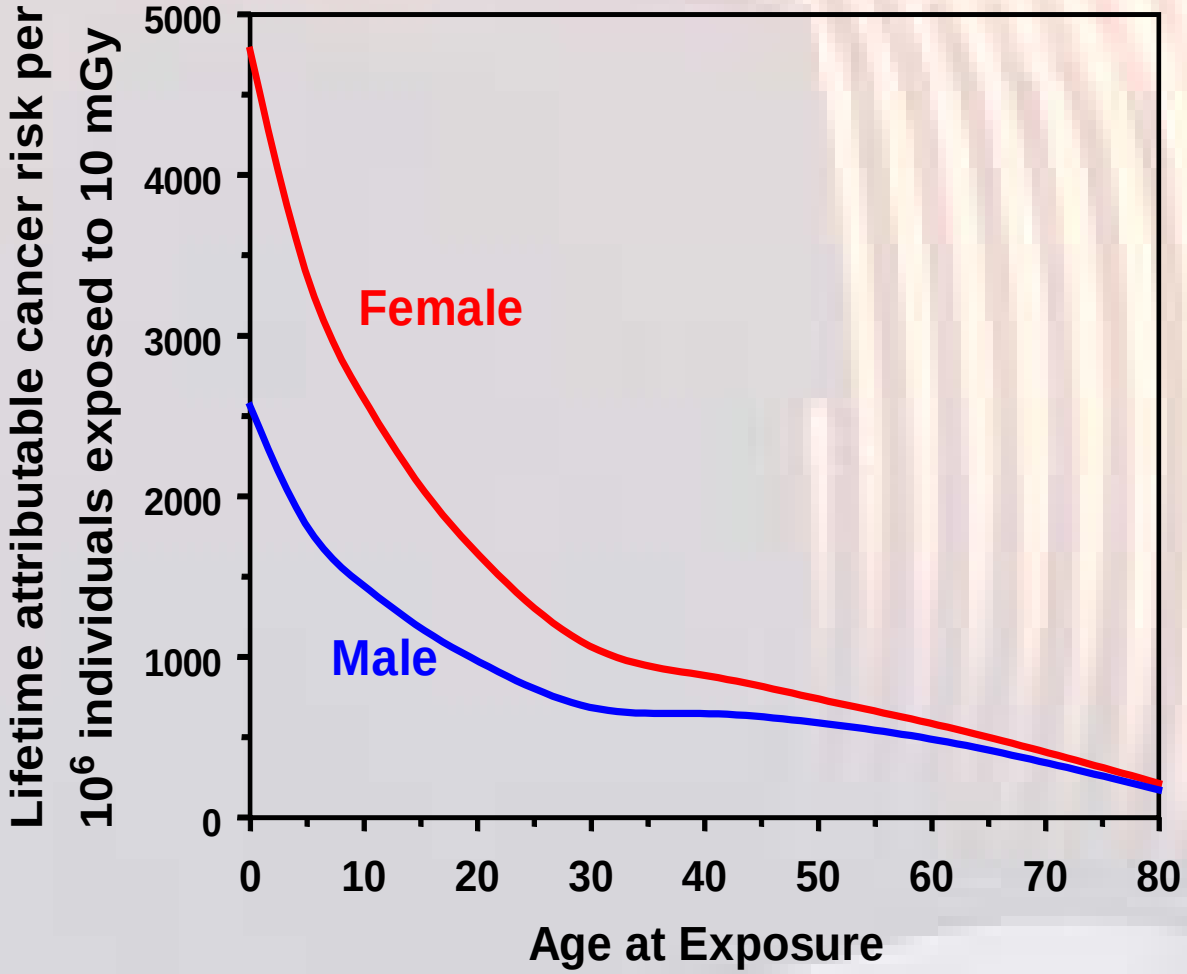

From BEIR-VII (2006)

Lifetime cancer risk patterns among A-bomb survivors as a function of age-at-exposure

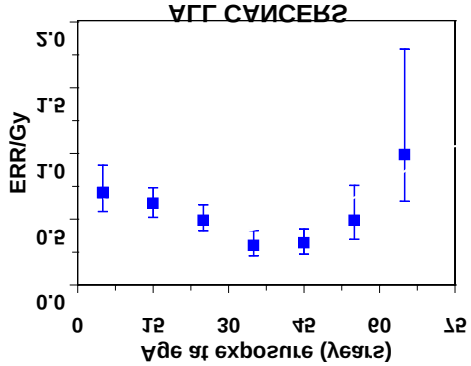

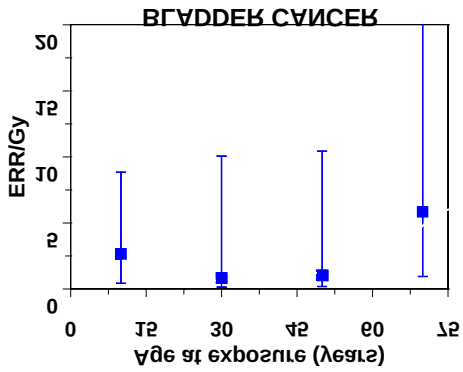

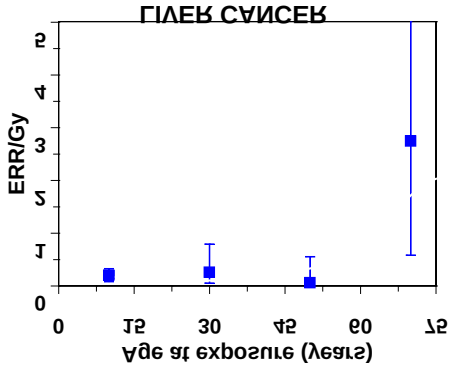

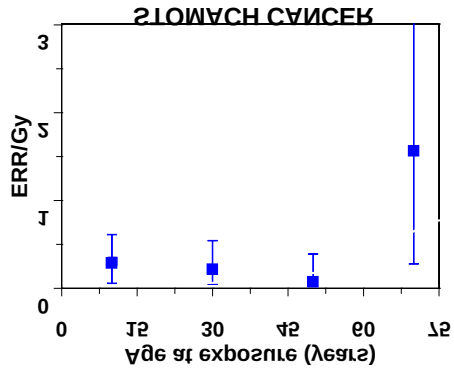

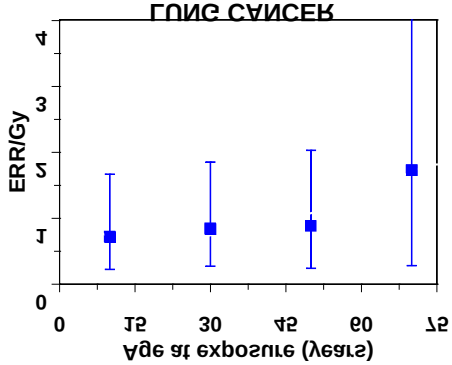

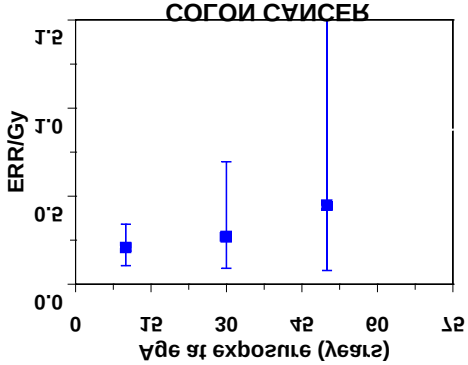

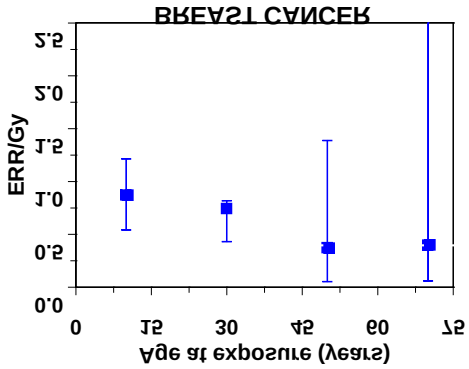

The actual data show very different age-at-exposure patterns relative to the monotonically decreasing risks modeled in BEIR VII

Multistage Carcinogenesis

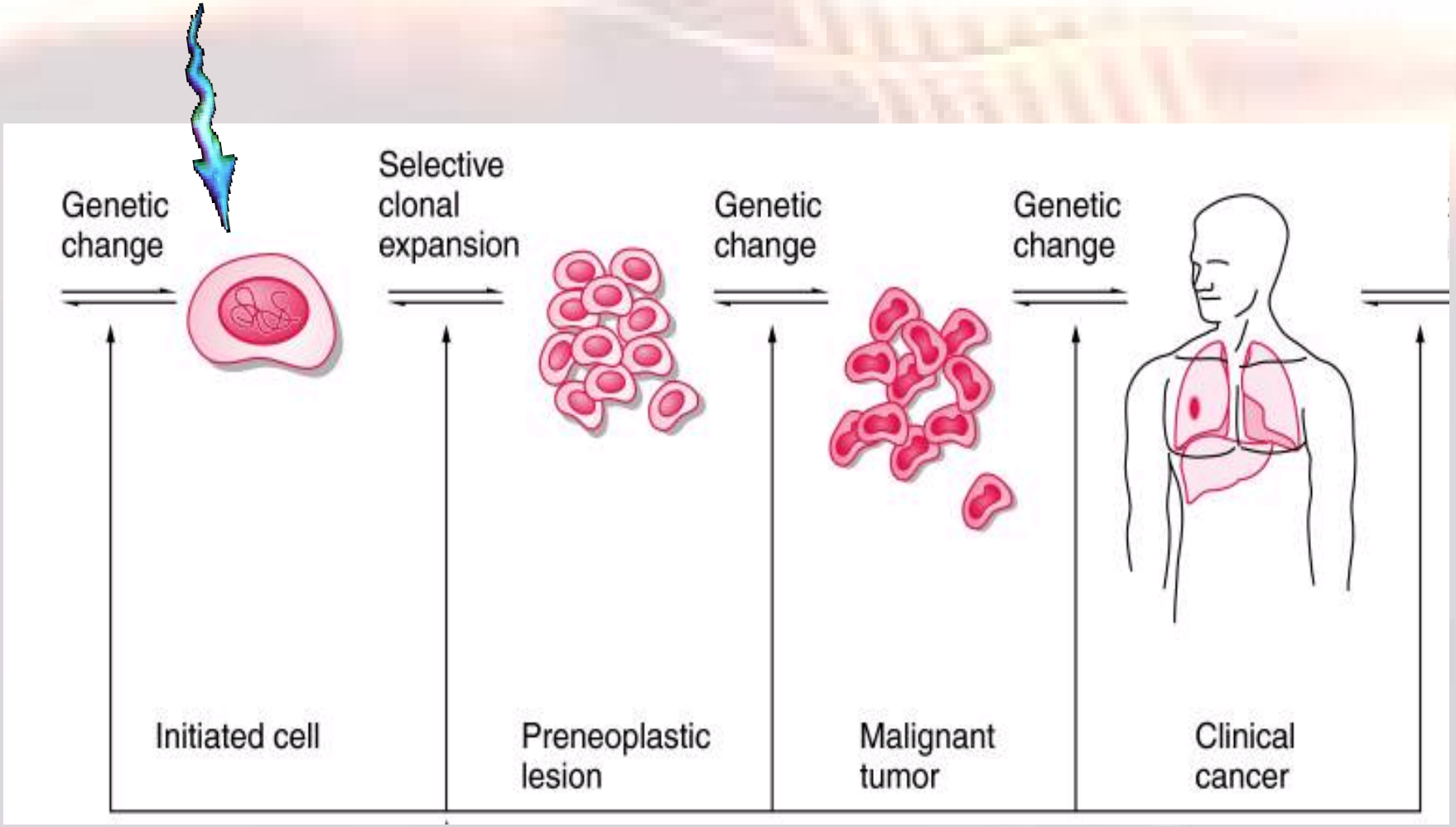

Lifetime cancer risk patterns as a function of age-at-exposure

Initiation: Here lifetime risk *decreases* with increasing age at exposure, because initiated cells have less time to exploit their growth advantage

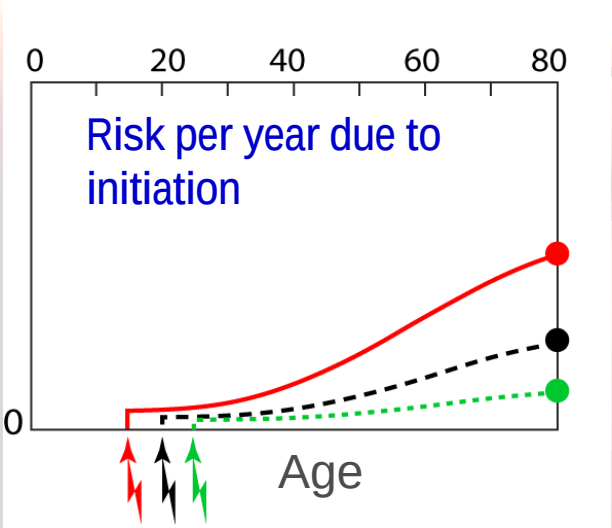

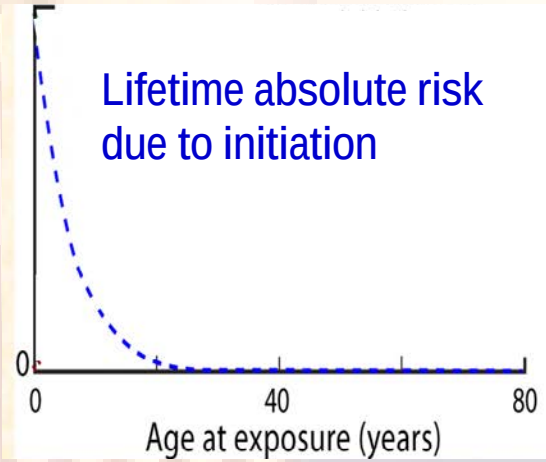

Multistage Carcinogenesis

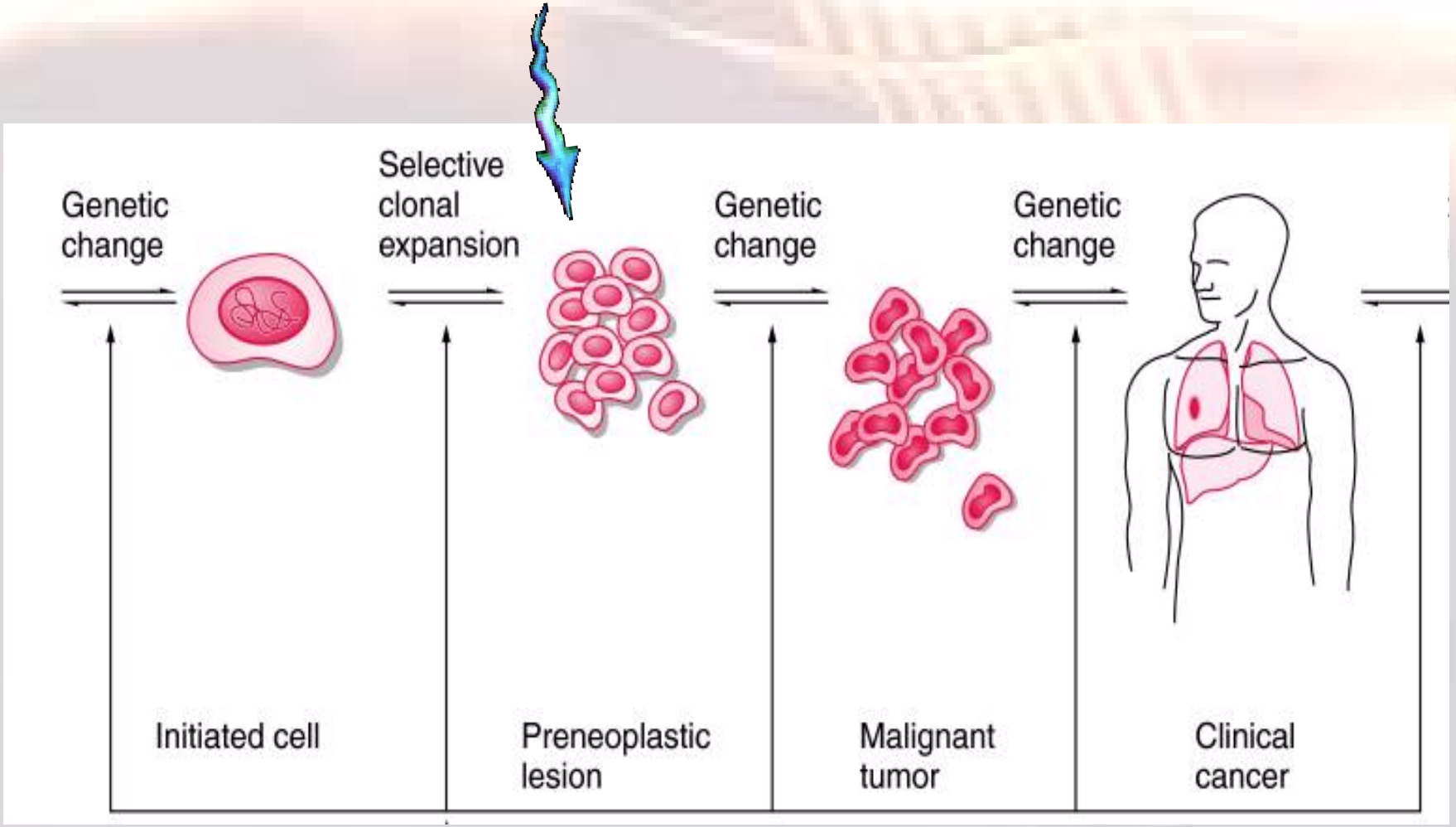

Lifetime cancer risk patterns as a function of age-at-exposure

Initiation: Here lifetime risk *decreases* with increasing age at exposure, because initiated cells have less time to exploit their growth advantage.

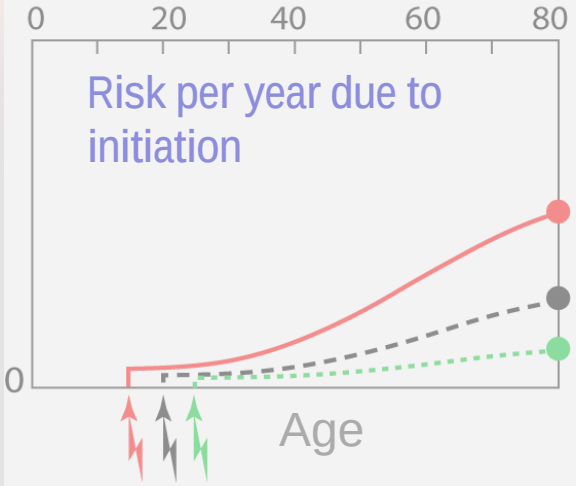

Promotion: In middle age, there are increasing numbers of pre-malignant cells to promote, so lifetime risk *increases* with increasing age at exposure.

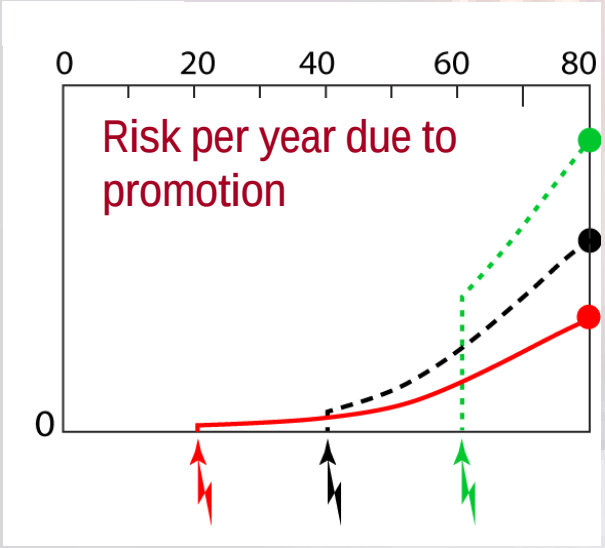

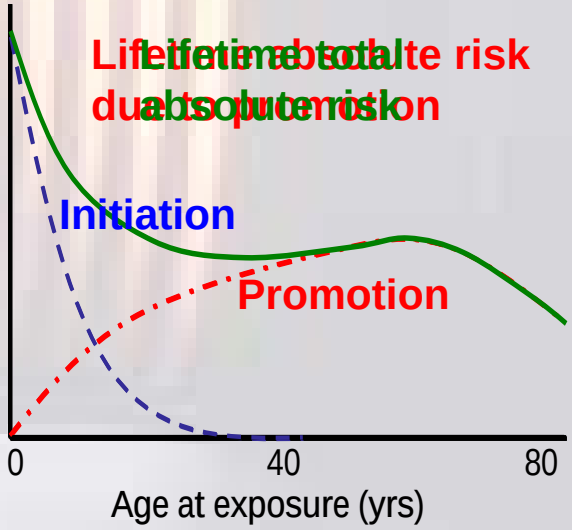

Observed age-at-exposure risk dependencies can be explained by an age-dependent balance between initiation and promotion

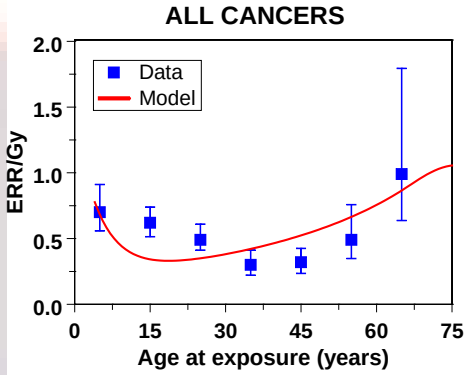

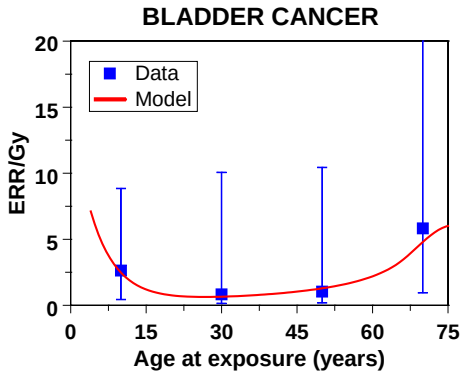

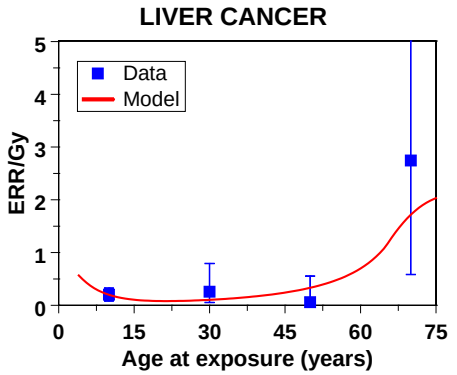

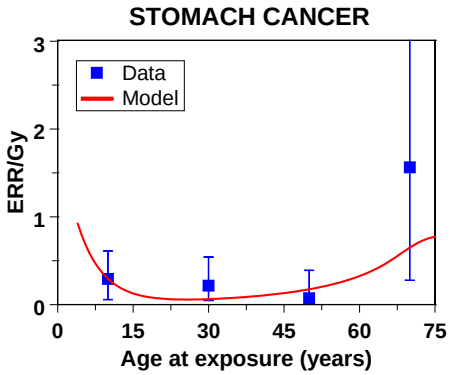

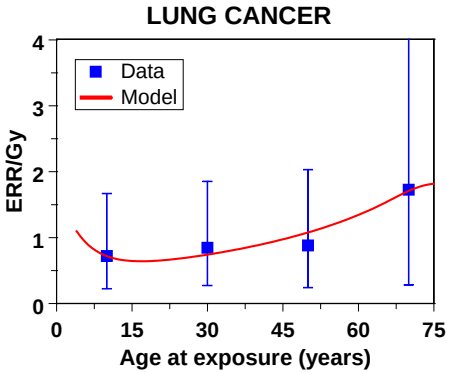

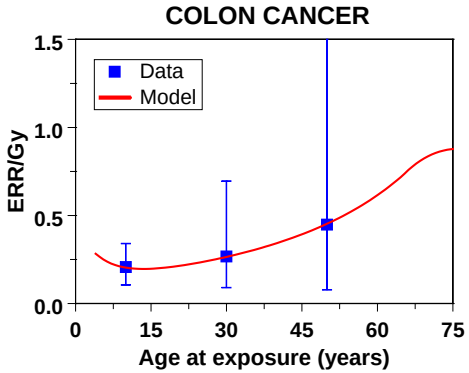

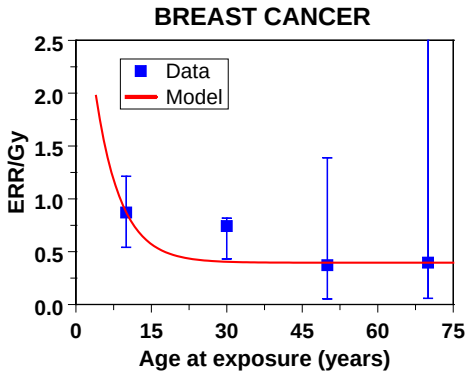

Red curves are the results from a radiation-induced initiation + promotion model

Shuryak et al JNCI 2010

Lifetime absolute risks, compared with BEIR-VII

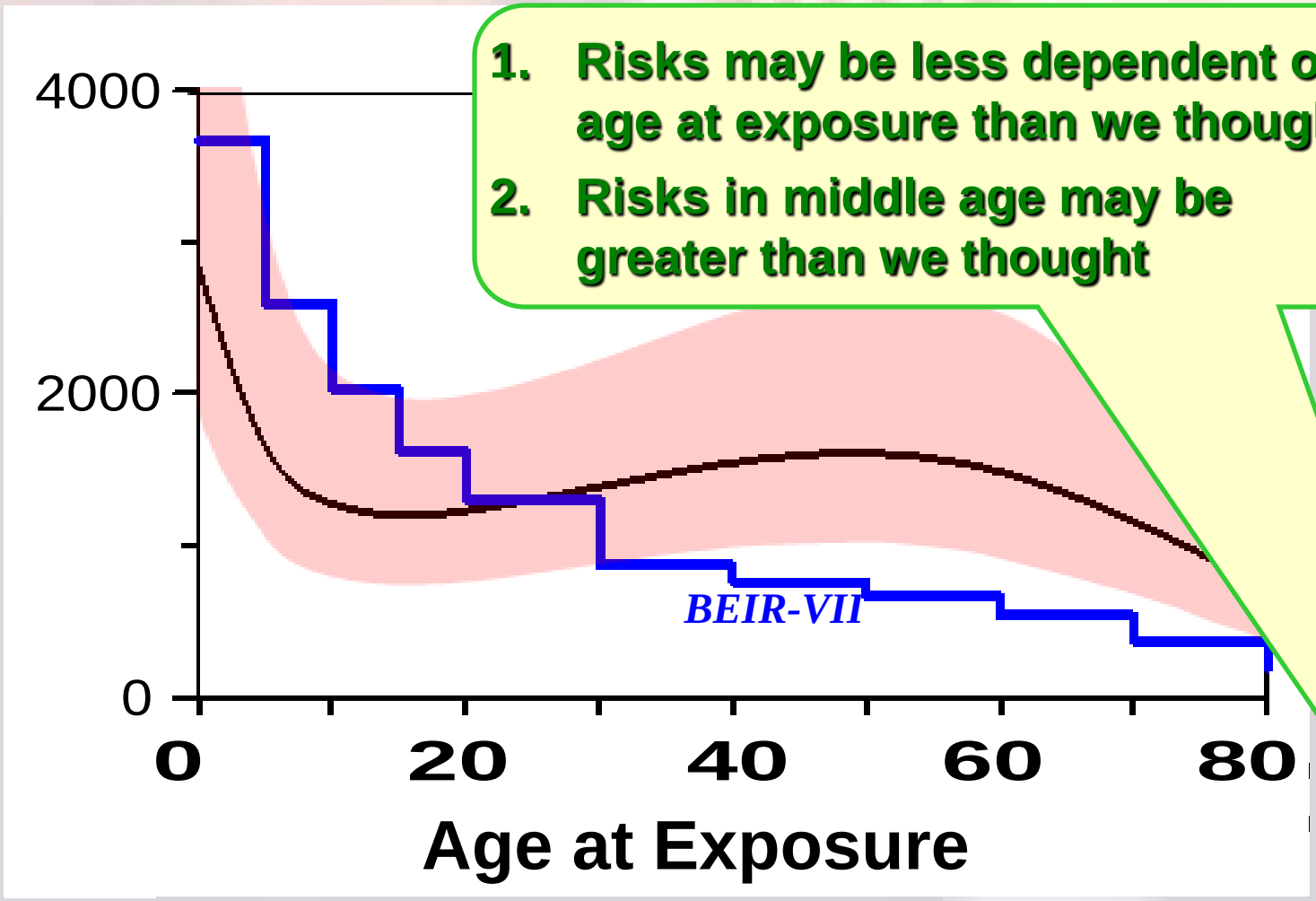

Shuryak et al JNCI 2010

… and of course most CT scans are given in middle age

Age distribution of CT scans, US, 2007

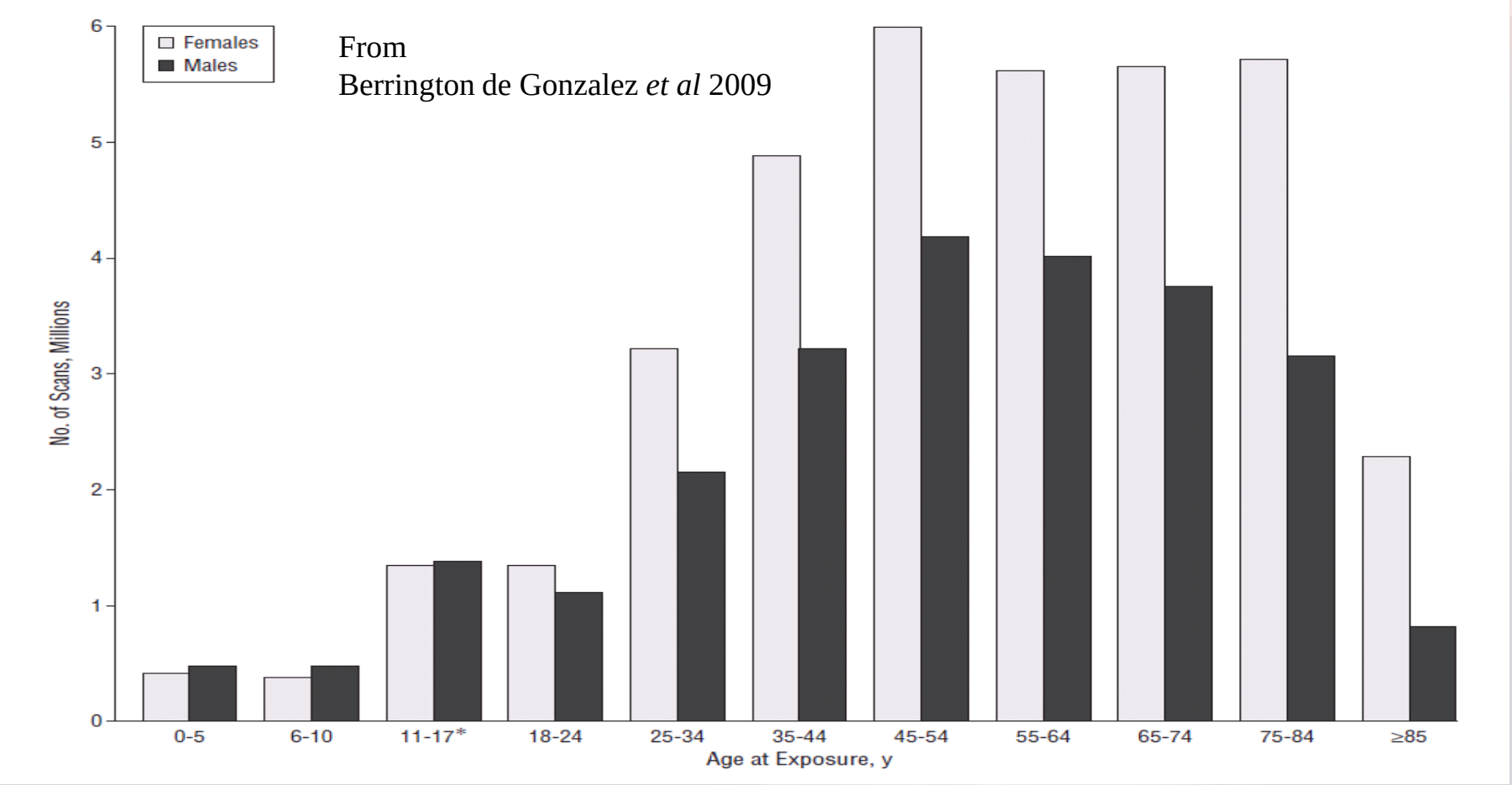

What do we know about risks from CT scans?

- **We have now passed a watershed in our field where it is no longer reasonable to suggest that CT risks are "*too low to be detectable and may be non-existent*"**
  - **We now know (almost) for sure that individual CT risks are small but real**
  - **Earlier CT risk estimates based on organ doses and A-bomb data have proved to be not unreasonable**
- **Because the individual risks are small, the individual benefits of any clinically-justified CT scan will by far outweigh the individual radiation risks**
  - **No need for super-accurate benefit-risk analyses for clinically-justified scans**
- **The CT risk issue is not confined to children**
  - **Radiation risks in middle age are probably somewhat larger than previously thought**
  - **Because there are far more adult CT scans, the population risks are larger for adults than for children**
- **While individual risks are small, because the number of CT scans is very large, and increasing, there will be significant population risks associated with CT**
  - **This population risk can be minimized by justifying and optimizing every CT scan**

A roadmap to reduce the long-term health consequences of radiation exposure from radiological exams

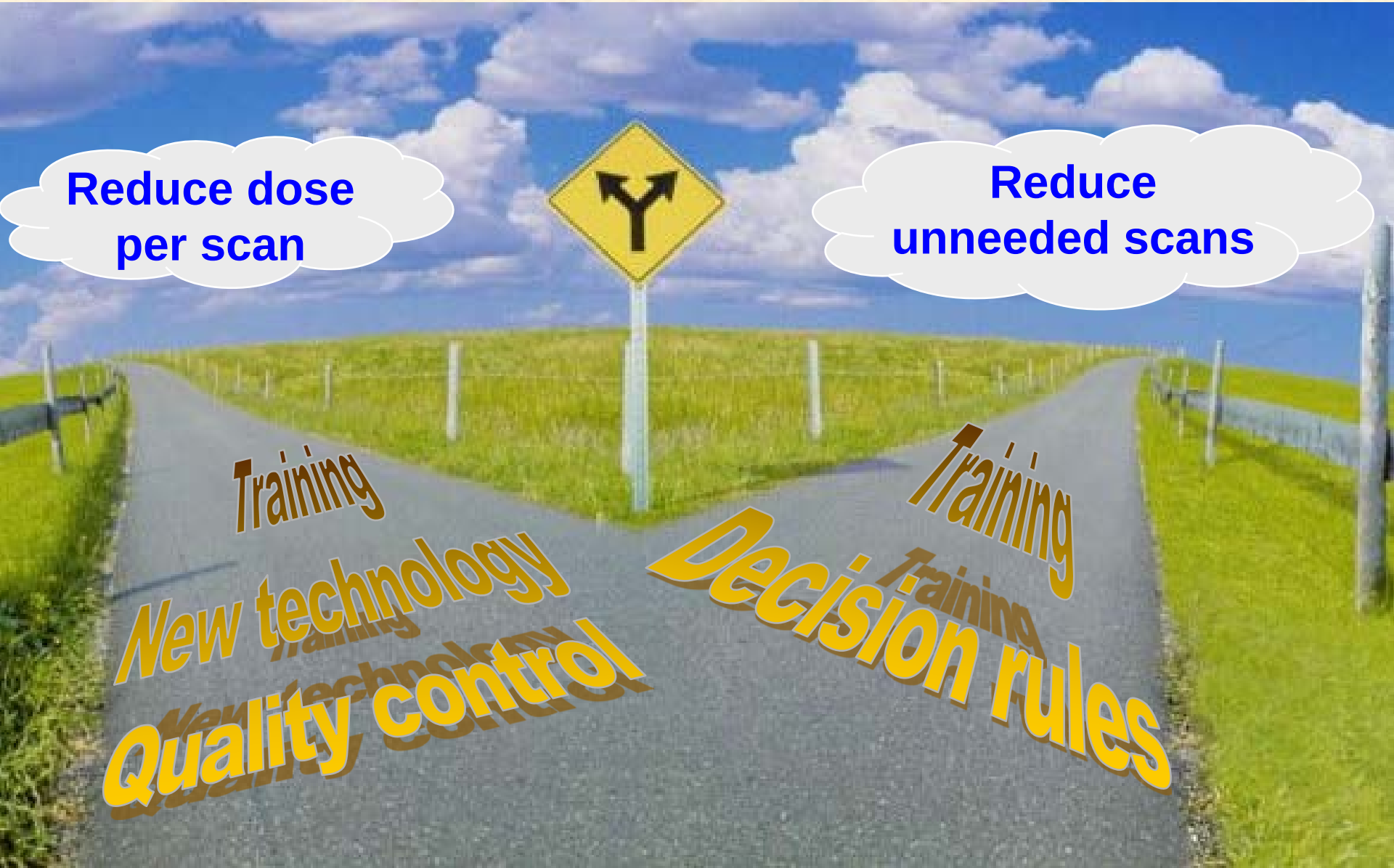

Inappropriate CT prescriptions rates:

Primary care physicians….
based on ACR Appropriateness Criteria

CT Exam	*Percent inappropriate*
Head / brain	62
Maxillofacial	36
Spine	53
Chest	12
Chest/abdomen/pelvis	30
Abdomen / pelvis	18
Miscellaneous + angiography	21
All CT exams	*27*

Lehnert and Bree 2010

Potential gains from CT justification…

- **~82 million CT scans done last year in the US**
- **~4 million pediatric CT scans / yr**
- **~2.5 million pediatric head CT scans / yr**
- **~1.5 million clinically-unnecessary pediatric head CT scans / year**
- ***1,500 unnecessary radiation-induced brain tumors produced each year***

Approaches for diagnosing pediatric appendicitis

100% CT

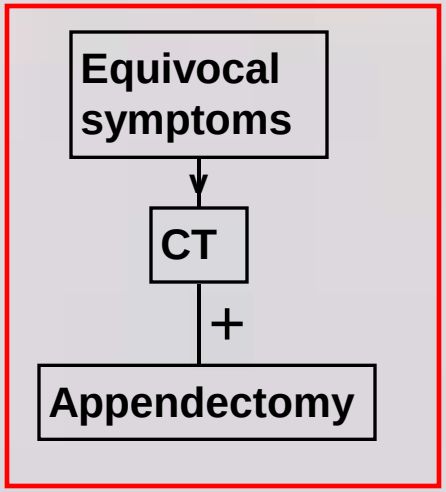

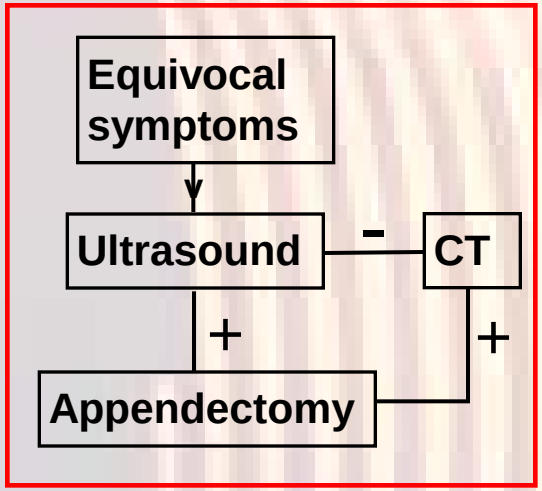

70% CT

Based on Garcia Pena 2004

Approaches for imaging patients with acute flank pain

AJR Am J Roentgenol. 2002 Feb;178(2):379-87.

Orlando Catalano[1,2]
Antonio Nunziata[3]
Francesco Altei[1]
Alfredo Siani[1]

Suspected Ureteral Colic: Primary Helical CT Versus Selective Helical CT After Unenhanced Radiography and Sonography

100% CT

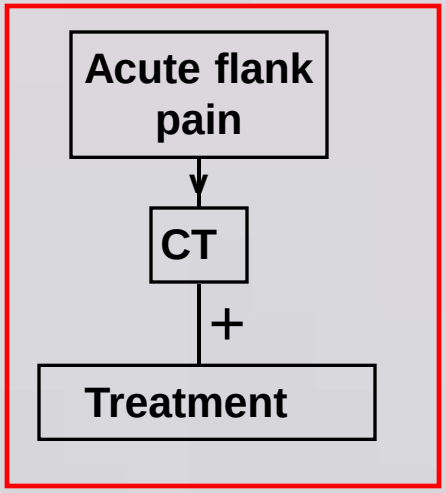

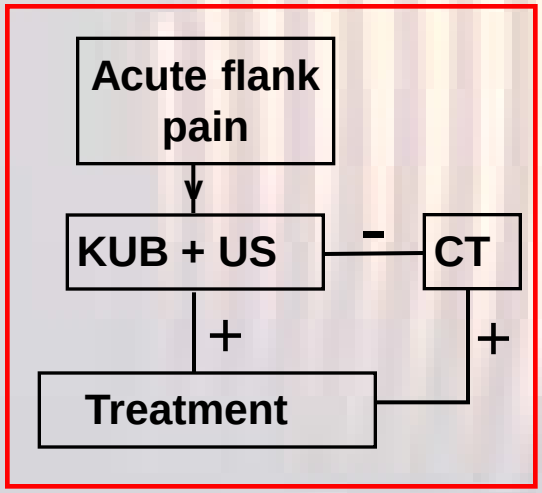

?% CT

Can CT usage be reduced?
(or the rate of increase slowed?)
without compromising patient care....

- **A significant fraction of CT scans (at least ¼ ??) could practically be replaced by alternate approaches, or need not be performed at all**

- **Targeting this “one quarter” is a [illegible]**

- **[illegible] s[illegible]**
  - [illegible]
  - [illegible]
  - **Economic**
  - **From patients**

Clinical Decision Rules

Do physicians actually use ACR appropriateness criteria?

- *What is your primary information resource in making imaging decisions for your patients?*

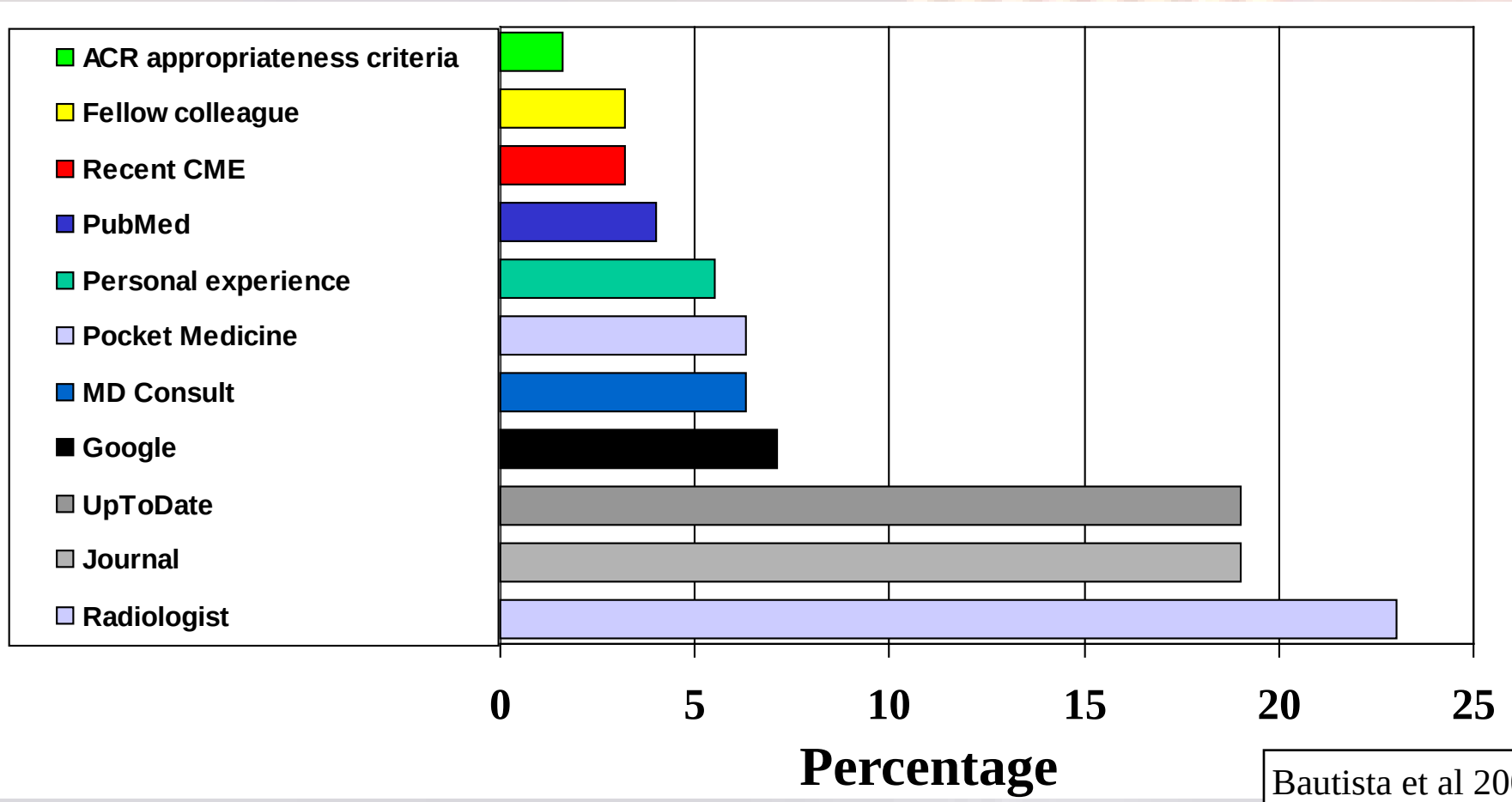

Bautista et al 2009

Radiology Decision-Support System

MGH Radiology Order Entry

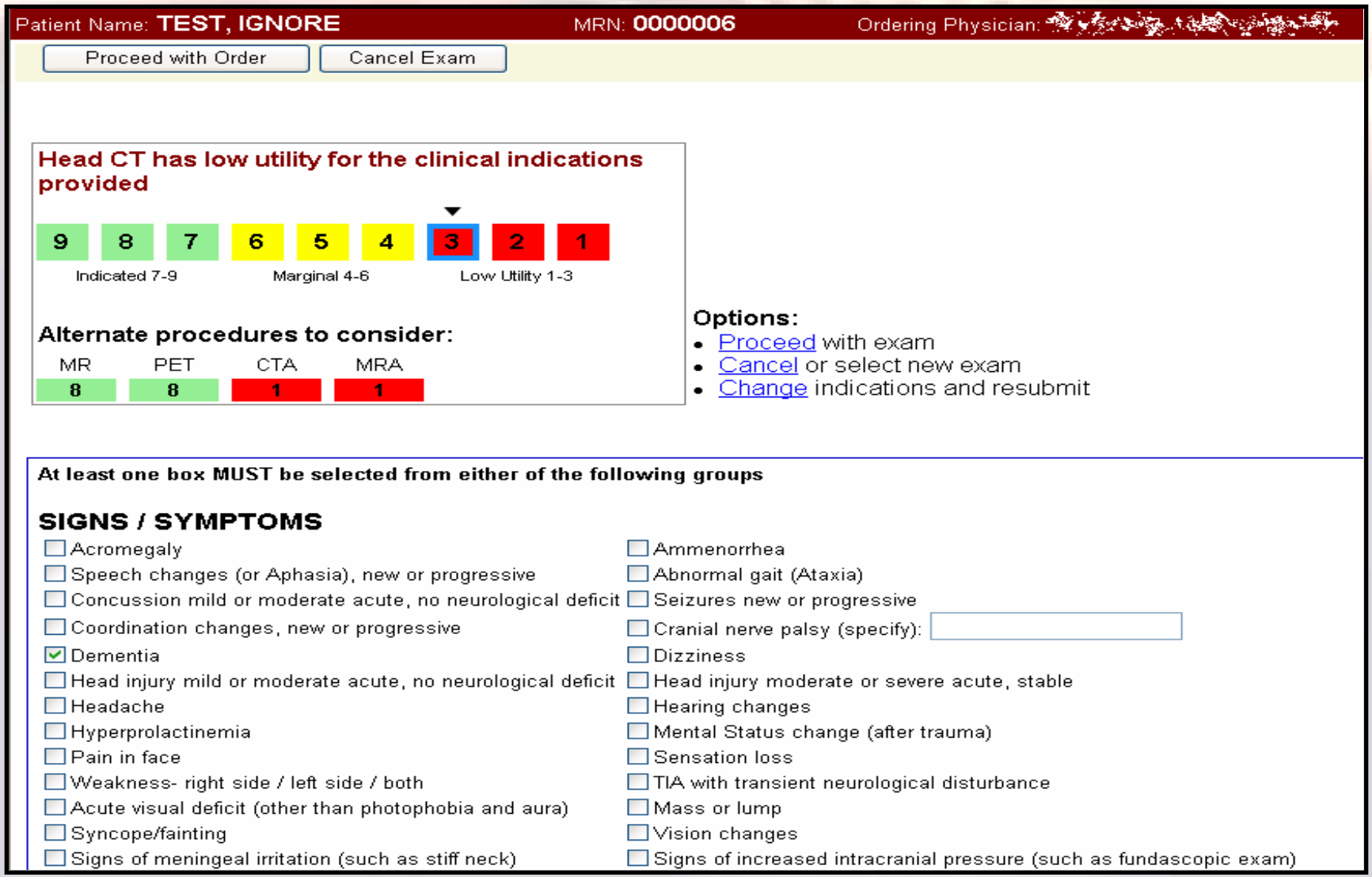

Sistrom, C. L. et al. Radiology 2009;251:147-55

Does putting decision support into order entry help?

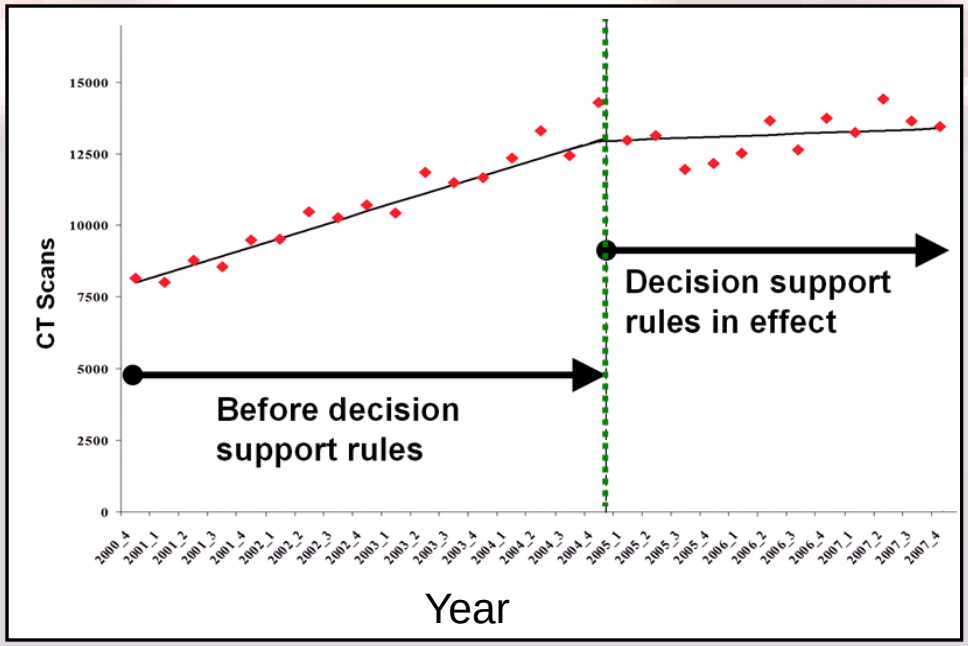

MGH outpatients

Virginia Mason, Seattle

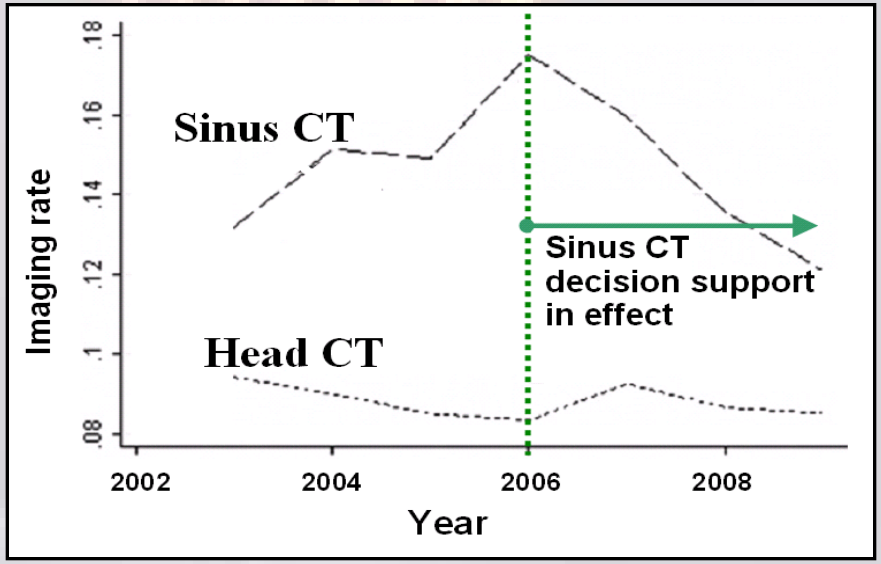

Conclusions

I: Are CT radiation risks real?

Yes

Conclusions

II. The individual risks are very small

- **When a CT scan is clinically warranted, the benefit will by far outweigh any possible individual radiation risk**

- ***(though of course we can and should continue to lower doses per scan)***

Conclusions

III. Reducing clinically unwarranted CT scans

- **The main concern is really about the population exposure from the roughly ¼ of CT scans that may not be clinically warranted**

Conclusions

IV. Reducing doses per scan is hard but doable; Reducing unwarranted CT scans is harder

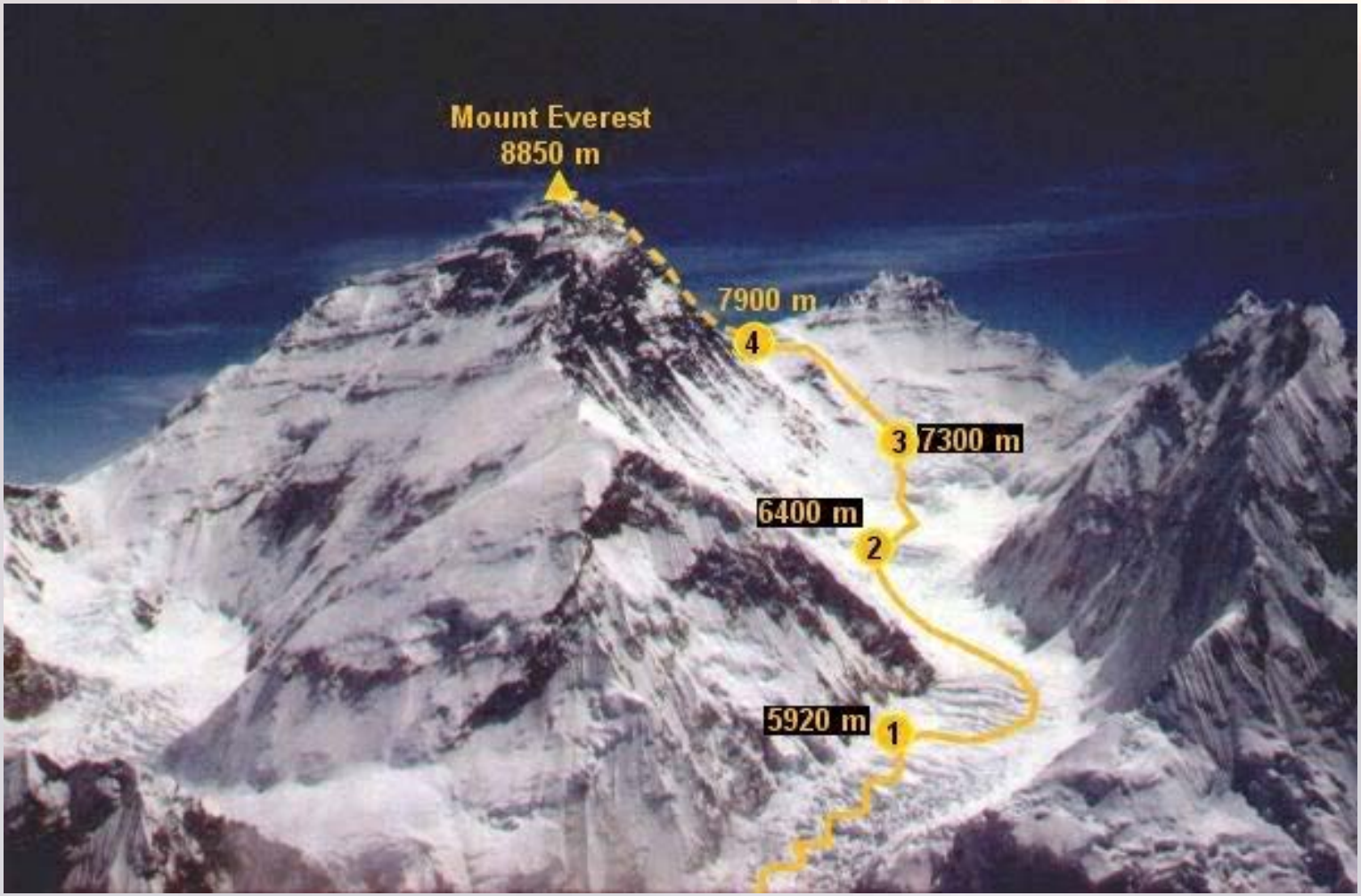

Connecticut Area Medical Physics Society (CAMPS) 2013 Summer Conference

May 14, 2013

Mattabesett Canoe Club
Middletown, CT

Advances in Robotic Brachytherapy

Yan Yu, Ph.D., MBA
Professor and Vice Chair, Director of Medical Physics

Department of Radiation Oncology, Thomas Jefferson University
Philadelphia, PA, 19107, U.S.A

May 14, 2013 AAPM CAMPS

Jefferson™ Kimmel Cancer Center
NCI-designated

Learning Objectives

1. Introduce the latest development in brachytherapy robotics.
2. Describe supporting laboratory investigations and clinical studies.
3. Outline future research directions

Conventional Prostate Seed Implant Brachytherapy

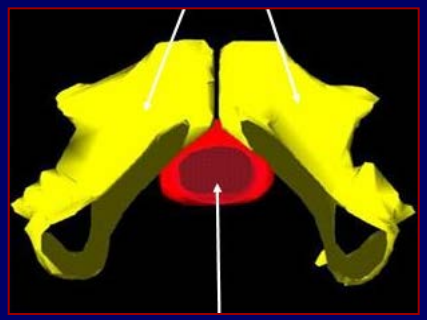

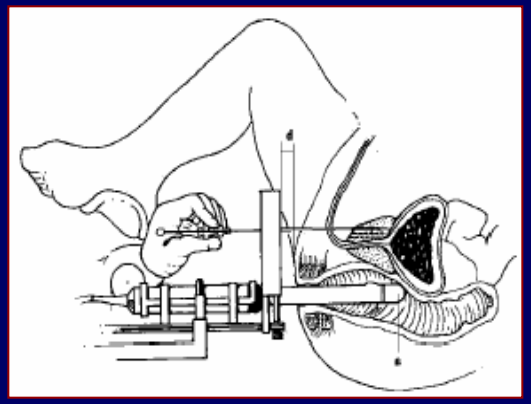

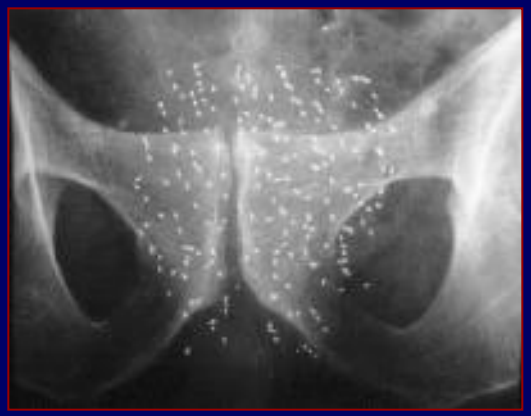

Fixed template

Needle angulation

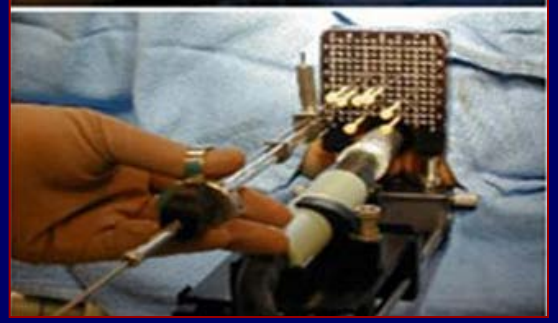

Fatigue & exposure

- Fixed template – limited maneuverability
- PAI – needle angulation difficult
- Consistency, accuracy, efficiency – techniques & human factors

Jefferson™ Kimmel Cancer Center
NCI-designated

What is a “ROBOT”?

“A robot is a reprogrammable multi-functional manipulator designed to move materials, parts, tools, or specialized devices, through variable programmed motions for performance of a variety of tasks.”

Jefferson™ Kimmel Cancer Center
NCI-designated

ROBOTs

Industrial robots

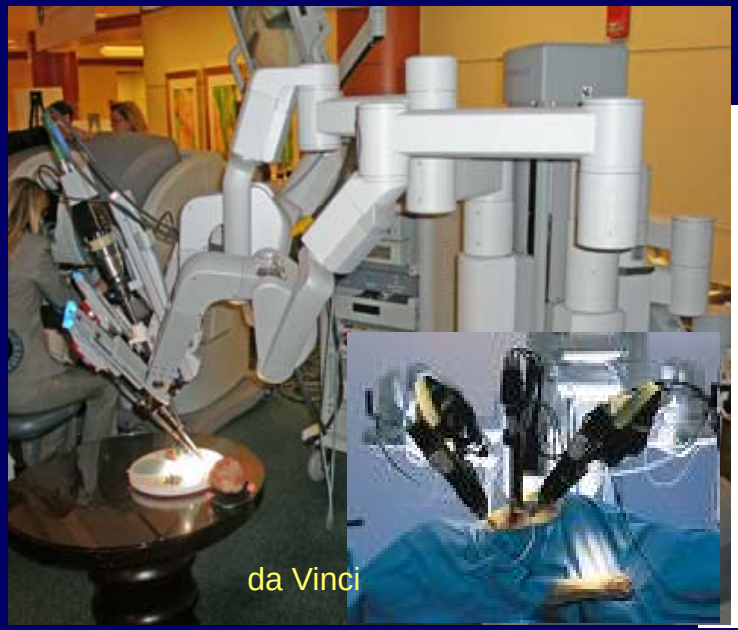

da Vinci

KUKA robot
(cyberknife)

Medical robots

Jefferson™
Kimmel Cancer Center
NCI-designated

Robotic IGBT System

IGBT: Image-Guided BrachyTherapy

Objectives:

- Increase accuracy and consistency of needle placement and seed delivery
- Increase avoidance of critical structures (urethra, pubic bone, rectum, etc.)
- Detect tissue heterogeneities and deformation via force sensing and imaging feedback
- Update dosimetry after each needle is implanted
- Reduce tediousness and assist clinicians
- Reduce trauma and edema
- Reduce radiation exposure
- Reduce learning curve
- Reduce OR time

Jefferson™ Kimmel Cancer Center
NCI-designated

The EUCLIDIAN Robotic System for IGBT

- EUCLIDIAN design & development
  - Positioning Module (3DOF cart, 6DOF platform)
  - Surgery Module (2DOF US driver, 3DOF gantry, 2DOF needle driver)
    - Robot workspace
    - In vivo force-torque & motion data collection
    - Needle bucking expt.
    - Force-reduction expt.
    - Reduction of tissue deformation expt.
    - Reduction of needle bending expt.
    - Improved prostate stabilization expt.
    - Friction reduction – needle coating expt.
    - Extended Kalman Filter for needle steering simulation & expt.
- EUCLIDIAN architecture
- EUCLIDIAN software
- Dosimetric planning
- Robotic IGBT procedures
- EUCLIDIAN performance

Jefferson™ Kimmel Cancer Center NCI-designated

Functional Requirements:

- Provision for reverting to conventional manual brachytherapy method at any time
- Quick and easy disengagement in case of emergency
- Improved of prostate immobilization
- Provision for periodic quality assurance
- Provision for reviewing and approving the motion plan and seed delivery
- Ability to modulate needle velocity by automatic feedback control
- Provision for needle tracking and seed detection
- Updating implant plan at any desired time
- Steering of the needle by automatic feedback control
- Visual/haptic force feedback during needle insertion
- Teach mode to simulate force/velocity patterns of expert practitioners
- Ease of operation and safety for the patient and OR environment

Workspace in the OR

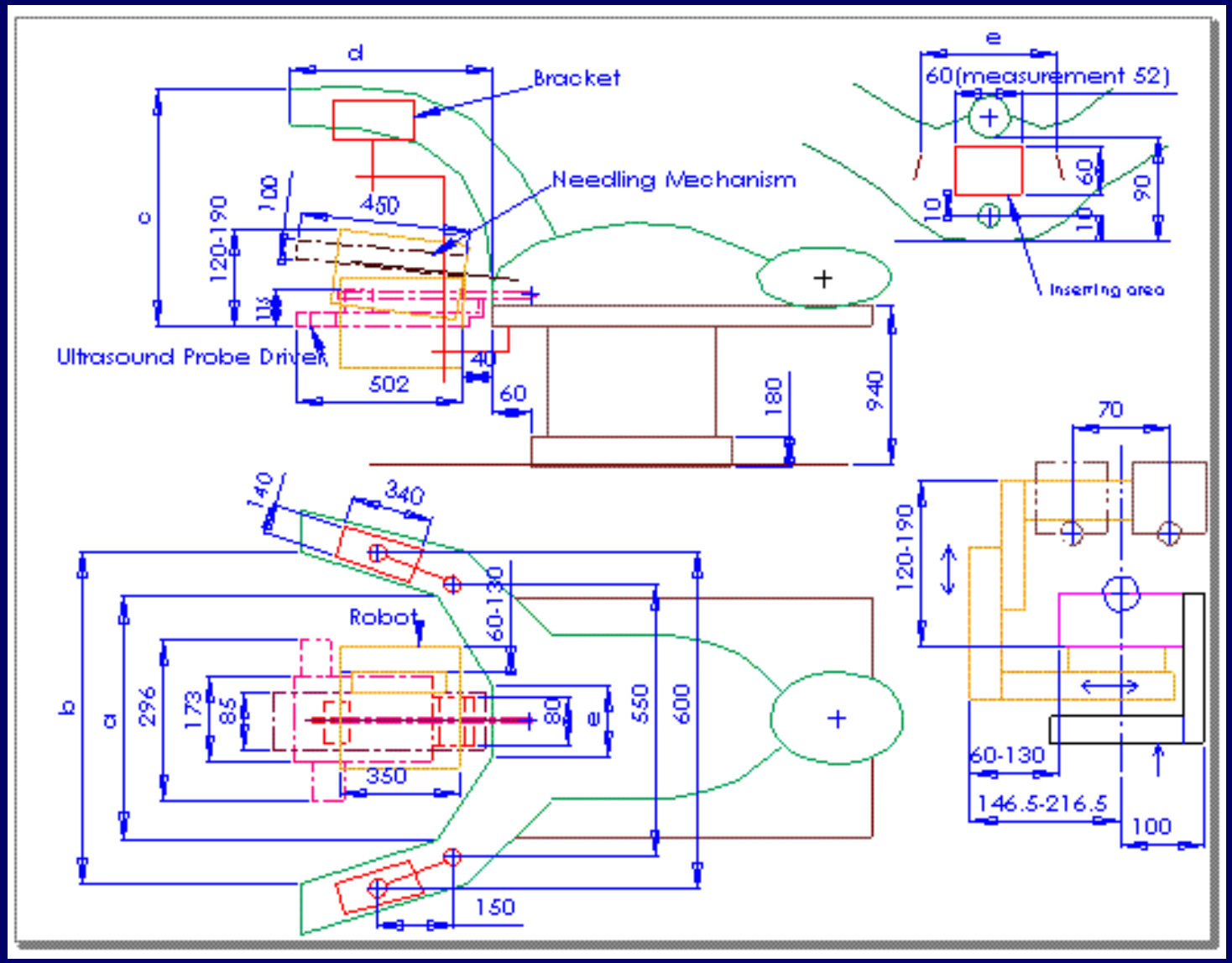

Jefferson™ Kimmel Cancer Center
NCI-designated

In Vivo Force Measurements

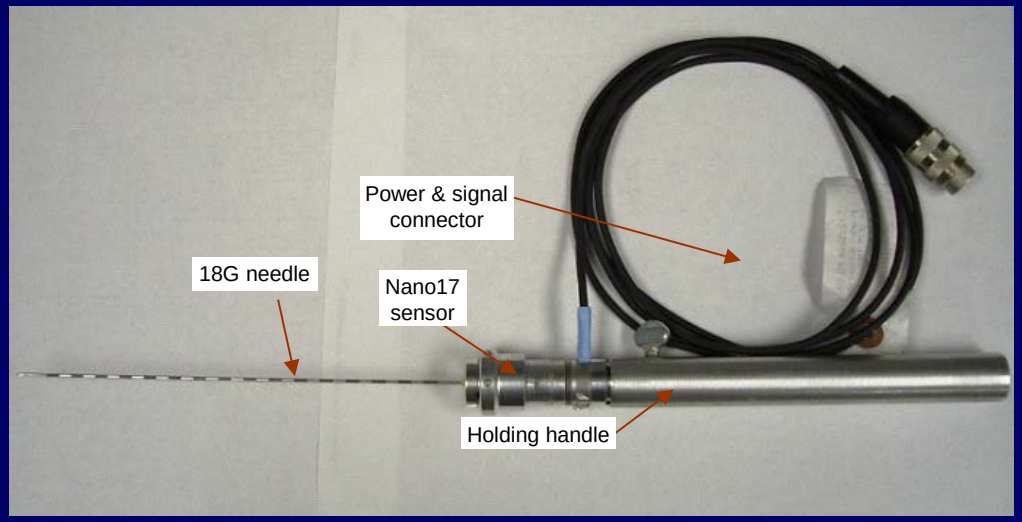

Hand-held adapter

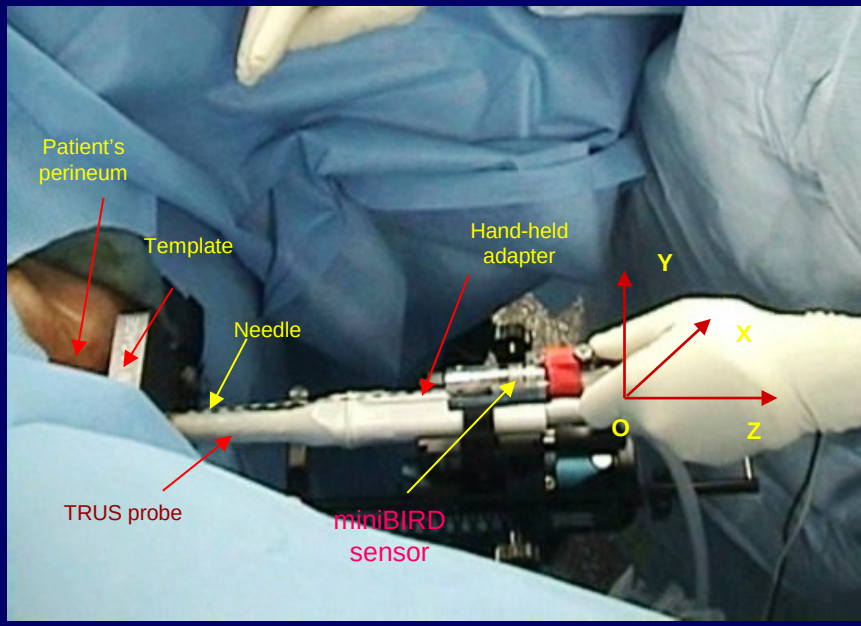

Force/torque and position data collection during actual brachytherapy procedure in the OR

Jefferson™ Kimmel Cancer Center NCI-designated

Patient #1, 17G Needle

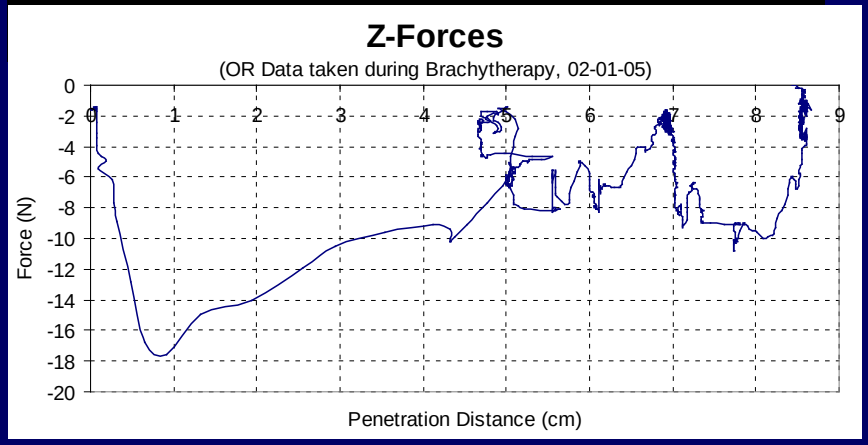

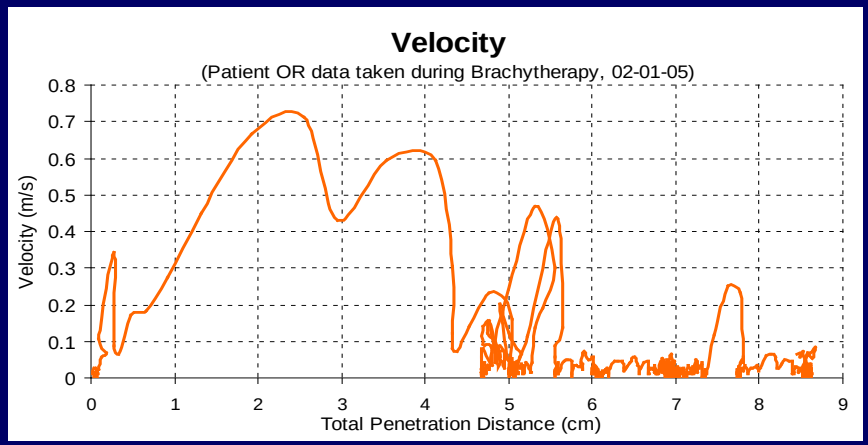

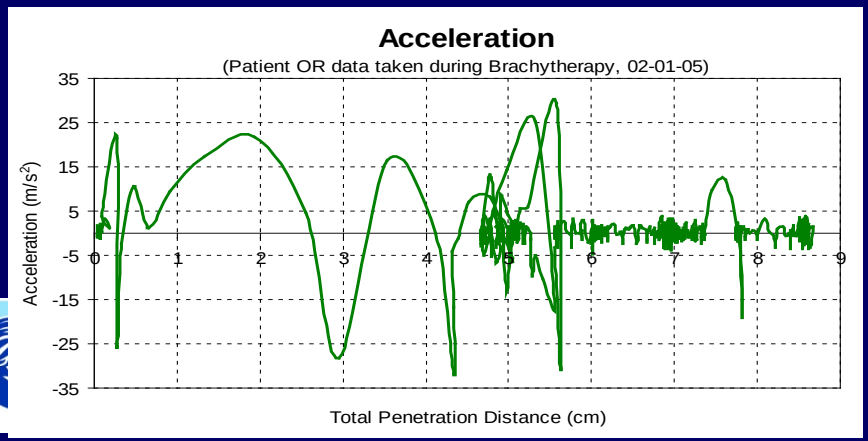

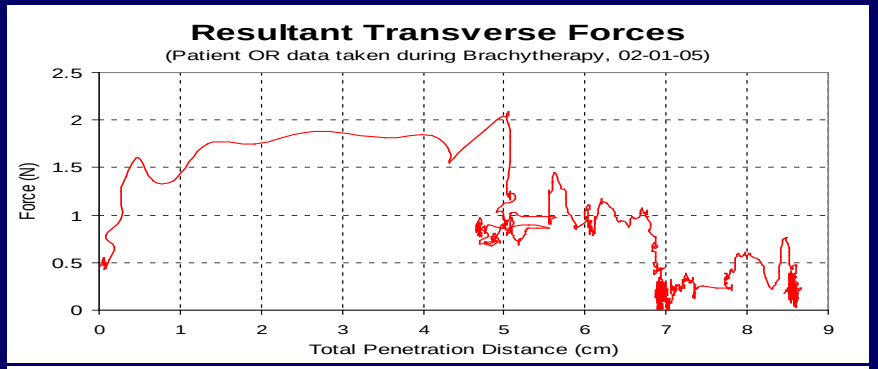

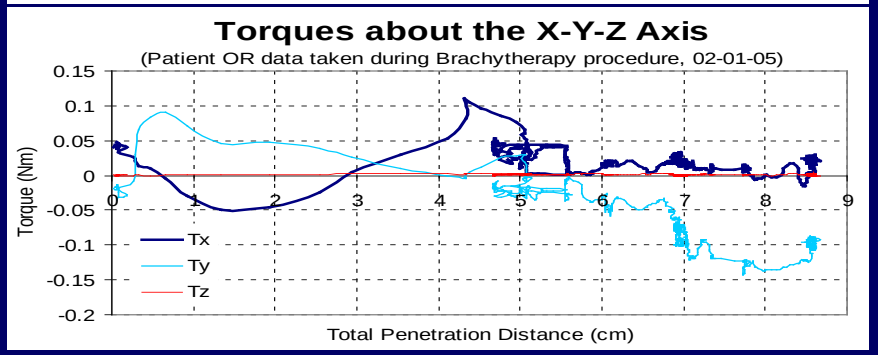

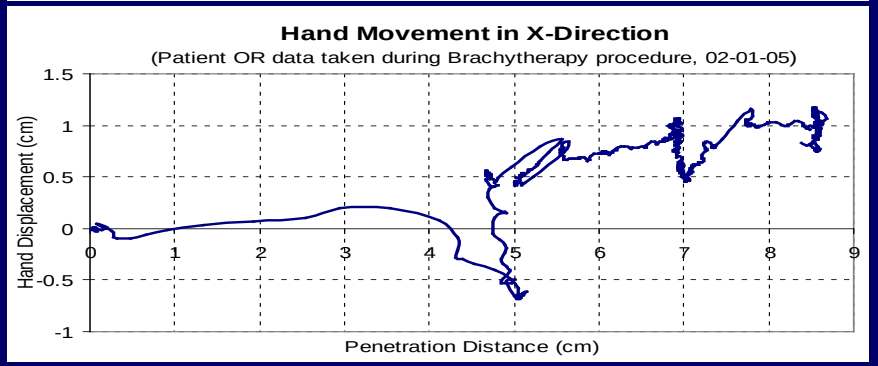

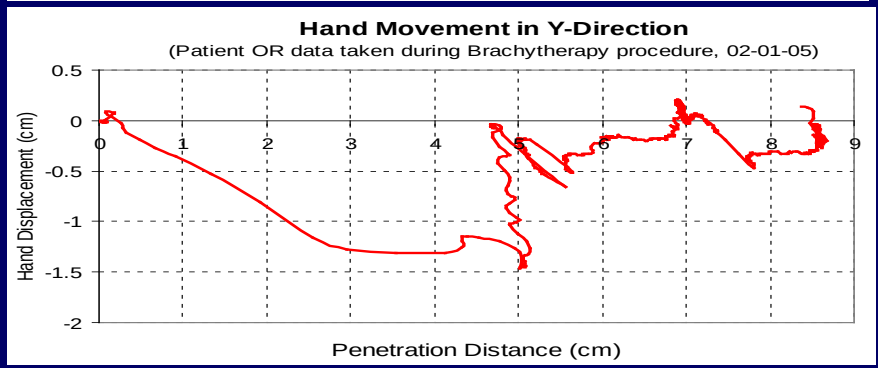

Prostate Deformation

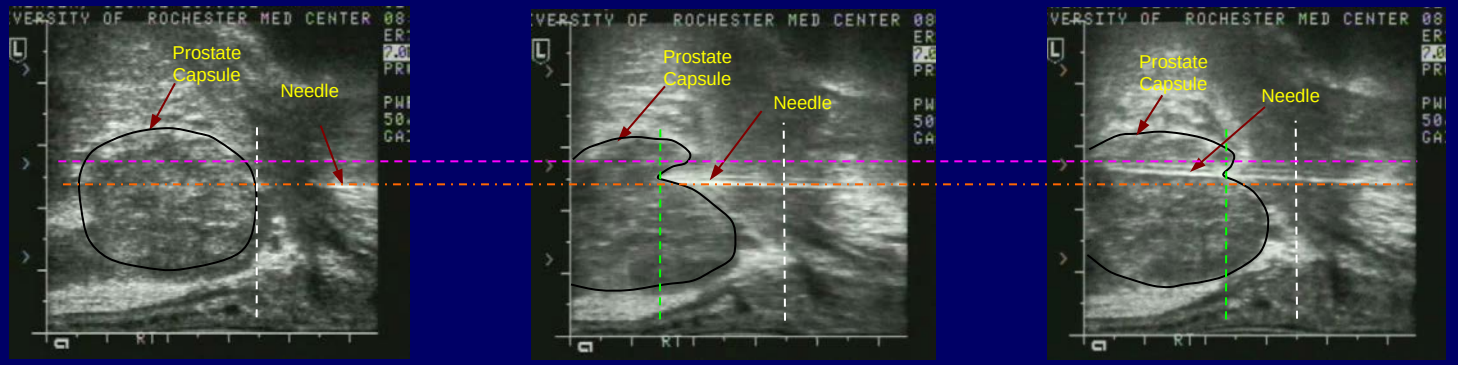

(a) Prior to capsule puncture

(b) During capsule puncture

(c) After full insertion

Video

Jefferson™ Kimmel Cancer Center
NCI-designated

Force & Target Deflection

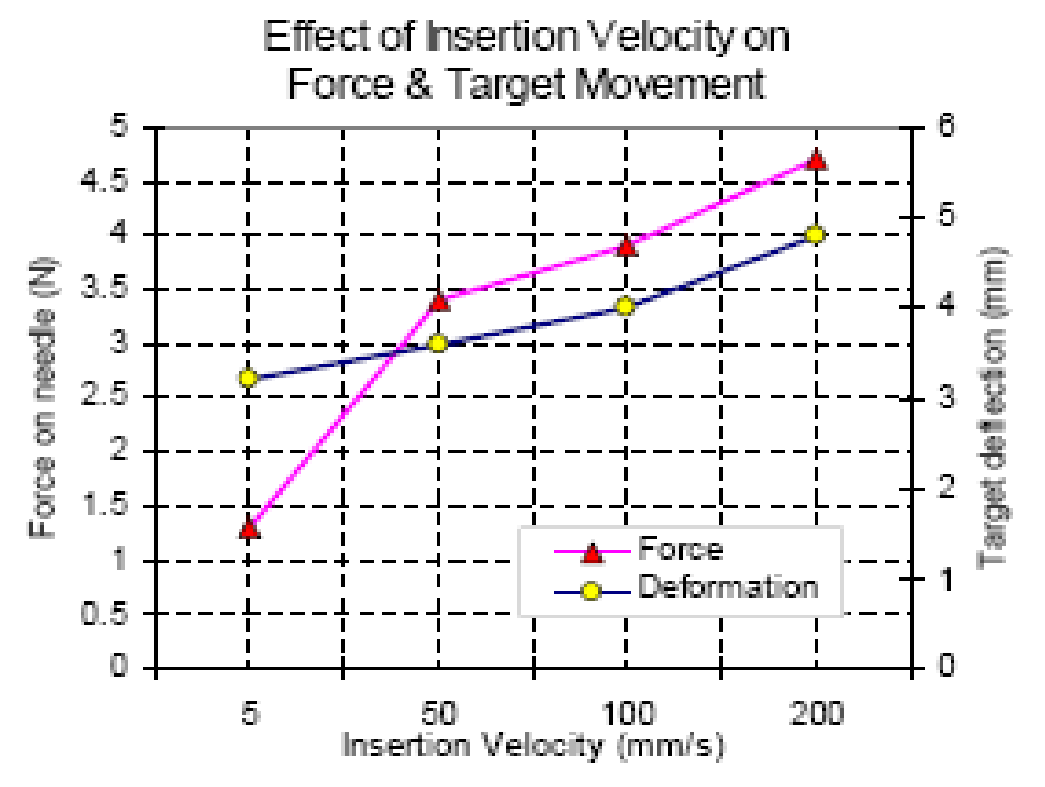

Jefferson™ Kimmel Cancer Center
NCI-designated

Rotational Velocity Modulation

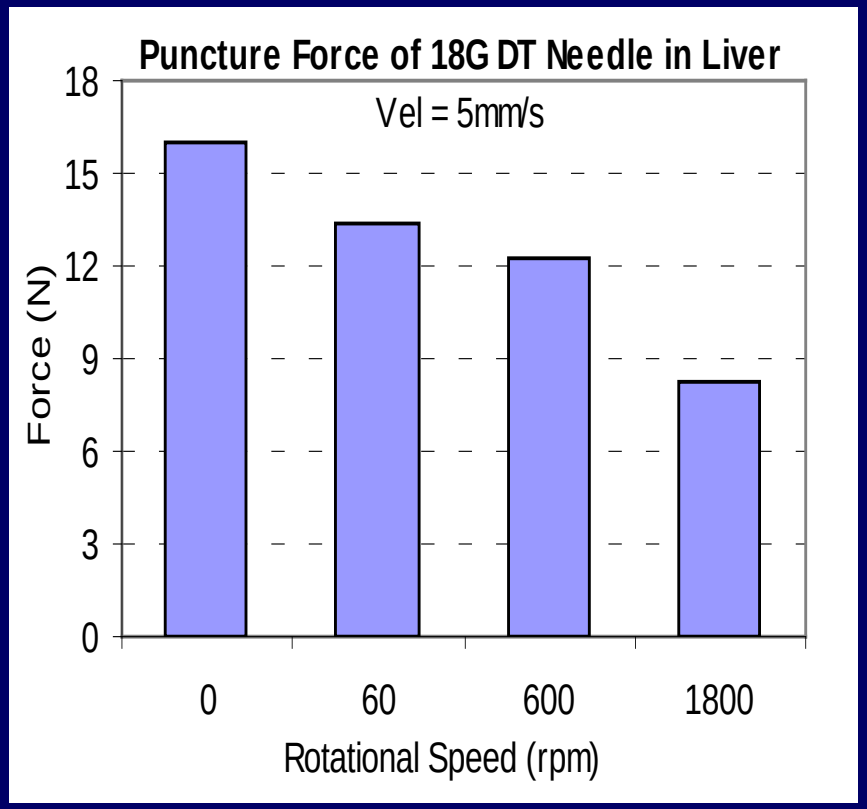

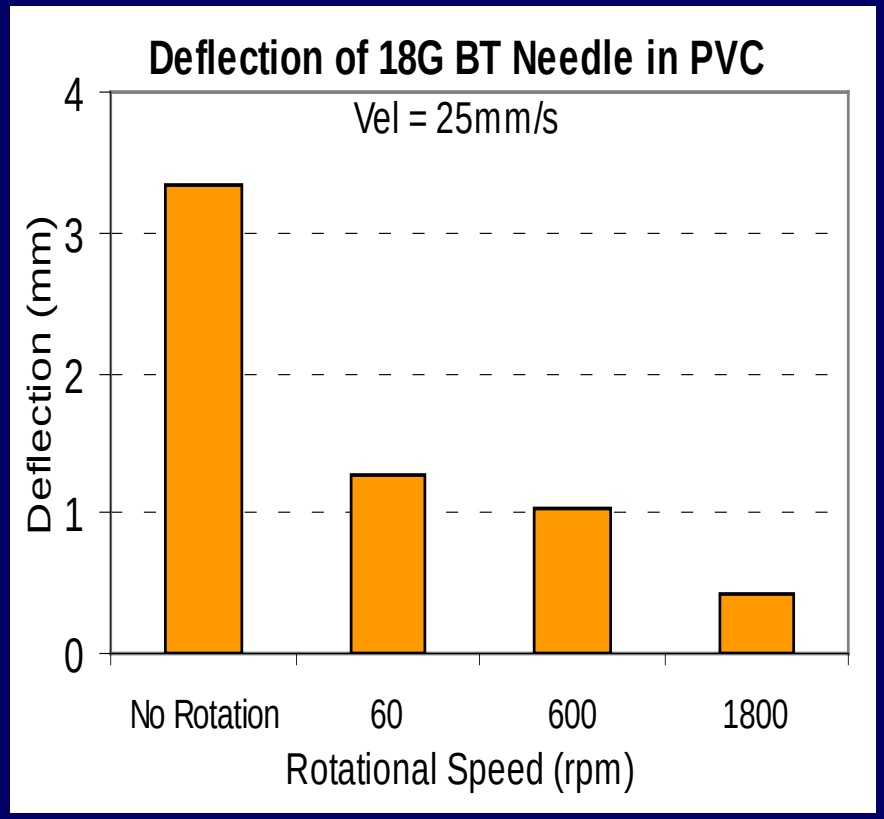

Jefferson™ Kimmel Cancer Center
NCI-designated

Robot Components for Brachytherapy

Hardware:

- Linkage/ mechanism
- Motors/ actuators
- Encoders/ sensors
- TRUS (CT, MR)
- Image acquisition board
- Industrial computer
- Power supply, amplifier

Software:

- Patient information handling
- Image acquisition
- Delineation of anatomic structures
- Dosimetric planning
- Needle tracking, seed detection
- Motion control and coordination
- 2D-3D visualization
- Position, velocity, force feedback

EUCLIDIAN OVERVIEW

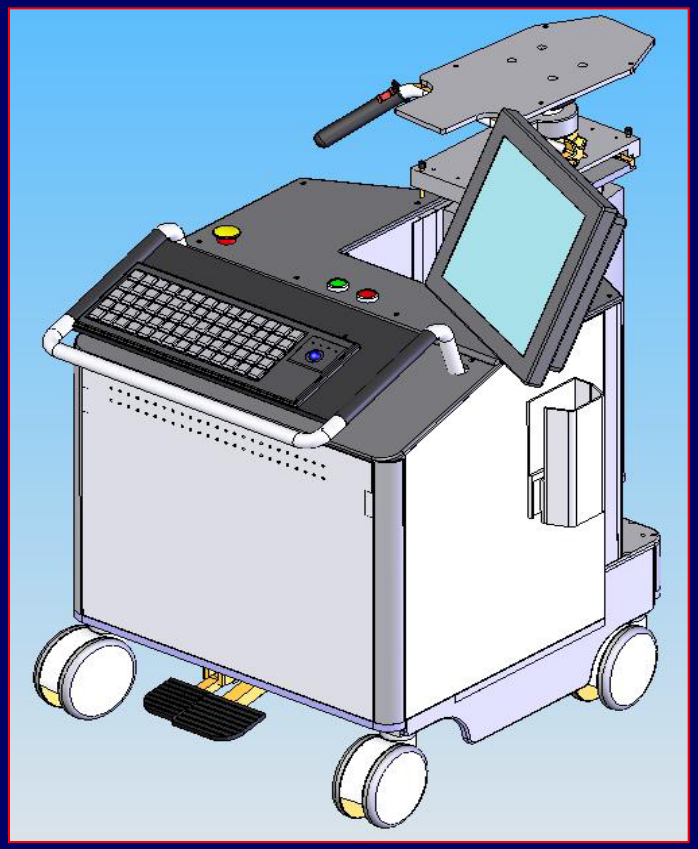

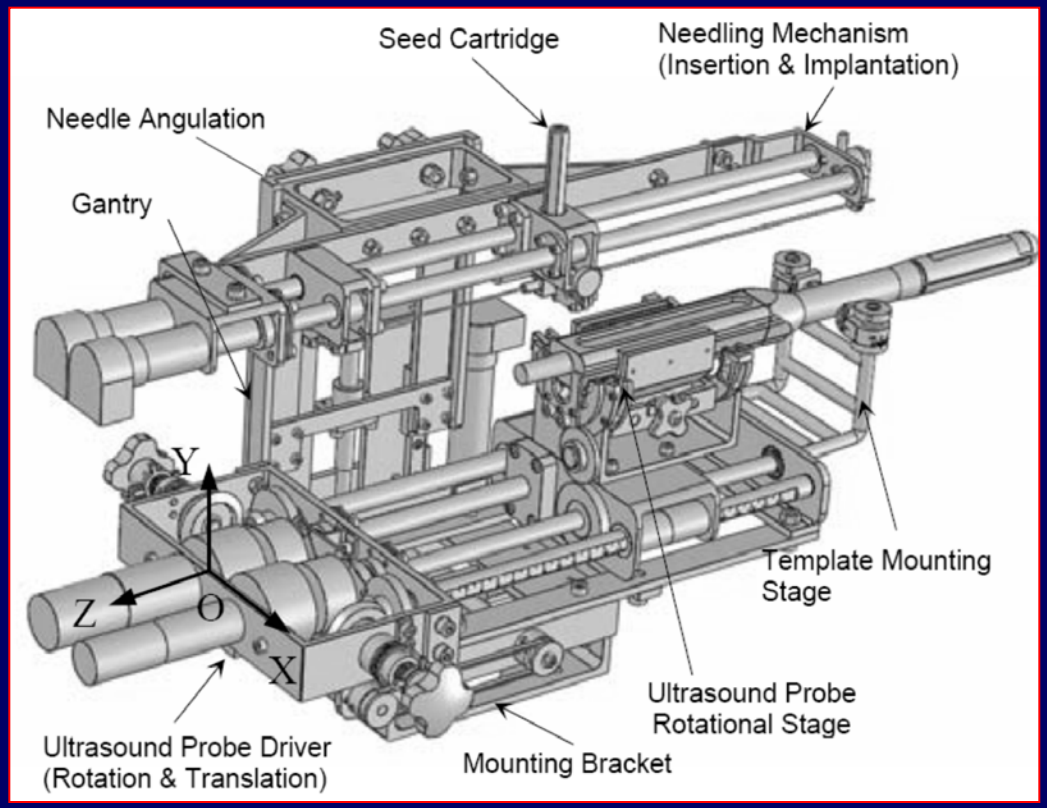

Jefferson™
Kimmel Cancer Center
NCI-designated

7 DOF Surgery Module

6DOF Supporting Platform

3 DOF Cart

Surgery Module

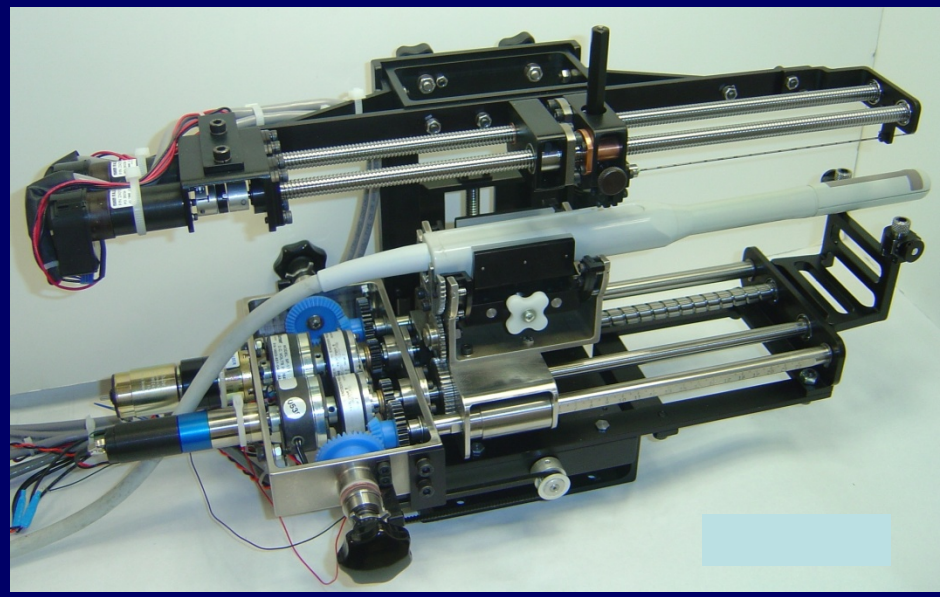

Jefferson™ Kimmel Cancer Center
NCI-designated

EUCLIDIAN in OR Setup

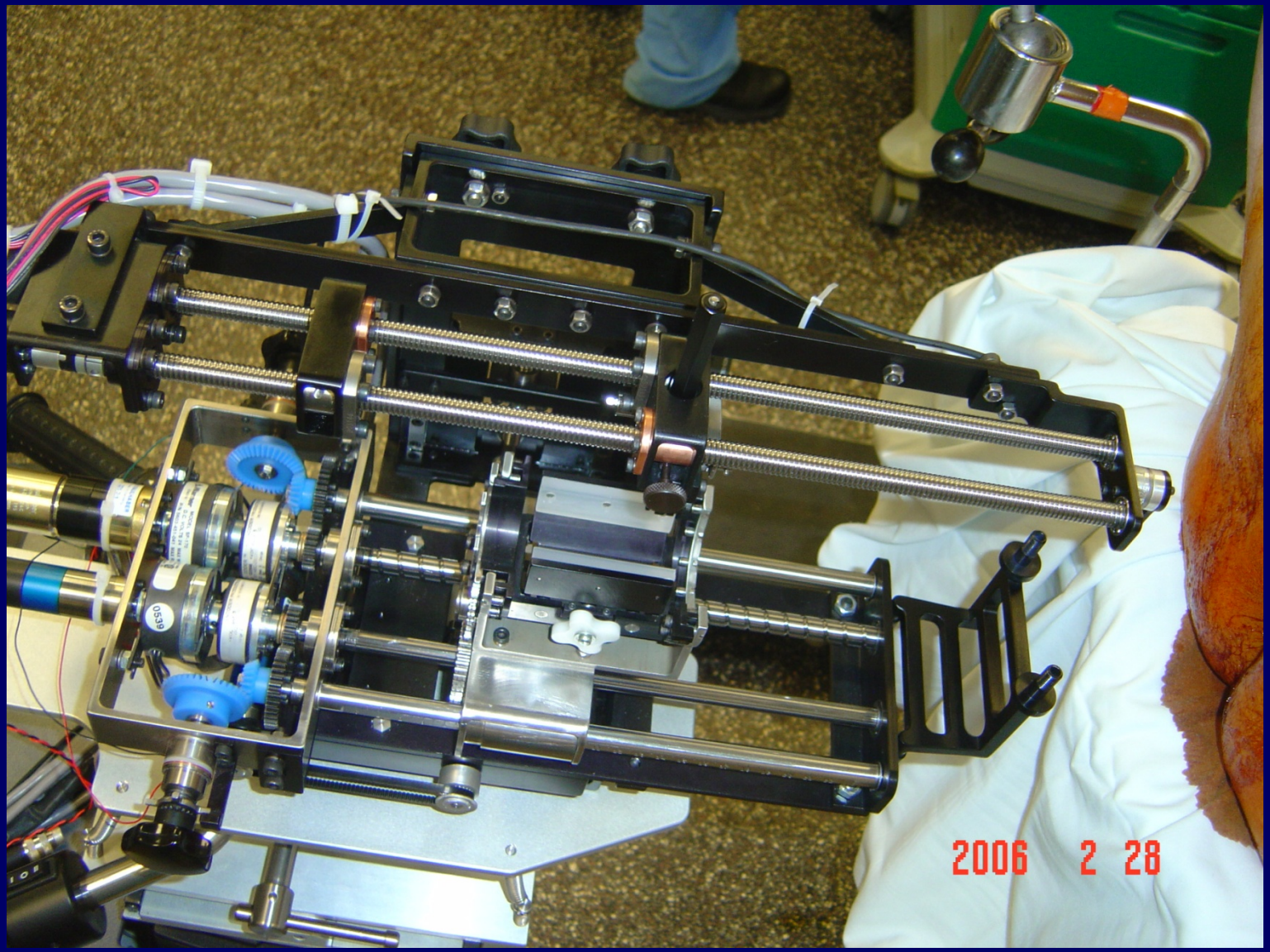

Jefferson™
Kimmel Cancer Center
NCI-designated

EUCLIDIAN - US Probe Driver

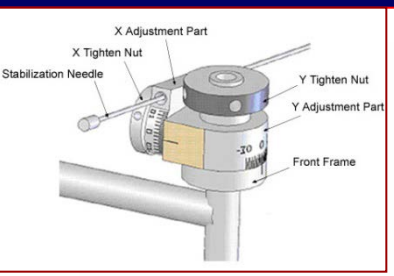

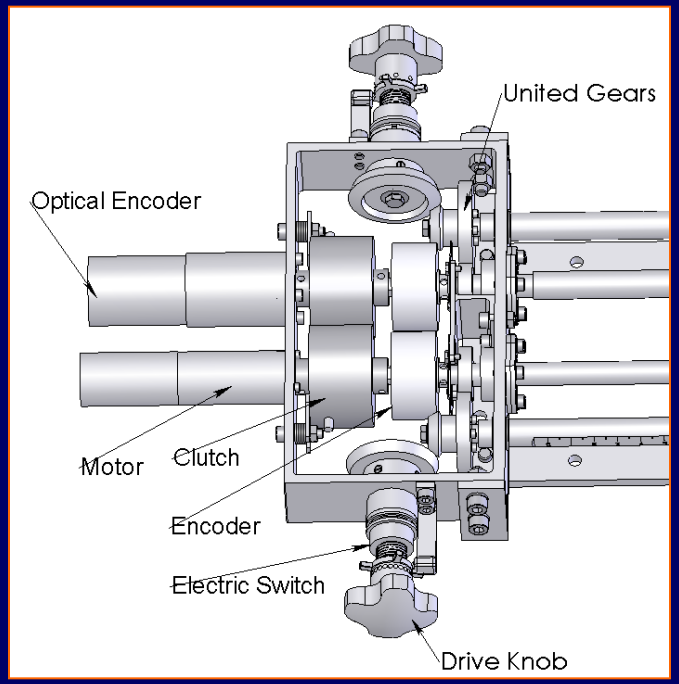

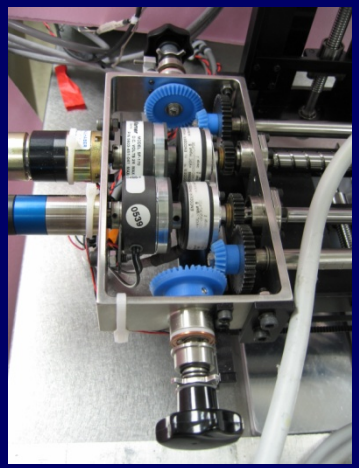

- Decoupled translation & rotation
- Motorized as well as manual
- Improved stabilization
- Provision for conventional method

Jefferson™ Kimmel Cancer Center
NCI-designated

EUCLIDIAN – Needle Insertion & Seed Delivery

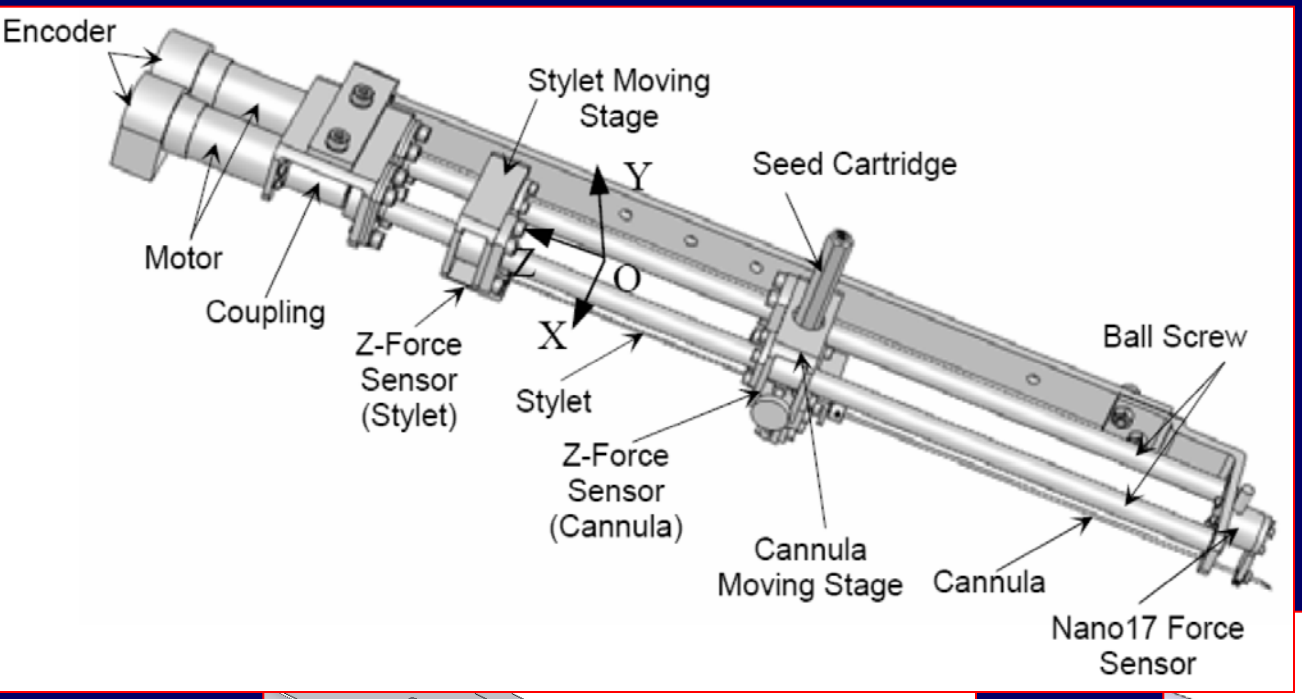

- 3 motorized motion
- Optical encoders
- Positive drive
- Cannula rotation
- 3 Force sensors
- Sterilizable seed passage

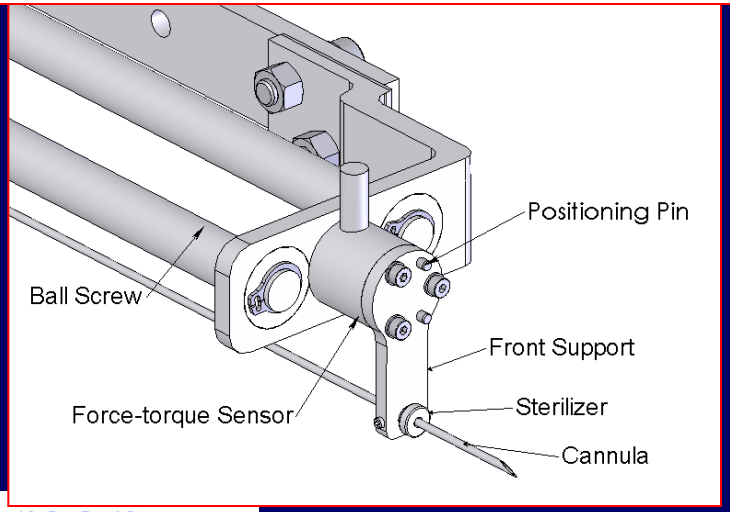

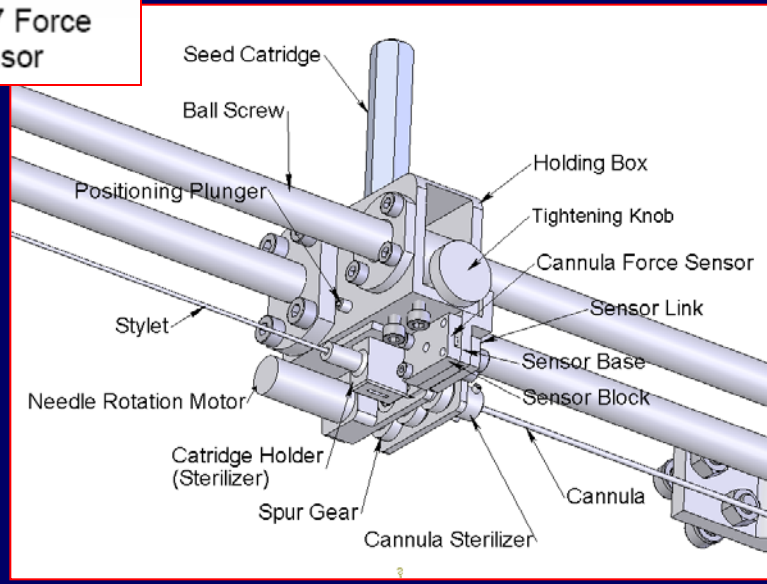

Jefferson™ Kimmel Cancer Center
NCI-designated

EUCLIDIAN – Gantry Robot

- Motorized x & y motion
- Angulation – up & down
- Optical encoders
- Positive drive – timing belt

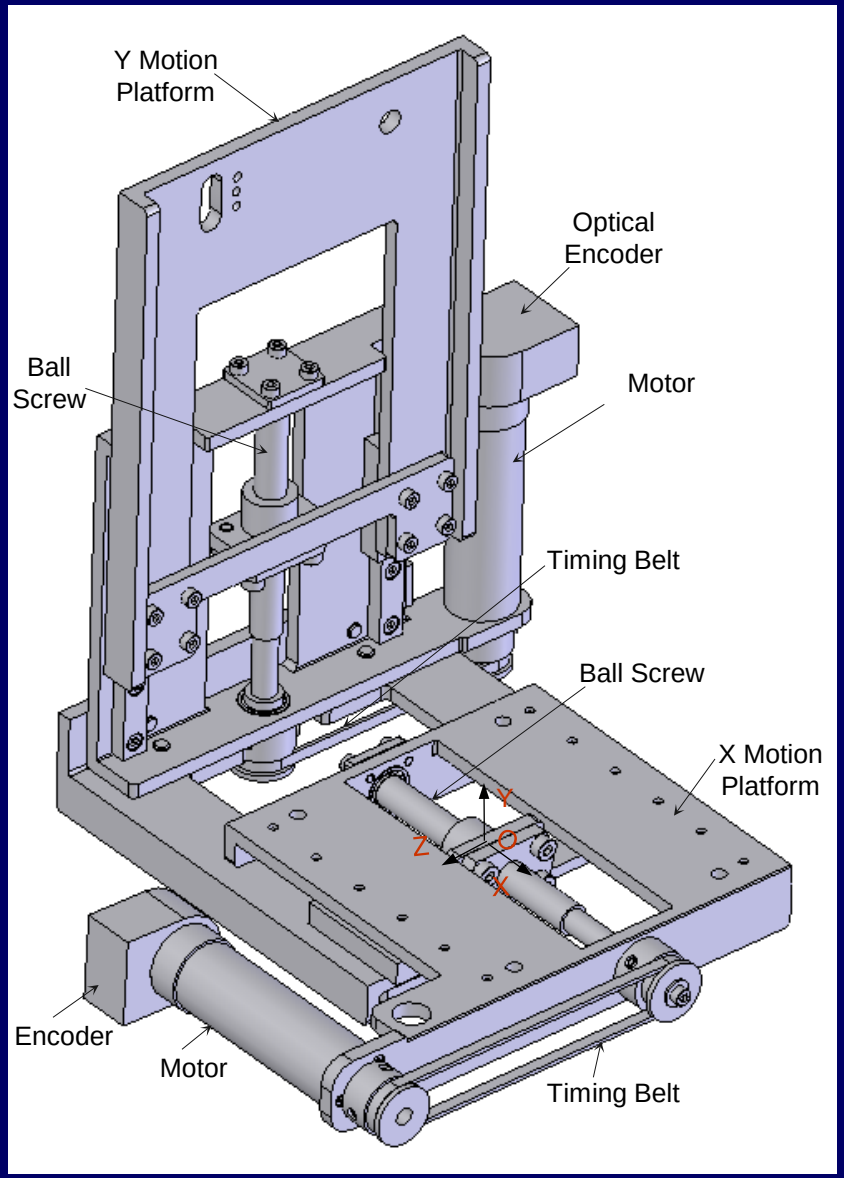

Jefferson™ Kimmel Cancer Center
NCI-designated

EUCLIDIAN Software

Tasks:

1. Patient record handling
2. Image acquisition
3. Model building (prostate, urethra, pubic bone, rectum)
4. Dose distribution planning
5. 3D visualization
6. Real-time monitoring
7. Loop back to #2, 3 or 4 if requested by user

EUCLIDIAN Software

- Tasks:
  - Patient record handling
  - Image acquisition
  - Model building (prostate, urethra, pubic bone, rectum)
  - Dose distribution planning
  - 3D visualization
  - Real-time monitoring

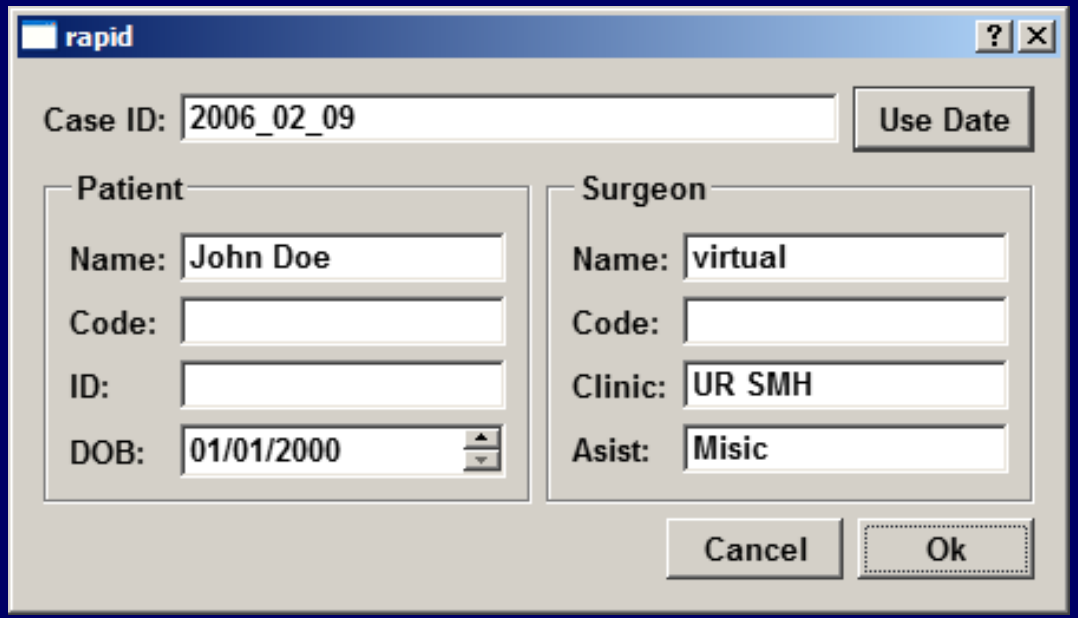

Jefferson™ Kimmel Cancer Center
NCI-designated

EUCLIDIAN Software

- Tasks:
  - Patient record handling
  - Image acquisition
  - Model building (prostate, urethra, pubic bone, rectum)
  - Dose distribution planning
  - 3D visualization
  - Real-time monitoring

- Transverse, para-sagittal, and coronal views of the compounded volume
- Seamless spline interpolation
- Depends on surgeon experience

EUCLIDIAN Software

- Tasks:
  - Patient record handling
  - Image acquisition
  - Model building (prostate, urethra, pubic bone, rectum)
  - Dose distribution planning
  - 3D visualization
  - Real-time monitoring

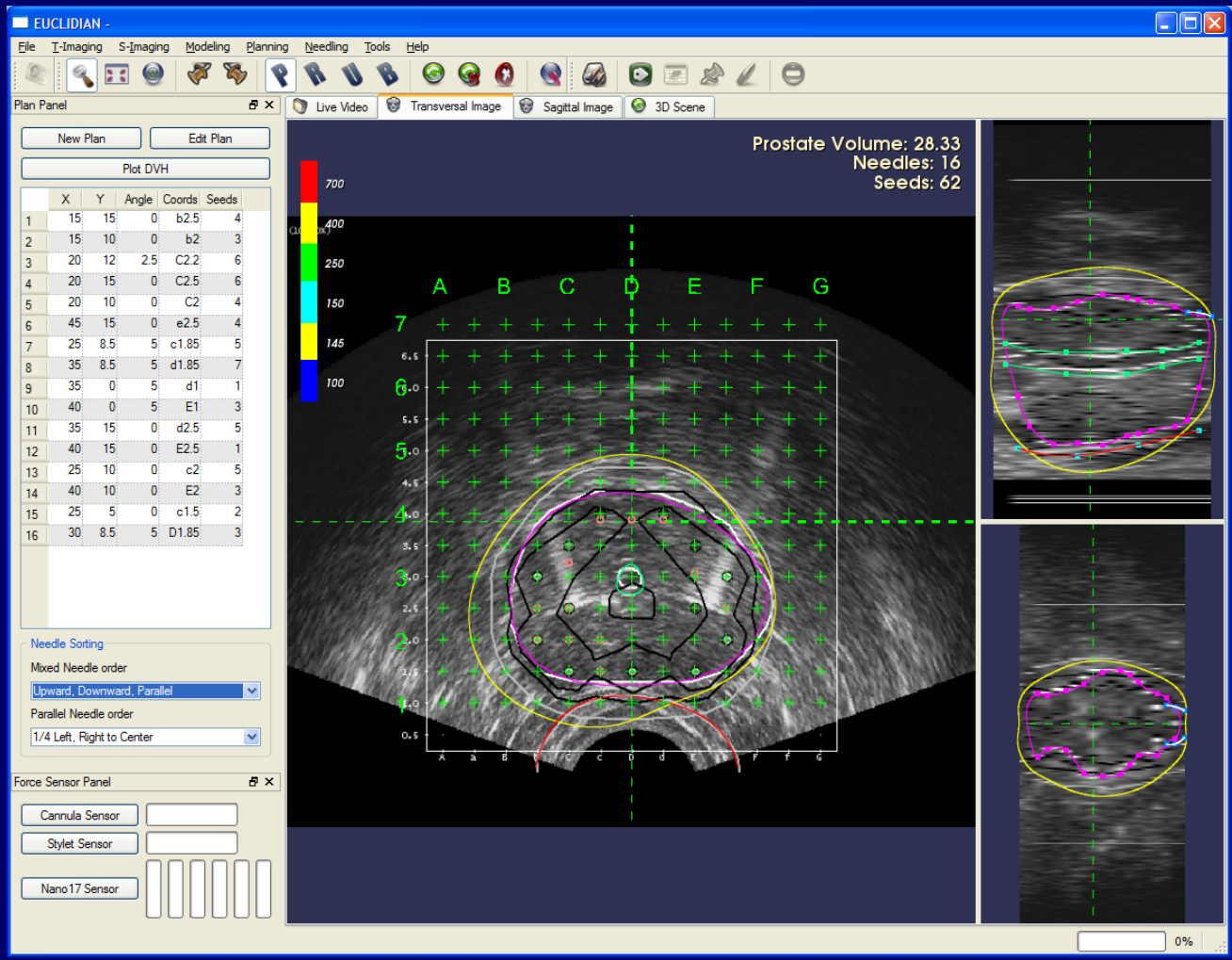

Jefferson™ Kimmel Cancer Center
NCI-designated

EUCLIDIAN Software

- Tasks:
  - Patient record handling
  - Image acquisition
  - Model building (prostate, urethra, pubic bone, rectum)
  - Dose distribution planning
  - 3D visualization
  - Real-time monitoring

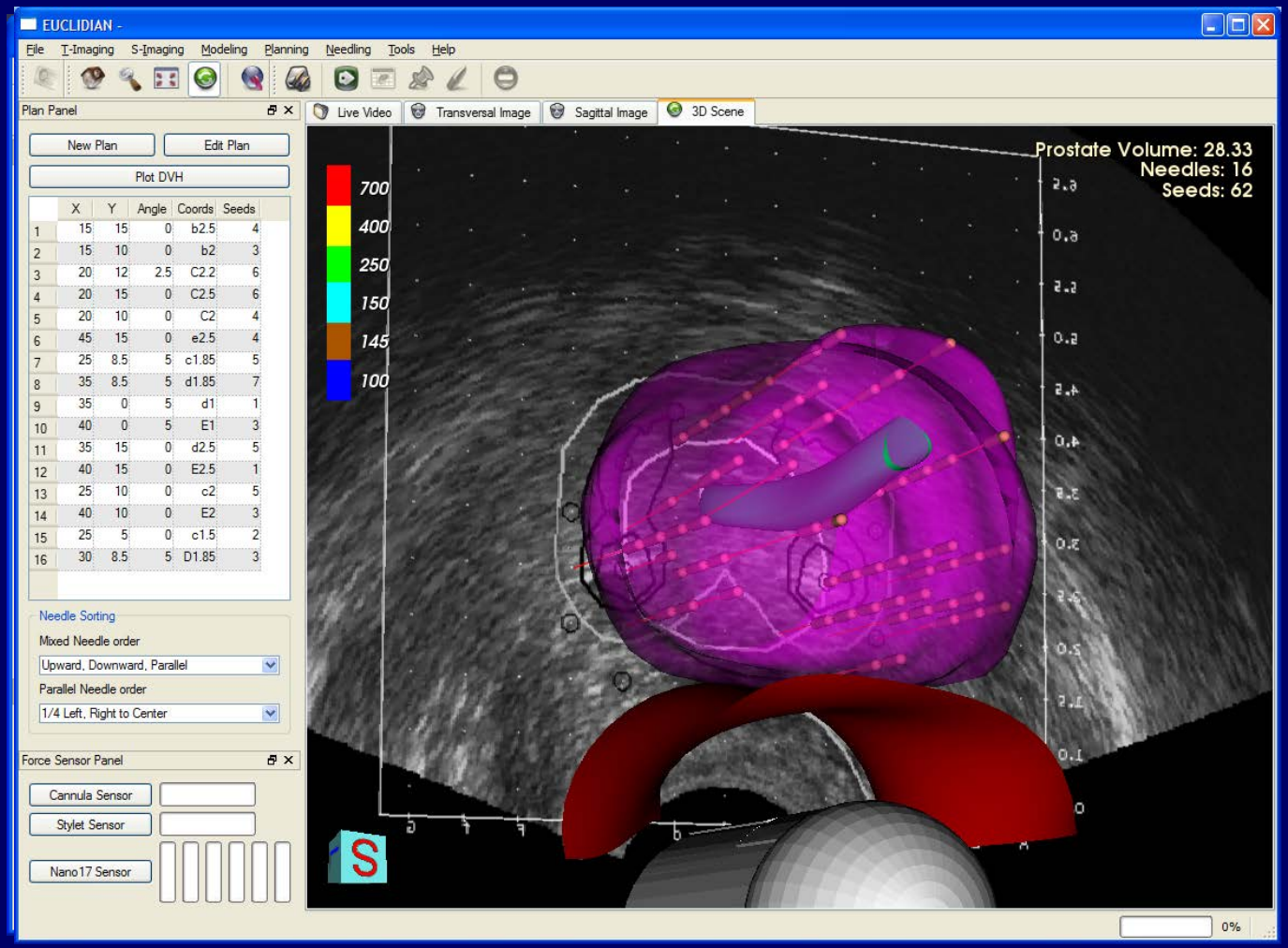

EUCLIDIAN Software

- Tasks:
  - Patient record handling
  - Image acquisition
  - Model building (prostate, urethra, pubic bone, rectum)
  - Dose distribution planning
  - 3D visualization
  - Real-time monitoring

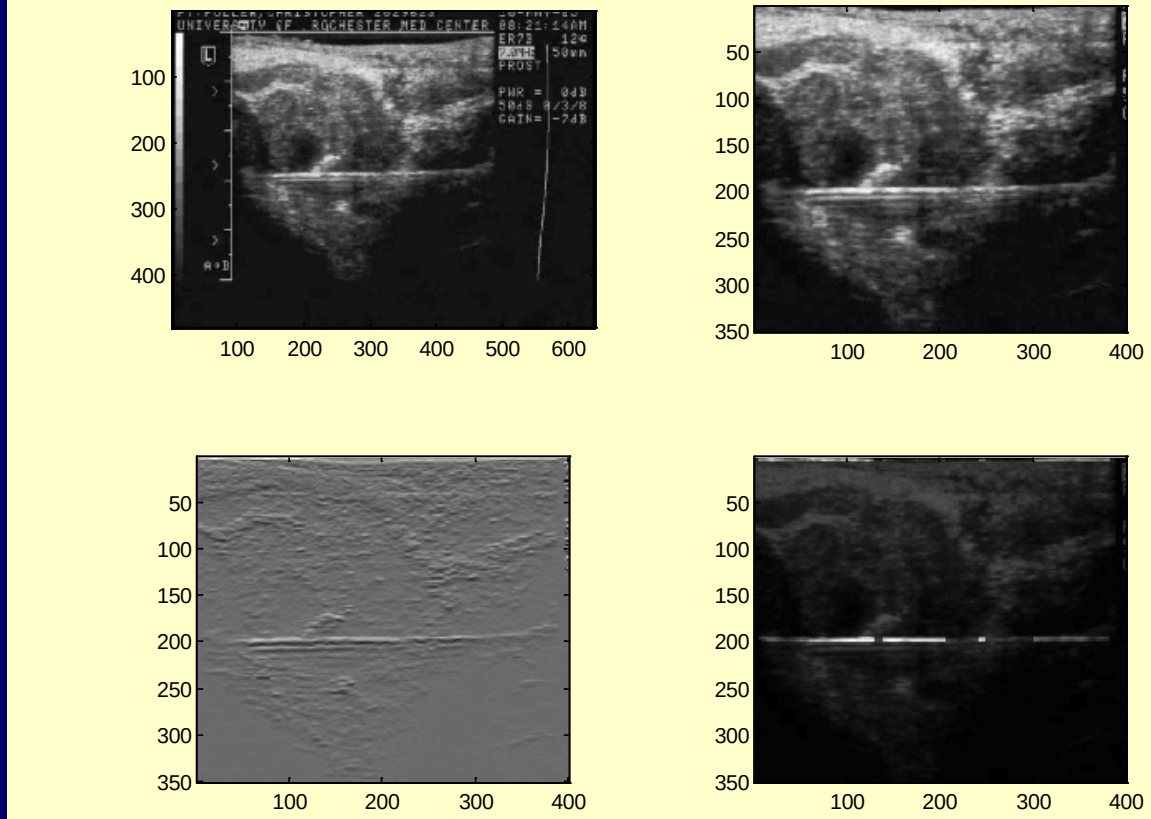

Jefferson™ Kimmel Cancer Center
NCI-designated

Kinematic calibration

Kinematic calibration determines

1)**System resolution** - the smallest incremental movement that the robot can physically perform

2)**Repeatability** - a measure of the ability of the robot to move back to the same position and orientation

3)**Accuracy** - the robot's ability to precisely move to a desired position in 3D space.

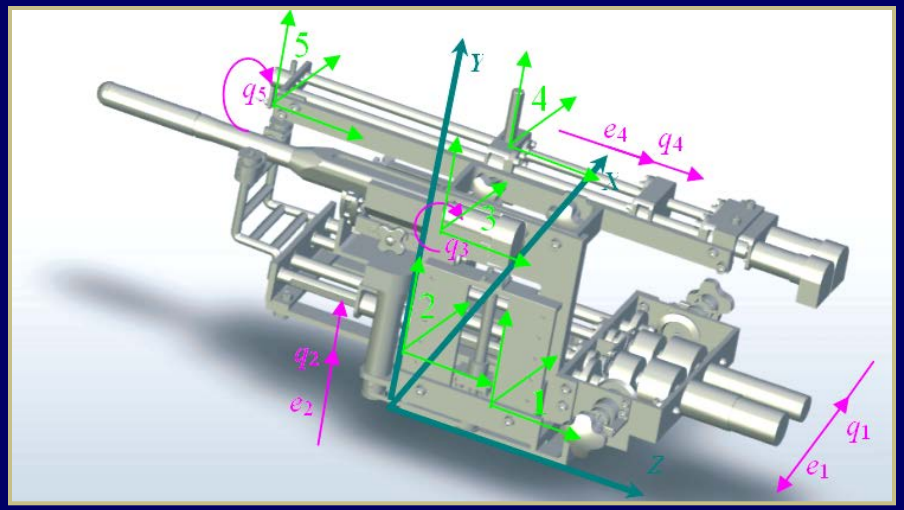

Generalized coordinates for Needling module

Jefferson™ Kimmel Cancer Center NCI-designated

Kinematic calibration - procedure

1) DH model and table definition for robotic system,
2) Matrix transformation,
3) Definition of composite matrices
4) Direct kinematics solution,
5) Inverse kinematics solution,
6) Definition of robot initial position,
7) Calculation of position error and
8) Error correction method

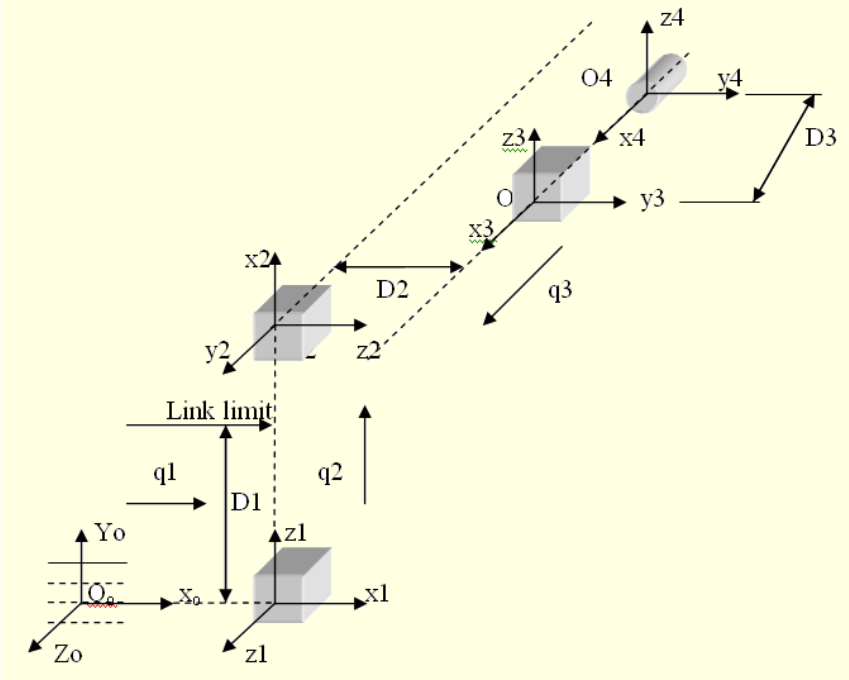

Kinematic DH calibration model

$$A = A_1 A_2 A_3 A_4 = \begin{bmatrix} 0 & \cos q_4 & -\sin q_4 & D_2 + q_1 + \delta_1 + \delta_4 \\ 0 & \sin q_4 & \cos q_4 & D_1 + q_2 + \delta_2 \\ 1 & 0 & 0 & D_3 + q_3 + \delta_3 + \delta_5 \\ 0 & 0 & 0 & 1 \end{bmatrix}$$

Real transformation matrix

$$\varepsilon = \sqrt{(p_{xid} - p_x)^2 + (p_{zid} - p_z)^2 + (p_{zid} - p_z)^2}$$

Position error

Imaging calibration

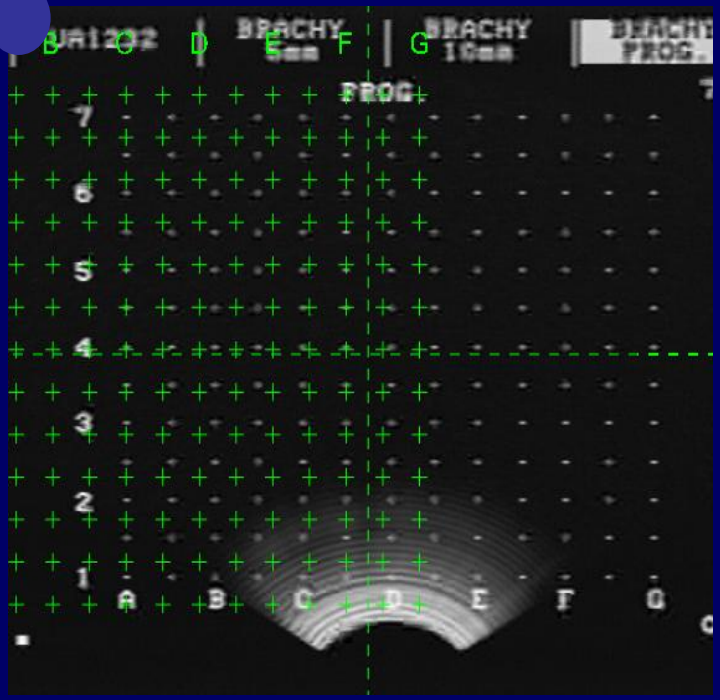

Imaging Calibration I – before image calibration

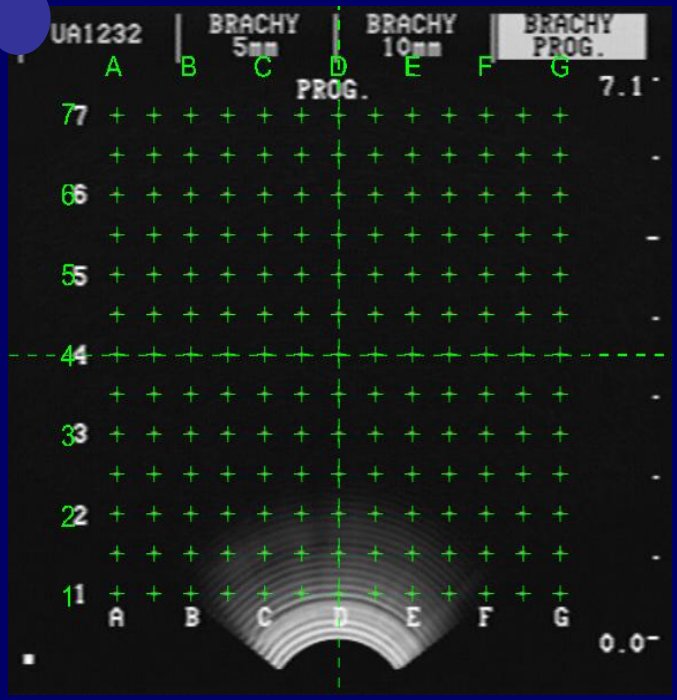

Imaging Calibration II – after image calibration

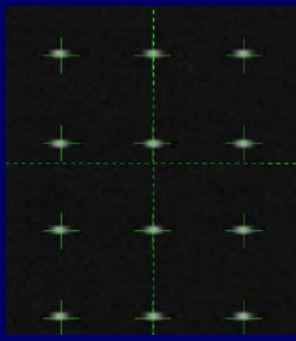

Jefferson™ Kimmel Cancer Center
NCI-designated

Mutual (overall) calibration

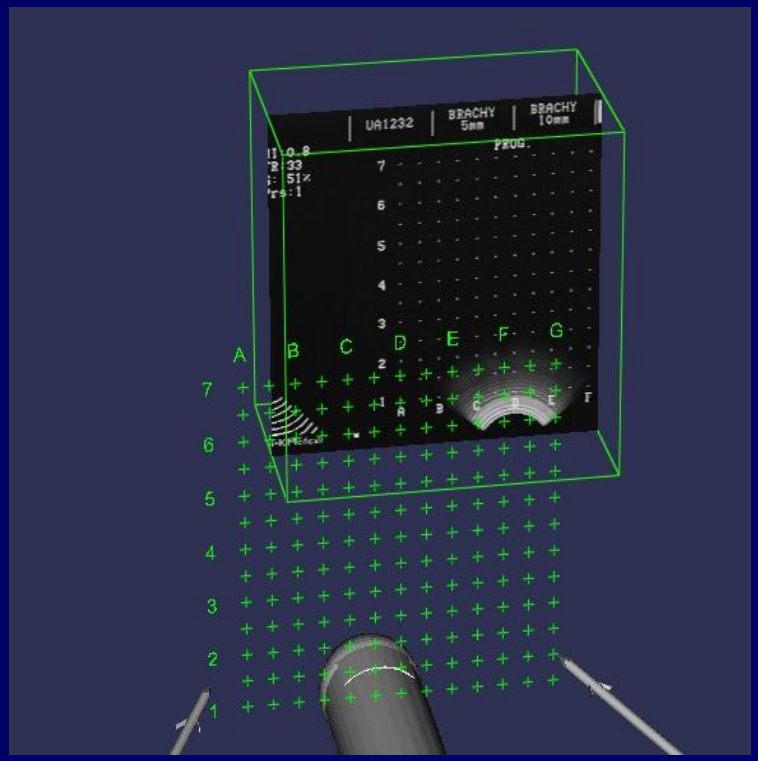

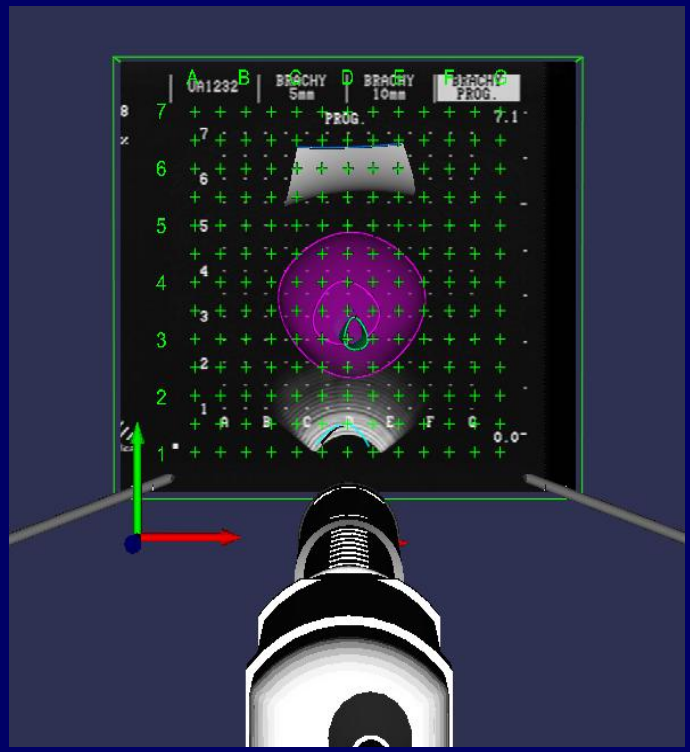

Overall Calibration I – before

Overall Calibration II – after

Jefferson™ Kimmel Cancer Center
NCI-designated

Calibration Results

Probe driver

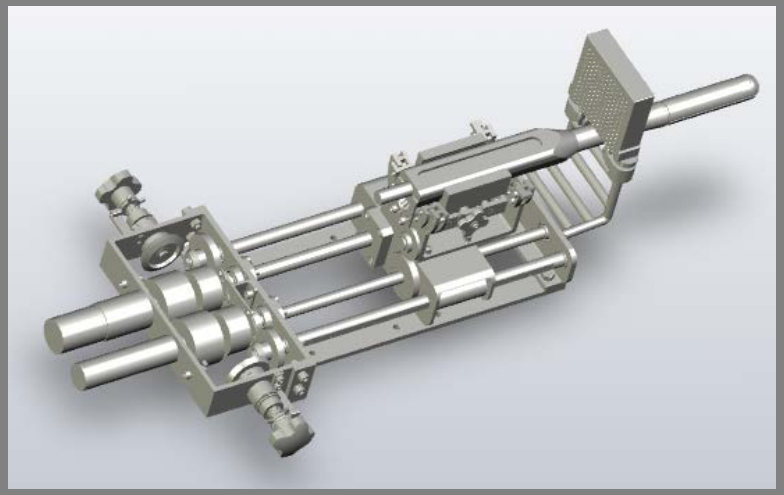

Accuracy: translation - 0.05mm
rotation - 0.1deg

	Measured value
Range	± 90 deg
Accuracy	0.1
Repeatability	± 0.03 deg

Table 1: US rotation performance

	Measured value
Parallelism	Axes Z and X
Accuracy (Z)	0.15 mm
Range (Z)	228.6 mm
Repeatability	0.03 mm
Accuracy (X)	0.05 mm
Range (X)	228.6 mm
Repeatability	0.03 mm

Table 2: US translation performance - parallelism

Jefferson™ Kimmel Cancer Center
NCI-designated

Calibration Results

Needling mechanism

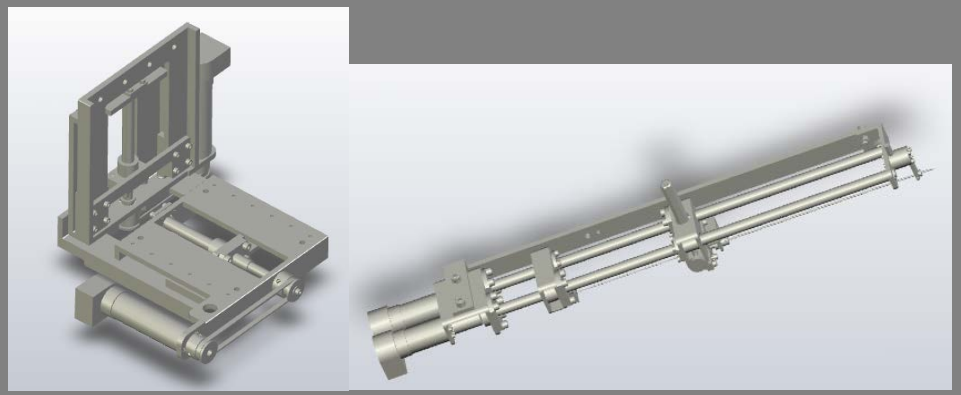

	Measured value
Parallelism	Axe Y
Accuracy (Z)	0.15 mm
Range (Z)	101.6 mm
Repeatability (Z)	0.03 mm

Table 1 Gantry vertical movement

	Measured value
Parallelism	Axes Z and X
Accuracy (Z)	0.15 mm
Range (Z)	279.4 mm
Repeatability	0.03 mm
Accuracy (X)	0.18 mm
Range (X)	279.4 mm
Repeatability	0.03 mm

Table 2: Gantry lateral movement performance

	Measured value
Accuracy	0.03 mm
Speed	± 0.01 rev/s

Table 3: Cannula rotation

	Measured value
Parallelism	Axes Z and X
Accuracy (Z)	0.15 mm
Range (Z)	279.4 mm
Repeatability	0.03 mm
Accuracy (X)	0.18 mm
Range (X)	279.4 mm
Repeatability	0.03 mm

movement performance

- ***Translation movements*** precision ***stylet and cannula*** are in the range of ***0.03-0.08mm***
- ***Lateral and vertical*** precision for ***gantry*** is 0.03mm
- The ***fiducial error*** for ***images*** is less than ***0.1mm*** in **x** and **y** image coordinates.

Jefferson™ Kimmel Cancer Center NCI-designated

Calibration Test - Seed Deposition

Assessment of the deposited seeds revealed that the accuracy (relative error) of seed placement is

0.15mm (SD=0.15mm) in x,
0.13mm (SD=0.11mm) in y
0.11mm (SD=0.11mm) in z

The 3D (Euclidean) rms error is 0.227 mm.

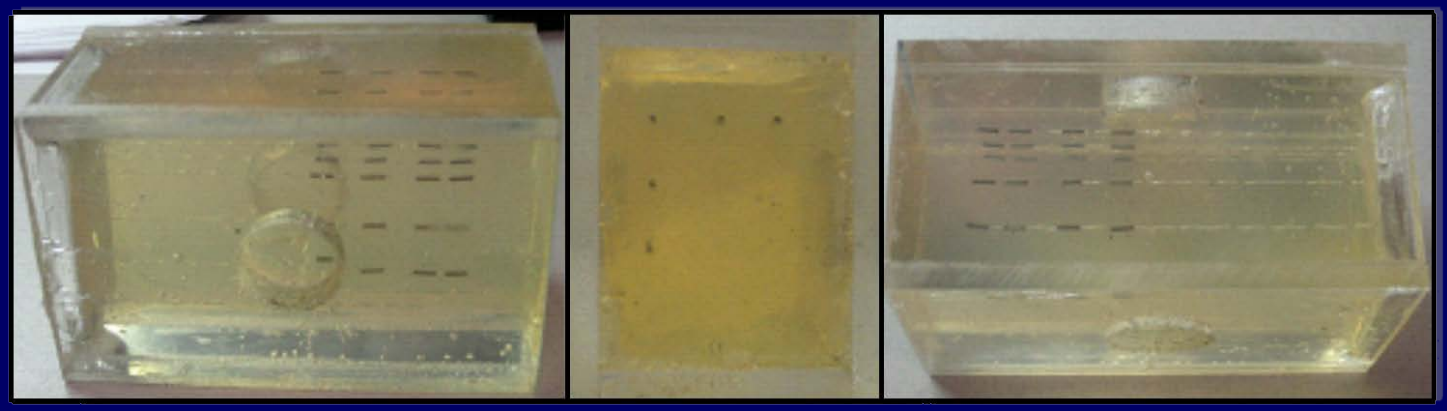

Seeds deposited into PVC phantom
(lateral, frontal and top view)

Jefferson™ Kimmel Cancer Center
NCI-designated

EUCLIDIAN Operation

Homing Procedure

Seed Delivery

Jefferson™ Kimmel Cancer Center
NCI-designated

Some pertinent features of EUCLIDIAN

- All the hardware and software are designed and developed in house
- Fully automated ultrasound-based IGBT system; however, at any time the physician can takeover the control using a teach/user-pendent
- 9dof positioning module – 3dof cart and 6dof platform motorized vertical lift (y), electro-magnetic locks on x, y and z axes, 3dof rotation has mechanical locking arrangement
- Motorized 7dof surgery module
- No physical template required
- 3 force sensors – to detect pubic arch interference (PAI), to confirm seed delivery, to detect needle deviation and bending, and potentially to sense tumor foci
- Can cover 62mm x 67mm surgical area; 10^0 angulation
- PID controller and sensor data acquisition algorithm
- Dosimetric planning, 3D visualization, needle tracking, seed detection in software
- Needle and seed passages are sterilizeable, other parts are easy to clean and decontamination
- Provision for quick manual takeover (if required)
- Preliminary results reveal seed delivery accuracy of 0.23mm

Jefferson™
Kimmel Cancer Center
NCI-designated

Multi-Channel Robotic System

MRDI (Multichannel Robot-assisted Delivery and Intervention)

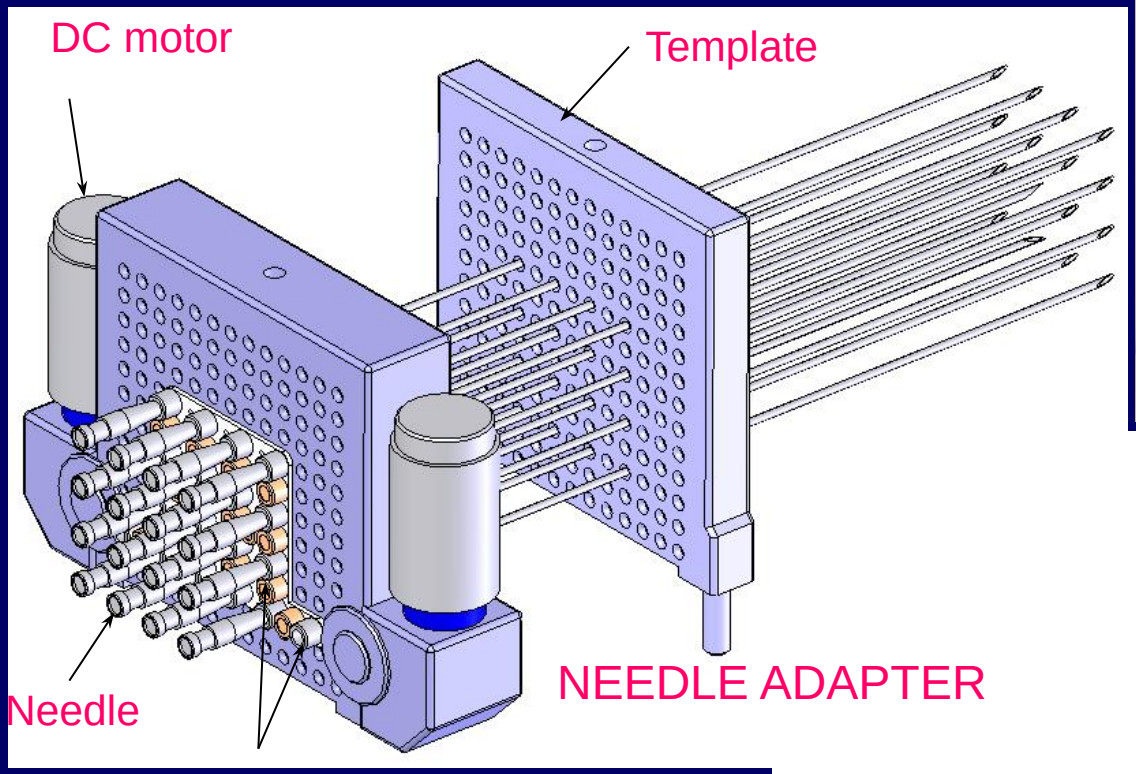

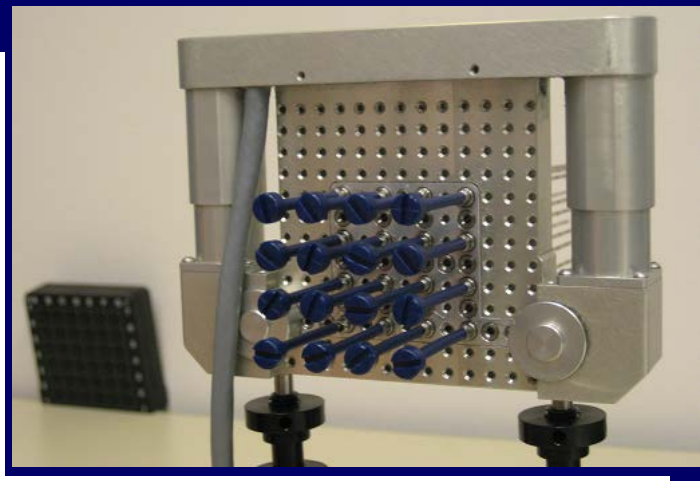

Miniature
spur gears

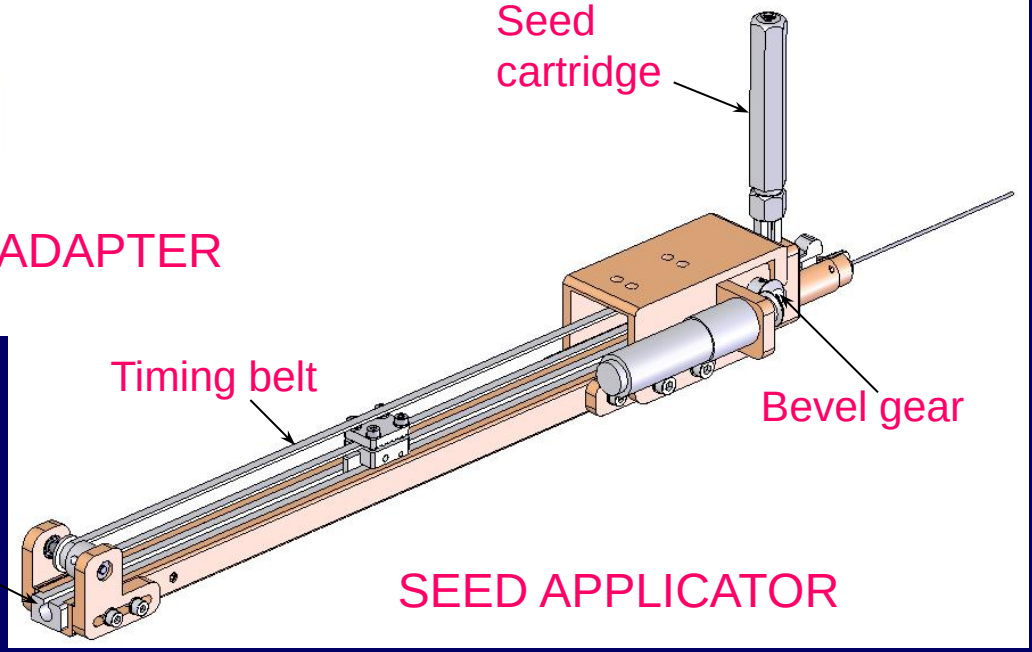

Jefferson™
Kimmel Cancer Center
NCI-designated

MRDI (Multichannel Robot-assisted Delivery and Intervention)

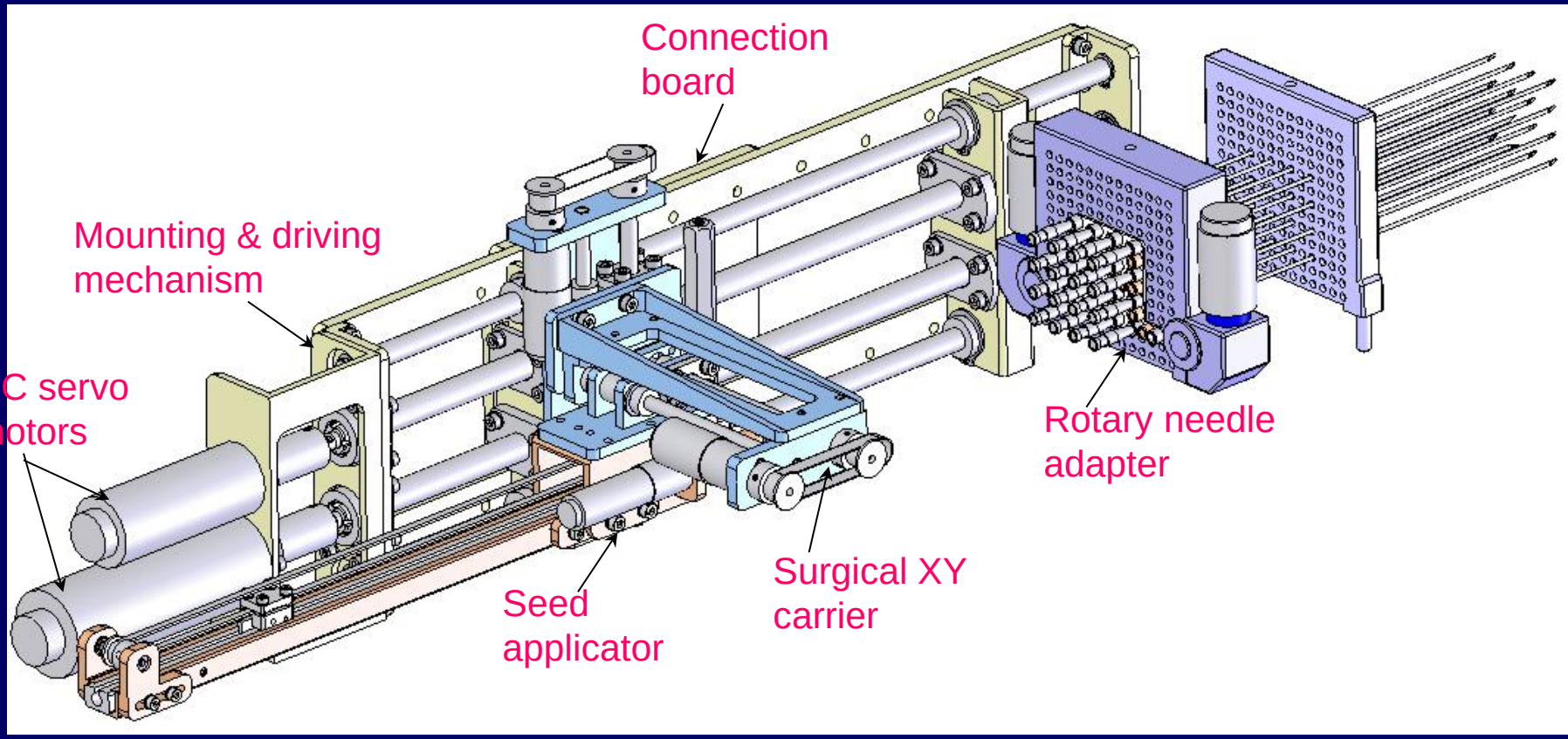

Jefferson™ Kimmel Cancer Center
NCI-designated

MRDI (Multichannel Robot-assisted Delivery and Intervention)

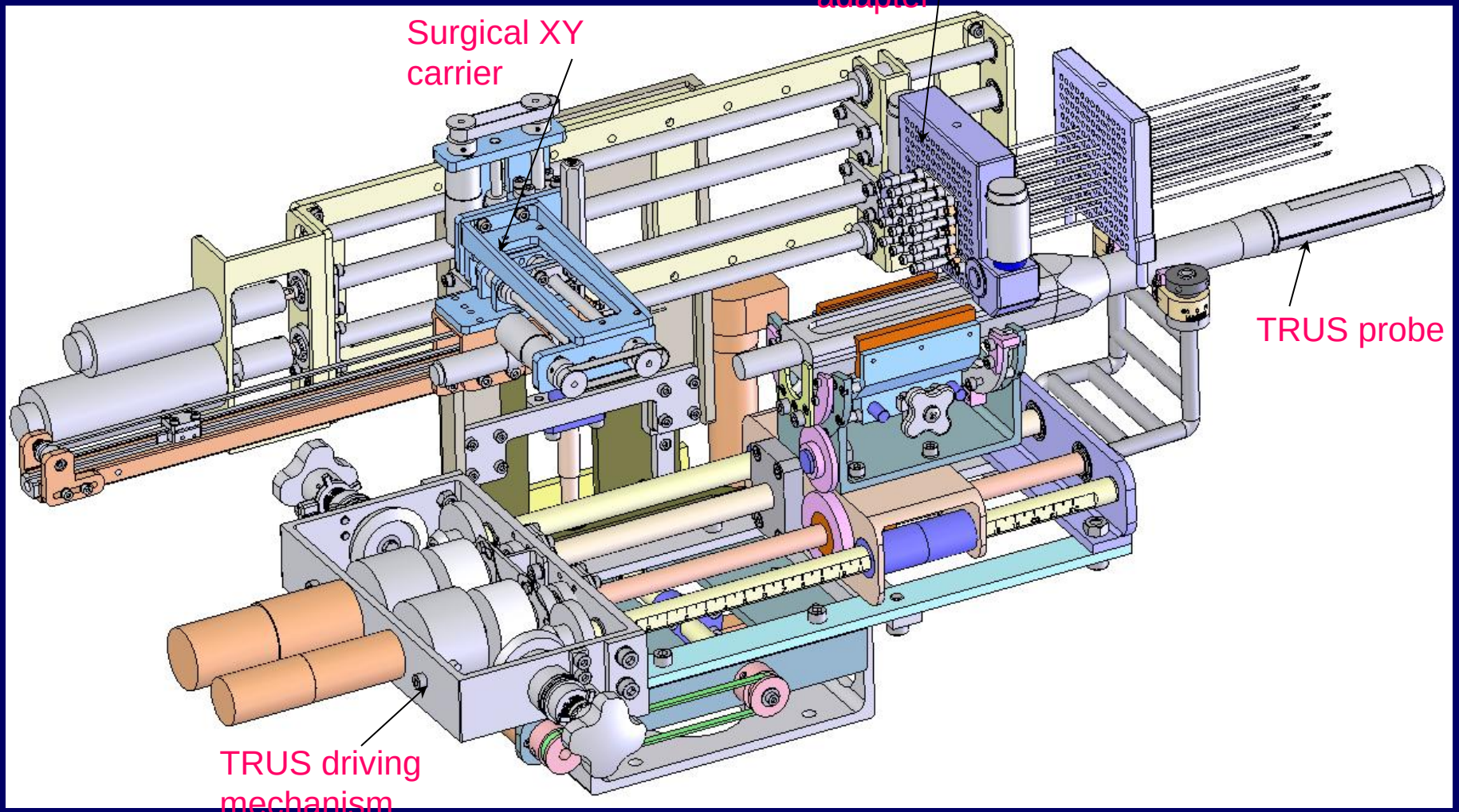

Jefferson™ Kimmel Cancer Center
NCI-designated

Tumor Sensing Study

OBJECTIVE

- To develop a real-time tissue sensing strategy by analyzing needle insertion forces combined with patient-specific criteria
  - Detect tumor foci “JIT” for targeted therapy
  - Maximize use of data that can be gathered during needle interventions under robotic assistance (e.g. during prostate brachytherapy)

HYPOTHESIS

- Tissue mechanical heterogeneities of tumor can be distinguished from those of normal variants (glandular, fibromuscular tissues) by accurate force-torque measurements during needle incursion

EVIDENCE SUPPORTING THE HYPOTHESIS

- Variations in stiffness between tumor and normal tissue [1], as well as between patients [2]
- Basis of tissue elastography imaging
  - Diseased tissues: changes in tissue composition, consistency, elasticity and stiffness
- DRE, BSE …
- Necrotic regions – potentially requiring selective, localized dose escalation

1. V. Jalkanen, B.M. Andersson, A. Bergh, B. Ljungberg, and O.A Lindahl., “Prostate tissue stiffness as measured with a resonance sensor system: a study on silicone and human prostate tissue in vitro”, Medical & Biological Engineering & Computing, 44 (7), 593-603 (2006).
2. V. Jalkanen, “Resonance Sensor Technology for Detection of Prostate Cancer”, Department of Applied Physics and Electronics, Umeå University, Umeå, Sweden (2006)

PATIENT-SPECIFIC FACTORS

- Age
- Ethnicity
- BMI
- Prostate volume
- Prostate density
- Gleason score
- PSA
- Clinical stage

METHOD: Patient-Specific Factors Modeling

- Regression model: Baseline mean force in normal tissue

$$F_b = \sum_{i=0}^{\mathbf{N}} \beta_i X_i^{n_i}$$

N = statistically significant terms

- Tumor detection model: threshold force in tumor

$$F_t = F_b + \Delta$$

Discriminator: sensitivity vs. specificity, i.e. ROC analysis

- Optimize diagnostic power
  - Objective: Max $F(\beta), \beta \in \Phi = \{\beta_{il} \le \beta_i \le \beta_{ih}, i = 0,1,2\}$
    - F_1 : area under curve (AUC) of ROC.
    - Sequential Quadratic Programming method

MATERIAL AND METHODS

- 23 patients who underwent radical prostatectomy enrolled in IRB-approved clinical study with informed consent
- Prostatectomy sample was brought to the research lab within 10 min of complete resection
- The prostate was placed into a pre-prepared PVC phantom
- Two stabilization needles were used to mimic the effect during brachytherapy procedure

MATERIAL AND METHODS (cont.)

- 18-gauge diamond tip brachytherapy needles (Mick Radio-Nuclear Instruments, Inc., NY)
- 6DOF robotic system equipped with 6DOF Force-Torque sensor (Nano17®, ATI Industrial Automation, NC)
- Insertion speed 10 mm/s; apex to base
- Needle progression into the prostate and 3D deformation were recorded in 2 orthogonal planes simultaneously under ultrasound (GE LOGIQ-9, model 2404587, Milwaukee, WI; Acuson model 128xP, Mountain View, CA)

Real-time Prostate Cancer Detection (needle insertion force)

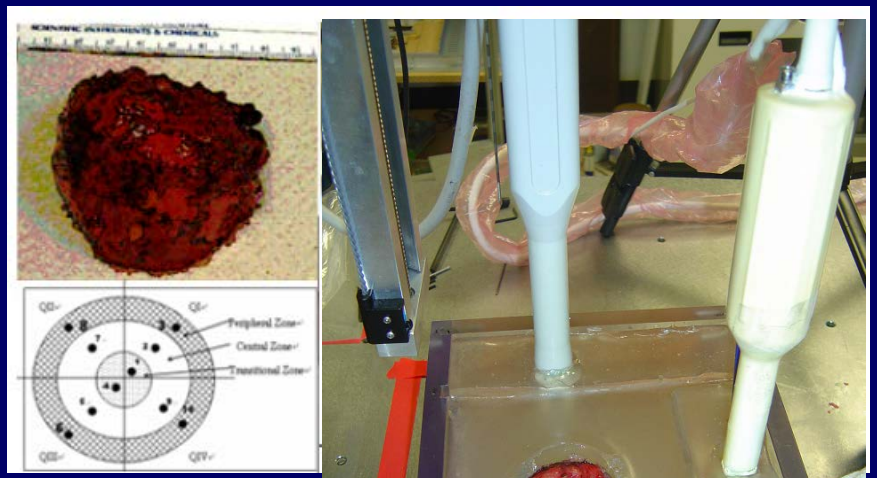

Needle insertion force experiment with Human Prostate (n=23)

Histopathology

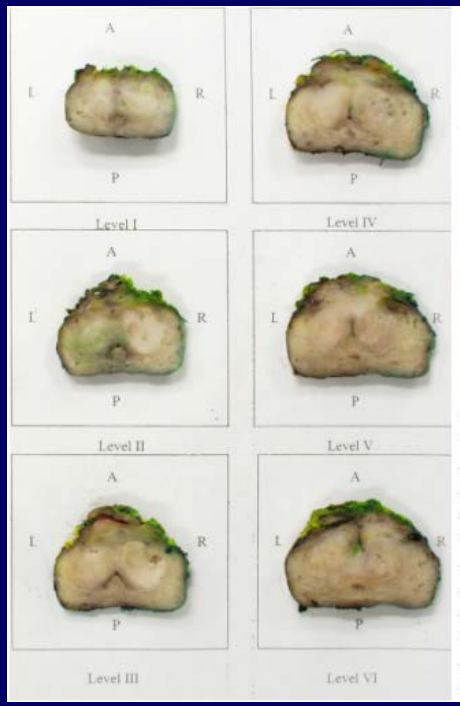

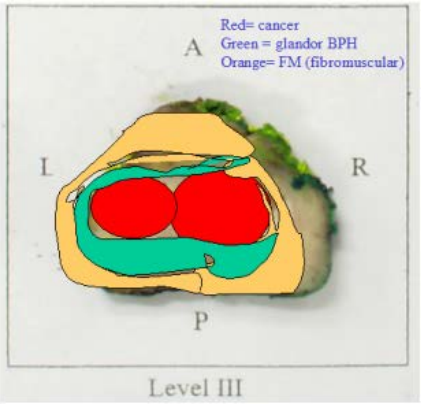

	Level III(midial)
1	BPH+FM(8:2)
2	G+FM(5:5)
3	G+FM(7:3))
4	CA+FM(8:2)
5	CA+FM(2:8)
6	FM(10)
7	CA (10)
8	G+FM(5:5)
9	BPH+G+FM(3:2:5)
10	FM(10)

G: Gland
FM: Fibromuscular
CA: Cancer
BPH: Benign Prostatic Hyperplasia

Jefferson™ Kimmel Cancer Center
NCI-designated

MATERIAL AND METHODS (cont.)

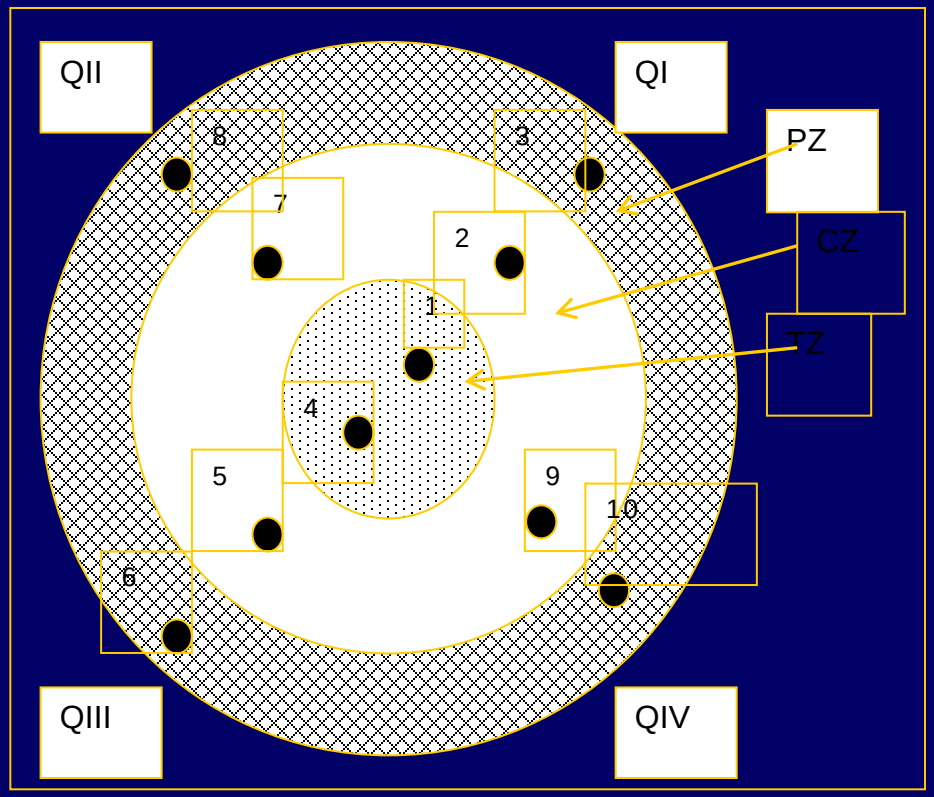

- 10 locations in three zones (peripheral, central and transitional) of the prostate
- Pathological analysis:
  - 4 mm sections through the prostate
  - Needle tracks identified
  - Histology reported at pre-selected levels from apex to base

Jefferson™ Kimmel Cancer Center
NCI-designated

Patient	case#5		Level I (Apex)	Level III (midial)	Level V (medial)	Level IX (base)
xyz	abcd	1	G(V, minute CA)+FM(5:5)	BPH+FM(8:2)	G+FM(4:6)	SV+G+FM(1:4:5)
56Y		2	G+FM (5:5)	G+FM(5:5)	G+FM(5:5)	G+FM(6:4)
43 gms		3	dilated G +FM (7:3)	G+FM(7:3))	G+FM(3:7)	G(dilated)+FM (5:5)
4.4 x 5 x 2.9 (cm)*		4	CA+G+FM(3:2:5)	CA+FM(8:2)	G+FM(2:8)	G+FM(pact) (4:6)
CA: 3+3=6/10		5	CA+BPH+FM (4:3:3)	CA+FM(2:8)	G+FM(2:8)	G+FM(pact) (4:6)
11 sections		6	G+FM(4:6)	FM(10)	G+FM(2:8)	G+FM (4:6)
		7	CA+FM (5:5)	CA (10)	CA+G+FM(1:2:7)	SV+G+FM(1:4:5)
		8	G+FM(4:6)	G+FM(5:5)	G+FM(4:6)	G(dilated with focal PIN) +FM(6:4)
		9	CA+G+FM(4:2;4)	BPH+G+FM(3:2:5)	G+FM(3:7)	BPH+G+FM(pact) (2:3:5)
		10	CA+G+FM(2:4:4)	FM(10)	G+FM(2:8)	G+FM(4:6)

Key:

SV=seminal vesicle; G=Gland; FM=fibromuscular tissue of prostate;

CA=adenocarcinoma of prostate; G(V)=Glands near Verumountanum.

MATERIAL AND METHODS (cont.)

- Pathology data used as ground truth
- Data from ~half of the study patients were used to optimize the model
- Data from the remaining patients were used to test/validate the model
  - ROC analysis: Area under the curve (AUC) used as measure of diagnostic power
- Selection of patients for modeling: factorial design

RESULTS

Needle Insertion Force Profiles

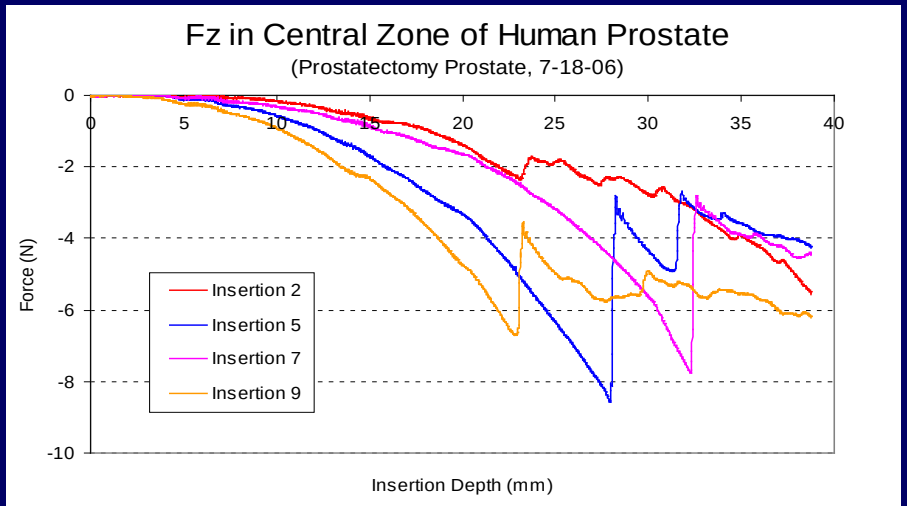

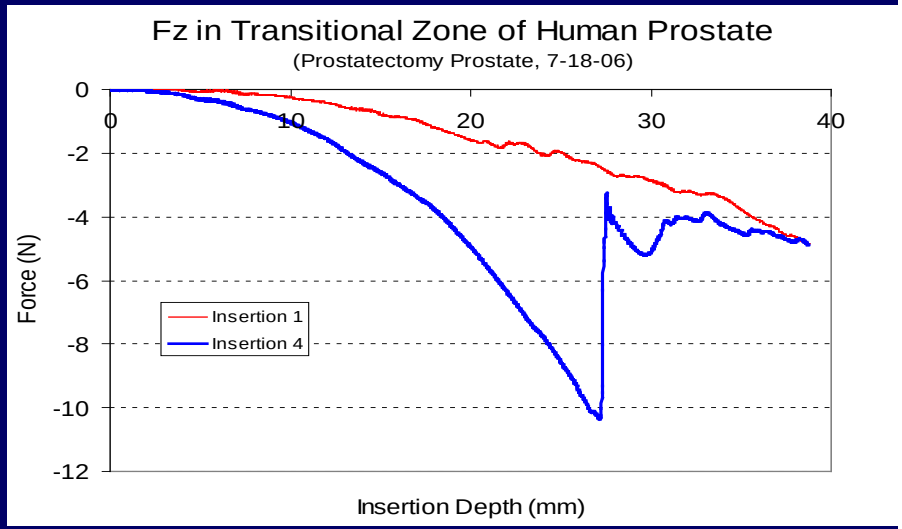

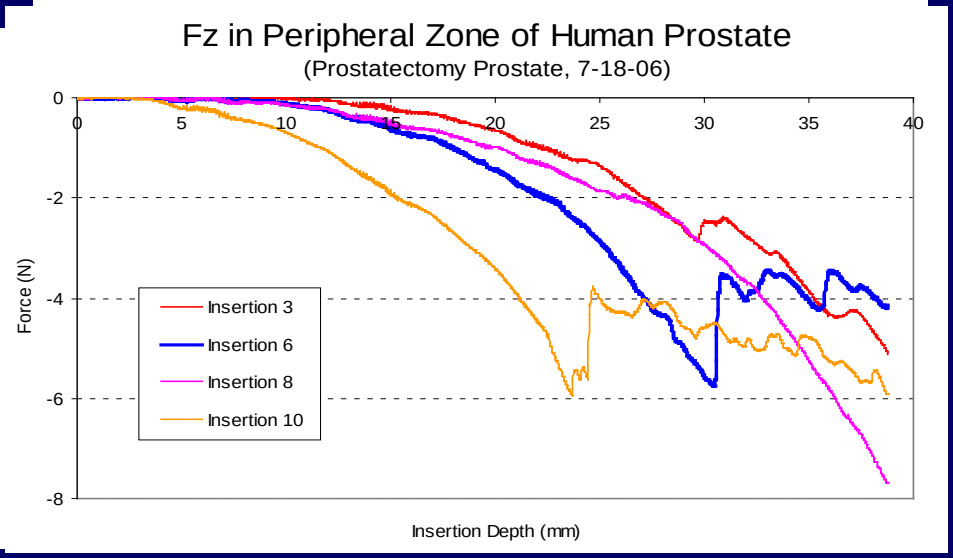

Jefferson™ Kimmel Cancer Center
NCI-designated

RESULTS: Force Analysis

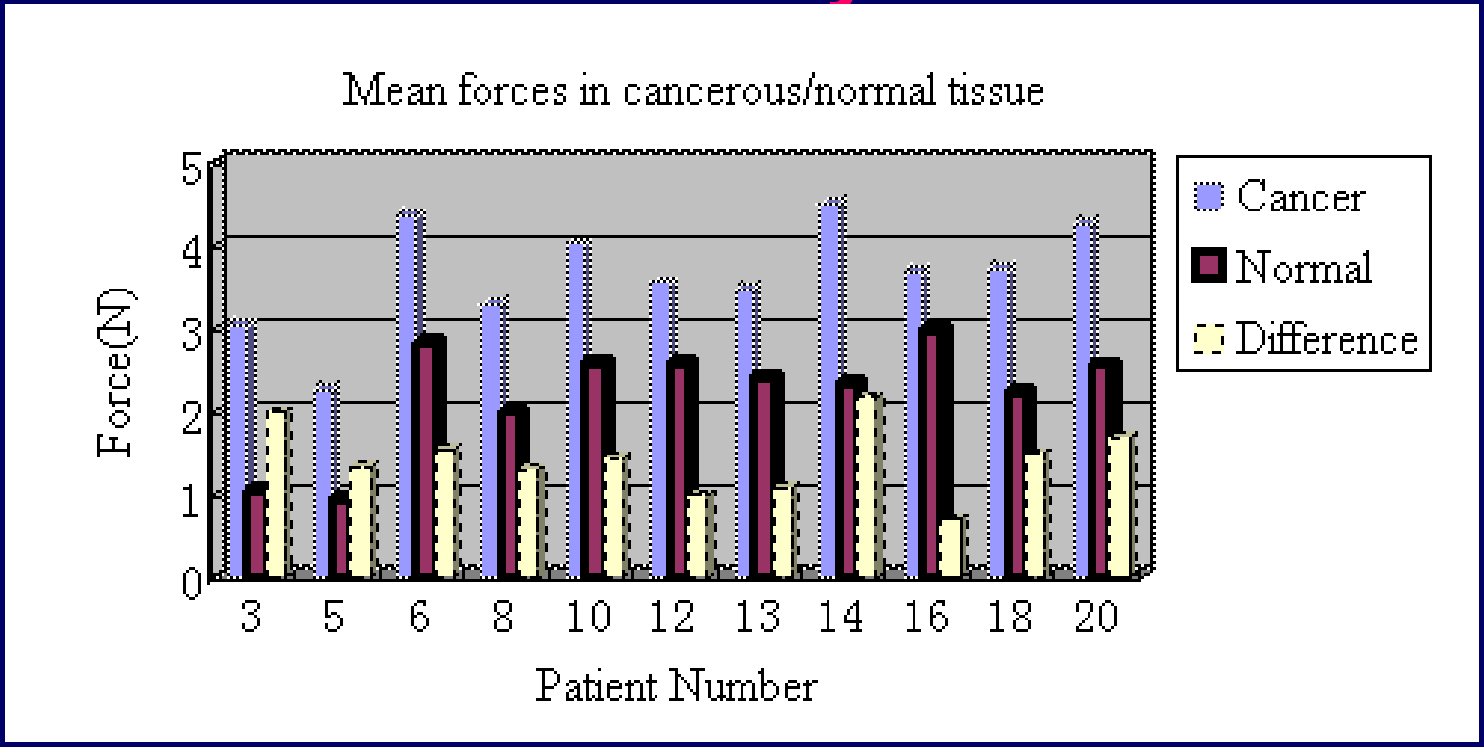

- Needle insertion force: cutting force + visco-elastic friction force
- Variation of the forces : indicator of tissue composition variability
- **$F_c > F_n$: 0.7N ~ 2.2N**

Jefferson™ Kimmel Cancer Center NCI-designated

RESULTS: Patient-specific Factors

- **Patient-specific factors**

  Start with all terms in constructing the model:

  patient age, ethnicity, BMI, clinical stage of cancer, Gleason score, prostate volume, prostate density and PSA

- **Backward stepwise regression**
  - p value: stepwise elimination of least significant terms in model
  - Multicolinearity: Variance inflation factors (VIF)
  - Autocorrelation of model residuals: Durbin-Watson number
- **Significant factors:** prostate density and PSA
  - Higher density and higher PSA value tend to predict larger insertion forces

RESULTS: Model Validation

- Model tuning: 10 patients
  - (x1:density, x2:PSA)
  - max(AUC)=0.80

$$F_b = \text{-}0.06\text{-}0.06x_1\text{-}0.175x_2$$

- Model validation: 11 patients

  - **AUC=0.90**

  - classifier 1.7: sensitivity 100%, specificity 76%
  - classifier 1.9: sensitivity 86%, specificity 79%

Jefferson™ Kimmel Cancer Center
NCI-designated

International Collaboration

Centre for Advanced Mechanisms and Robotics

School of Mechanical Engineering

Tianjin University

Division of Medical Physics, Department of Radiation Oncology

Thomas Jefferson University

2013

(1) MRI-guided surgical robot

a. Mechanism Design
b. Control System Design
c. Machinability Research
d. Reliability Analysis

(2) Ultrasound-guided surgical robot

a. Introduction on robot
b. Treatment Planning Software (TPS) Design

(3) Needle-tissue interaction

a. Tissue-equivalent material preparation
b. Needle-tissue interaction forces investigation

(1) MRI-guided surgical robot

a. Mechanism Design: The first generation of the robot

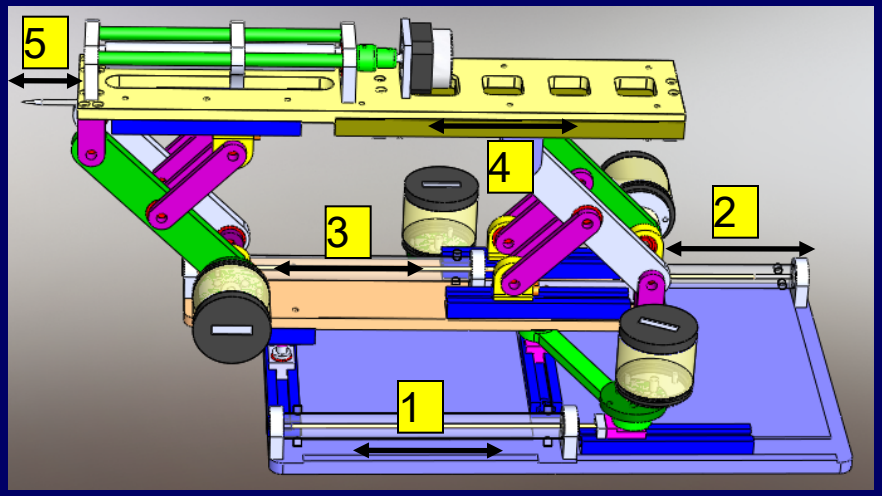

Fig.1 Virtual prototype of the surgical robot

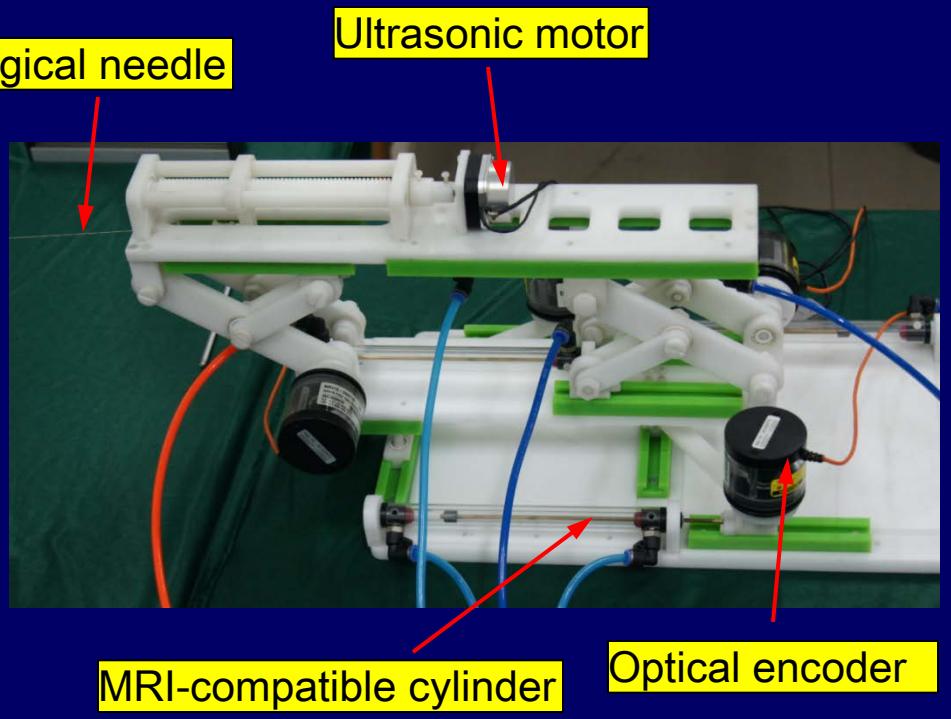

Fig.2 Physical prototype of the surgical robot

Jefferson™ Kimmel Cancer Center NCI-designated

(1) MRI-guided surgical robot

a. Mechanism Design: The second generation of the robot

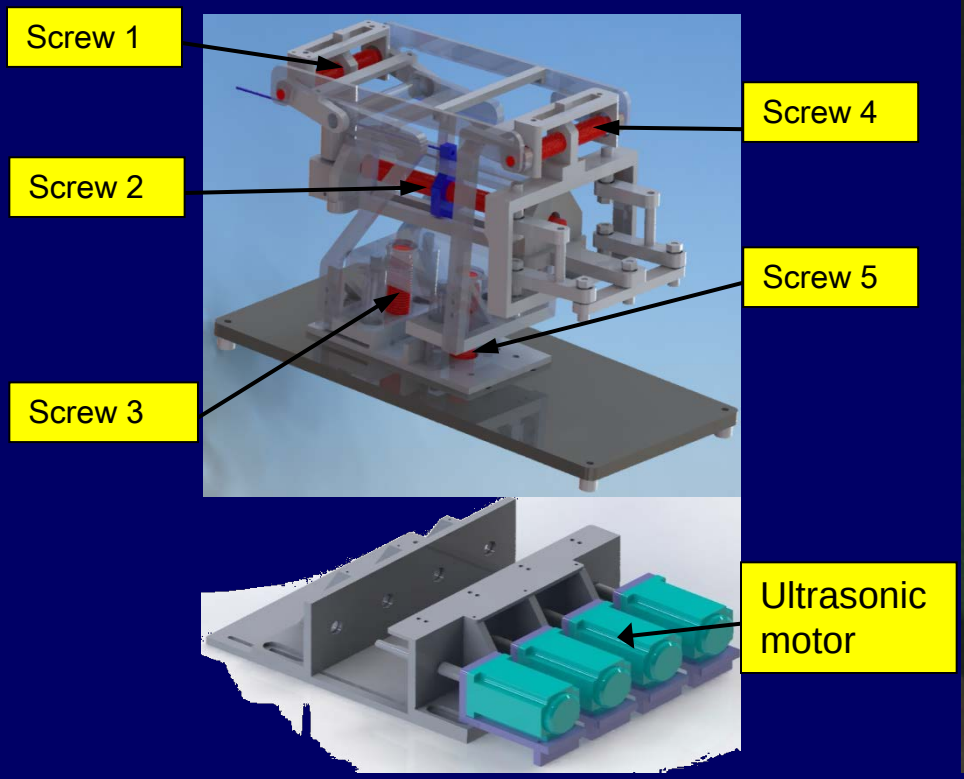

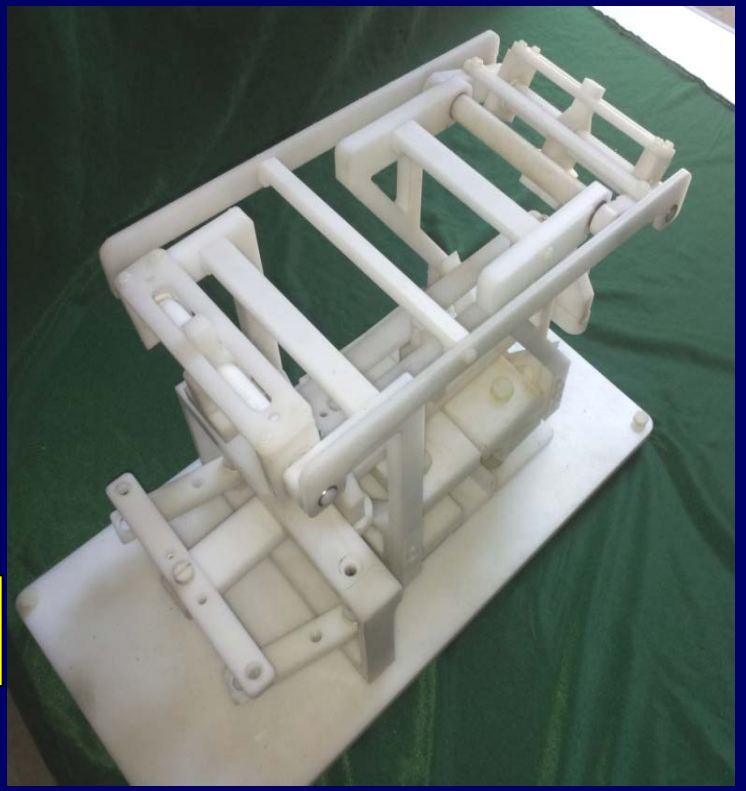

Fig.3 Virtual prototype of the surgical robot Fig.4 Physical prototype of the surgical robot

Jefferson™ Kimmel Cancer Center NCI-designated

(1) MRI-guided surgical robot

a. Mechanism Design：The third generation of the robot

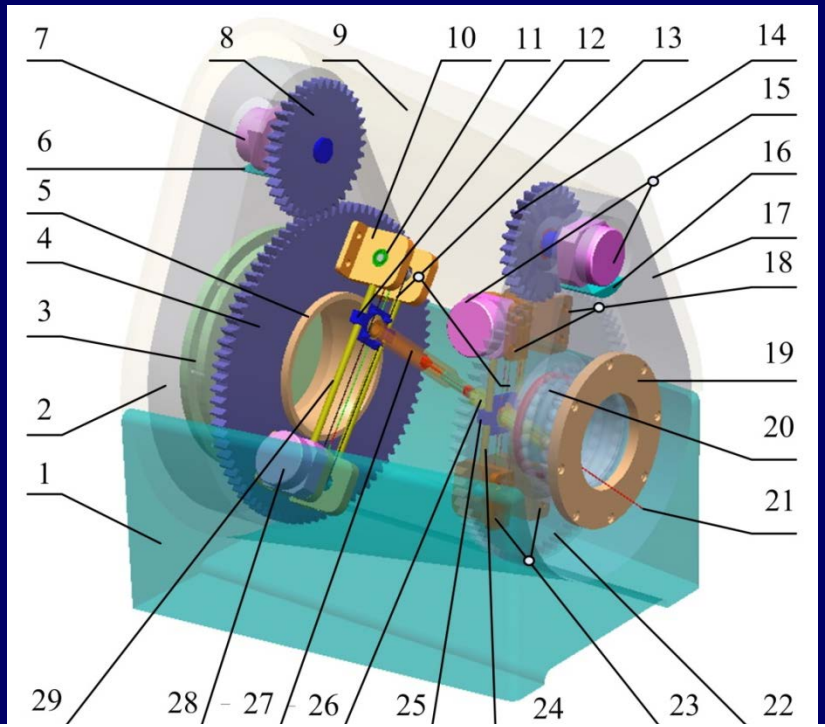

1-base, 2,17-bracket, 3,19-bearing end plate, 4,22-gearwheel, 5-gear shaft, 6,16-motor base, 7,15,28-ultrasonic motor, 8,14-pinion, 9-cover, 10,18,23-bearing pedestal, 11,20-bearing, 12, 25-slider, 13-transmission wire, 21-puncture needle(end effector), 24,29-guiding bar, 26, 27-needle guards

Fig.5. Virtual prototype of the third generation of the surgical robot

(1) MRI-guided surgical robot

b. Control System Design

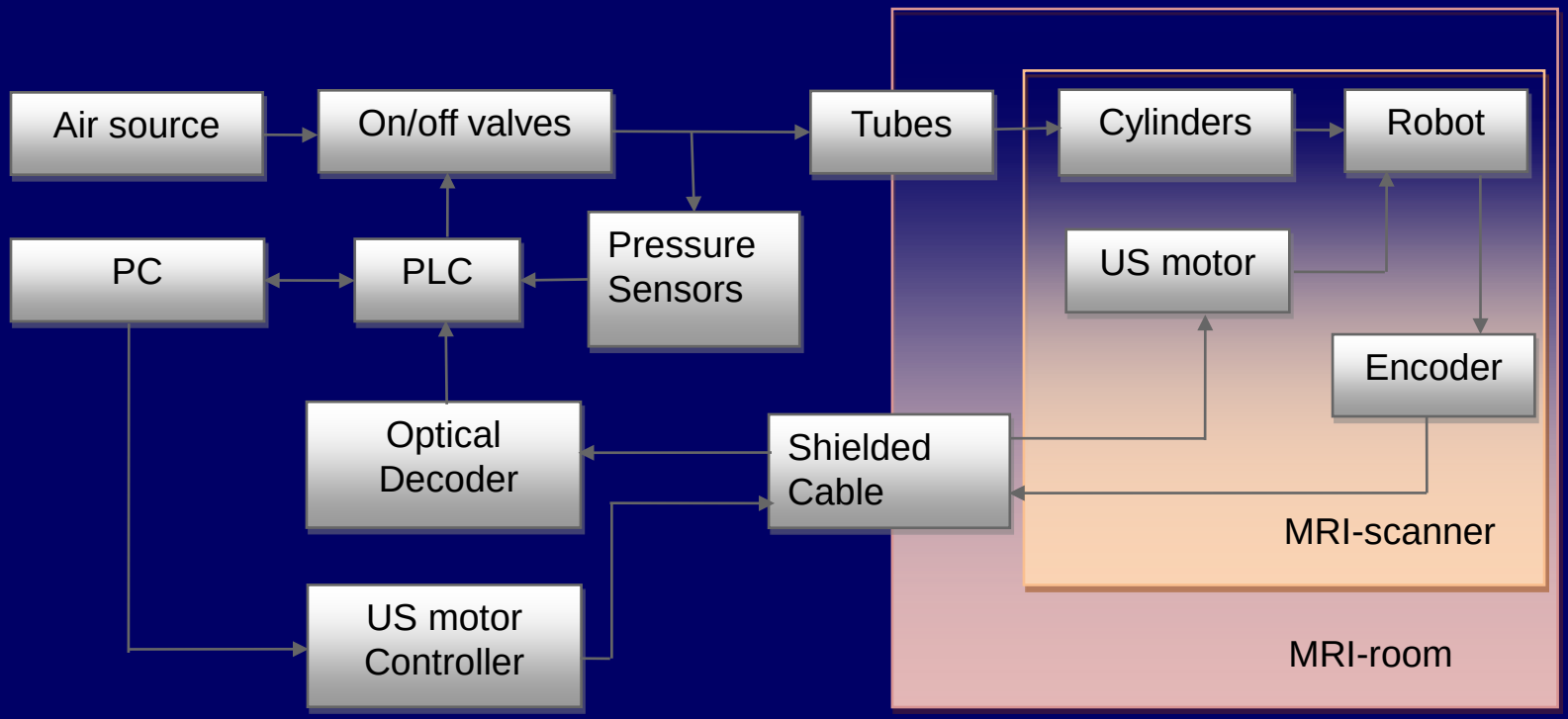

Fig.6. Flow diagram the control system

Jefferson™ Kimmel Cancer Center NCI-designated

(1) MRI-guided surgical robot

b. Control System Design

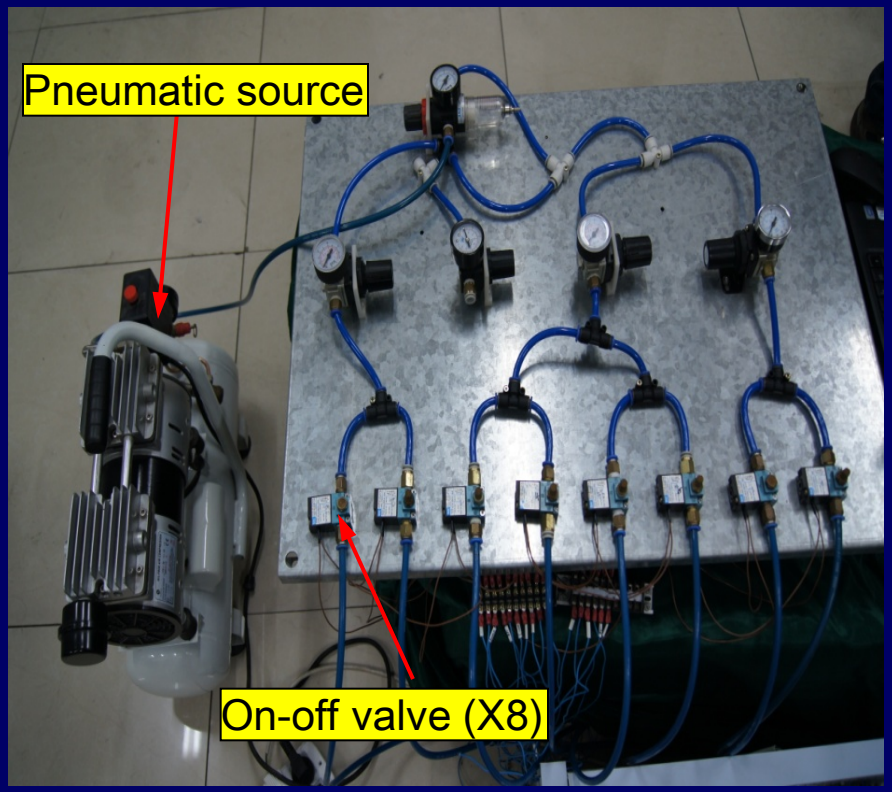

Fig.7. Pneumatic system

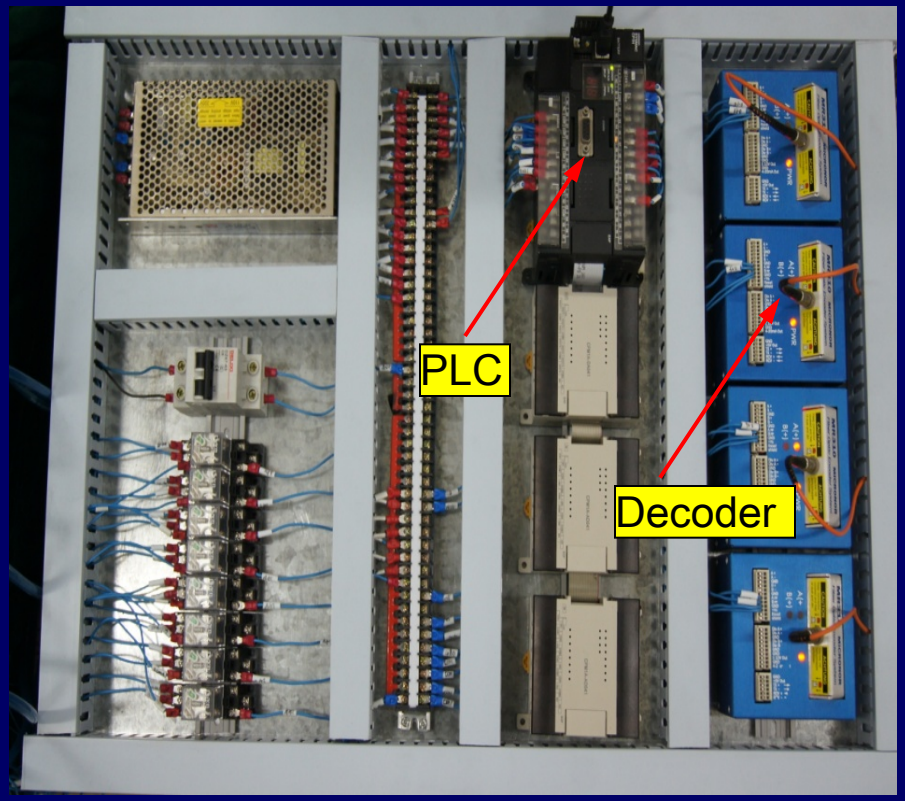

Fig.8. Electrical system

Jefferson™ Kimmel Cancer Center NCI-designated

(1) MRI-guided surgical robot

b. Control System Design

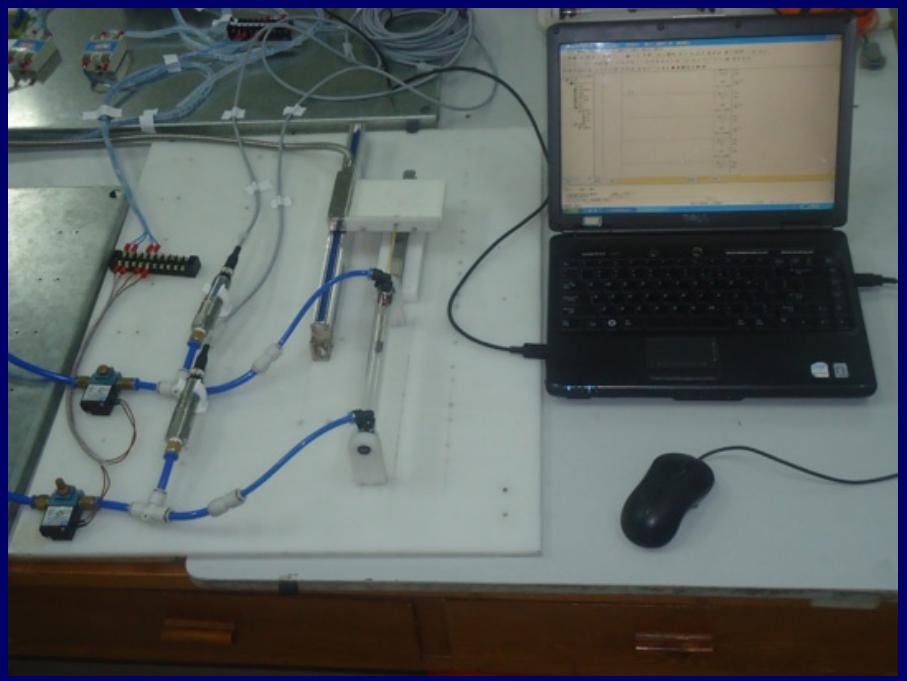

Fig.9. Experimental setup on different length tubes.

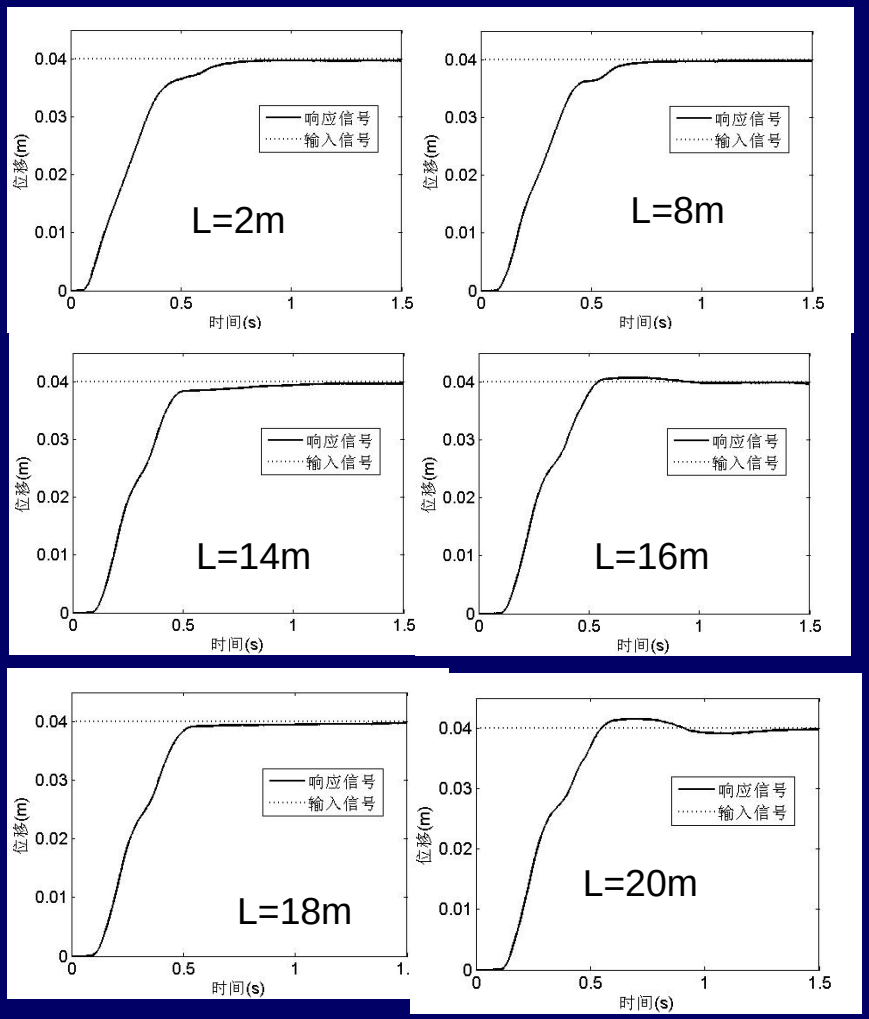

Fig.10. Experimental results

Jefferson™ Kimmel Cancer Center NCI-designated

(1) MRI-guided surgical robot

c. Machinability Research

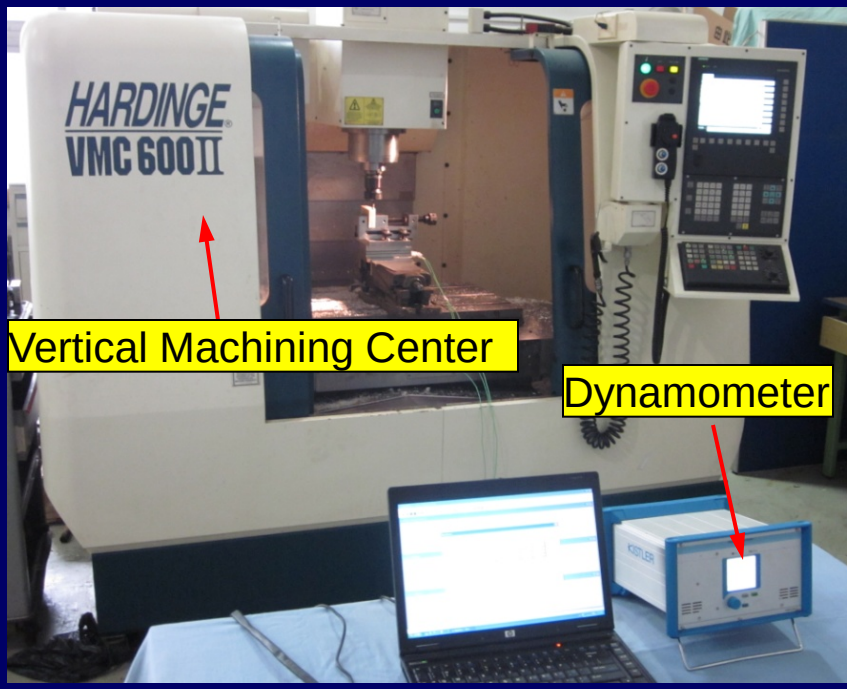

(a) Experimental setup

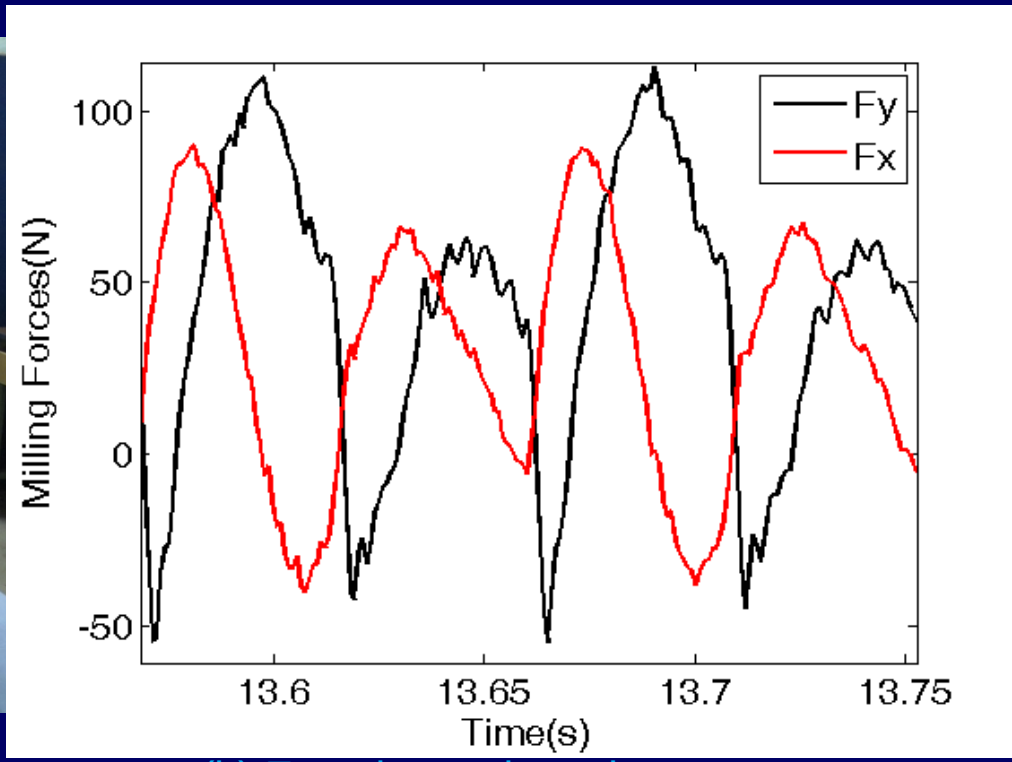

(b) Experimental results

Fig.11. Milling force experiment

Jefferson™ Kimmel Cancer Center NCI-designated

(1) MRI-guided surgical robot

c. Machinability Research

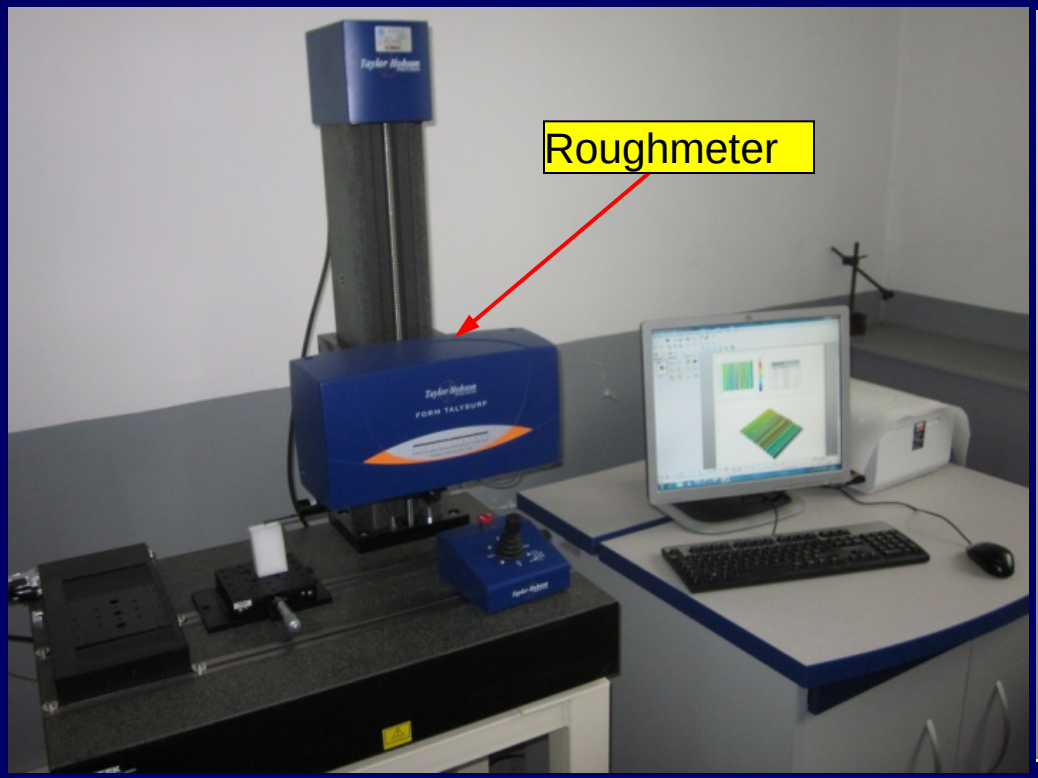

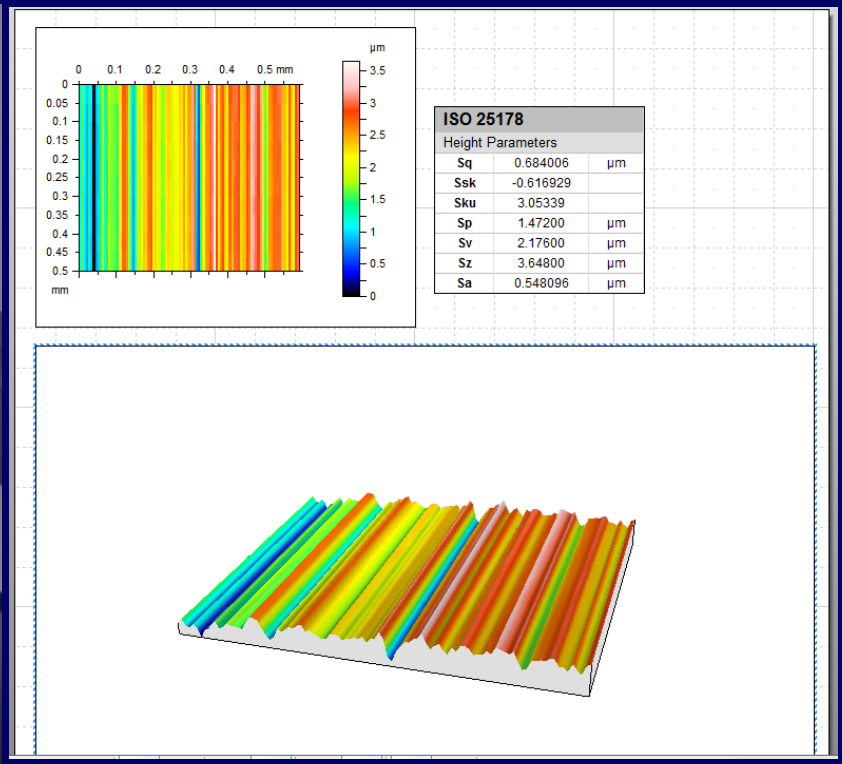

(a) Experimental setup (b) Experimental results

Fig.12. surface roughness experiment

(1) MRI-guided surgical robot

d. Reliability Analysis

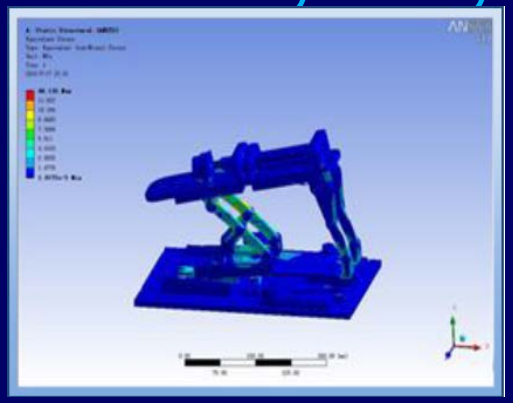

Fig.13. FEM analysis of the surgical robot

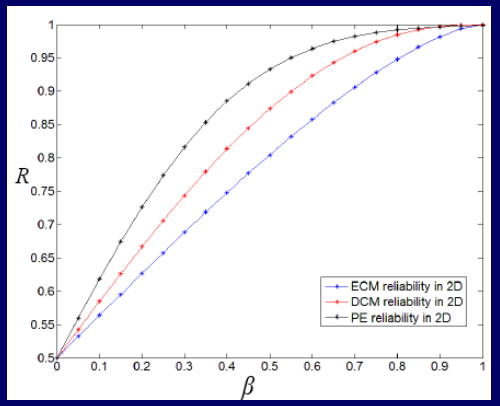

Fig.14. Relation curves between reliability and reliability index ² in 2D

.

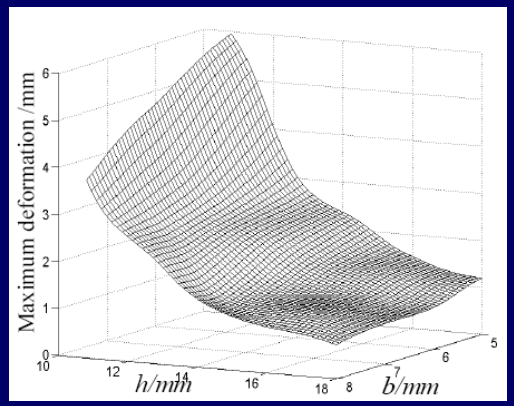

Fig.15. Response surface of maximum deformation

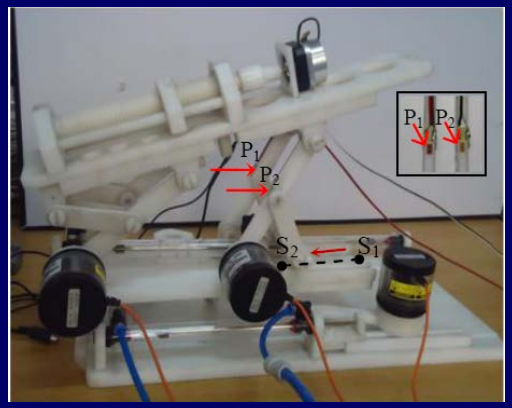

Fig.16. Sample robot based on optimization

Jefferson™ Kimmel Cancer Center NCI-designated

(2) Ultrasound-guided surgical robot

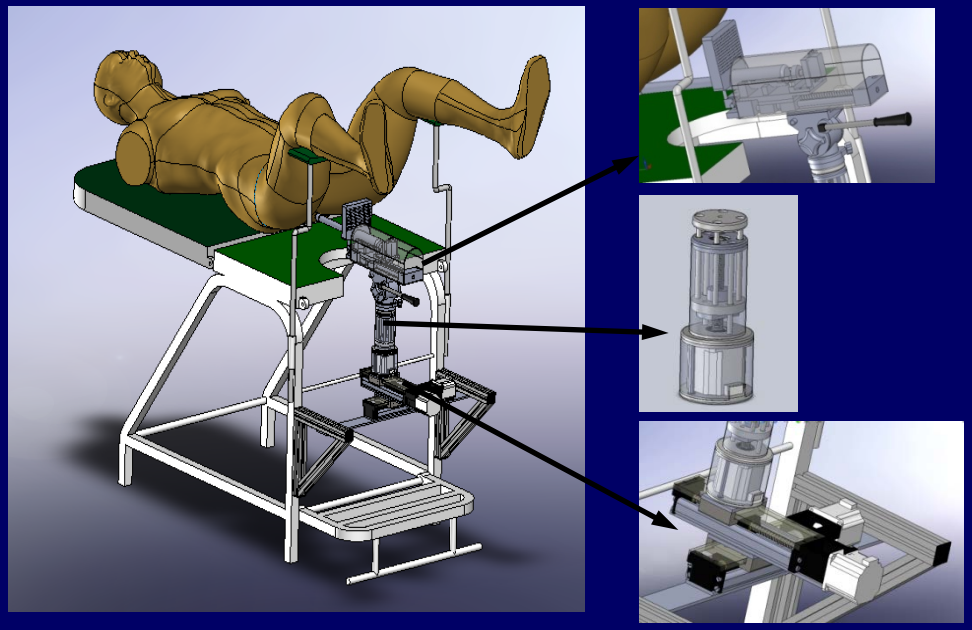

Fig.17. Ultrasound-guided surgical robot

(3) Needle-tissue interaction

a. Tissue-equivalent material preparation

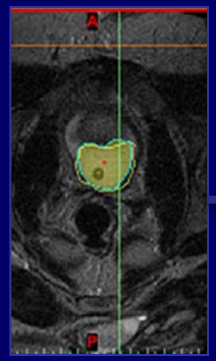

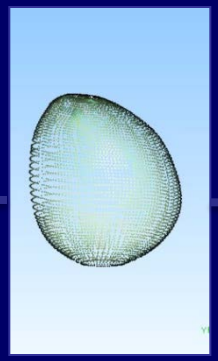

Image → Reverse Engineering → Rapid Prototyping → PVA Material Preparation → Artificial Organ

Uniaxial tensile test setup

Scanning Electron Microscope

Fig. 18. The preparation process of the artificial organ

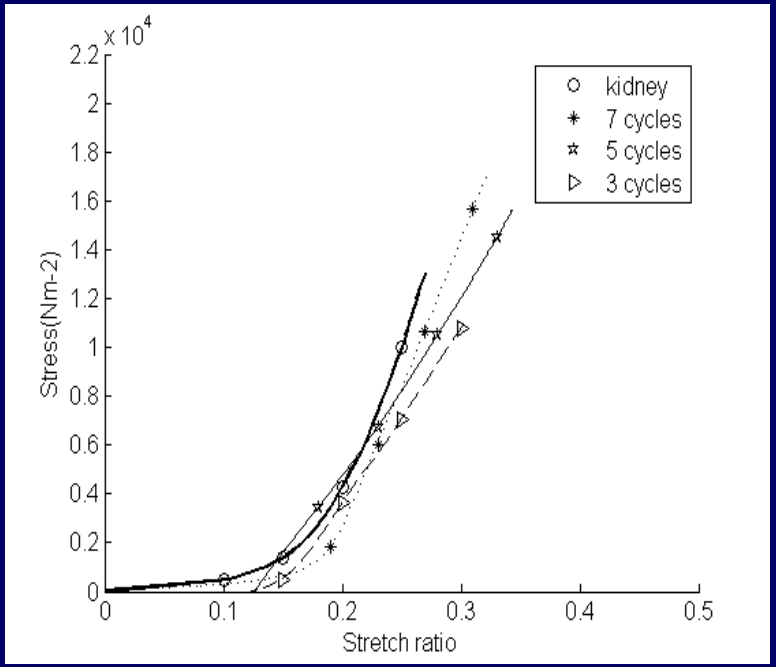

(a)

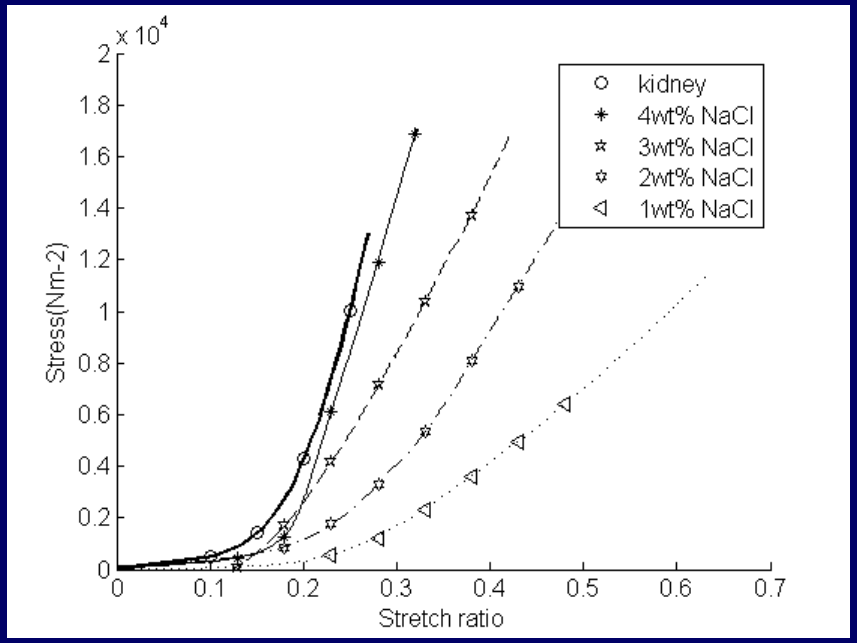

(b)

Fig. 19. The stress-strain diagram used to compare biomechanical properties of PVA materials and porcine kidney tissue

a. Tissue-equivalent material preparation

- Morphology characterization

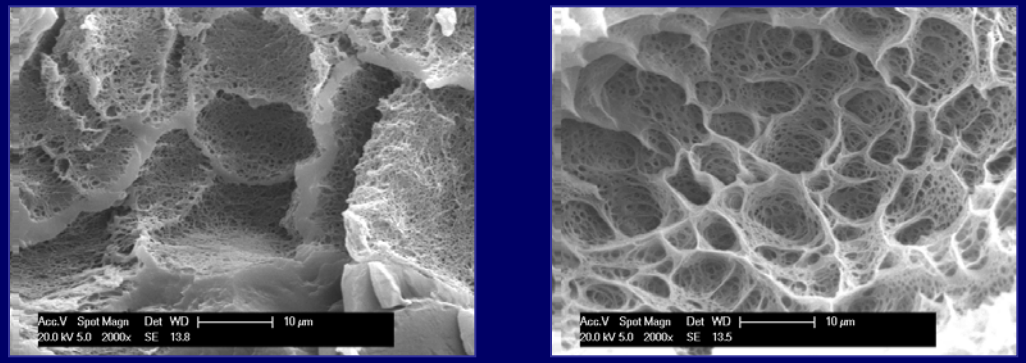

Fig. 20. The SEM images of different NaCl concentrations

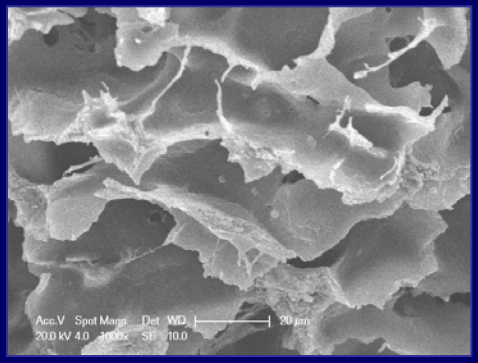

Fig. 22.The SEM images of porcine liver

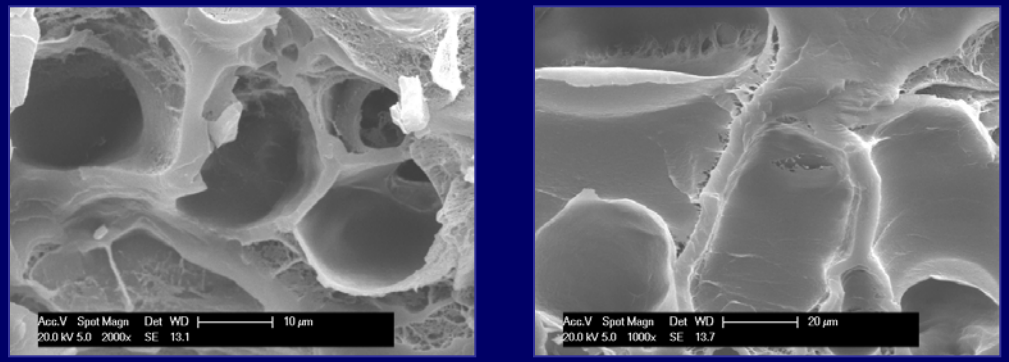

Fig. 21. The SEM images of different cross-linking cycles

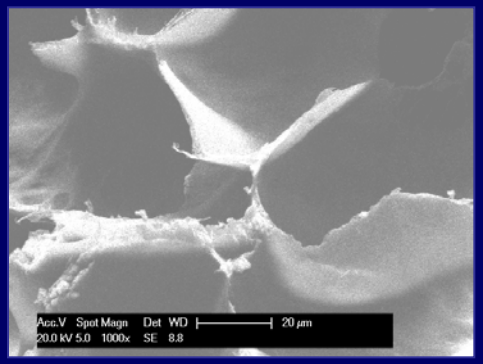

Fig. 23.The SEM images of porcine kidney

Jefferson™ Kimmel Cancer Center
NCI-designated

(3) Needle-tissue interaction

b. Needle-tissue interaction forces investigation

- Force modeling for needle insertion

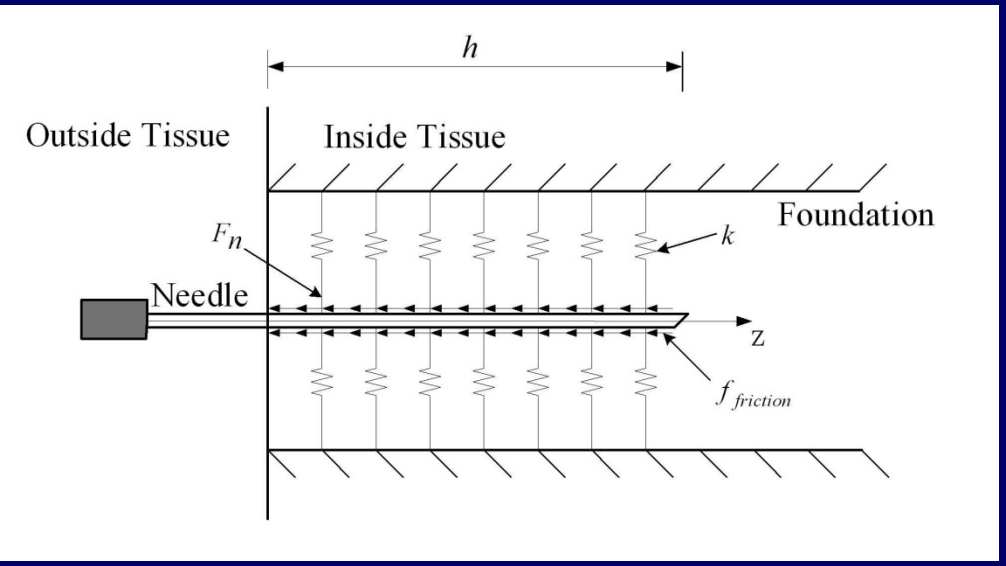

Fig.24. Modified Winkler's foundation model

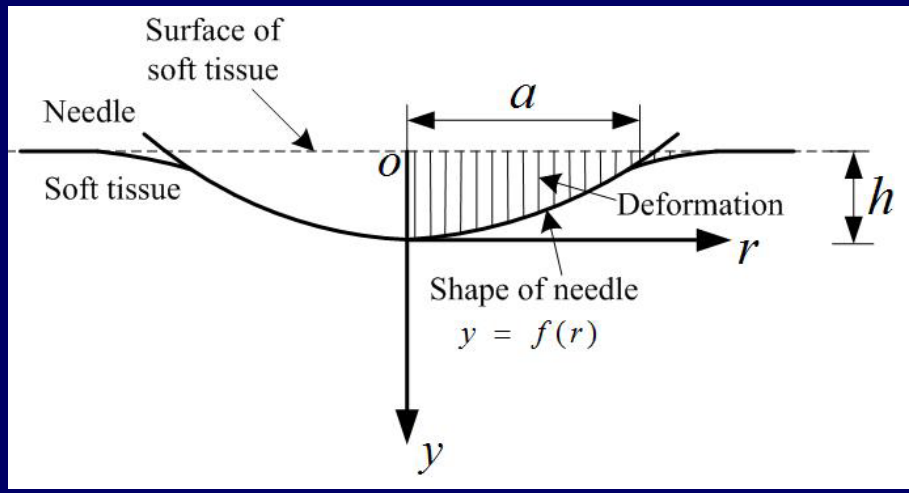

Fig.25. The sketch of the contact model

(3) Needle-tissue interaction

b. Needle-tissue interaction forces investigation

- Experimental setup

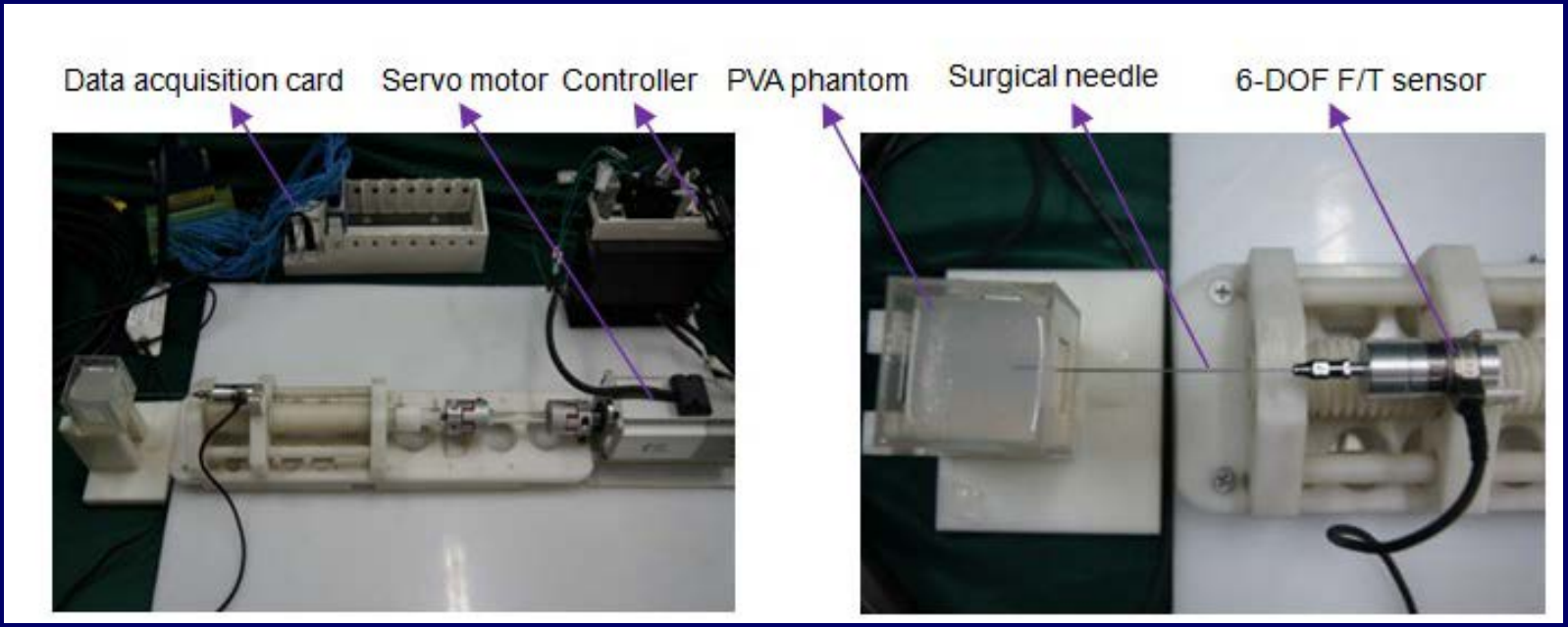

(a) 1 DOF experimental setup for needle insertion

(b) 6 DOF F/T sensor and the PVA phantom

Fig.26 Experimental setup for needle-tissue interaction forces

(3) Needle-tissue interaction

b. Needle-tissue interaction forces investigation

- Experiment results

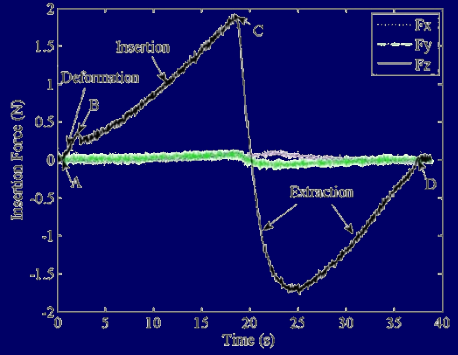

Fig.27 . Forces versus time curve for needle insertion

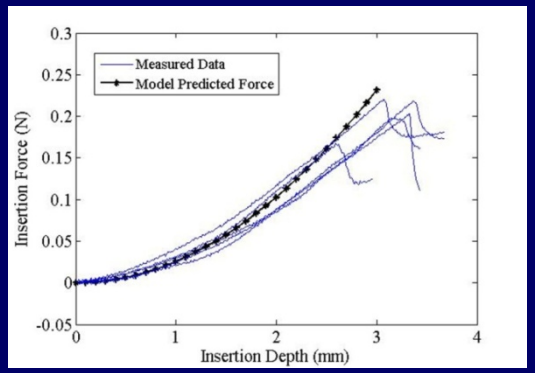

Fig.28 . The stiffness force phantom puncture of the capsule

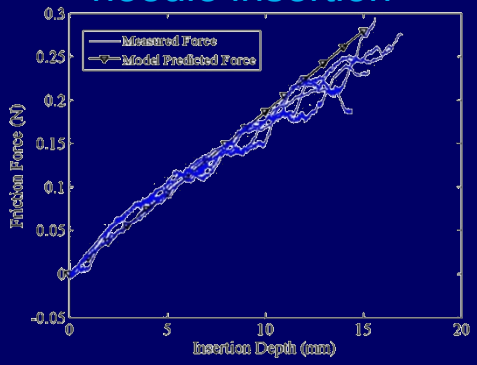

Fig.29. The friction model predicted force and the measured force

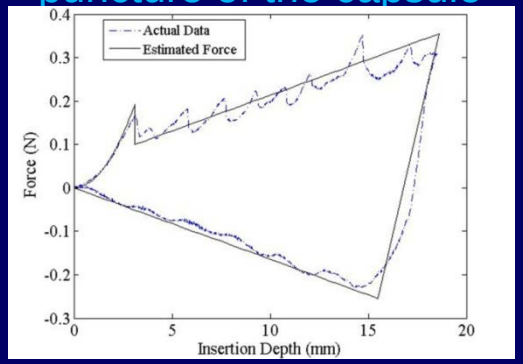

Fig.30. The needle insertion force model is compared to interaction force on PVA phantom.

Jefferson™ Kimmel Cancer Center NCI-designated

(3) Needle-tissue interaction

b. Needle-tissue interaction forces investigation

- Trajectory planning

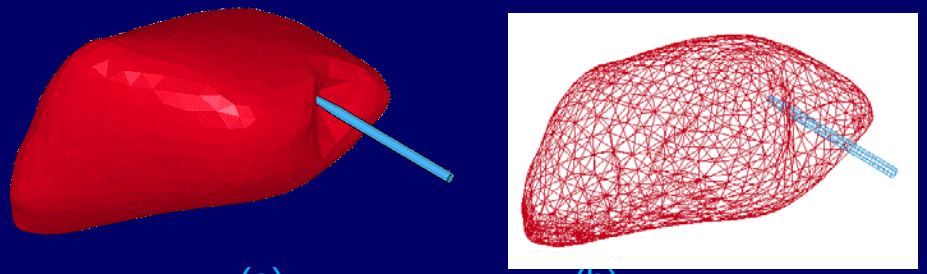

(a) (b)

Fig.31. The dynamic FEA model of prostate

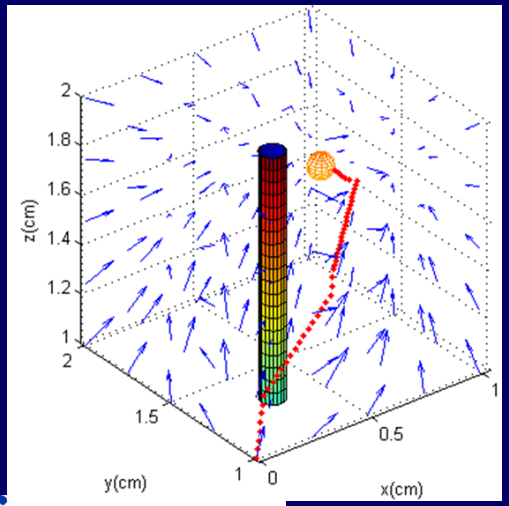

Fig.32. Trajectory planning result without considering deformation with a sphere target and cylinder obstacle.

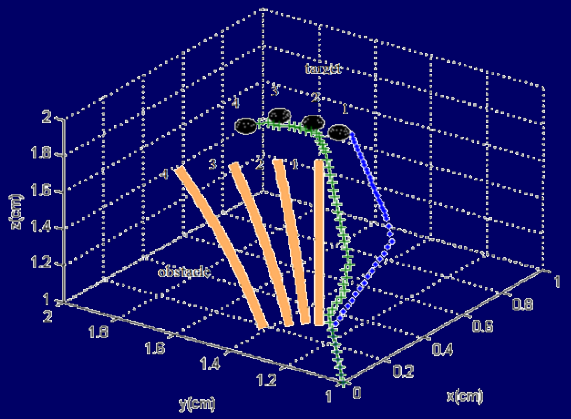

Fig.33. Trajectory planning result considering deformation

Jefferson™ Kimmel Cancer Center NCI-designated

Curved and Smart (Active) Needles

Thomas Jefferson University

Temple University

Case Western Reserve University

Needle Steering Techniques

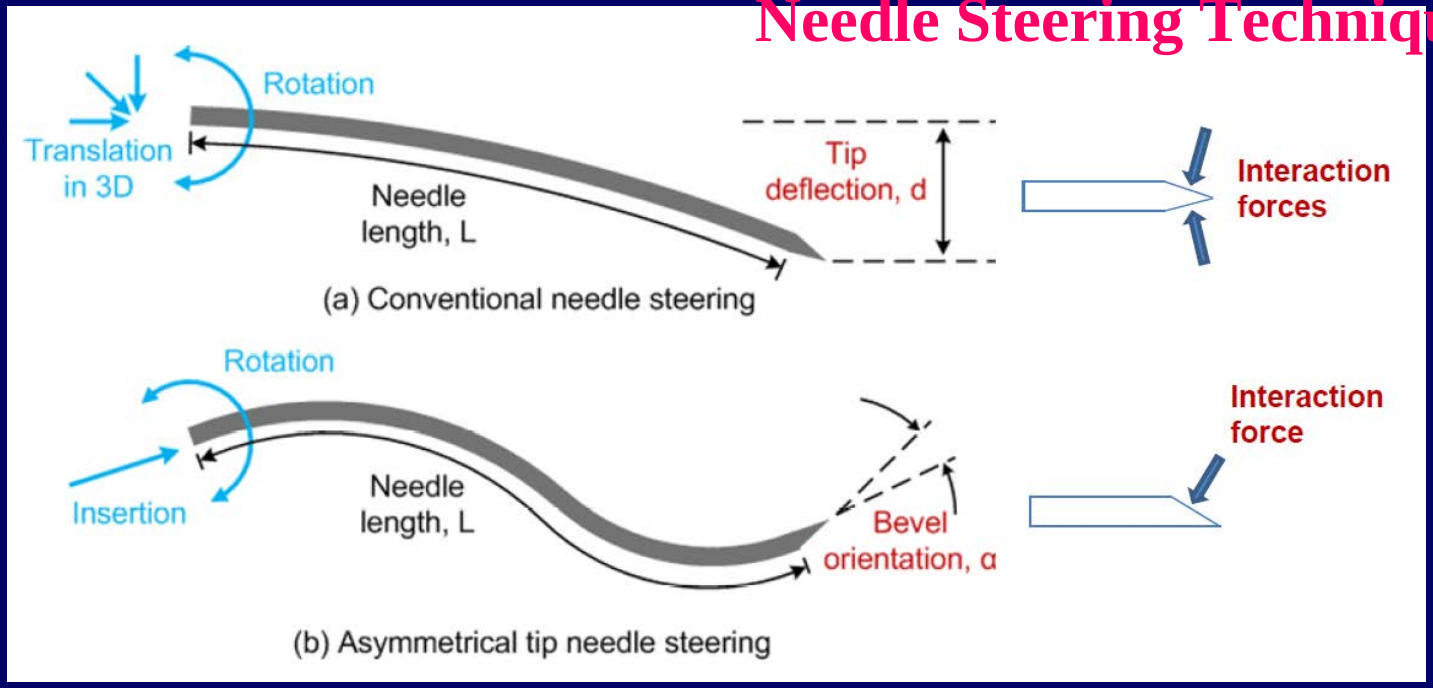

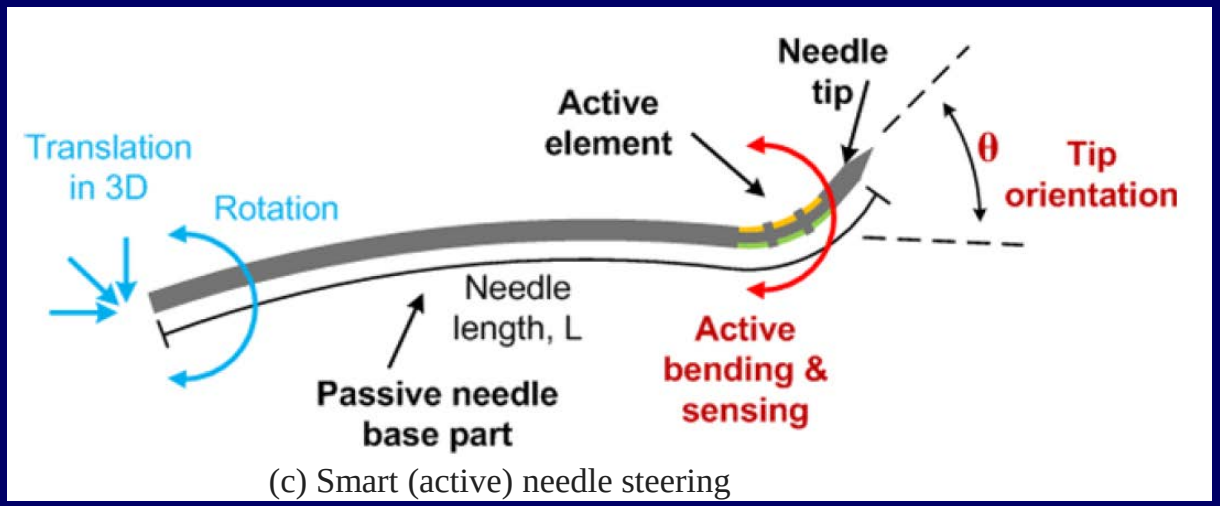

(c) Smart (active) needle steering

Ryu, PhD Thesis, 2012

Rectilinear and Curvilinear Techniques for Prostate Brachytherapy

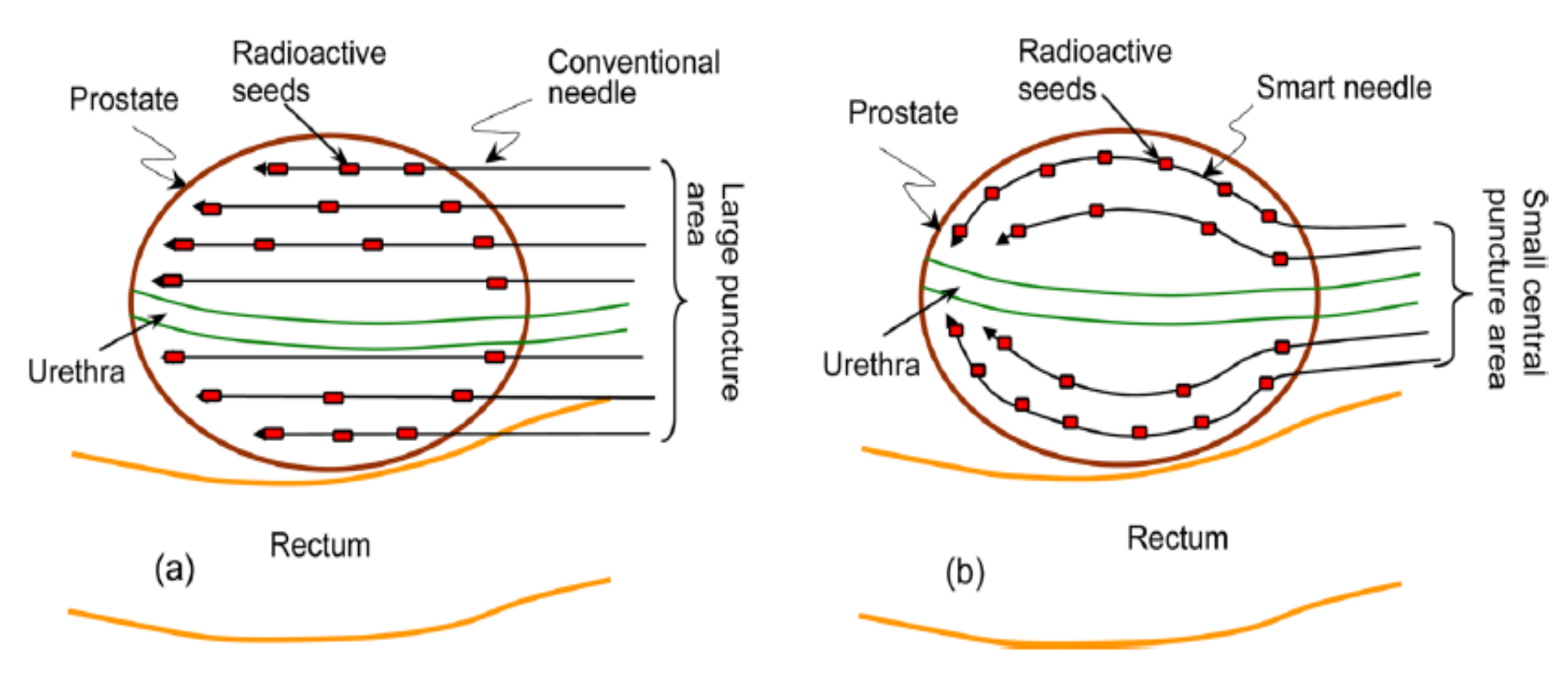

(a) Conventional rectilinear approach.

(b) Curvilinear conformal smart needle insertion.

Podder et al., MedPhys 2012

Jefferson™ Kimmel Cancer Center NCI-designated

Dose Distribution in Rectilinear Technique

A Representative Case

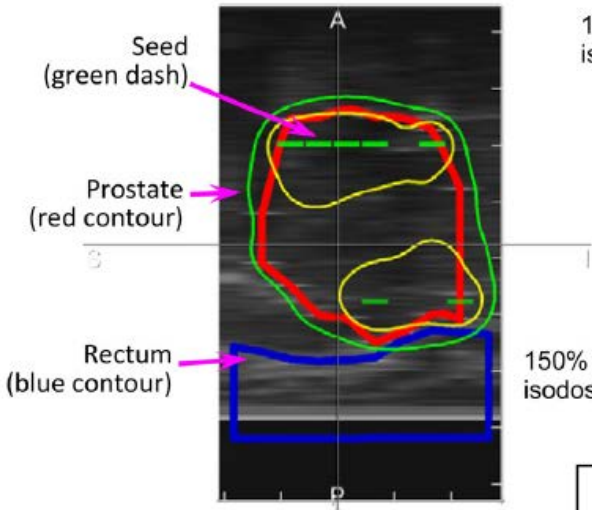

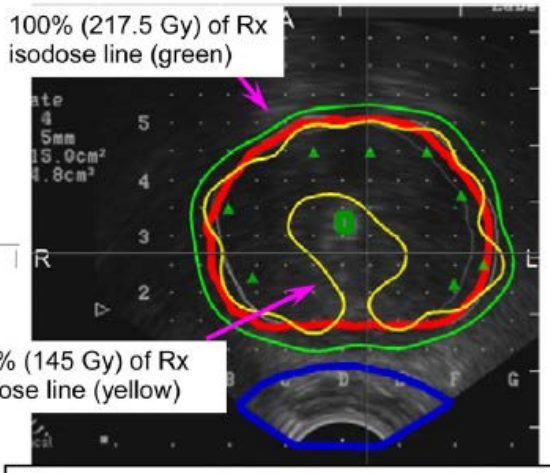

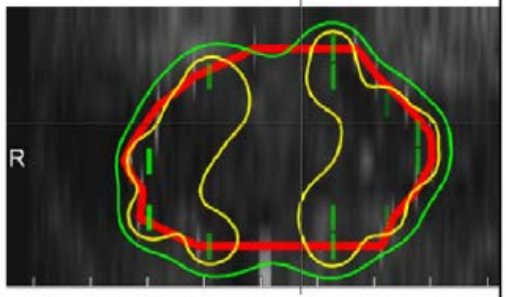

(a) Rectilinear implantation
(22 needles, 68 seeds, 41.68 U, 1cc = $1cm^3$)

Dose Information

Prostate:			
	Total Volume:	44.01 cc	
	V200%:	14.40 cc	[32.72%]
	V150%:	33.20 cc	[75.44%]
	V100%:	43.84 cc	[99.61%]
	D100%:	132.46 Gy	[91.35%]
	D90%:	194.58 Gy	[134.20%]
	D80%:	210.48 Gy	[145.16%]
	D50%:	253.81 Gy	[175.04%]
Urethra:			
	Total Volume:	0.25 cc	
	D100%:	96.74 Gy	[66.72%]
	D90%:	121.39 Gy	[83.72%]
	D30%:	187.66 Gy	[129.42%]
	D10%:	191.17 Gy	[131.84%]
Rectum:			
	Total Volume:	19.43 cc	
	V100%:	0.40 cc	[2.04%]
	D30%:	65.56 Gy	[45.22%]
	D5%:	119.07 Gy	[82.12%]

Dose Distribution in Curvilinear Technique

A Representative Case

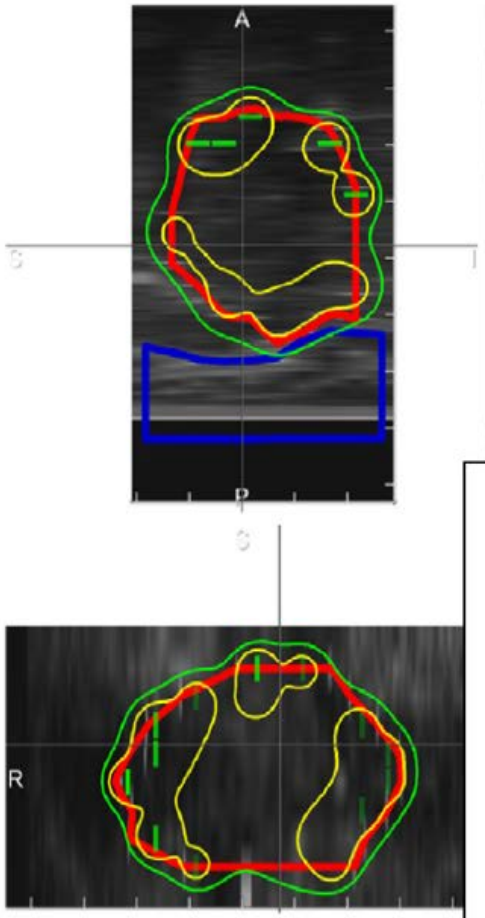

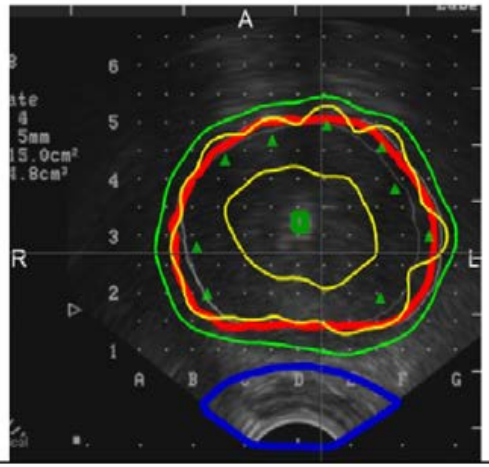

(b) Curvilinear implantation
(14 needles, 63 seeds, 38.43 U, 1cc = 1cm^3)

Dose Information

Prostate:			
	Total Volume:	44.01 cc	
	V200%:	11.38 cc	[25.85%]
	V150%:	25.60 cc	[58.16%]
	V100%:	43.90 cc	[99.76%]
	D100%:	132.43 Gy	[91.33%]
	D90%:	174.22 Gy	[120.15%]
	D80%:	188.23 Gy	[129.81%]
	D50%:	229.62 Gy	[158.36%]
Urethra:			
	Total Volume:	0.25 cc	
	D100%:	91.54 Gy	[63.13%]
	D90%:	109.43 Gy	[75.47%]
	D30%:	163.58 Gy	[112.81%]
	D10%:	168.94 Gy	[116.51%]
Rectum:			
	Total Volume:	19.43 cc	
	V100%:	0.08 cc	[0.42%]
	D30%:	61.29 Gy	[42.27%]
	D5%:	106.37 Gy	[73.36%]

DVH for Rectilinear vs. Curvilinear Techniques

A Representative Case

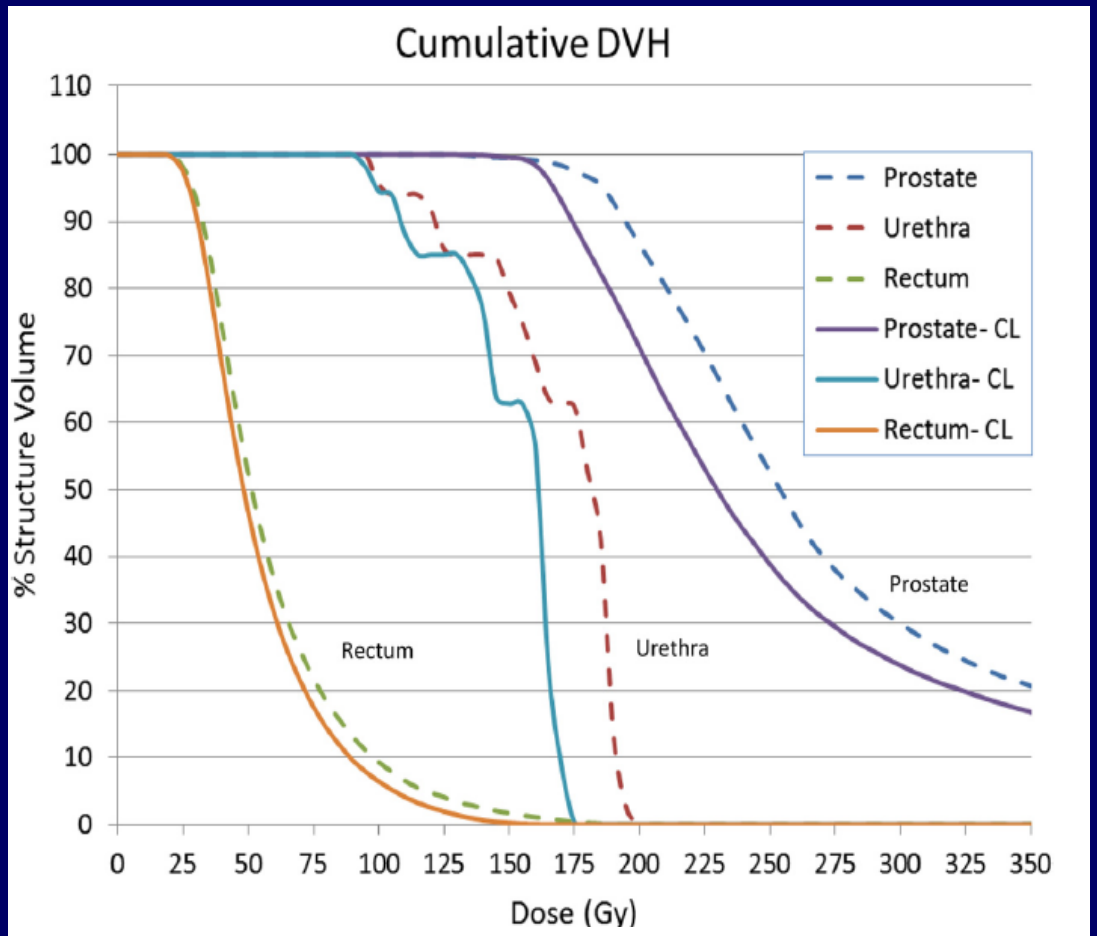

- Conventional **rectilinear** implantation (**dotted** lines)
- Proposed **curvilinear** implantation (**solid** lines)

Jefferson™ Kimmel Cancer Center NCI-designated

Rectilinear and Curvilinear Techniques for Prostate Brachytherapy

TABLE I. Comparison of proposed curvilinear approach and conventional rectilinear approach.

20 patient PSI cases

Parameter ($n = 20$)	Rectilinear method Average ± SD (range)	Curvilinear method Average ± SD (range)	Difference	p-value (two-tailed)
Total needle	19.2 ± 2.6 (14–23)	13.2 ± 1.4 (10–15)	−6.0 (−30.5%)	< 0.001
Total seed	62.5 ± 11.2 (43–85)	55.1 ± 10.4 (38–74)	−7.4 (−11.8%)	< 0.49
Total activity (mCi)	38.3 ± 6.3 (28.3–47.3)	33.8 ± 4.9 (25.3–40.3)	−4.5 (−11.8%)	< 0.37
Prostate (average = 41.3 cm^3, range = 26.6–53.2 cm^3):				
D_{90} (Gy)	198.7 ± 9.9 (182.9–215.2)	183.3 ± 6.8 (176.3–194.5)	−15.4 (−7.8%)	< 0.04
V_{100} (cm^3)	99.98 ± 0.06 (99.8–100)	99.97 ± 0.06 (99.83–100)	−0.01 (−0.01%)	< 0.85
V_{150} (cm^3)	80.9 ± 6.8 (68.5–89.8)	65.7 ± 5.3 (57.8–75.9)	−15.2 (−18.8%)	< 0.01
V_{200} (cm^3)	43.7 ± 6.0 (32.7–53.4)	28.9 ± 3.3 (26.0–35.5)	−14.8 (−33.9%)	< 0.001
Urethra:				
D_{10} (Gy)	209.9 ± 12.2 (186.2–228.7)	189.2 ± 8.1 (178.3–208.8)	−20.7 (−9.9%)	< 0.02
D_{30} (Gy)	205.1 ± 10.4 (184.3–219.9)	184.3 ± 7.4 (172.5–200.2)	−20.8 (−10.1%)	< 0.01
Rectum:				
D_5 (Gy)	160.2 ± 15.9 (137.9–196.8)	130.5 ± 12.3 (111.0–151.1)	−29.7 (−18.5%)	< 0.03
V_{100} (cm^3)	0.93 ± 0.51 (0.19–2.0)	0.21 ± 0.17 (0.03–0.61)	−0.72 (−77.8%)	< 0.001

Jefferson™ Kimmel Cancer Center NCI-designated

Curvilinear vs. Rectilinear Approach for PSI

- Small puncture area
- Accurate needle placement
- Improved dose distribution
- Better sparing of OARs
- Less needles, seeds
- Expected less traumas
- Expected reduction of toxicities

Curved Needles for Surgical Procedures

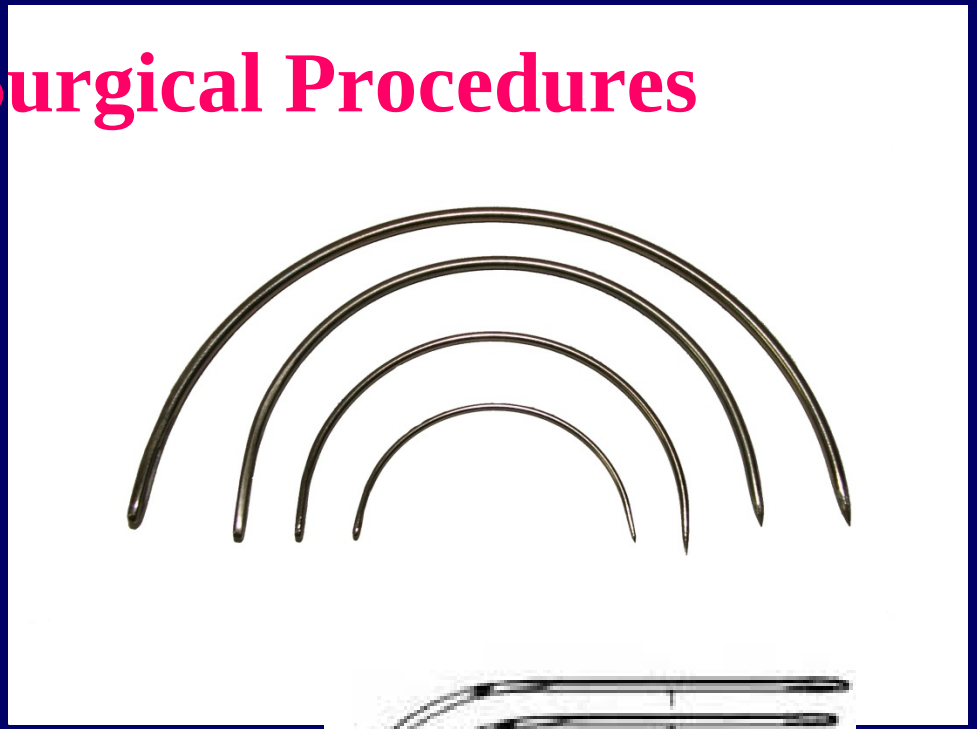

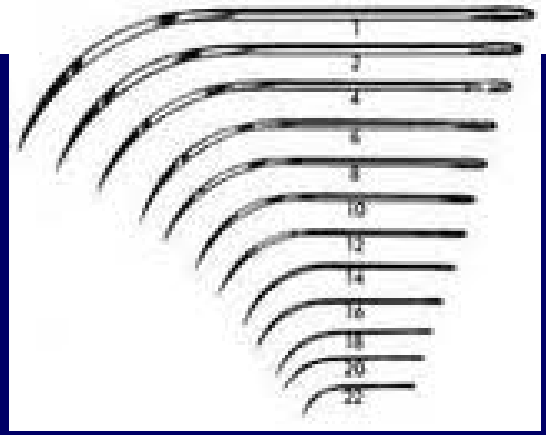

Jefferson™
Kimmel Cancer Center
NCI-designated

Smart (active) needle

- Planning & control computer
- Interface with clinician

- Robotic (mechanized) interface
- Closed-loop feedback controller

Passage for needle

Needle

Concerned gland (prostate)

- Distributed actuation (SMA, piezoelectric, magnetic, etc..)
- Distributed sensors (EM, optical, imaging, F/T, etc..)

Curved Needle vs. Smart (active) Needle

Curved needle:

o Fixed geometrical configuration

- rigid body
- less conformity
- challenging for insertion in organ
- actuation from proximal end only
- limited sensory feedback

Smart (active) needle:

o Variable controlled configuration

- flexible configuration
- distributed actuation
- good geometric conformity
- distributed sensory system (EM, imaging, F/T, optical, etc.)
- distributed actuation and control

Jefferson™ Kimmel Cancer Center NCI-designated

Modeling and Control of Pre-curved Needle Continuum

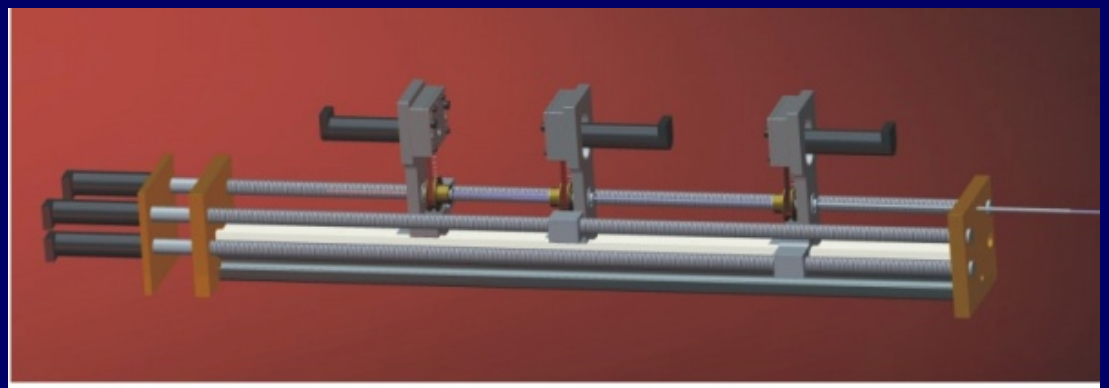

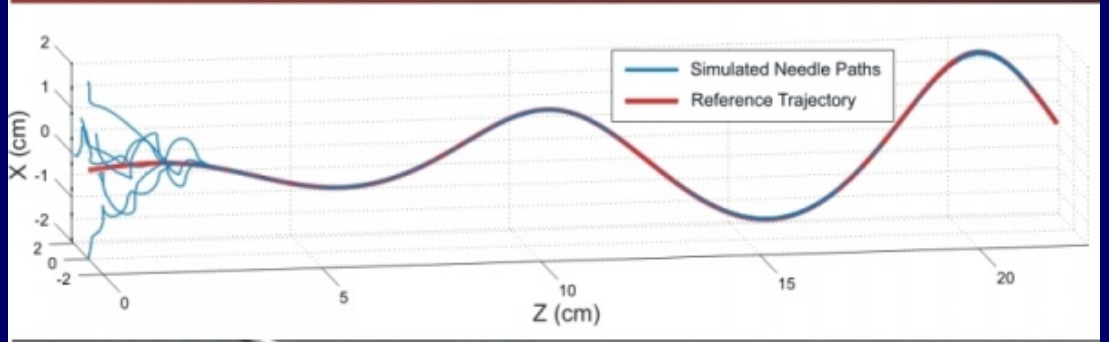

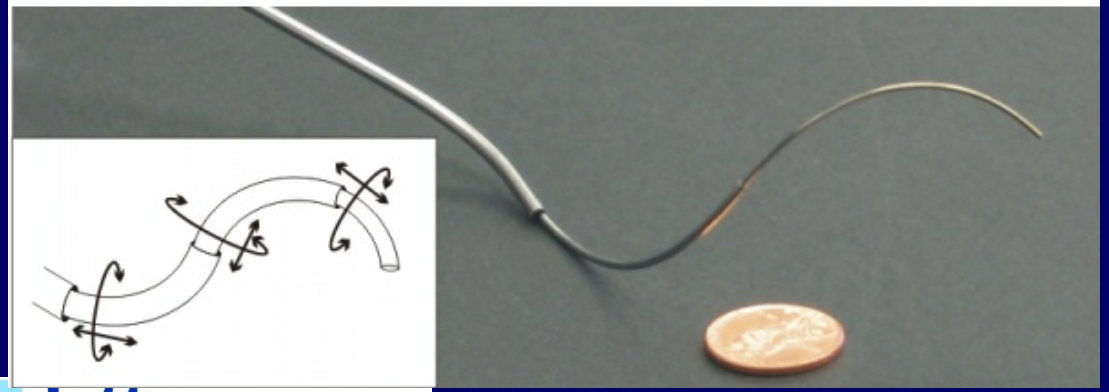

The figures (from top to bottom) show-

(1) a CAD drawing of a new active cannula or steerable needle actuation unit,

(2) a simulation showing that controller can stabilize bevel-steered needles to a 3D reference trajectory from various initial poses,

(3) an active cannula prototype with inset line drawing indicating DOF.

Webster et al., MICCAI 2008

Jefferson™ Kimmel Cancer Center
NCI-designated

Steerable Needle (bevel-tip)

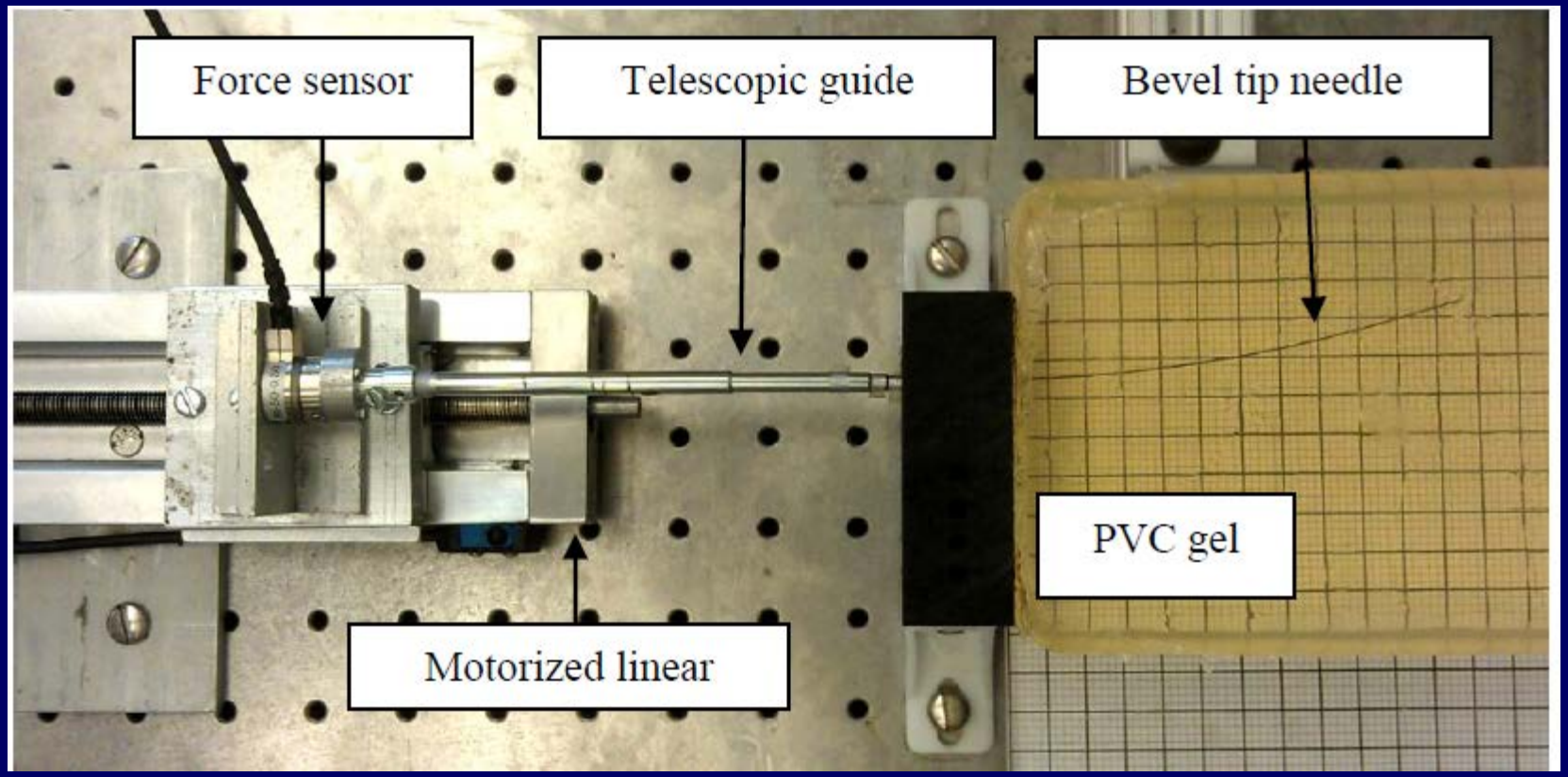

Image-Guided Flexible Needle Steering by Robotic Arm

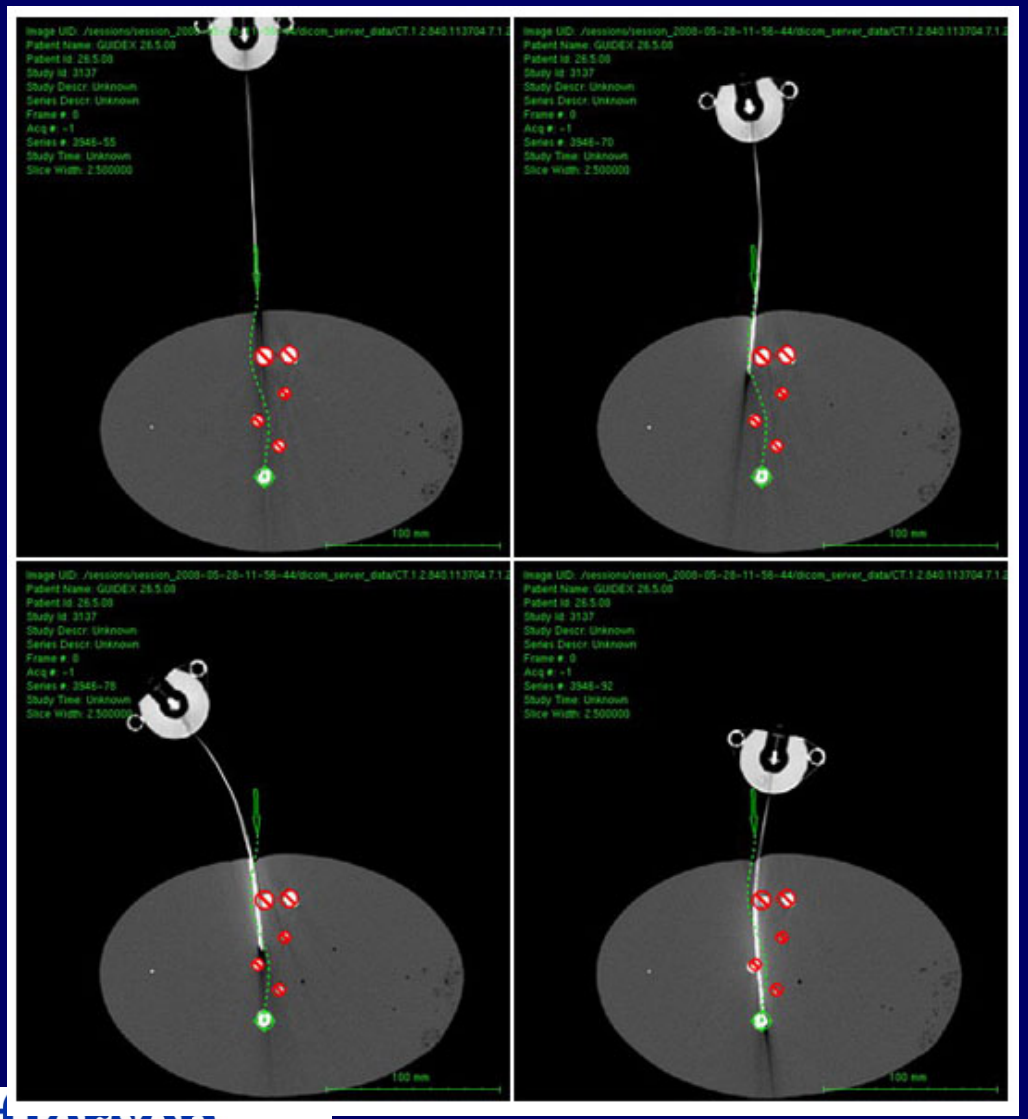

This example illustrates trajectory planning and realization of curved trajectory by a robot. The whole movement is done in the same CT slice and the needle is kept in plane.

Glozman et al., MICCAI 2008

Motion Planning for Steerable Medical Needles

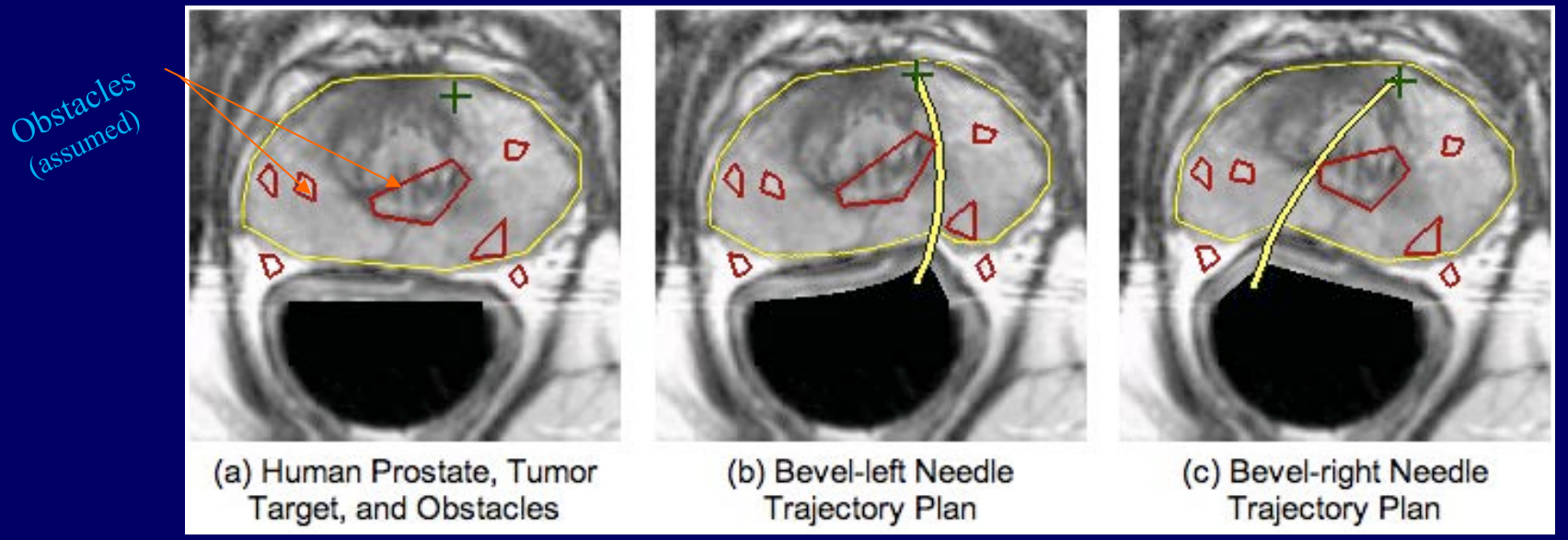

In this example based on an MR image of the prostate, a biopsy needle attached to a rigid rectal probe (black half-circle) is inserted into the prostate (outlined in yellow) using simulation. Obstacles (red polygons) and the target (green cross) are overlaid on the image (a). The target is not accessible from the rigid probe by a straight line path without intersecting obstacles. However, bevel-tip needles bend as they are inserted into soft tissue. The planner computes a locally optimal bevel-left needle insertion plan that reaches the target, avoids obstacles, and minimizes insertion distance (b). Using different initial conditions, the planner generates a plan for a bevel-right needle (c). Due to tissue deformation, the needle paths do not have constant curvature.

Alterovitz et al., MICCAI 2008

Needle (flexible) Steering via Duty-cycled Spinning

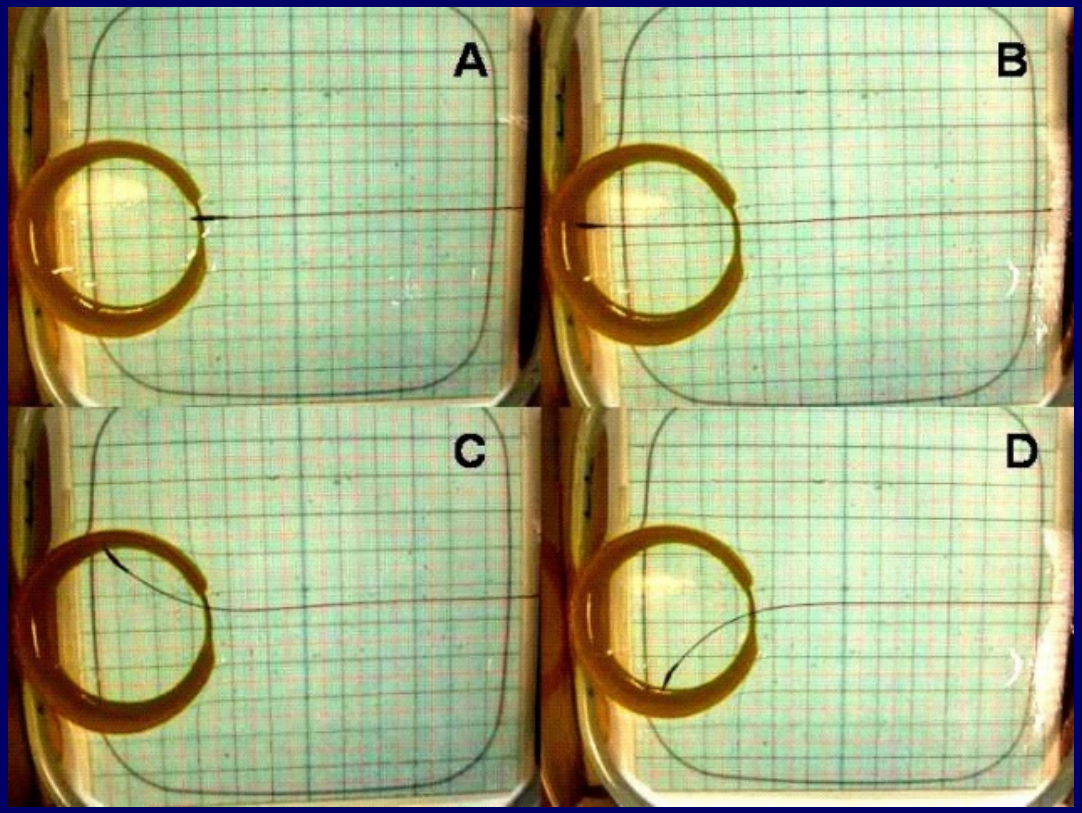

Simulation in a gelatin sample of multi-point "coverage" of a lesion zone using duty-cycled spinning of a bevel-tip needle. The needle is steered to the edge of a treatment zone (A). The needle is then advanced straight forward to the boundary (B). Then the needle returns to the entry point (A), and is advanced to other points in the treatment zone (C, then D), each time returning to the same starting point (as in A). The black gridlines are 1 cm apart.

Riviere et al., MICCAI 2008,

IEEE EMBS 2012

Jefferson™ Kimmel Cancer Center
NCI-designated

Modeling and Planning of Needle Insertions in Deformable Tissue

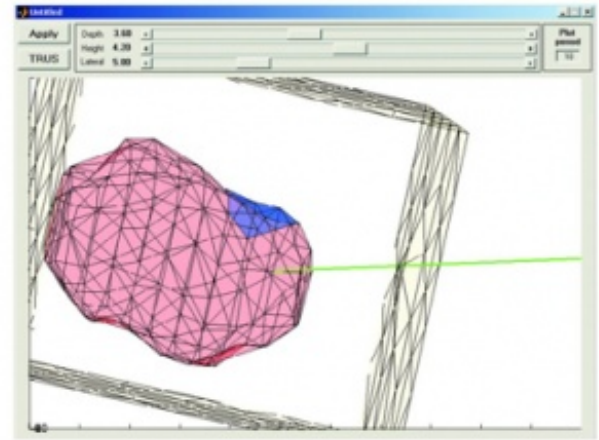

(a)

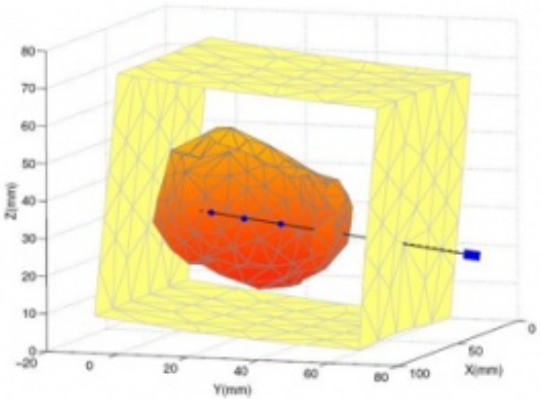

(b)

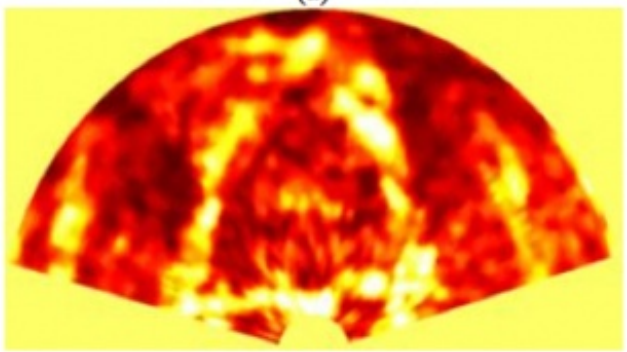

(c)

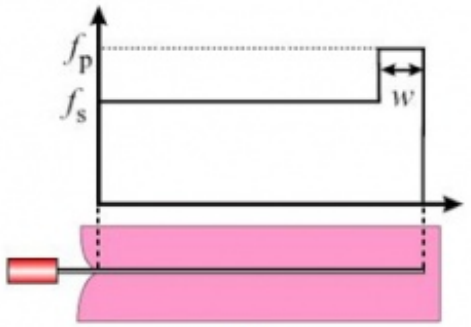

(d)

(a) shows the needle insertion simulator with a simplified mesh of the prostate and the surrounding tissue.

(b) shows the needle inserted with optimal initial insertion parameters. In this situation the needle passed through the targets in the presence of the tissue deformation.

(c) Vibro-elastographic image of the prostate in the transverse view.

(d) the three-parameter force distribution along the needle shaft.

Salcudean et al., MICCAI 2008

Jefferson™ Kimmel Cancer Center
NCI-designated

Optically Actuated MR-compatible Active Needle

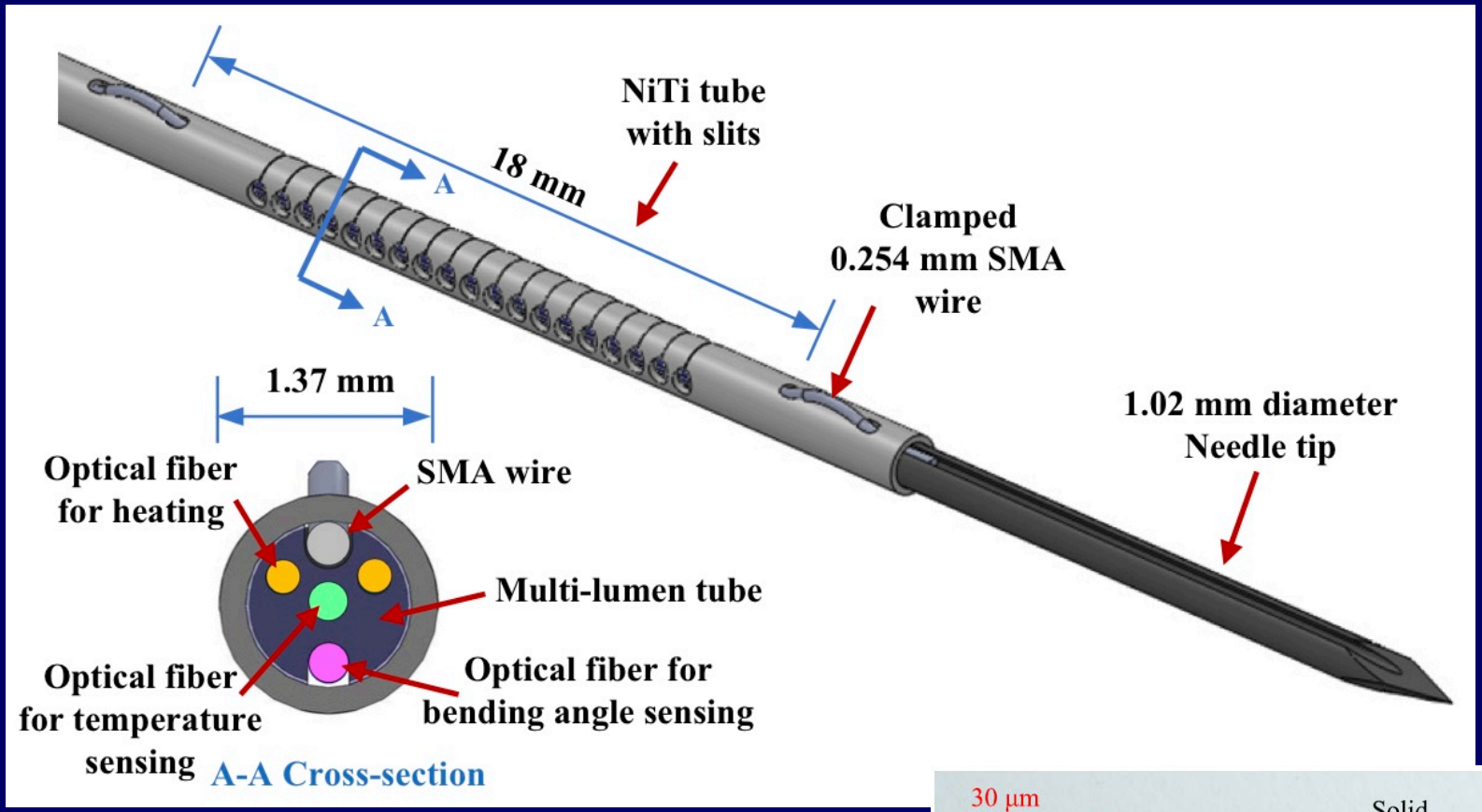

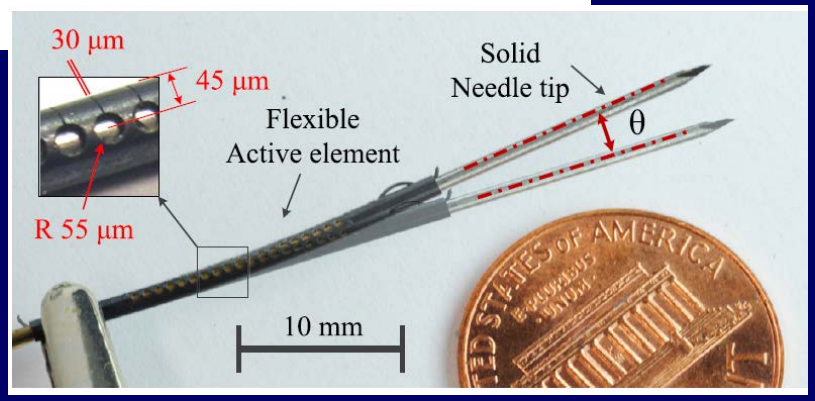

Ryu, IEEE IROS 2011

Jefferson™ Kimmel Cancer Center
NCI-designated

Optically Actuated MR-compatible Active Needle

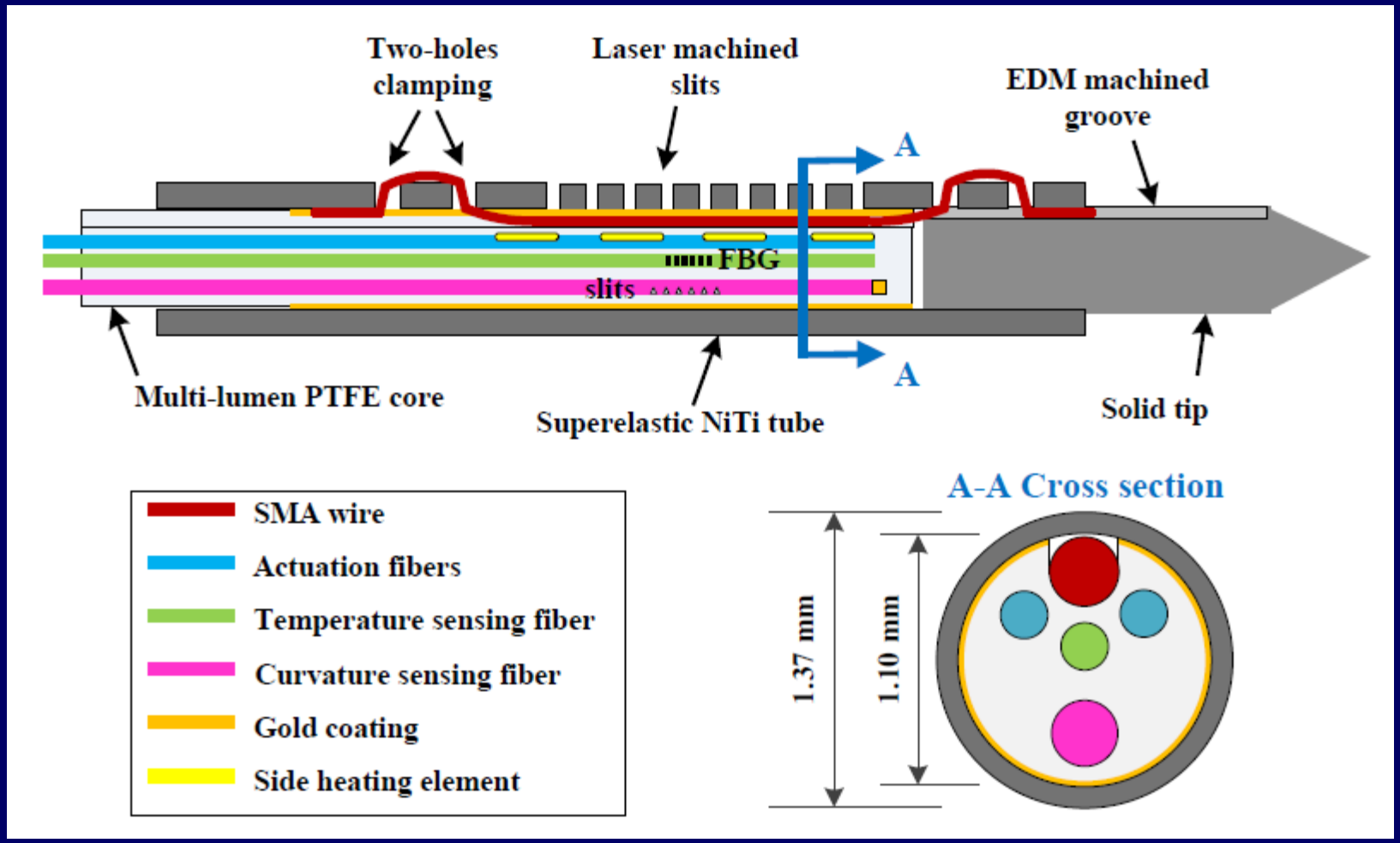

Ryu, PhD Thesis, 2012

Jefferson™ Kimmel Cancer Center
NCI-designated

Optically Actuated MR-compatible Active Needle

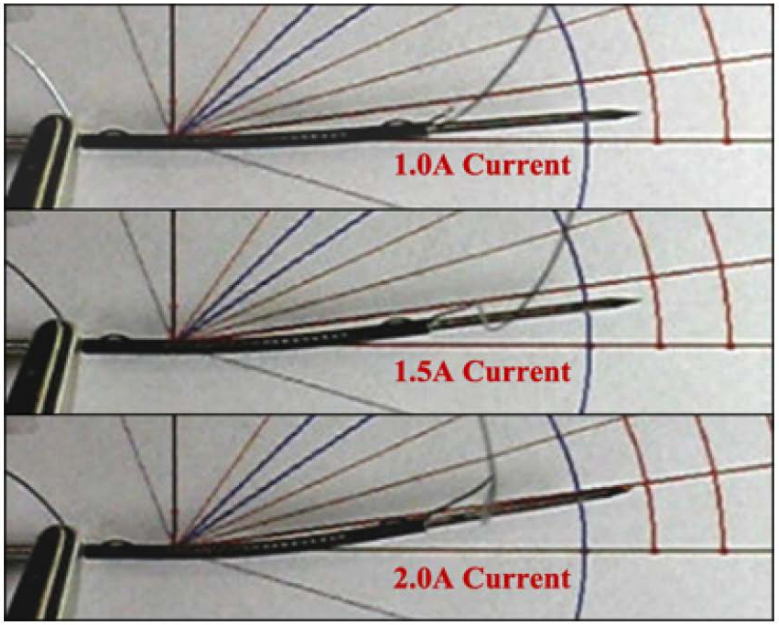

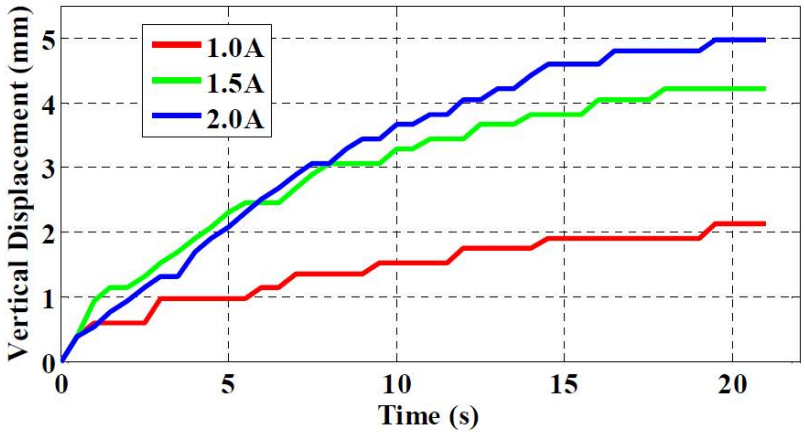

Vertical deflection of the active needle tip with Joule heating.

Ryu, IEEE IROS, 2011

Jefferson™ Kimmel Cancer Center
NCI-designated

Optically Actuated MR-compatible Active Needle

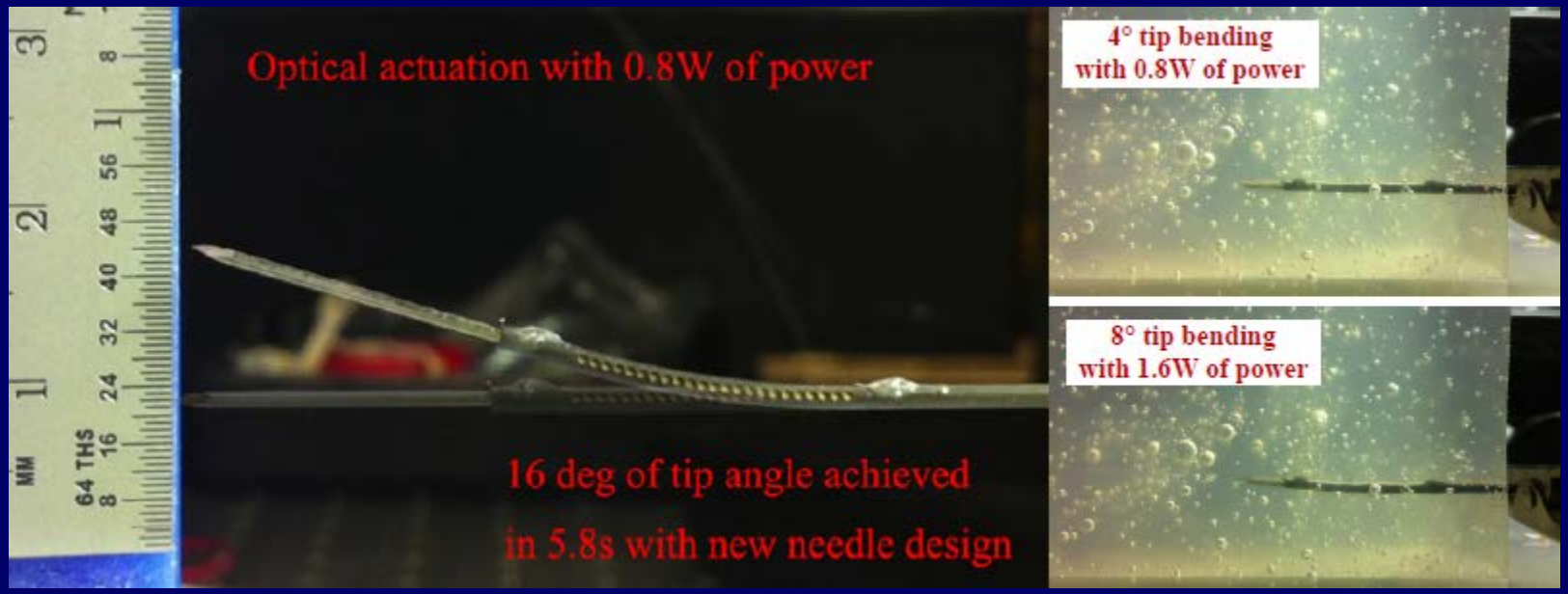

Optical activation of the new needle prototype and mechanical phantom tests: (left) as expected, two times faster bending achieved (right) bending capability in tissue phantom slightly increased but limited by heat loss and tissue reaction force

Ryu, PhD Thesis, 2012

Jefferson™ Kimmel Cancer Center
NCI-designated

SMA-actuated Smart (active) Needle Design

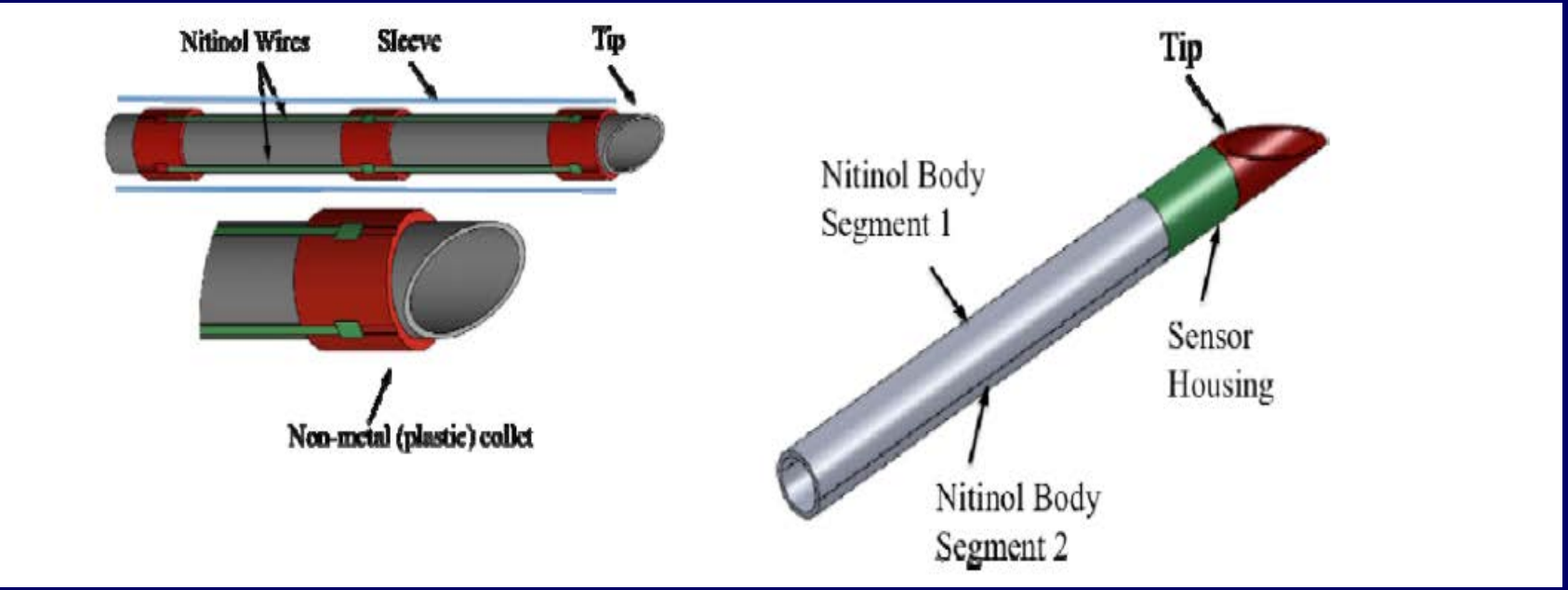

Two types of needle design and actuation techniques: Longitudinal body segment design (left) and lateral body segment design (right).

Podder et al., MedPhys 2012

SMA-actuated Smart (active) Needle Control

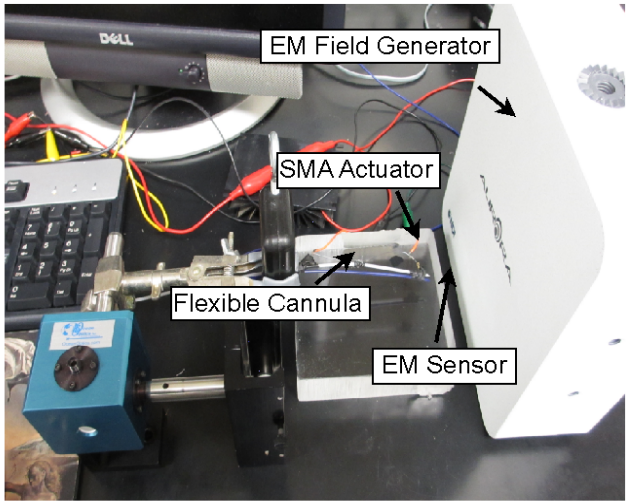

(a)

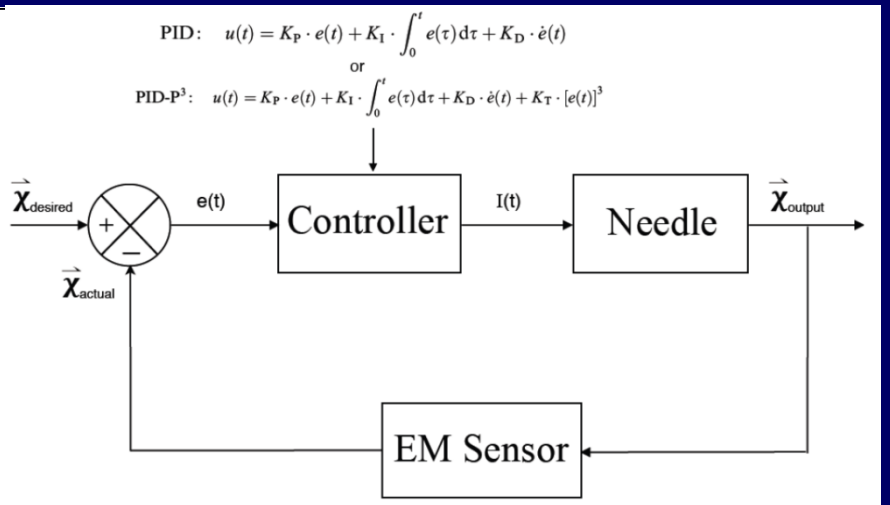

(b)

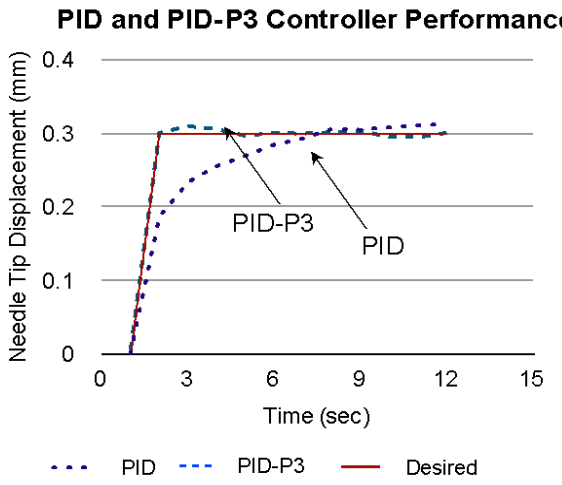

(c)

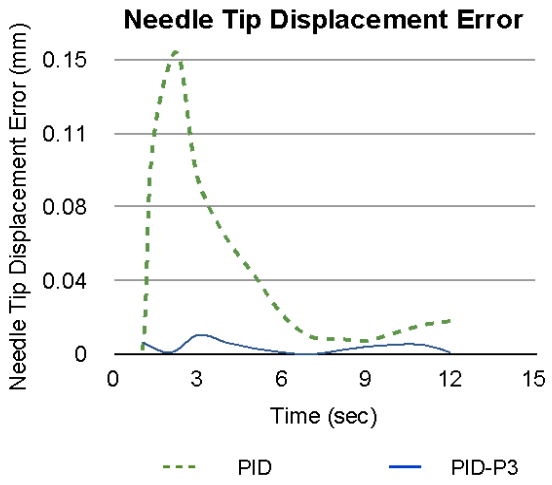

(d)

(a) Experimental setup, (b) control block diagram, (c) control performance, (d) errors.

SUMMARY

- IGBT robotic platforms are in active development and testing in preclinical settings.
  - About 15 robotic systems developed in 5 countries.
- Accuracy in needle placement and seed delivery as assessed in phantoms are promising.
  - The 3D seed placement error is at sub-millimeter level (EUCLIDIAN).
- Clinical study is the next step.
  - Where applicable, FDA Investigational Device Exemption (IDE) has been obtained (EUCLIDIAN).
- AAPM Working Group on Robotic Brachytherapy was formed in 2008
  - AAPM TG192 formed in 2009, to produce report in <1 yr

SUMMARY (cont.)

- The feasibility of cancer discrimination in real time along interstitial needle tracks is demonstrated.
  - ROC analysis: validation set achieved AUC = 0.90
  - The proposed technique may be implemented in robotic brachytherapy with online force sensing and real-time planning to achieve targeted dose painting.
- Investigation in tissue-mimicking phantom materials, needle-tissue interaction models, flexible needle control and “smart” (active) needle prototypes further broadens the landscape of interstitial interventions such as implantation therapy and targeted biopsy/tissue resection under robotic assistance.

Thank you!

Work supported by:

NCI BRP Grant

R01 CA91763

"Robotic-Assisted Platform for Intratumoral Delivery"

DoD CDMRP PCRP Idea Development Grant

PC050733

"Multi-channel Robotic System for Concurrent Delivery and Immobilization of Interstitial Therapeutic Agents"

and

DoD CDMRP PCRP Synergistic Grant

W81XWH-11-1-0397

"Development of a Smart Needling Device for Image-Guided Percutaneous Intervention and Delivery of Therapeutic Agents in Prostate"

Tarun Podder, PhD

Wan Sing Ng, PhD

Deborah Rubens, MD

John Strang, MD

Edward Messing, MD

Lydia Liao, MD, PhD, MPH

Yongde Zhang, PhD

Yida Hu, PhD

Ivan Buzurovic, MS

Lei Fu, MS, ME

Kaiguo Yan, PhD

Jason Sherman, MS

Adam Dicker, MD, PhD

Shan Jiang, PhD

Parsaoran Hutapea, PhD

Jefferson™ Kimmel Cancer Center NCI-designated

Connecticut Area Medical Physics Society (CAMPS) 2013 Fall Conference

October 3, 2013

University of Connecticut Health Center
Farmington, CT

Evolving Role of Physics in Radiation Therapy --- Technology and Beyond

John Wong, Ph.D.

Johns Hopkins University

Acknowledgments

- *Radiation Oncology Physics*
  - T McNutt, E Tryggestad, K Wang, T Roland, ……
- *Radiation Oncology Clinical & Molecular Radiation Sciences*
  - J Herman, P Tran, D Song, H Quon, T DeWeese
- *JHU Computer Science/Robotic Engineering*
  - R Taylor, P Kazanzides, I Iordachita
- *Radiology, Neurosurgery, Neurology, ICMIC, Oncology*
- *JHU Physics & Astronomy*
  - Alex Szalay

Disclosure

- *Small animal platform*
  - *NCI R01 CA158100*
  - *Gulmay Medical Inc. (Xstrahl) Research Agreement Tech transfer and Consultancy*
- *Integrated x-ray CBCT and Ultrasound imaging*
  - *NCI R01 CA 161613*
  - *Elekta Research Agreement and Royalty*
- *Philips Research Agreement*
- *QA Box --- MD Biotech, MD TEDCO, JPLC Associates*

Technology Challenge: TG 142 QA

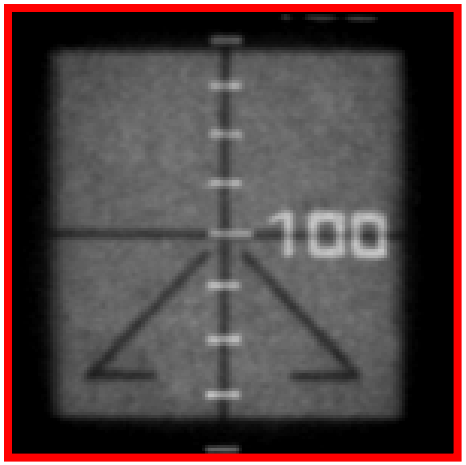

Light field with ODI

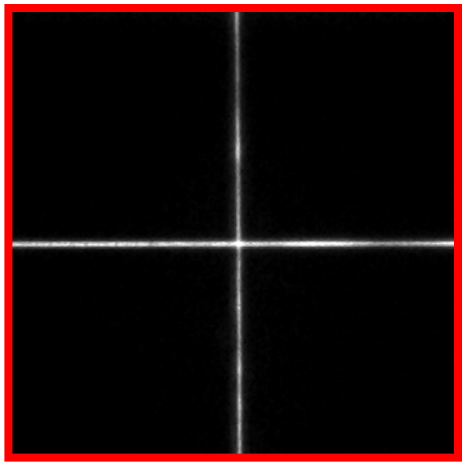

Room Lateral Laser

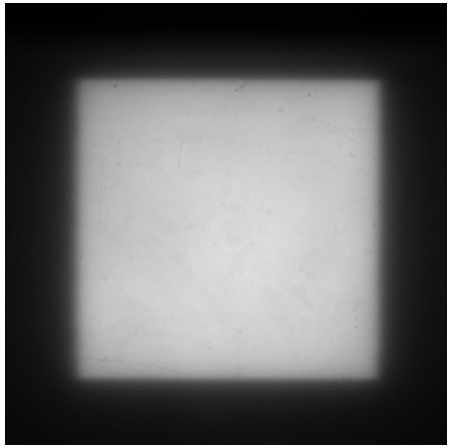

6 MV x-ray at dmax

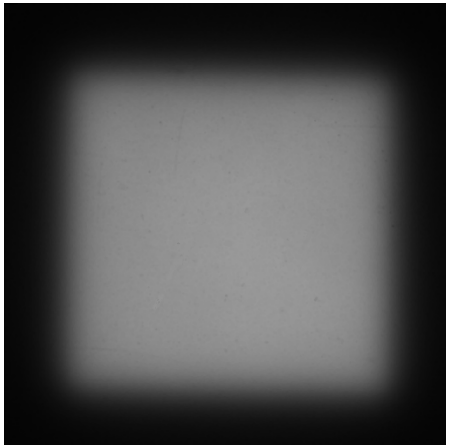

12 MeV electron at dmax

- 1.4 Mpixels, 16-bit, CCD camera to provide 0.2 mm x 0.2 mm per pixel resolution for a 20 cm x 20 cm image
- CCD operates at integration mode
- Optical / Laser imaging *without* buildup on phosphor
- Radiation imaging *with* buildup on phosphor

An Unified QA System for TG 142

- A mirror system that allows capturing images at the isocenter plane with a stationary camera

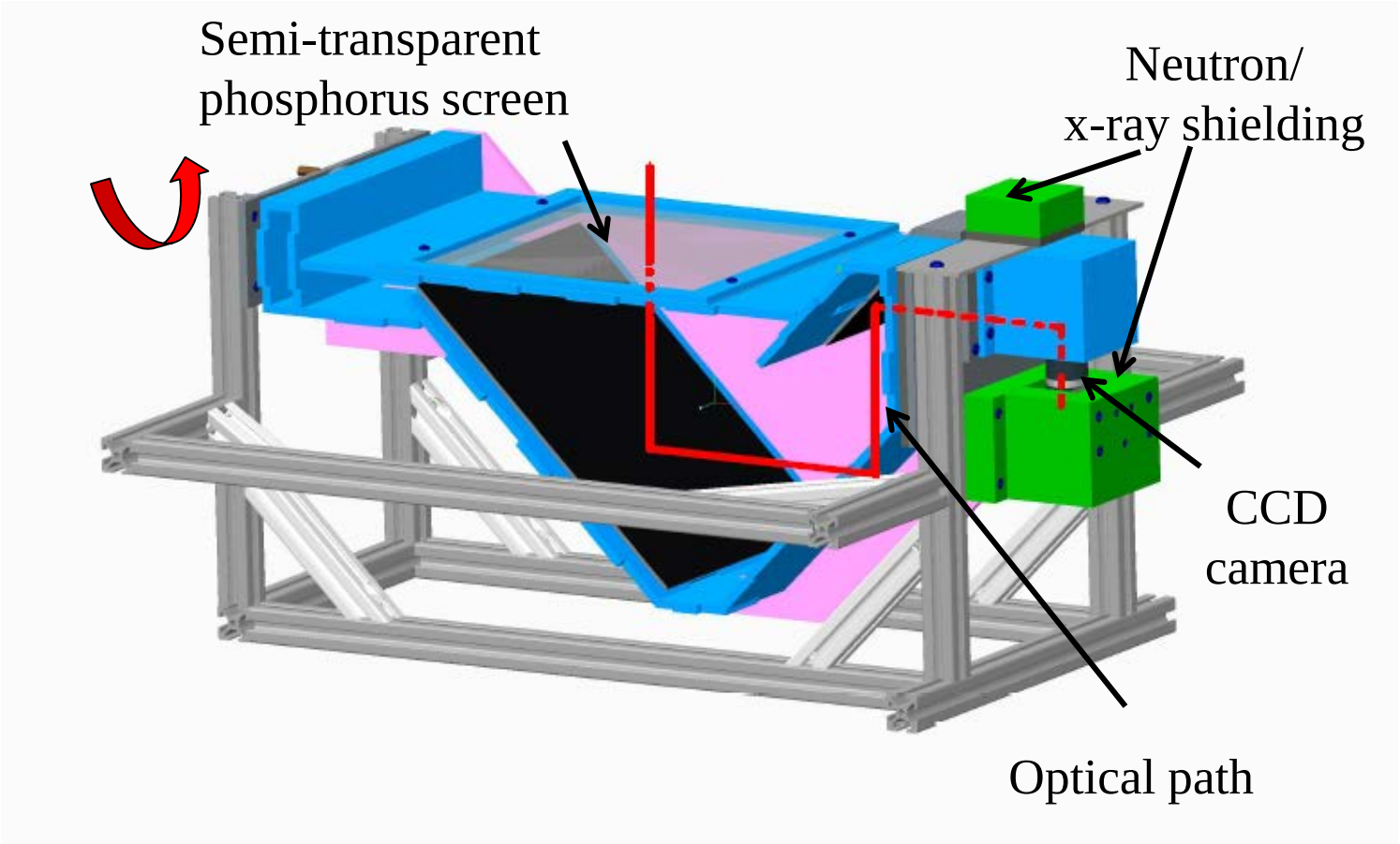

1st prototype

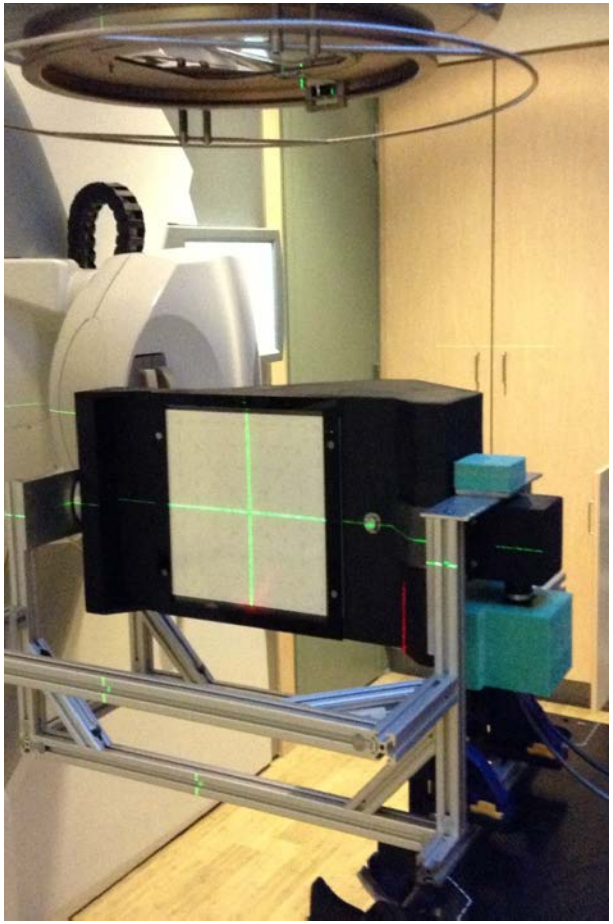

Suspended setup for gantry rotation measurements

Radiation Isocenter QA

- Results of isocentricity
  - Gantry Starshot diameter
  - Collimator Starshot diameter

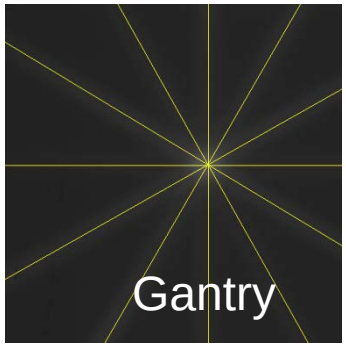

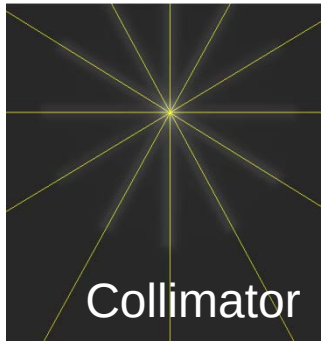

- The use of ***Center Of Mass (COM)*** calculations of a small field (2x2 cm) for collimator, table and gantry rotation
- For collimator:

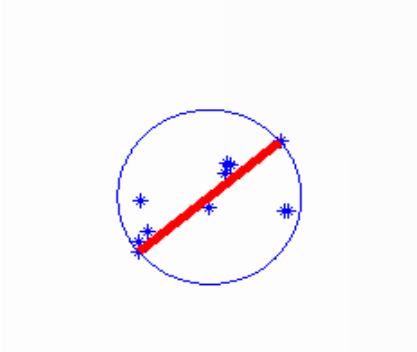

COM diameter = 0.3 mm

Film star-shot,
diameter = 0.7 mm

Method can be applied to gantry rotation instead of gantry star-shot

Raven QA: Product-Grade Prototype

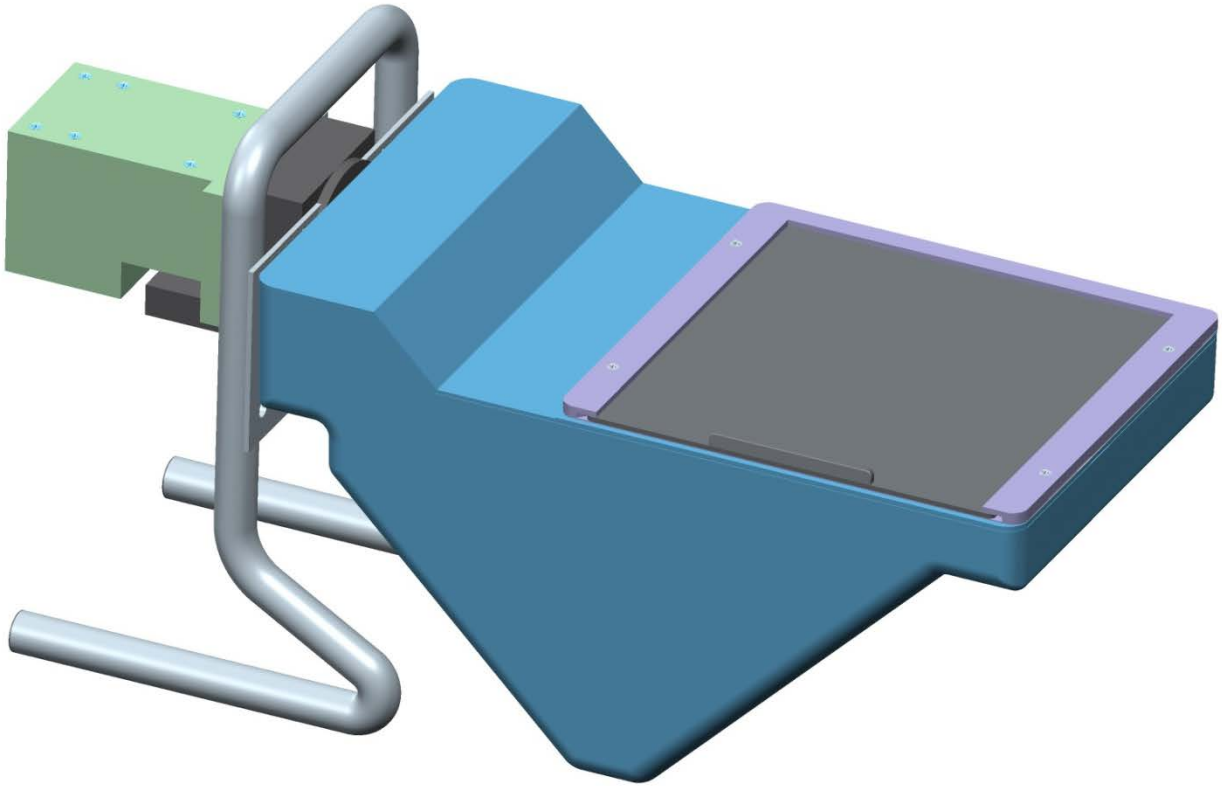

Technology Challenges: IGRT of Soft Tissue Targets

Inter-fraction methods: Cone beam CT, MV CT			
Pros	Adaptive Radiation Therapy	Cons	Ionizing radiation
			Image Quality
Inter-fraction methods: Intra-modal ultrasound imaging			
Pros	Soft tissue information	Cons	Snap Shot (at present)
	Non-ionizing		Expertise/operator dependence
Intra-fraction methods: Implanted Markers			
Pros	Real-time monitoring	Cons	Invasive
	Non-ionizing option		Ionizing radiation
			Soft tissue surrogate (truth?)

- Emergence of MRI-Radiation Machines

Phase 1 Prototype MRI-GRT

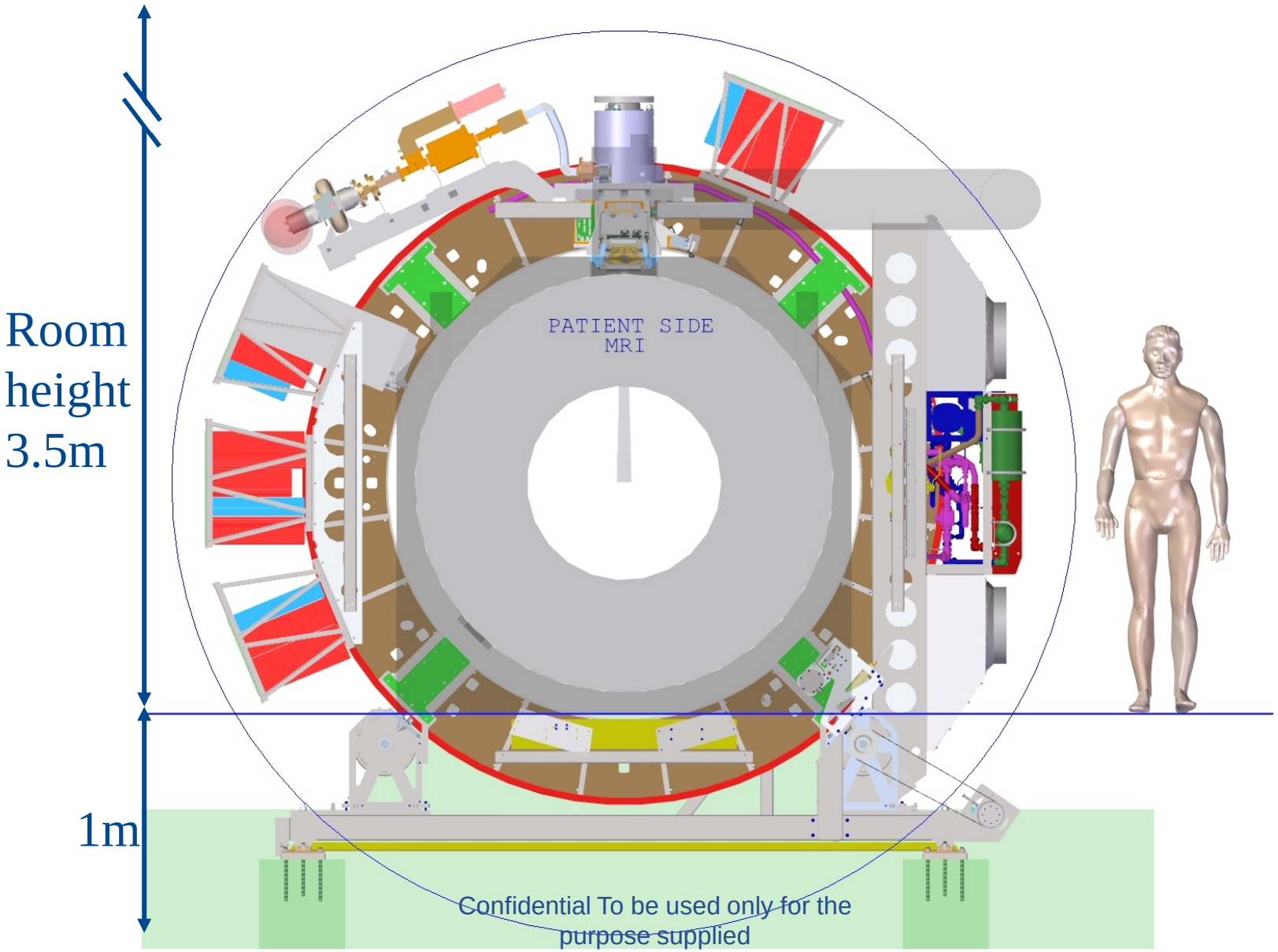

MRI-GRT project : Current Status

- MRI Magnet full on at 1.5T and able to image
- Linac able to radiate
- MLC able to move leaves
- Gantry able to rotate

At the same time !

Cine MRI on MRI-GRT concept platform

- 2 frames per second
- Kidneys, liver and spleen can be followed in real time

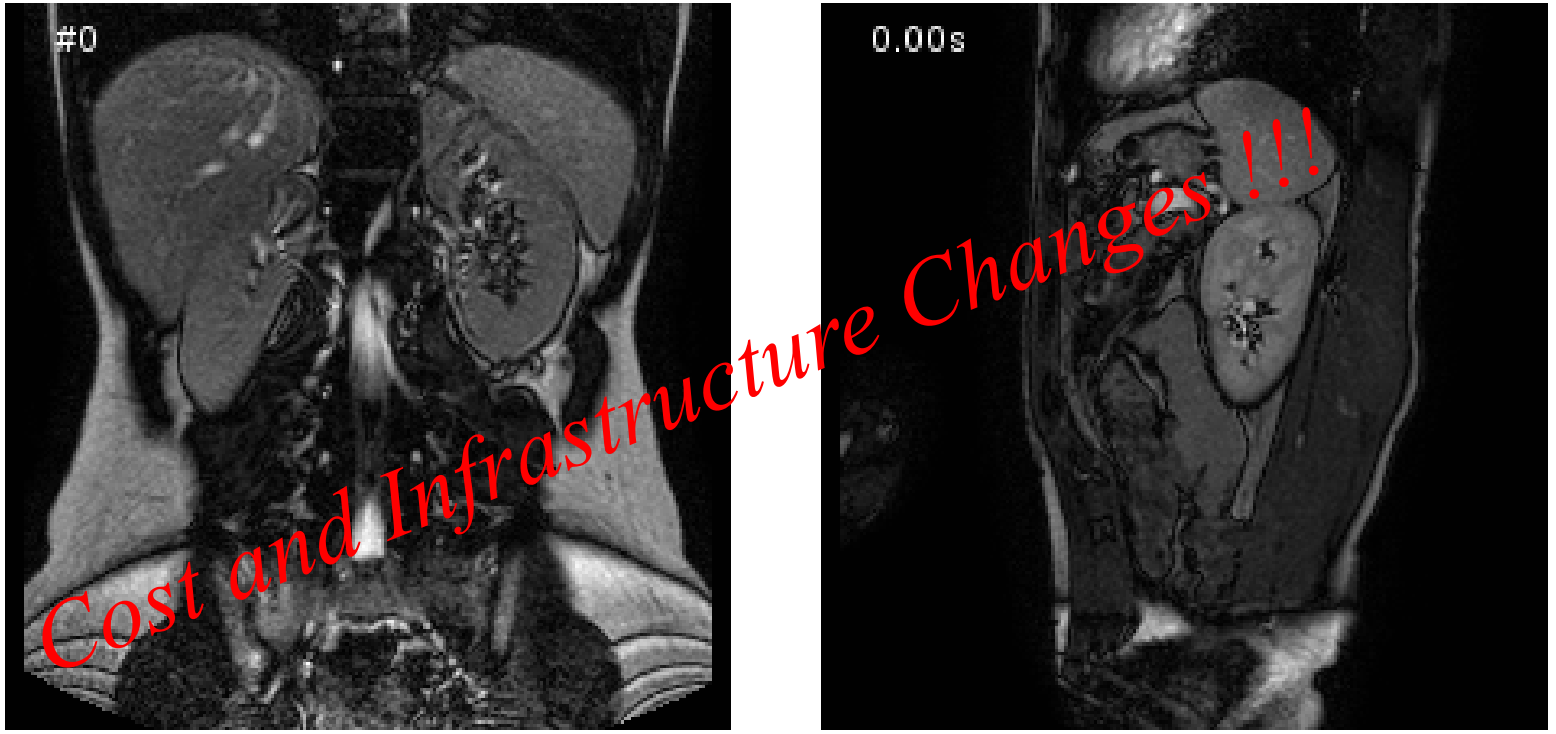

Courtesy UMC Utrecht

Integrated 3D ultrasound/CBCT imaging for soft tissue IGRT

Hypothesis:

- US-CBCT offers an non-ionizing, non-invasive inter- and intra-fraction solution for soft tissue targets
- Prostate, liver, pancreas

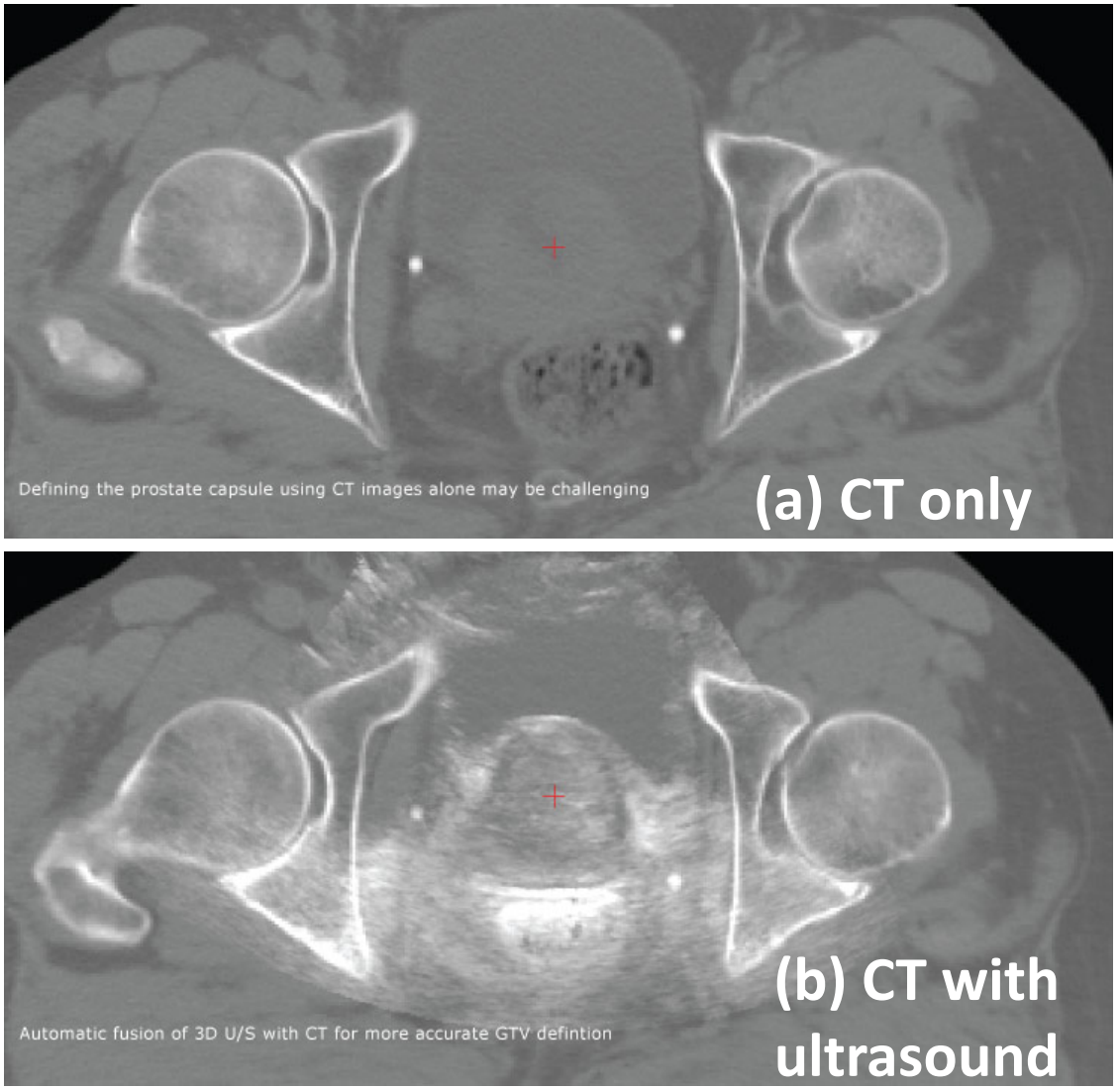

Challenges of US imaging	Solutions
Reproducibility / operator dependence	Robotic placement of a 3D probe
Deformation of anatomy	Keep US probe in place during irradiation while avoiding beams → Intra-fraction monitoring
Soft tissue registration	By definition, auto-fusion of CBCT and real-time US

Require simulation/planning of patient in treatment position with the ultrasound/CBCT system in place

Passive robotic arm and gel phantom

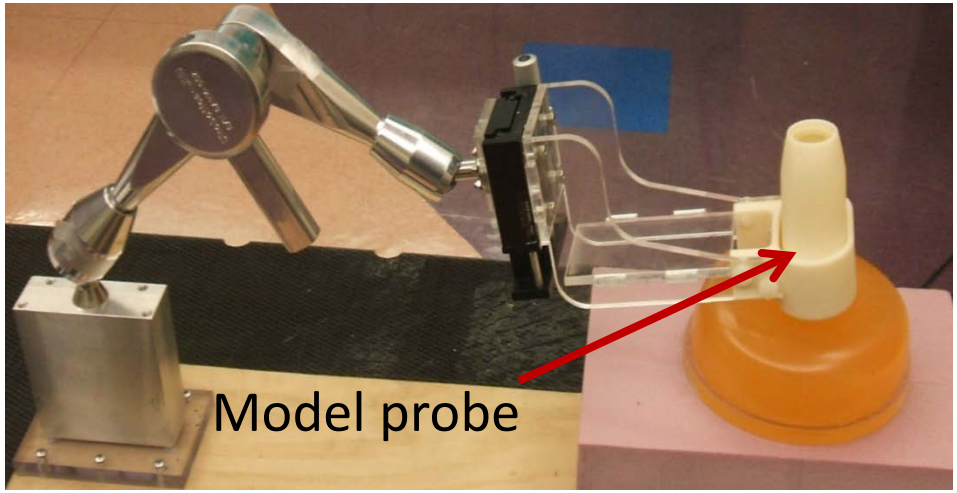

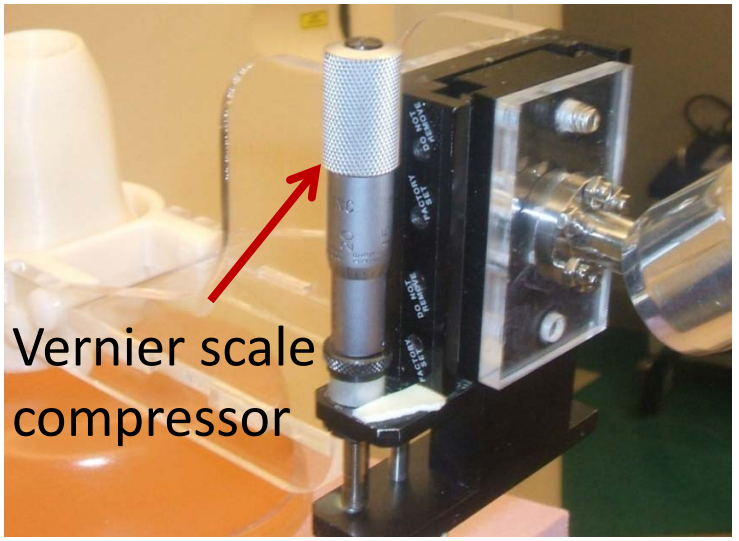

- A passive robotic arm with 1D linear (vernier scale) actuator
- Deformable gel phantoms with embedded 12 PMMA beads (1.2, 2.8, 3.2 mm in diameter)
- CT scans of repeat cycles compress/release to determine reproducibility
- Intra-, inter-fraction reproducibility all within 1 mm

Ex-vivo Bovine Liver in gel phantom

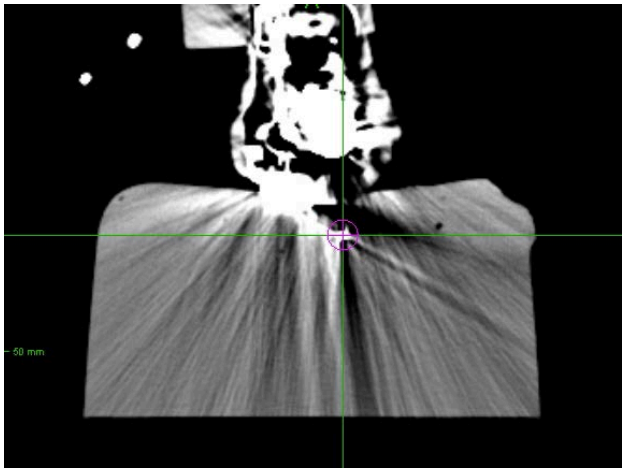

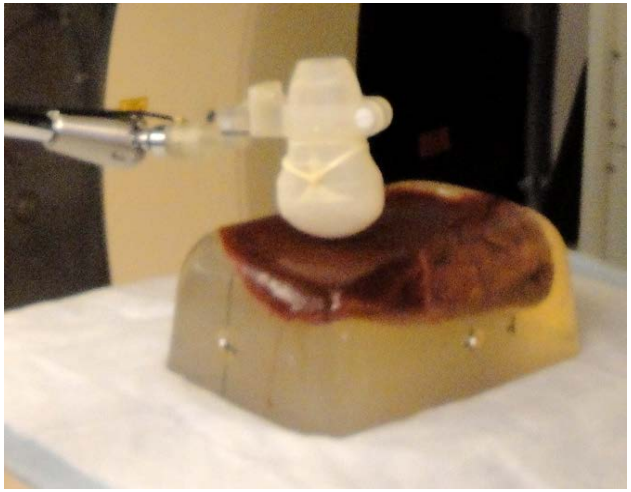

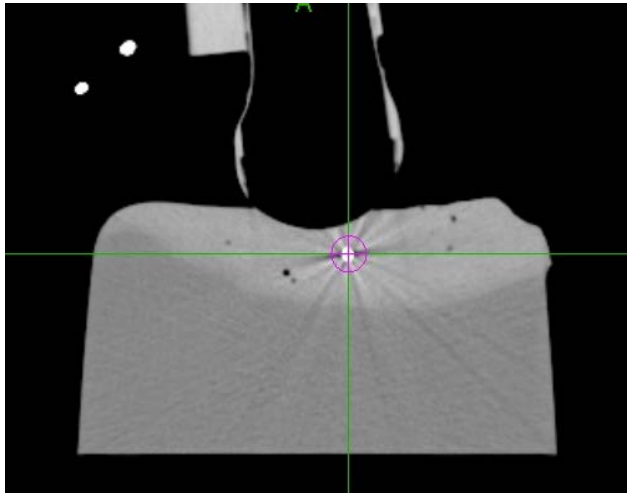

- Gel phantom was overly simplistic with uniform deformation
- A more realistic ex-vivo liver phantom was devised
- Comparison of deformation was made between ultrasound and model probe.

Reproducibility of Deformation

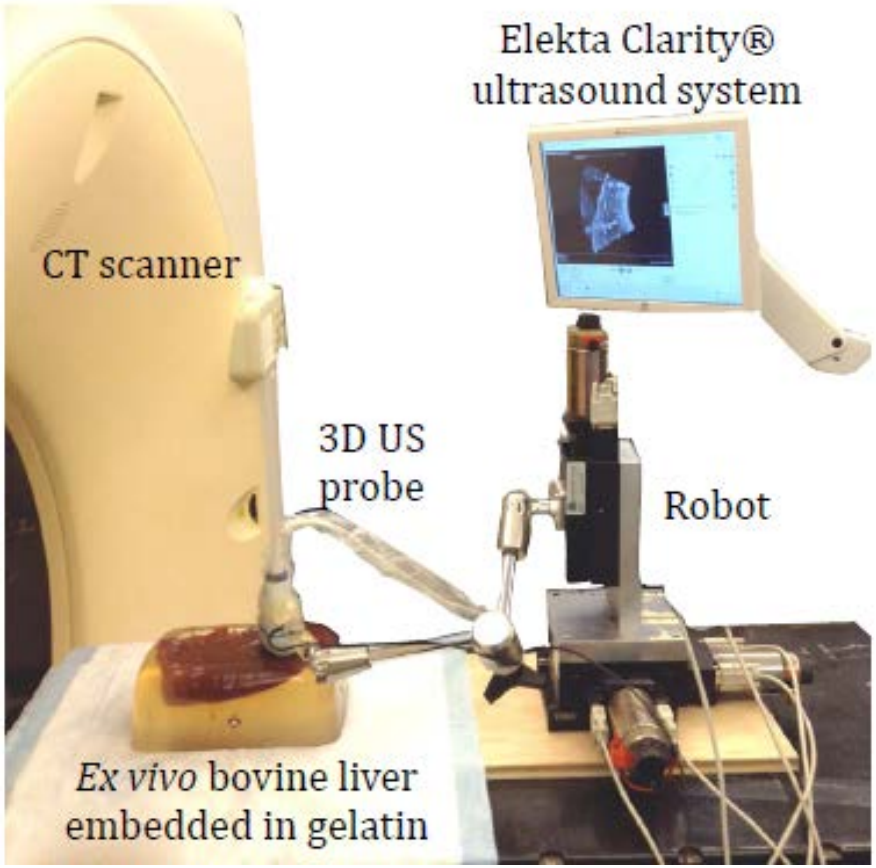

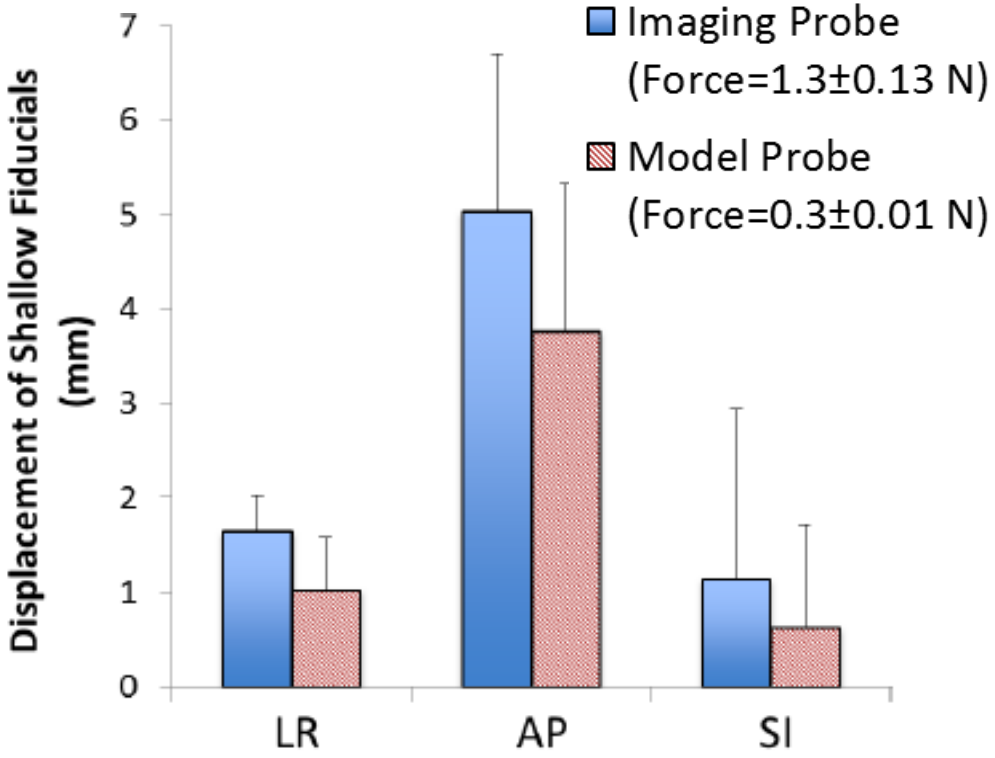

Contact forces lower with model probe
The robotic arm needs to be stiffened

- Significant compression force differences between gel and liver phantom
- Suitability of phantom material is of concern


PHILIPS

Prostate (Force = 14 N)

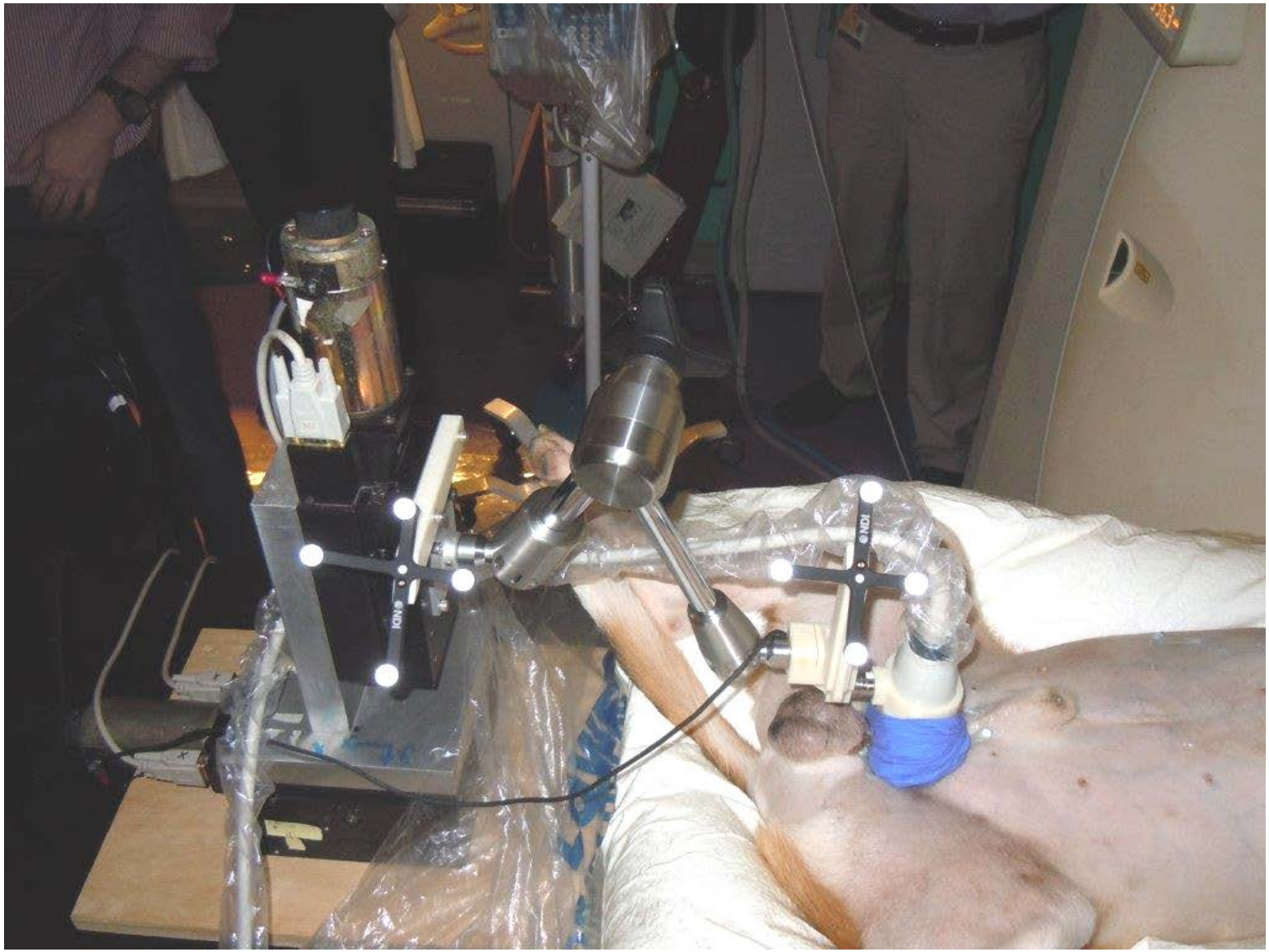

Prostate Images

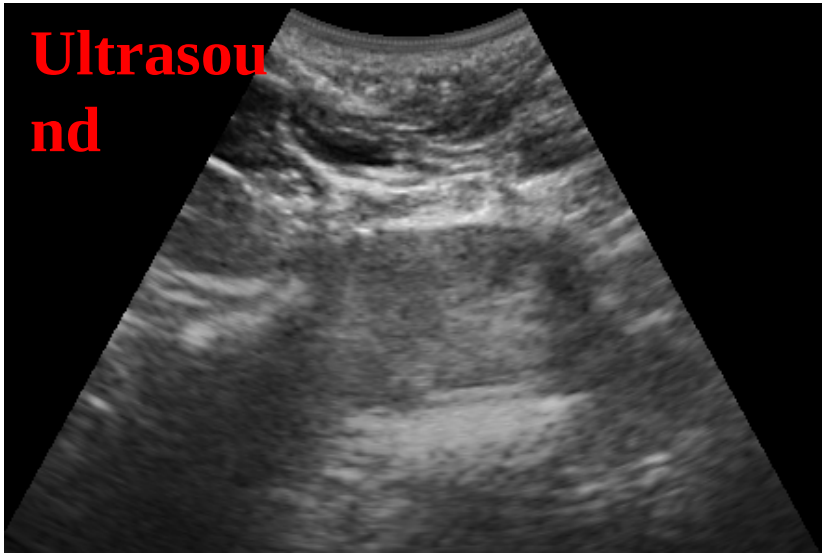

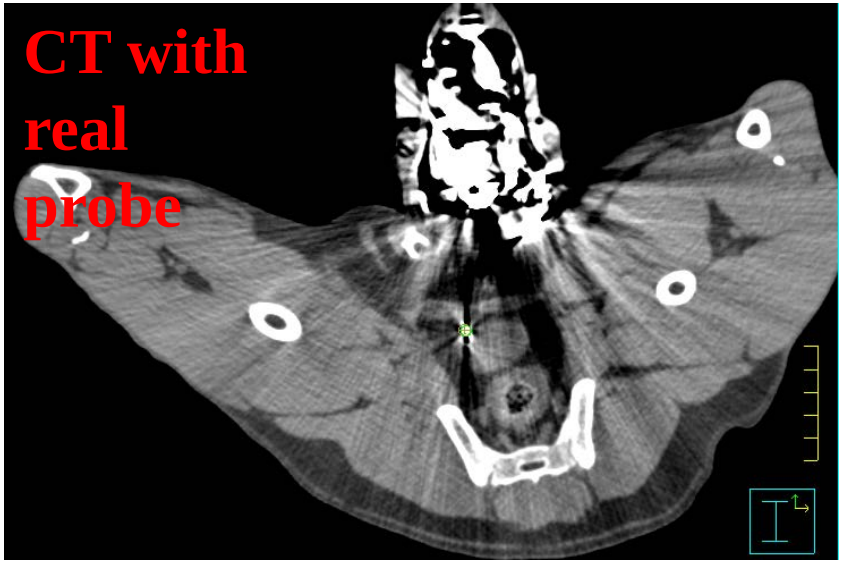

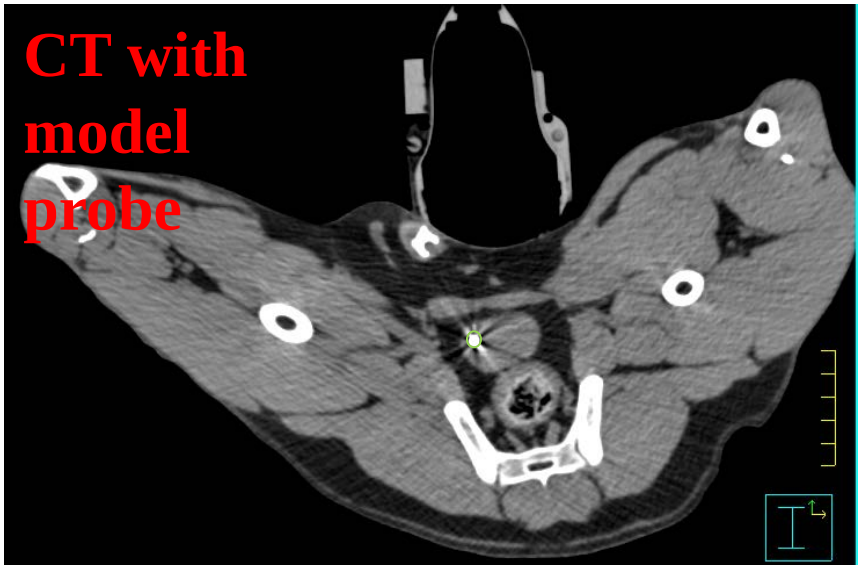

Prostate (Force = 14 N; 10 N ~ 1 kg):
Marker Position Reproducibility in Interquartile Range

Real Probe: 3D mean error=0.6 mm

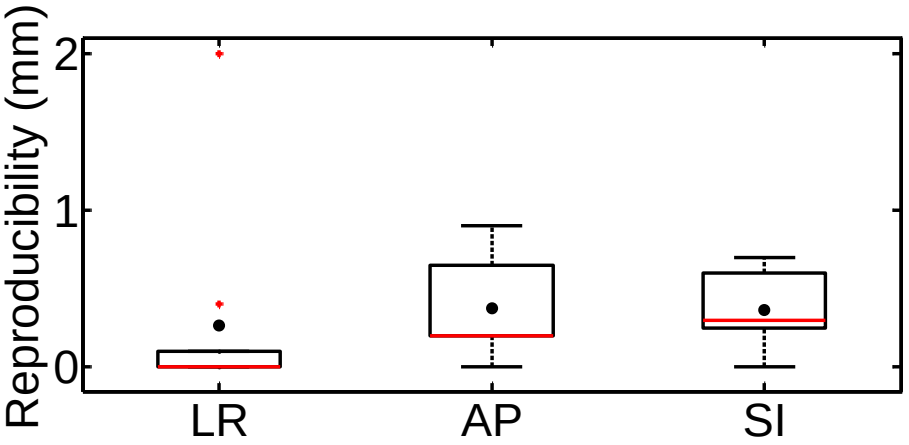

Model Probe: 3D mean error = 0.7mm

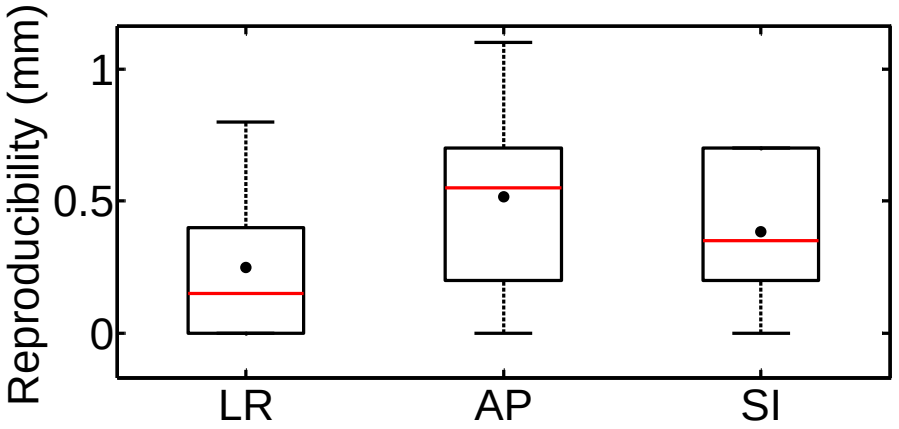

No Probe: 3D mean error = 0.4mm

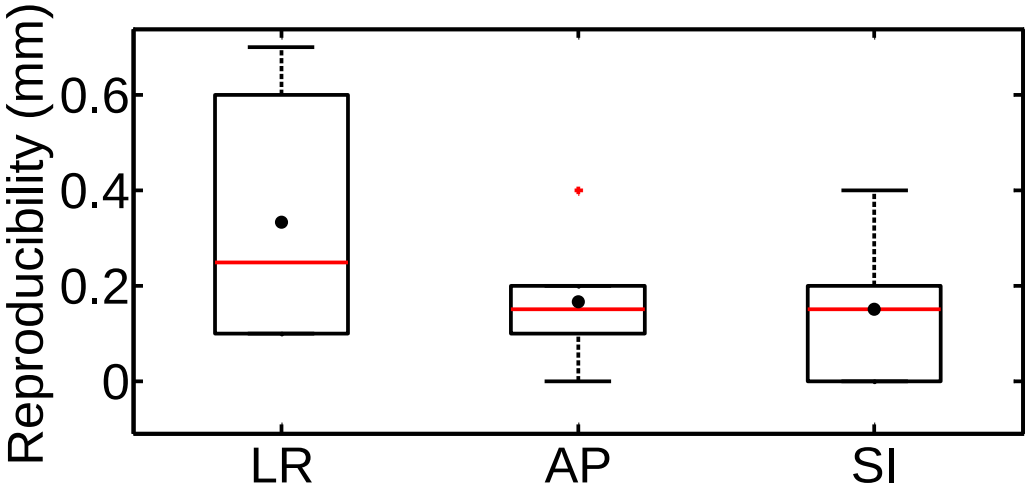

Prostate:
Probe-Induced Marker Displacement (from no probe)

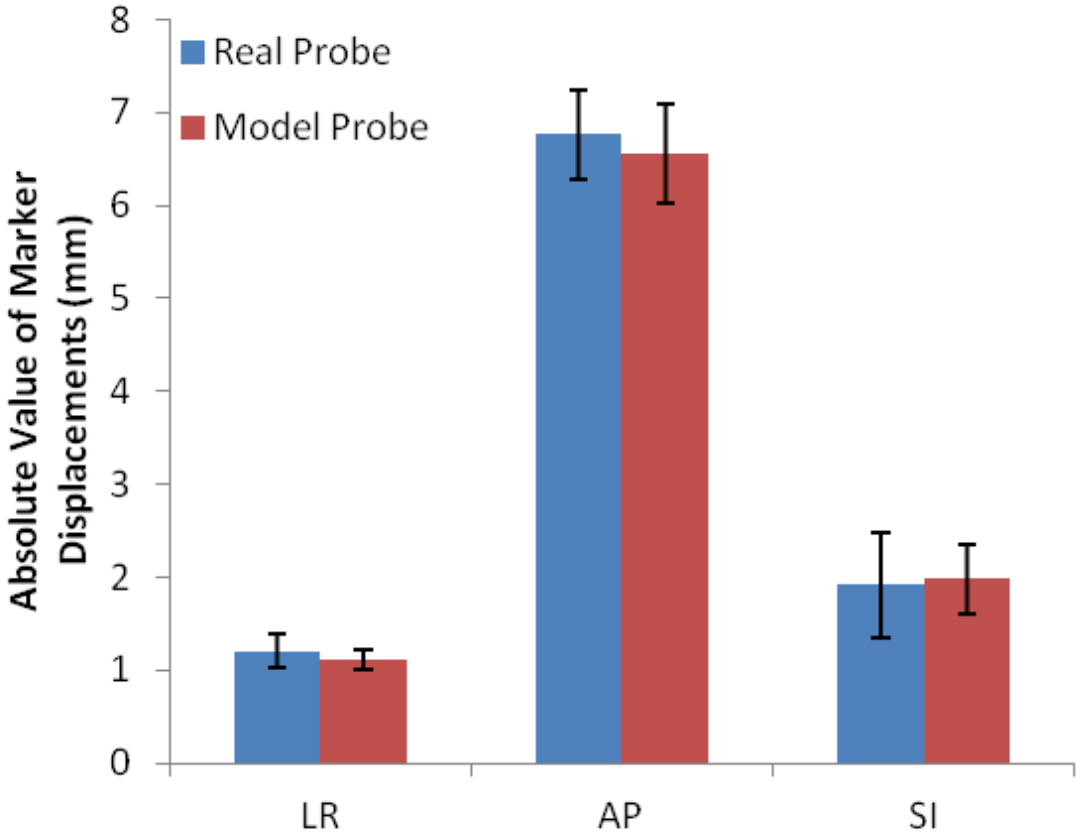

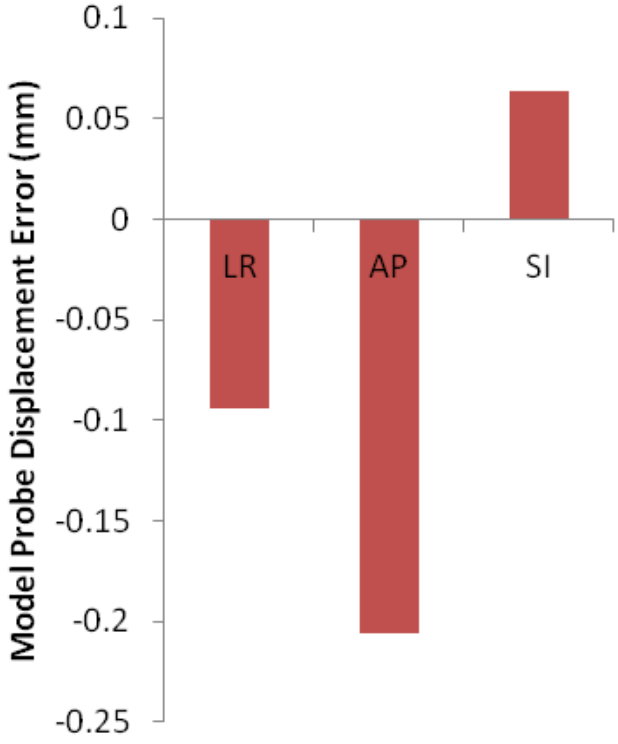

3D mean error
= 0.2mm

Liver at Breath-hold (Force = 40 N)

Liver CT and Ultrasound Images

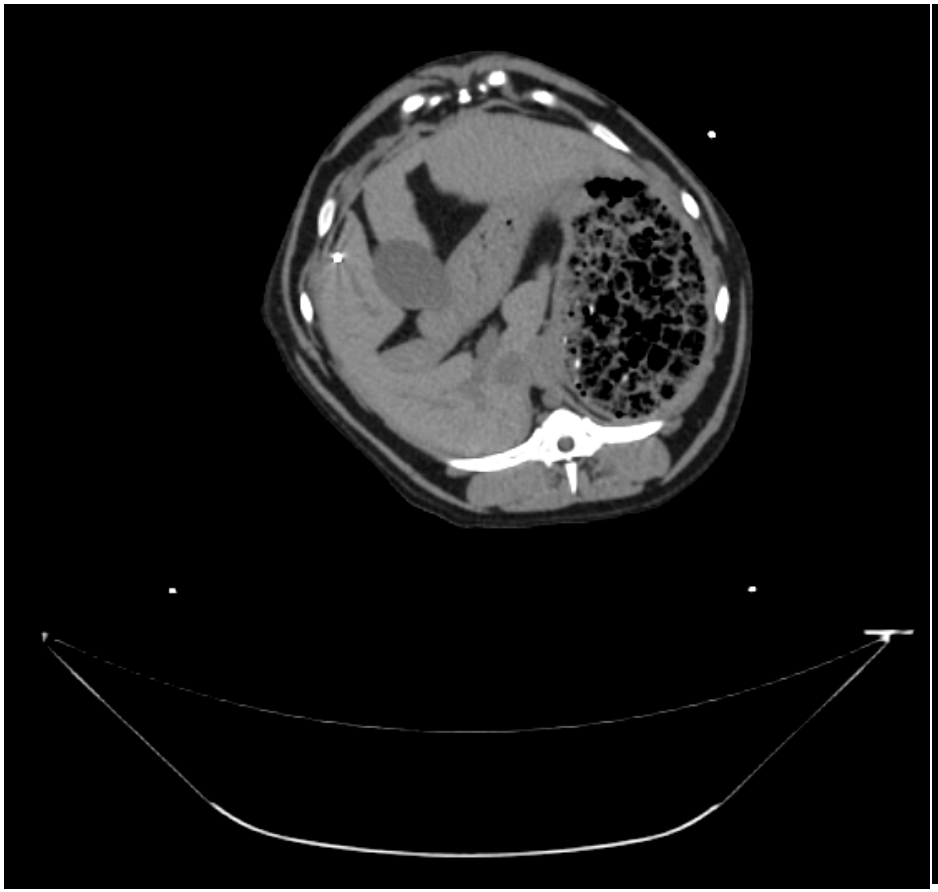

Liver (at Breath-hold): Probe-Induced Marker Displacement

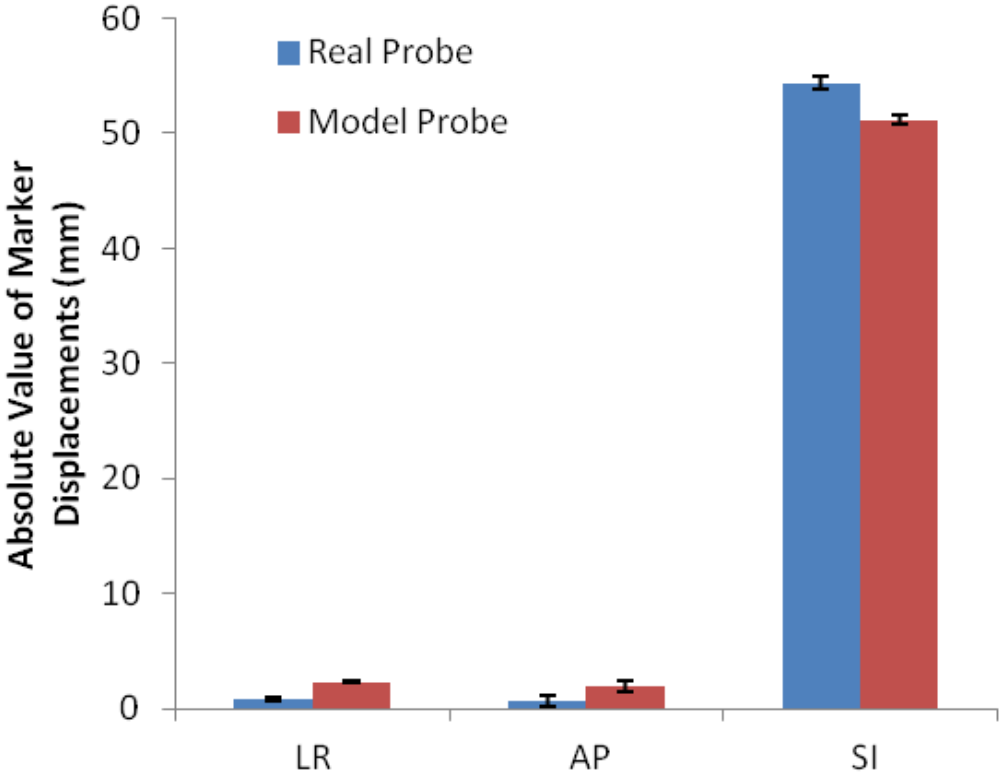

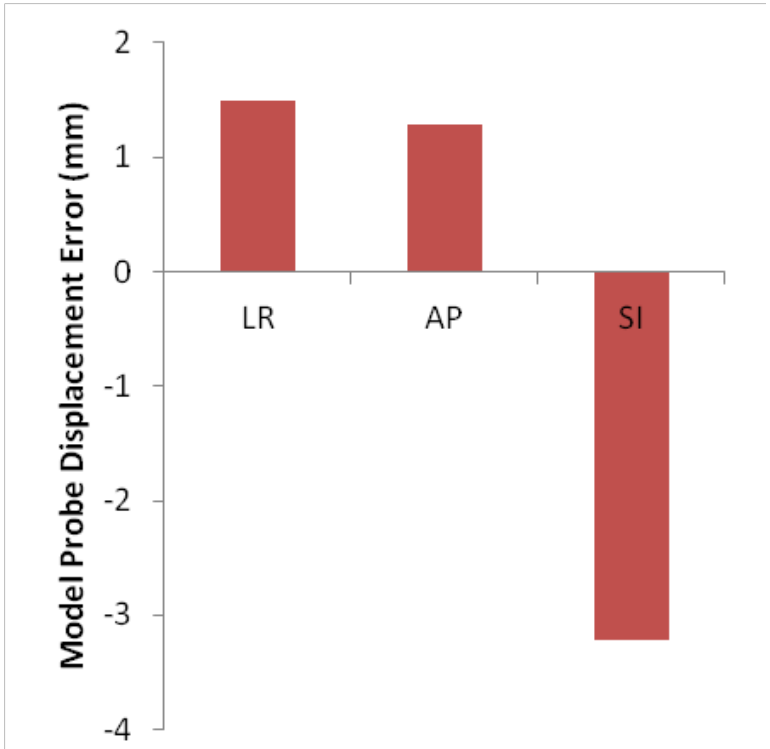

3D mean error
= 4.1 mm

Model of Elekta-Resonant 4D prostate system: Novel transperineal (TPUS) scan

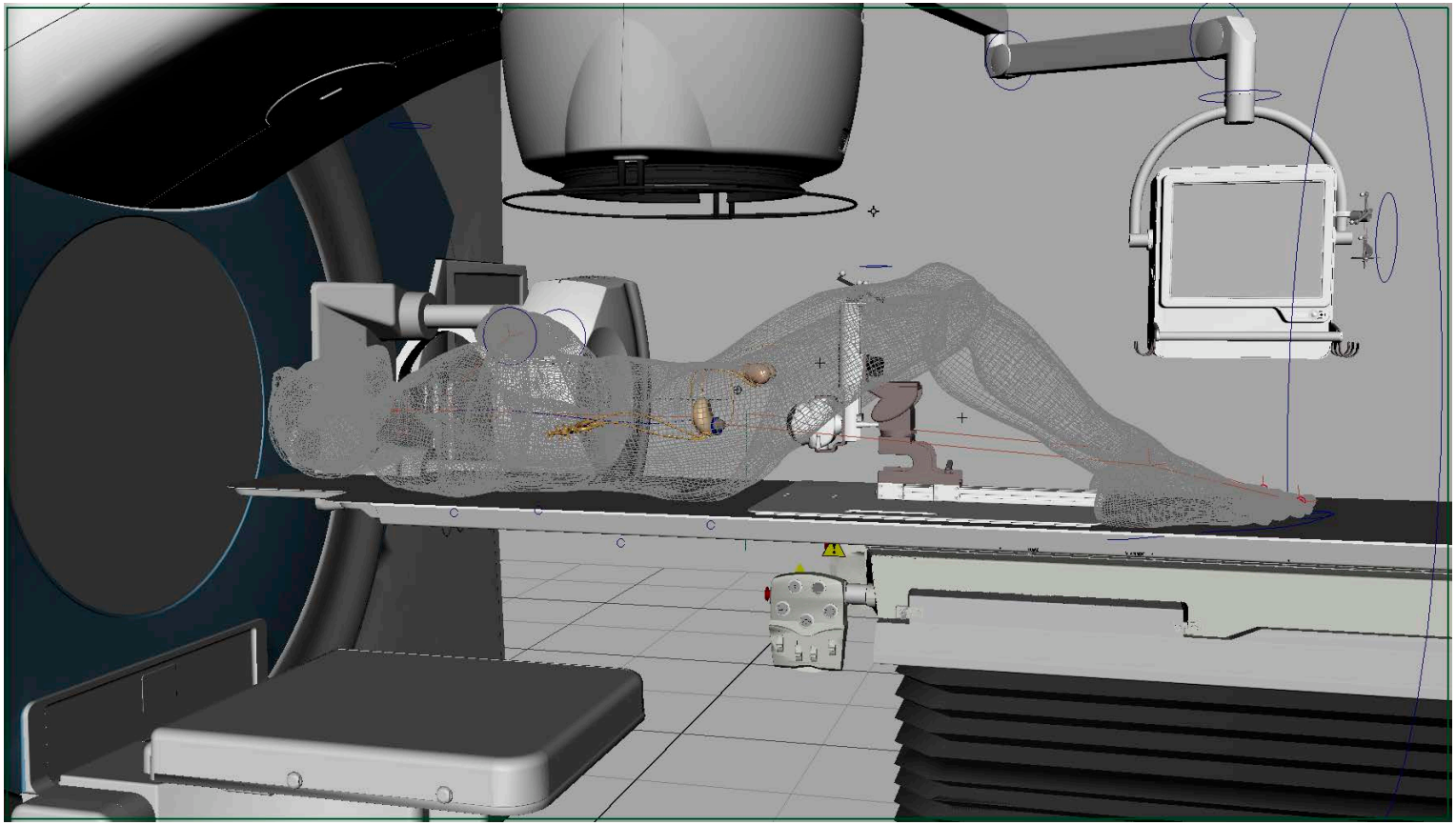

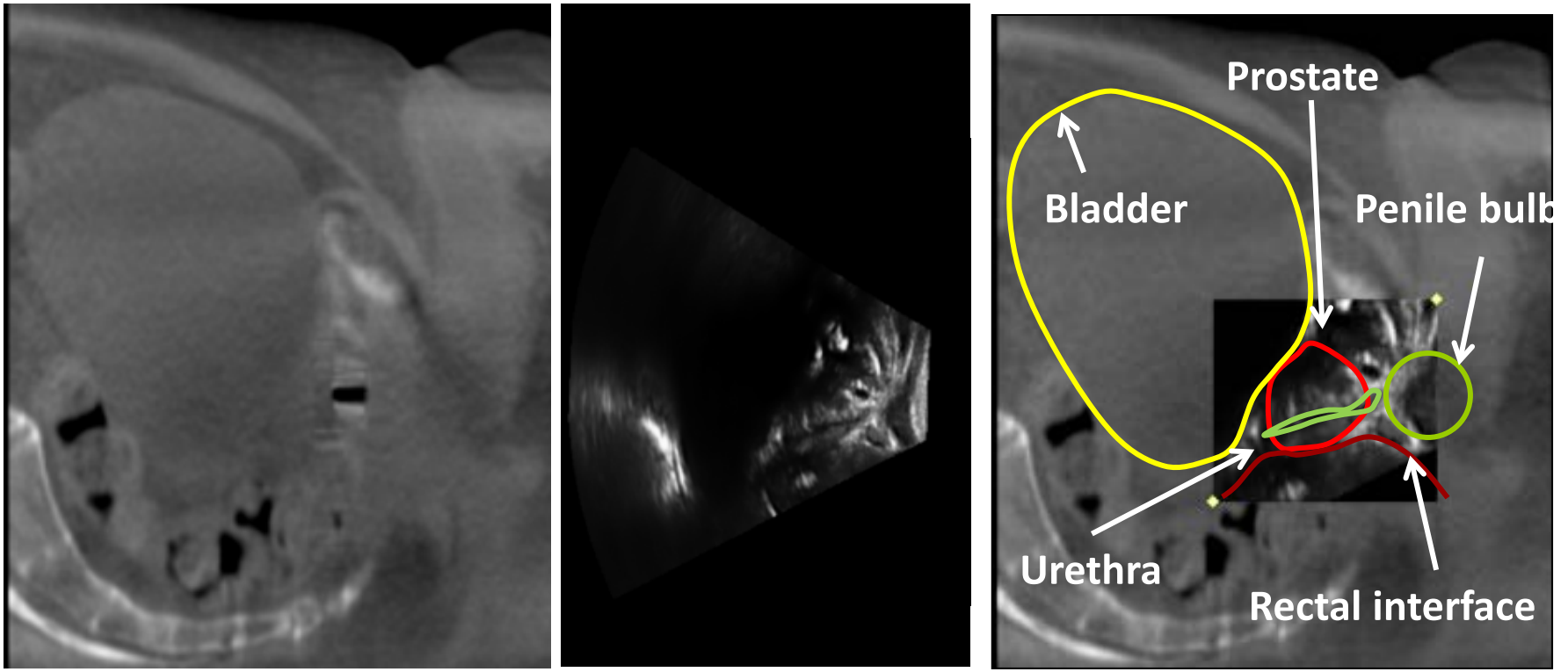
Prostate
Bladder
Penile bulb
Urethra
Rectal interface

stop monitoring

Capturing reference volume.

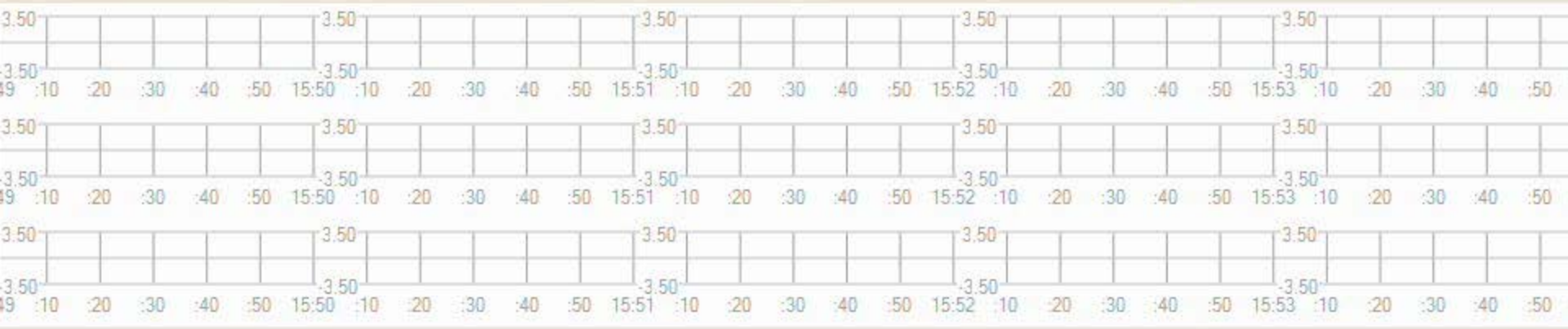

Oncospace

JOHNS HOPKINS
MEDICINE

Analytic database for personalized medicine and data sharing in radiation oncology

Radiation Oncology and Molecular Radiation Sciences
Johns Hopkins University

Re-engineering the Cooperative Research Model

Present (RTOG)

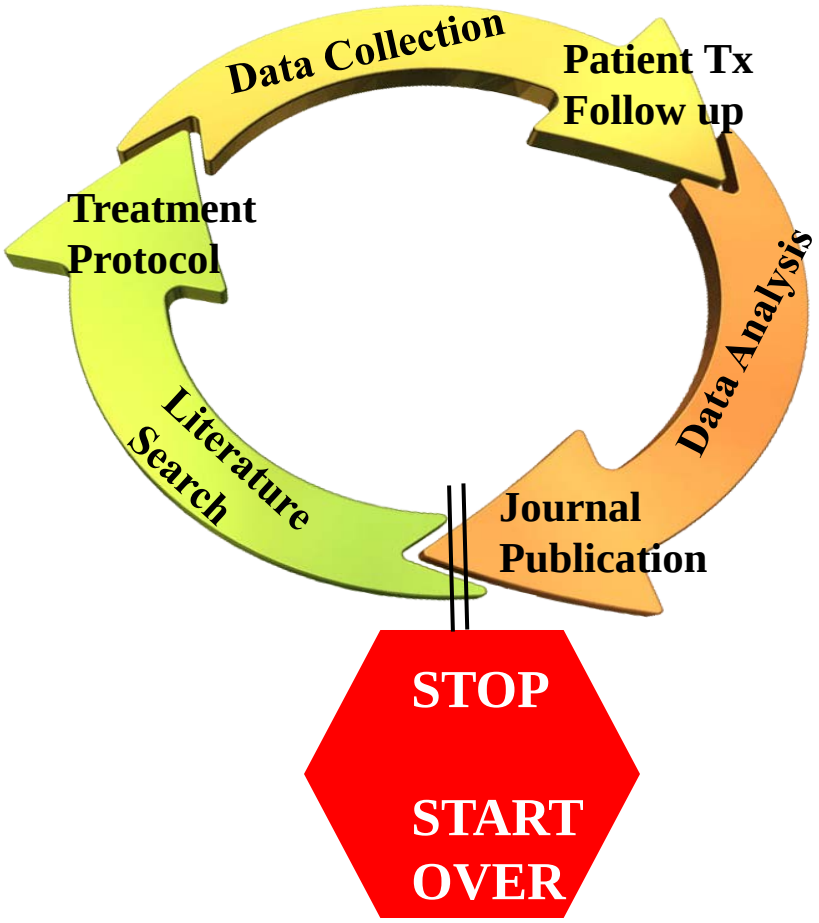

- < 3% of patients treated are enrolled in cooperative clinical trials
- Required data submission for QA and approval – *"big problem"*
- Average duration to complete a clinical trial
  - > 5years
  - outpaced by advances
- No feedback from community practice
- Data limited for re-use
  - Data/Knowledge lost

JHU: Re-engineering the Cooperative Research Model

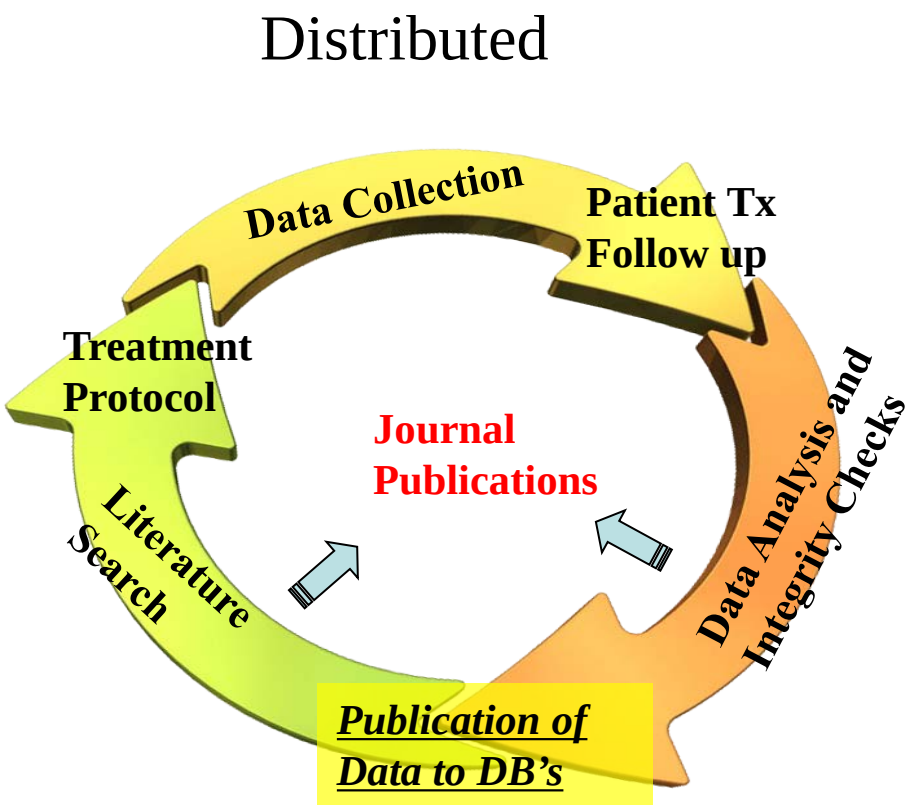

- Keep data local and available in an active database
- Send queries to data, extracting only answers
  - e.g. Validate the PTV margin prescribed for lung SBRT
- Facilitate data-reuse, decision support and education
- Promote data sharing for CER
- *Tools for data capture to populate OncoSpace*

OncoSpace: Radiaton Oncology Model for Data Sharing and Decision Support

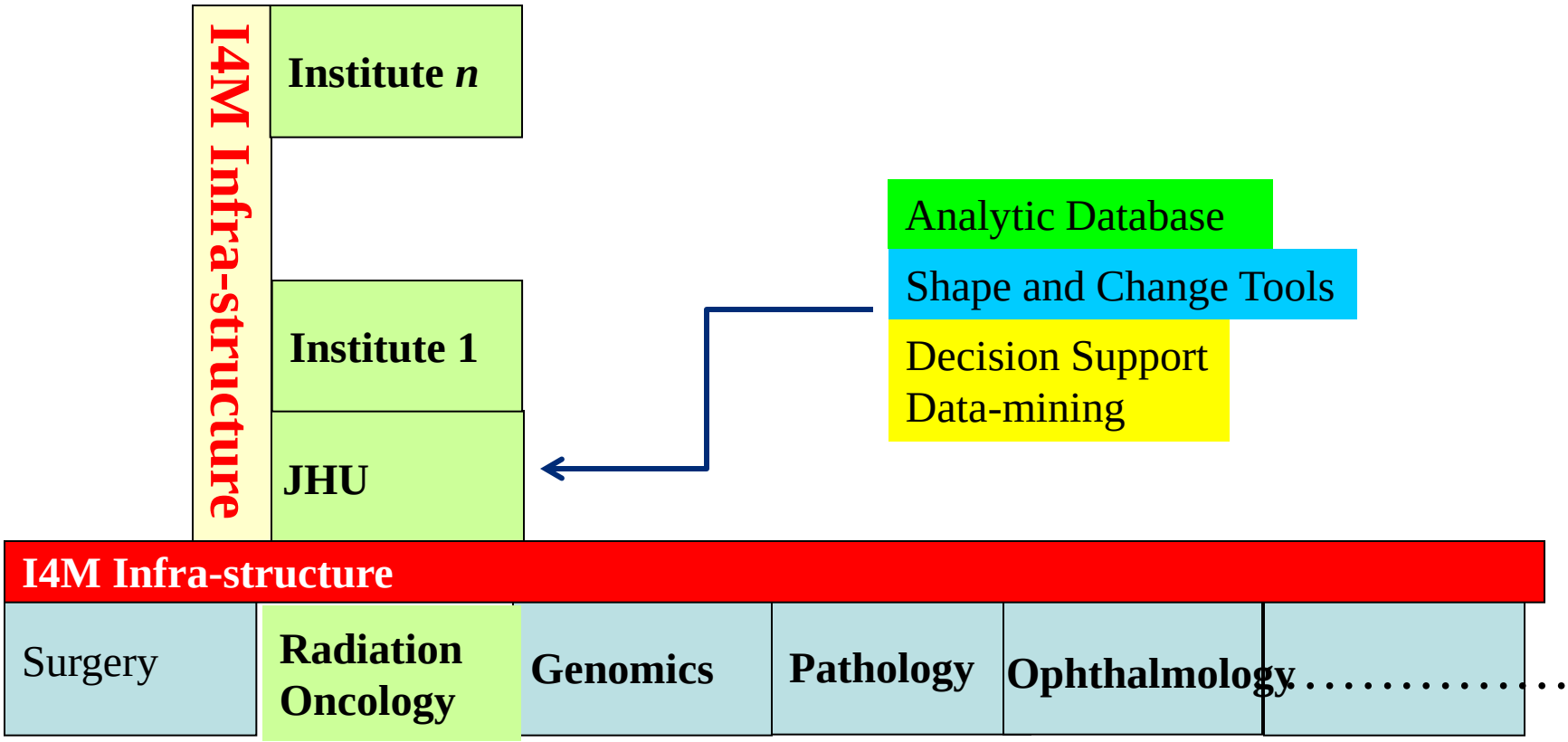

I4M: Integration of Imaging, Information and Intervention in Medicine

Hopkins OncoSpace

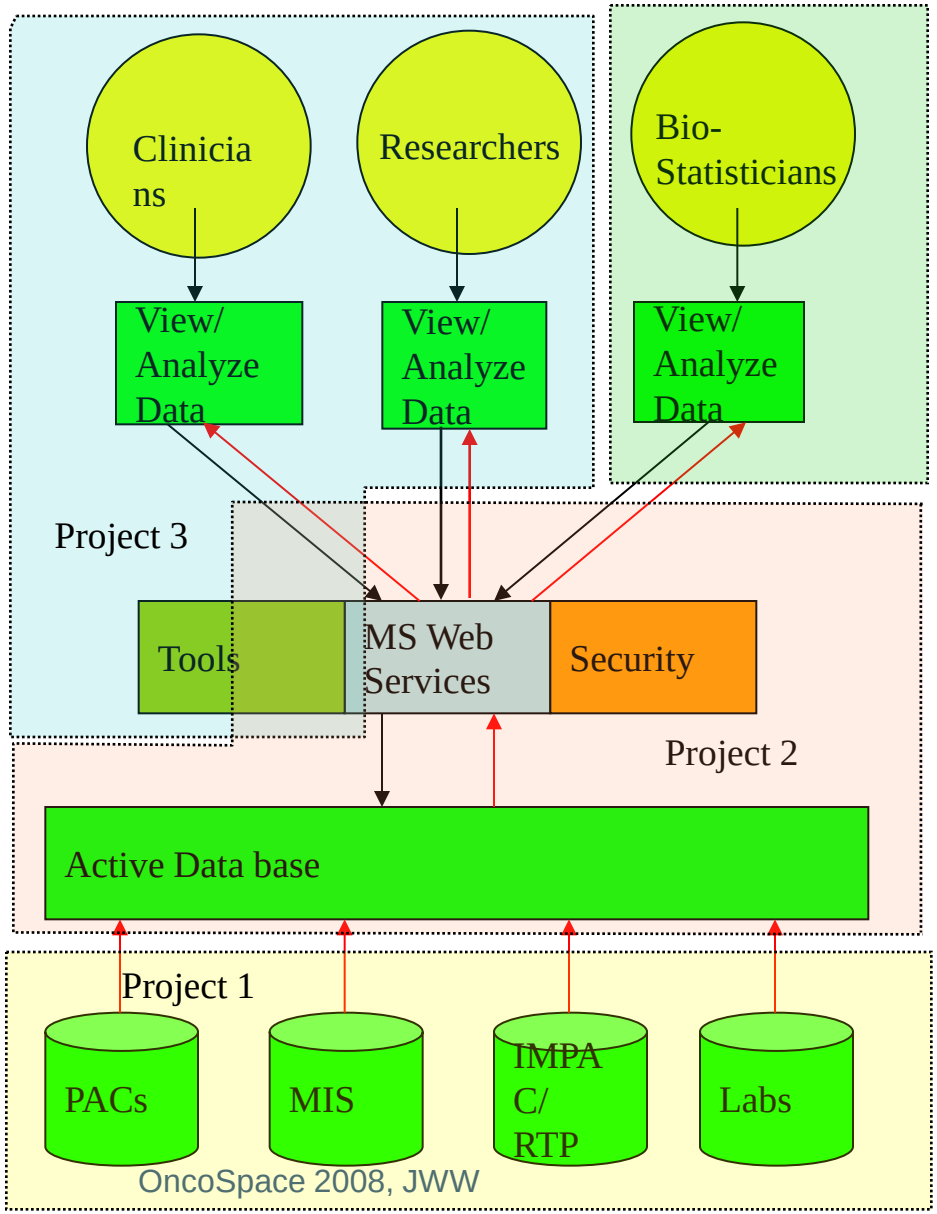

1. Integration of clinical workflow with data collection to populate OncoSpace.
   - ***Enable Mosaiq/Aria and TPS to capture data***
2. Optimize database architecture for secured distributed web-access
3. Tools for query, analysis, navigation and decision support
4. Data mining, decision support and bio-statistic research

Database organization

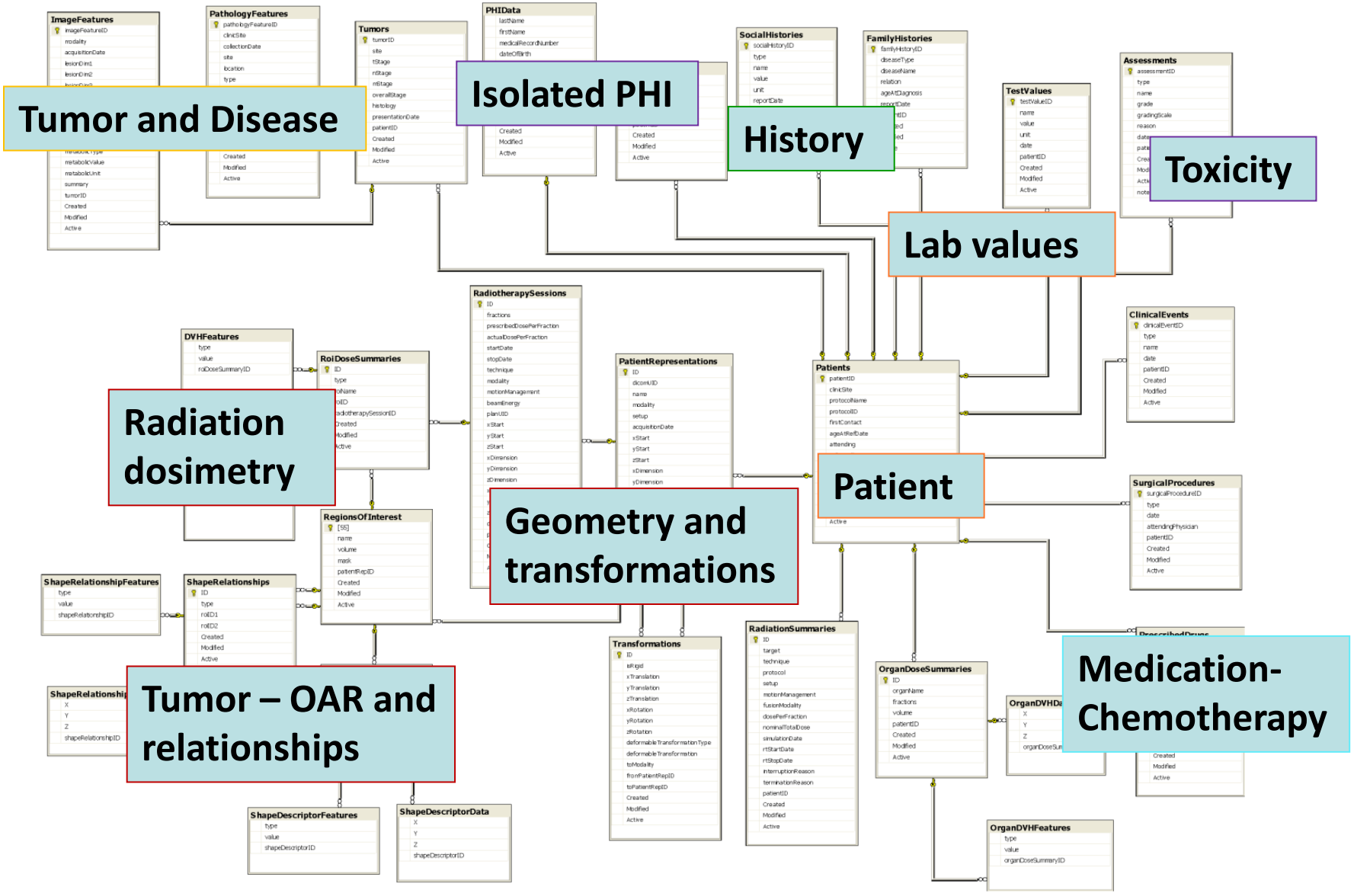

MOSAIQ RO information system

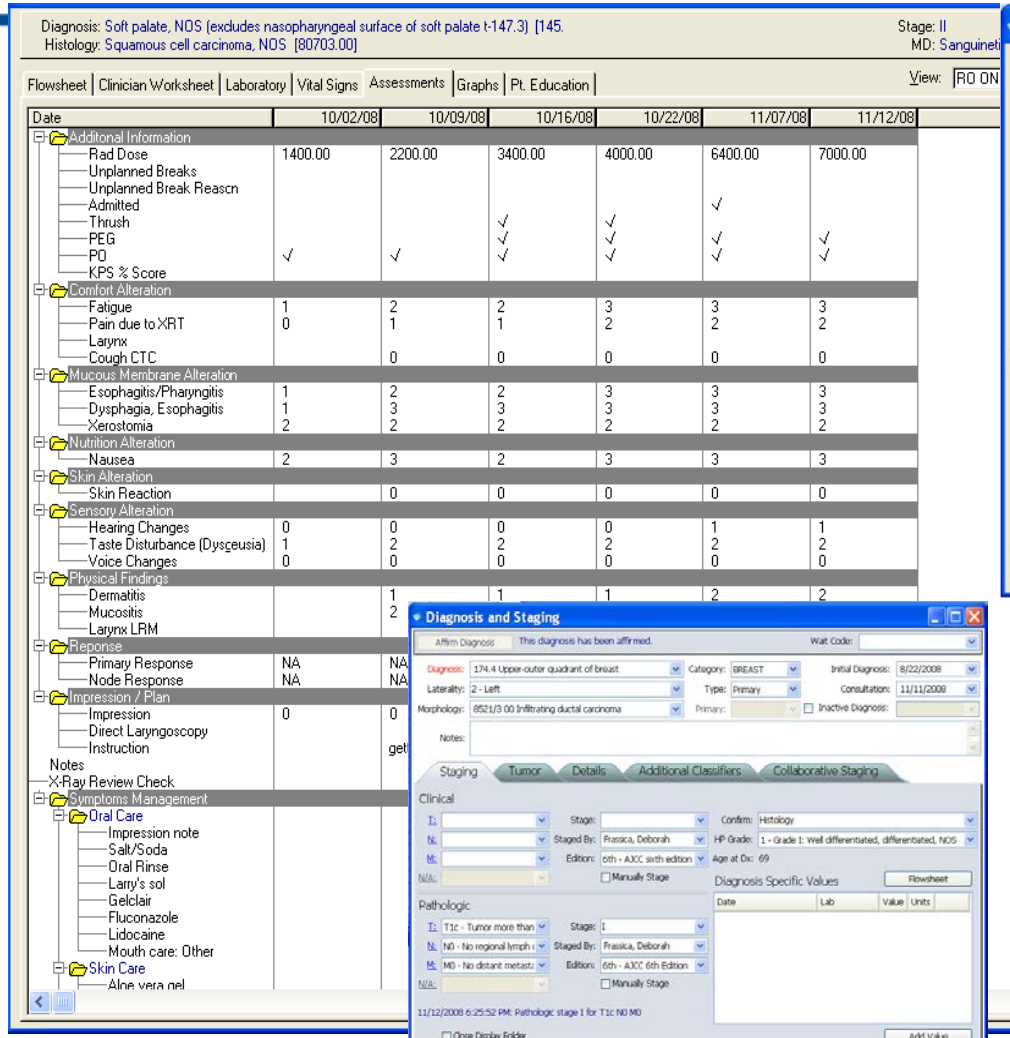

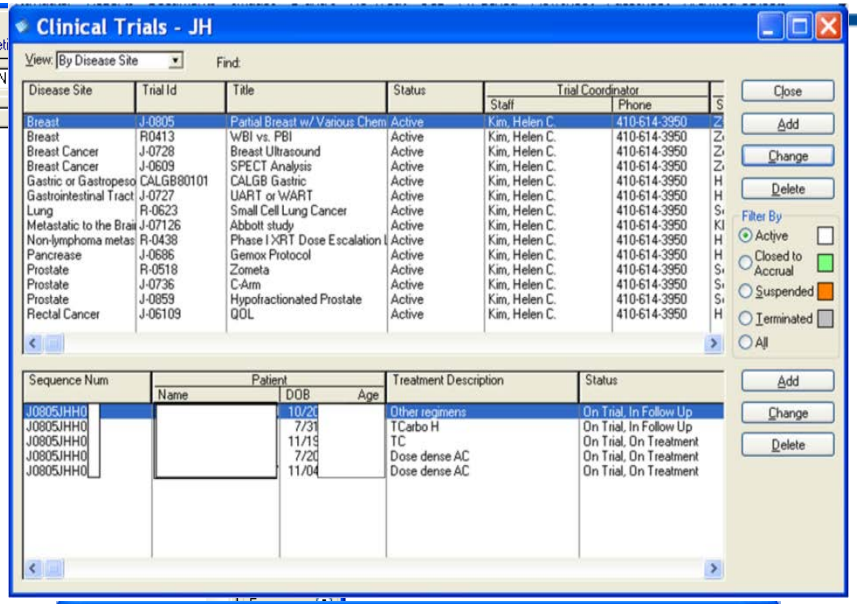

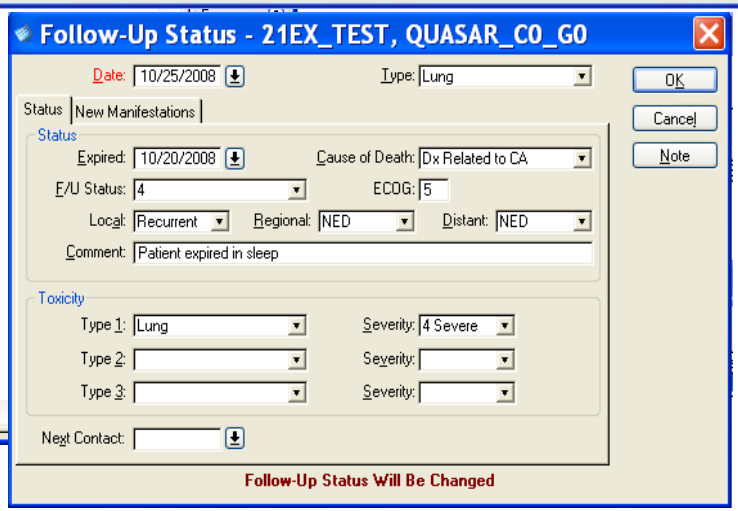

Mobile devices for specific tasks

Plan Approval

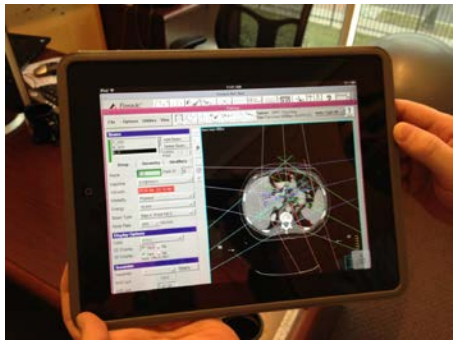

Patient summary

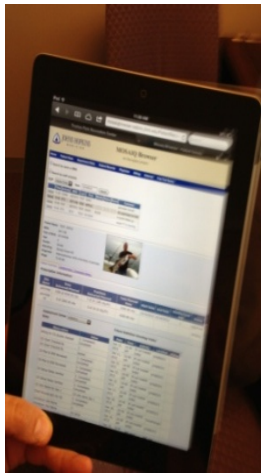

Clinical assessment

Clinical notes

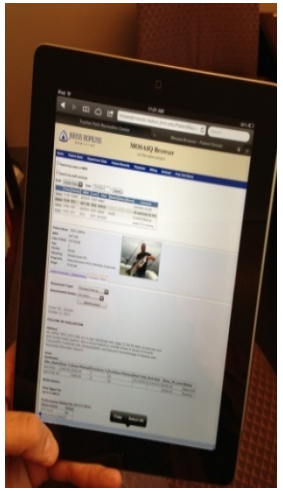

Patient Quality of Life

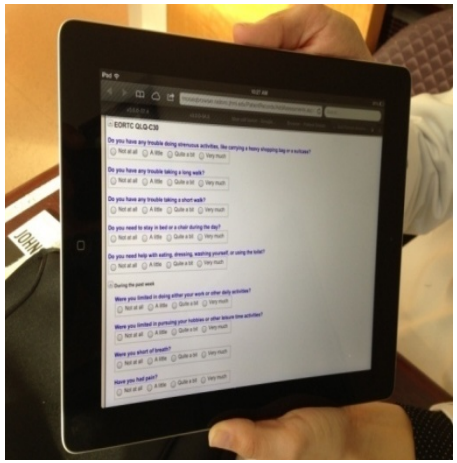

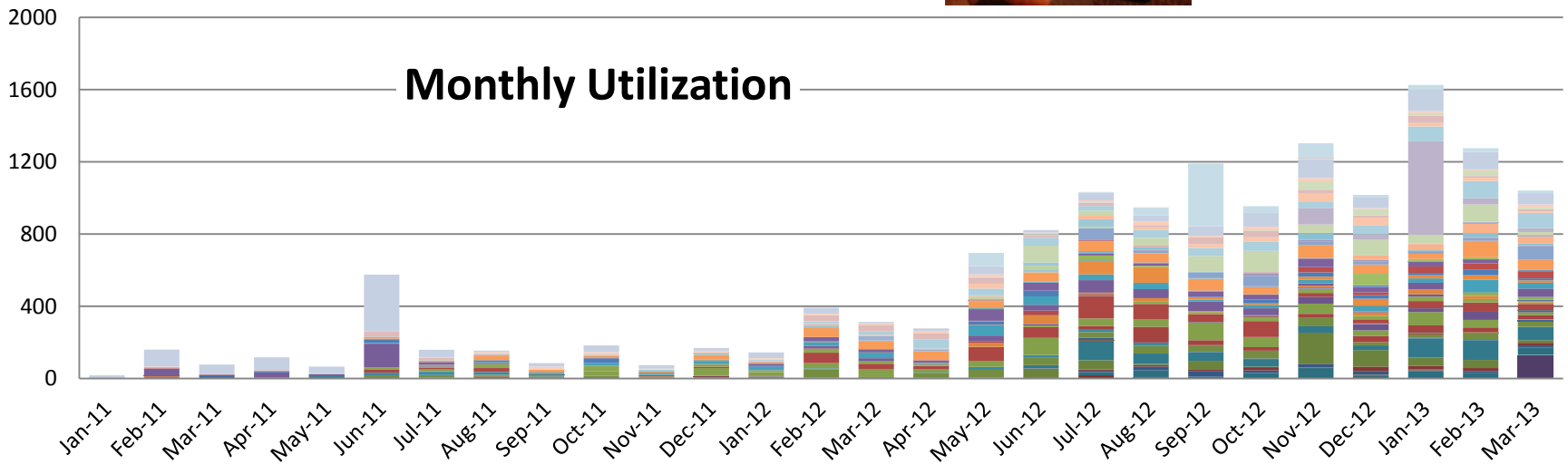

Safety and Quality
Oncospace: Query & Analysis

- How to ask questions of the data?
  - Given this DVH, what is the risk of toxicity?

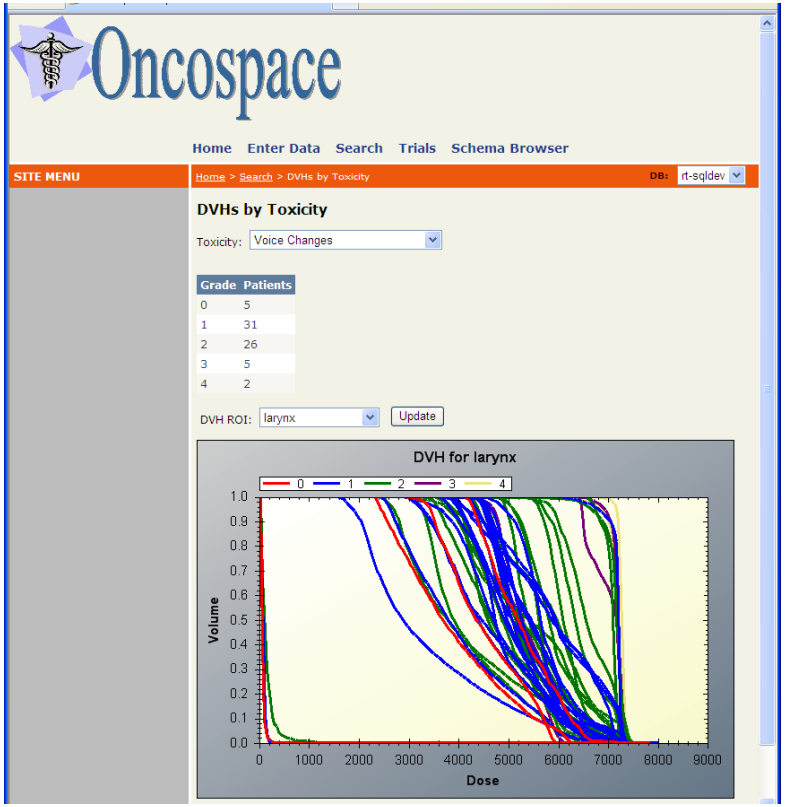

Safety and Quality
Oncospace: Query & Analysis

- How to ask questions of the data?
  - Given this DVH, what is the risk of toxicity?

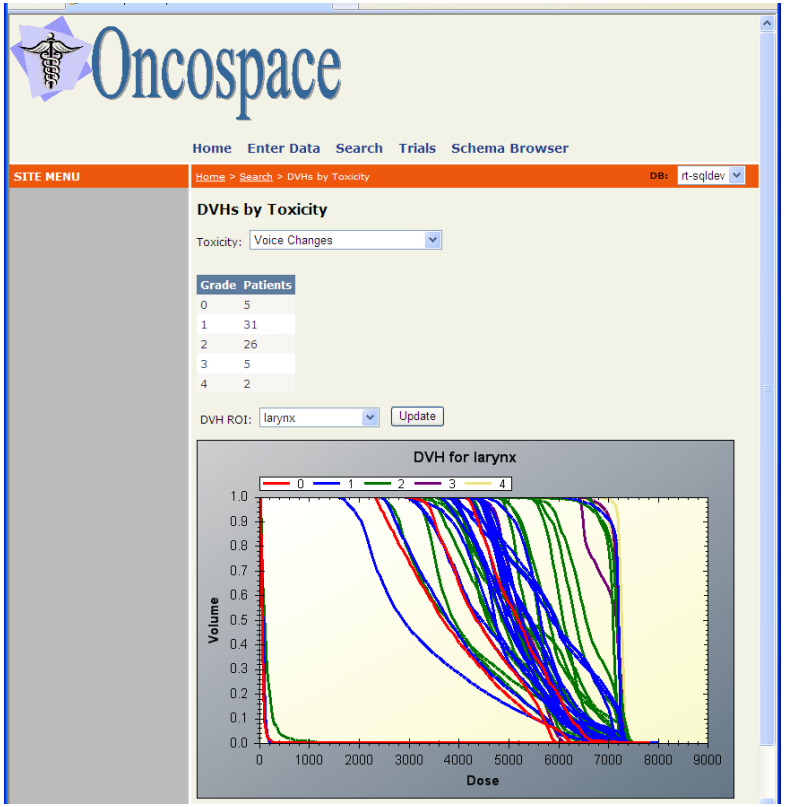

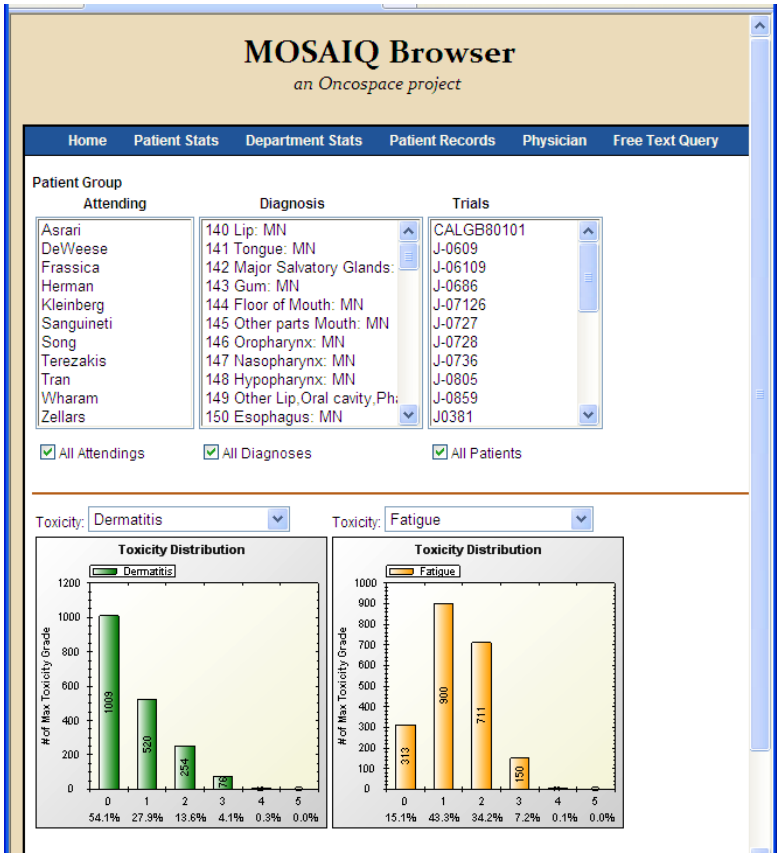

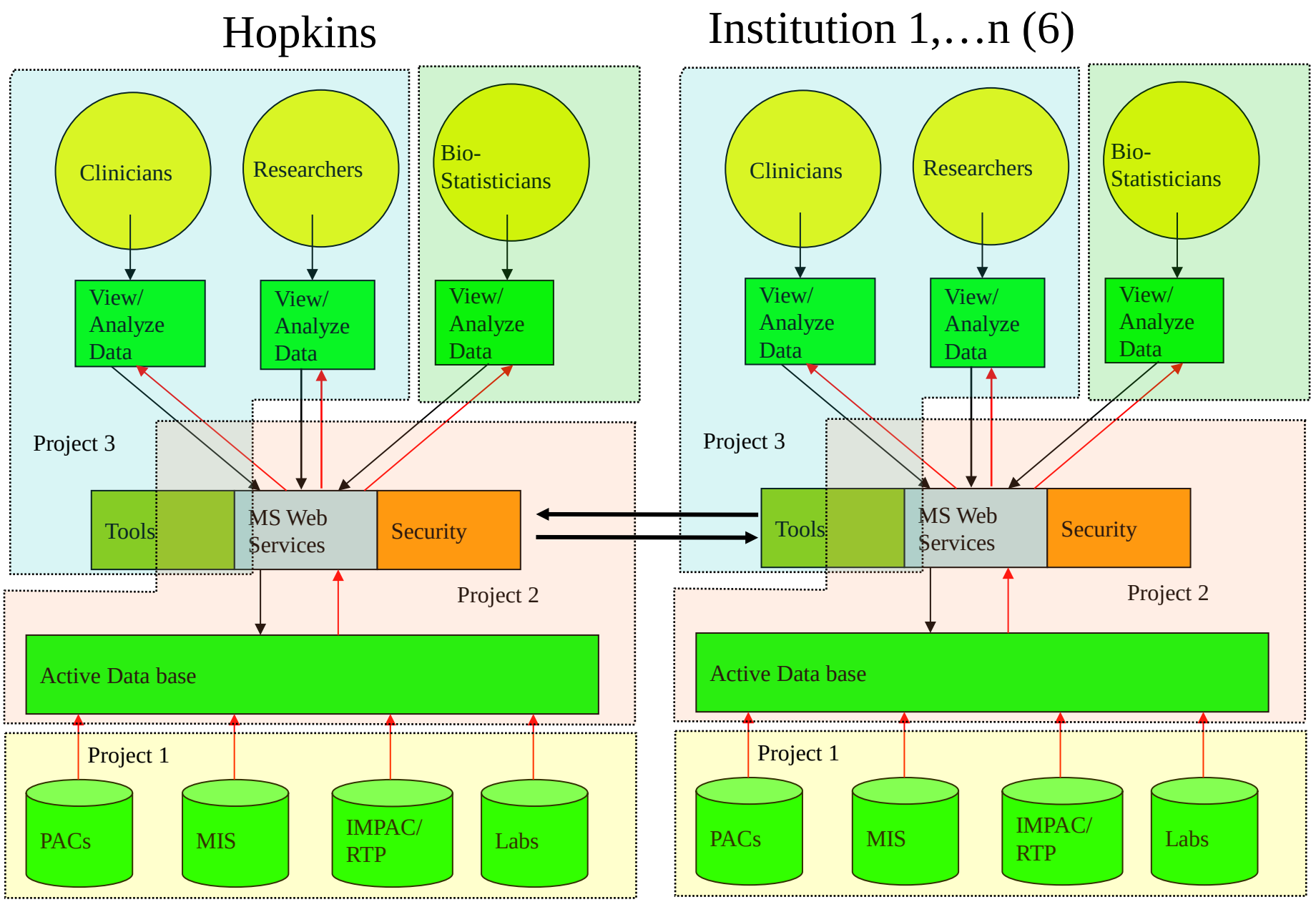
Hopkins
Institution 1,…n (6)
Clinicians
Researchers
Bio-
Statisticians
View/
Analyze
Data
Project 3
Tools
MS Web
Services
Security
Project 2
Active Data base
Project 1
PACs
MIS
IMPAC/
RTP
Labs

DVHs by Toxicity - Windows Internet Explorer

http://localhost:1251/Oncospace/Search/DVHToxicity.aspx

DVHs by Toxicity

Oncospace

Home Enter Data Search Trials Schema Browser

SITE MENU

- Enter Data
- Search
- Trials
- Schema Browser

Home > Search > DVHs by Toxicity DB: local

DVHs by Toxicity

Selected Patient: 120

Toxicity: Xerostomia

Grade	Patients
0	1
1	5
2	43
3	20

DVH ROI: rt_parotid Update

Display

☑ Grade 0 ☑ Grade 1 ☑ Grade 2 ☑ Grade 3 ☑ Grade 4 ☑ Grade 5

Institution

☐ JHU ☐ UCD

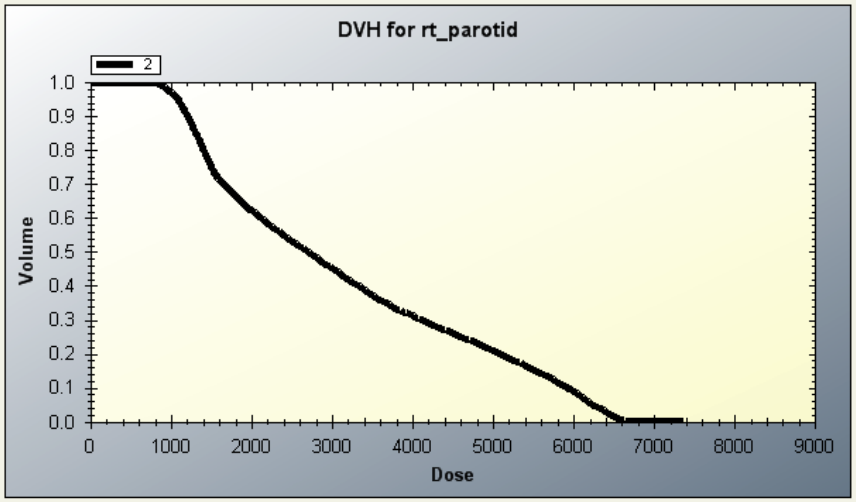

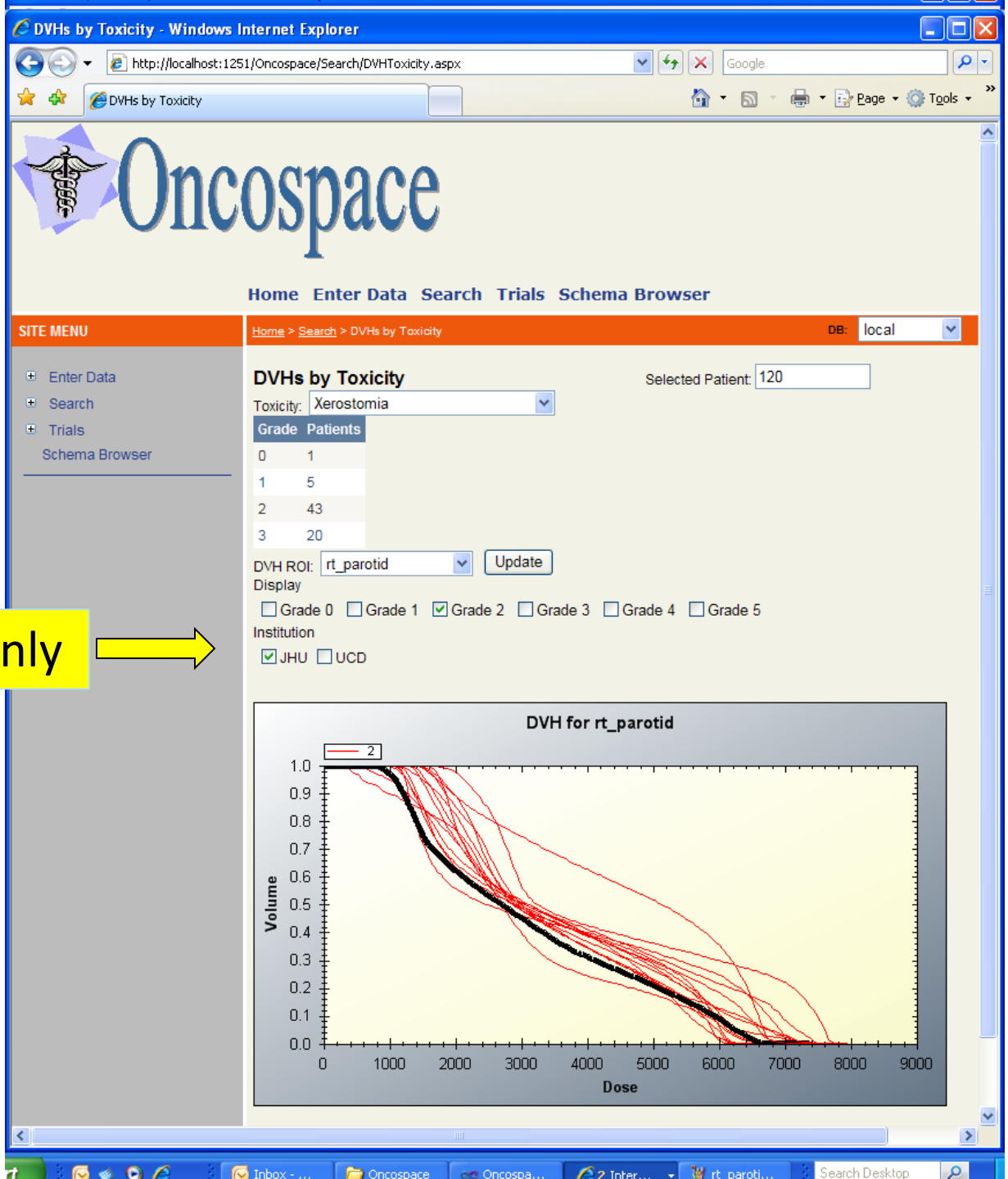
DVHs by Toxicity - Windows Internet Explorer
http://localhost:1251/Oncospace/Search/DVHToxicity.aspx
DVHs by Toxicity
Oncospace
Home Enter Data Search Trials Schema Browser
SITE MENU
Enter Data
Search
Trials
Schema Browser
Home > Search > DVHs by Toxicity
DB: local
DVHs by Toxicity
Selected Patient: 120
Toxicity: Xerostomia
Grade Patients
0 1
1 5
2 43
3 20
DVH ROI: rt_parotid
Update
Display
Grade 0 Grade 1 Grade 2 Grade 3 Grade 4 Grade 5
Institution
JHU UCD
DVH for rt_parotid
2
Volume
Dose
0.0 0.1 0.2 0.3 0.4 0.5 0.6 0.7 0.8 0.9 1.0
0 1000 2000 3000 4000 5000 6000 7000 8000 9000

JHU Only

DVHs by Toxicity - Windows Internet Explorer

http://localhost:1251/Oncospace/Search/DVHToxicity.aspx

DVHs by Toxicity

Oncospace

Home Enter Data Search Trials Schema Browser

SITE MENU

- Enter Data
- Search
- Trials
- Schema Browser

Home > Search > DVHs by Toxicity

DB: local

DVHs by Toxicity

Selected Patient: 120

Toxicity: Xerostomia

Grade	Patients
0	1
1	5
2	43
3	20

DVH ROI: rt_parotid Update

Display

☐ Grade 0 ☐ Grade 1 ☑ Grade 2 ☐ Grade 3 ☐ Grade 4 ☐ Grade 5

Institution

☑ JHU ☑ UCD

JHU & UCD

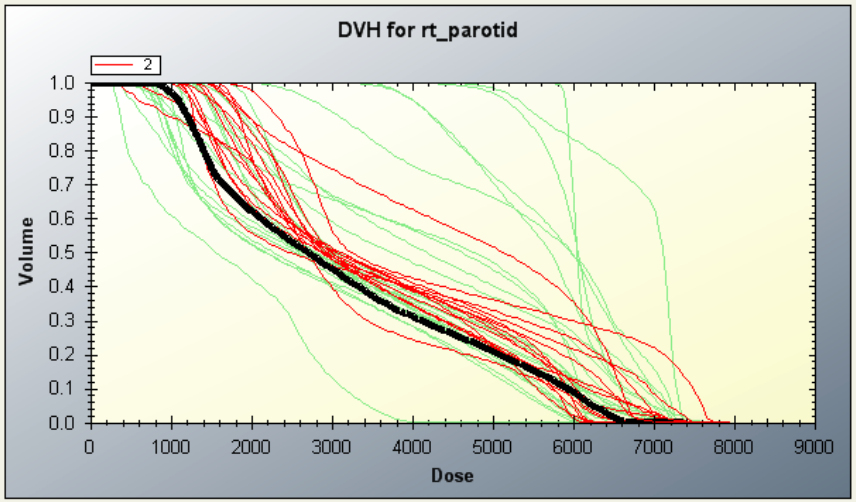

Physics to engage Biology in Radiation Therapy

- Questions and Challenges:
  - The validity of EUD, NTCP, ……
  - Validation and optimization of biological image guided or molecular targeted radiation therapy
  - Others questions: biological target volume???
- Present small animal radiation research methods bear little resemblance to human treatment
- A pressing need to down-size human treatment to bridge small animal laboratory research

Small Animal Radiation Research Platform

- Hopkins-Xstrahl partnership
- Integrated 3D-Slicer-GPU based treatment planning system
- Computer controlled
  - 360^{o} gantry rotation
  - Non-coplanar delivery

SARRP CBCT: “Pancake” geometry

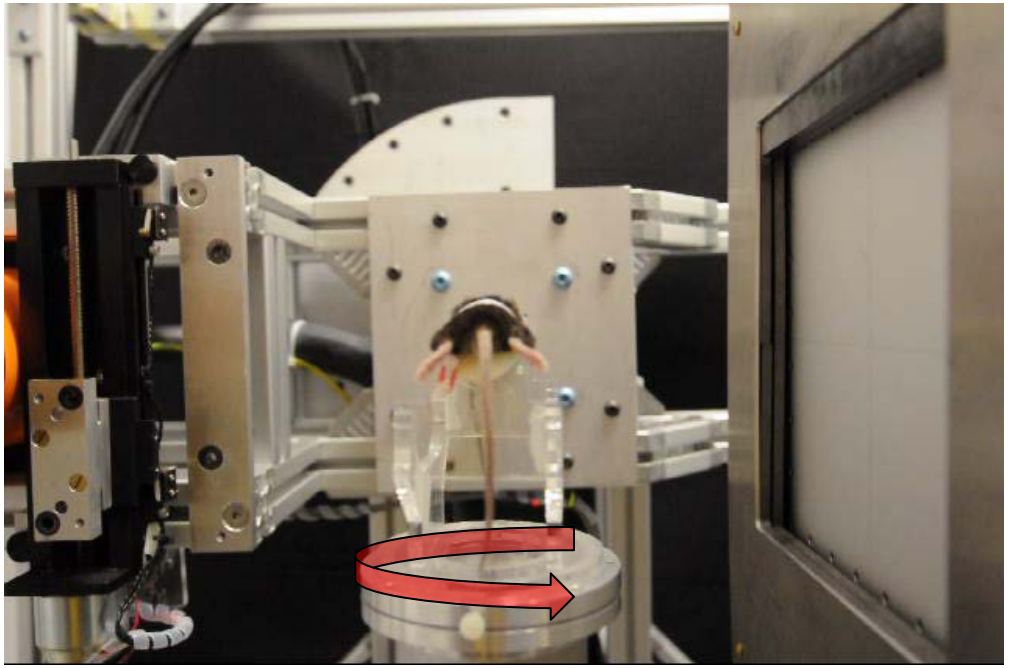

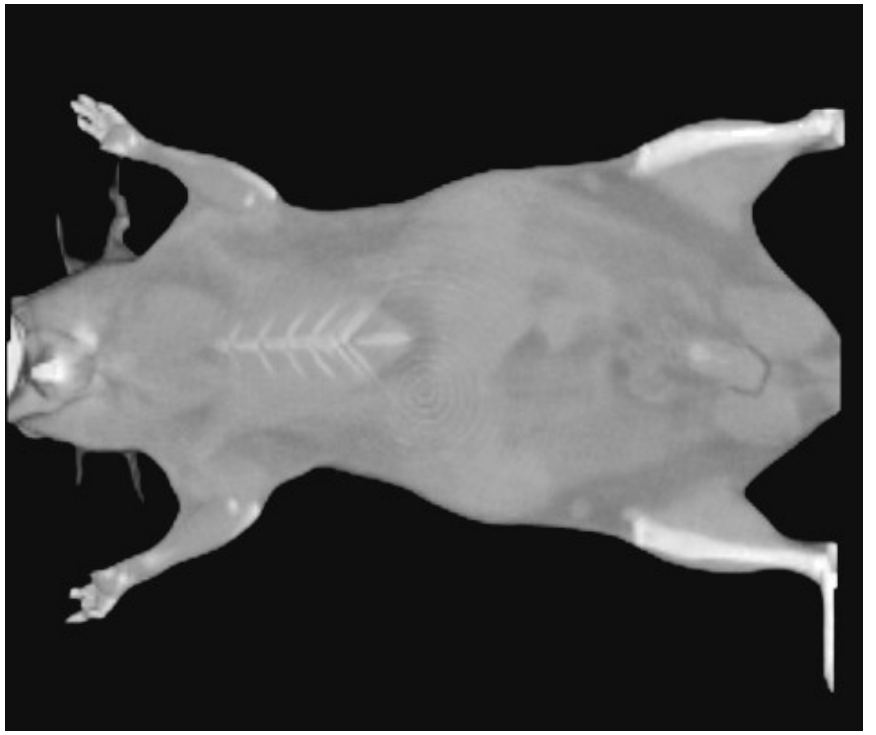

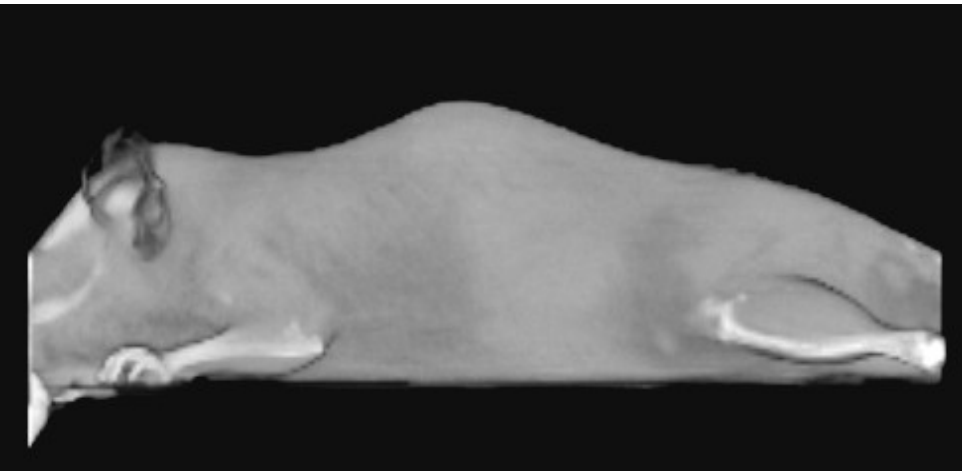

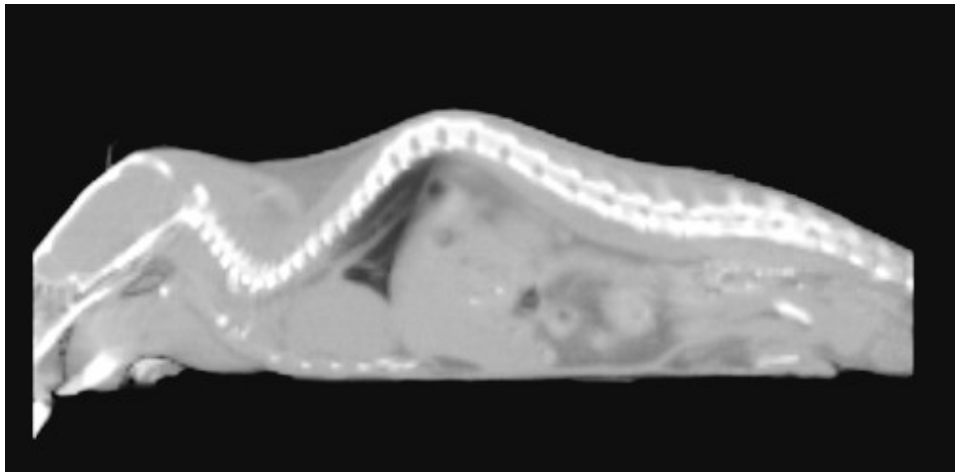

Small Animal Treatment Console

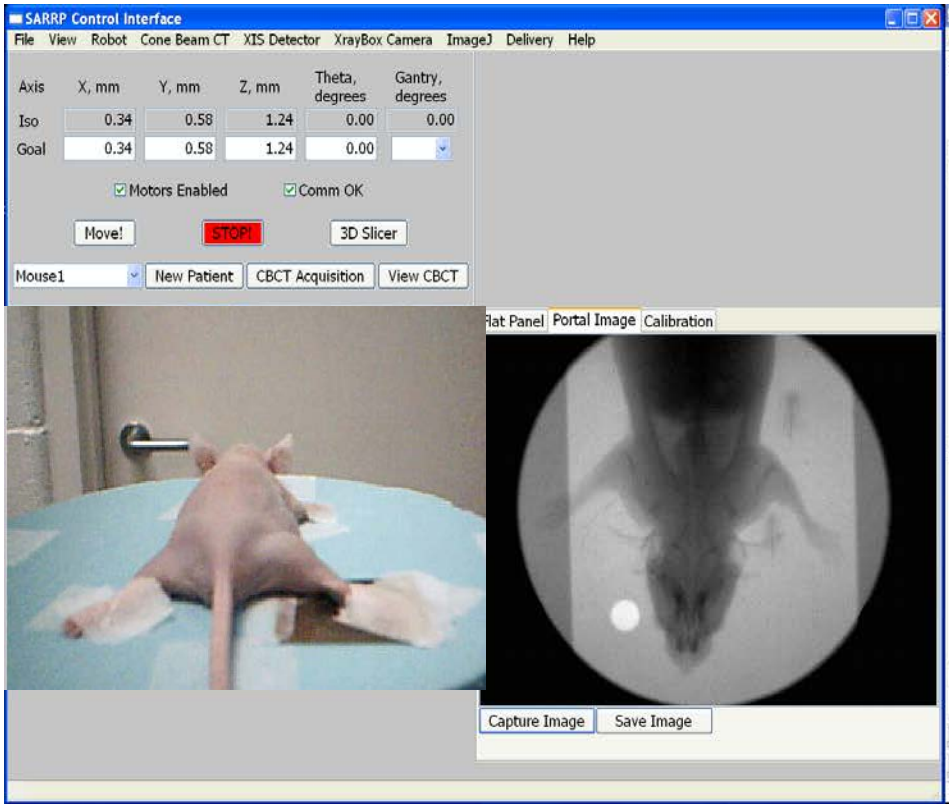

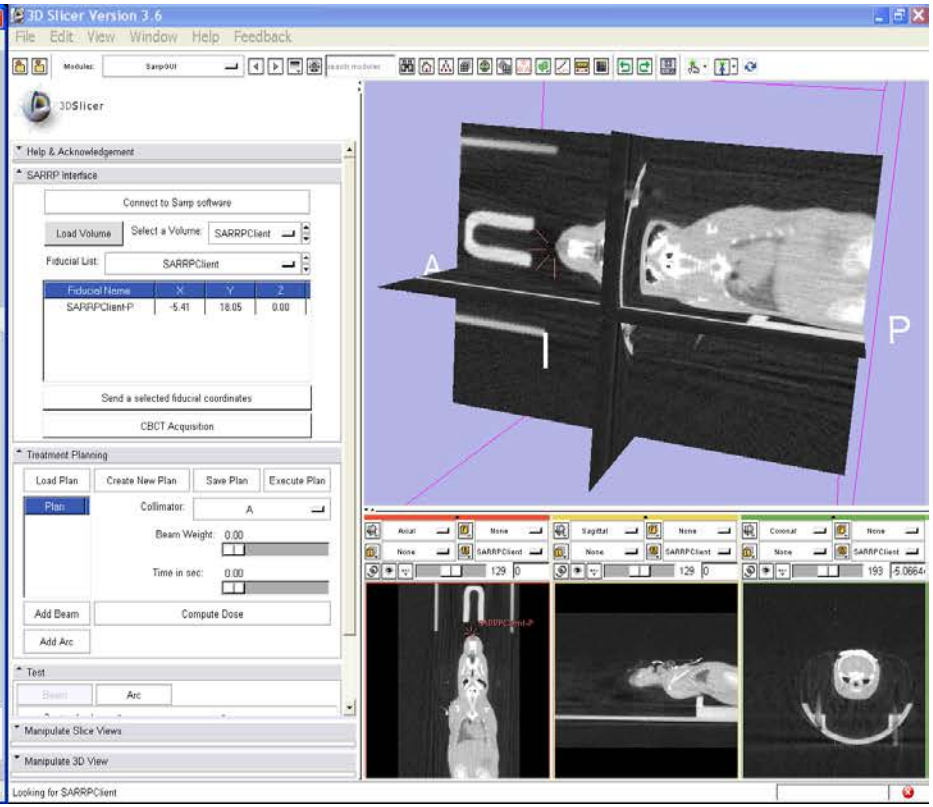

SARRP Slicer- 3D RTP: GPU Dose – CBCT Engine

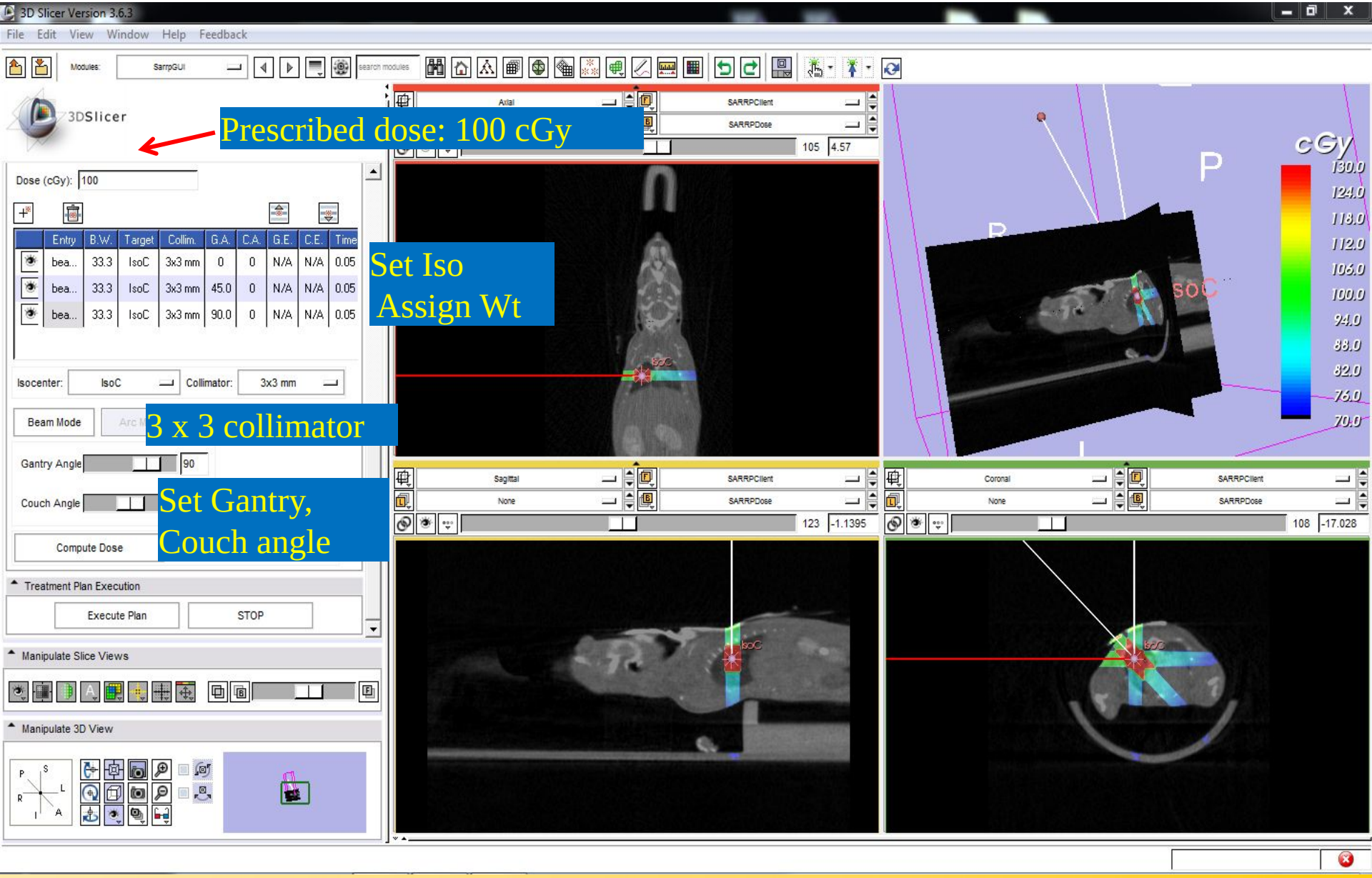

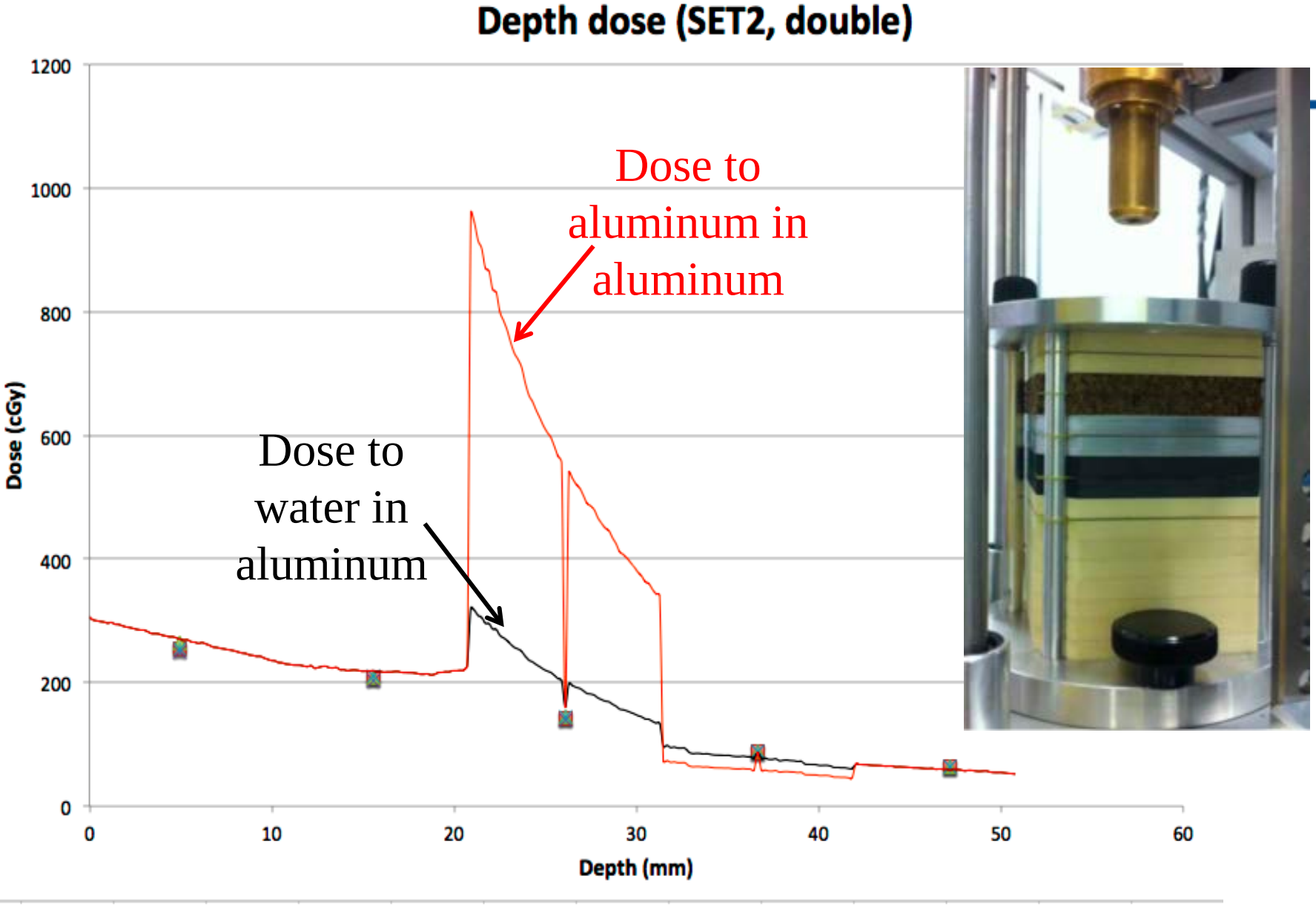
Depth dose (SET2, double)
Dose (cGy)
1200
1000
800
600
400
200
0
0
10
20
30
40
50
60
Depth (mm)
Dose to aluminum in aluminum
Dose to water in aluminum

Comparison of SC to Monte Carlo

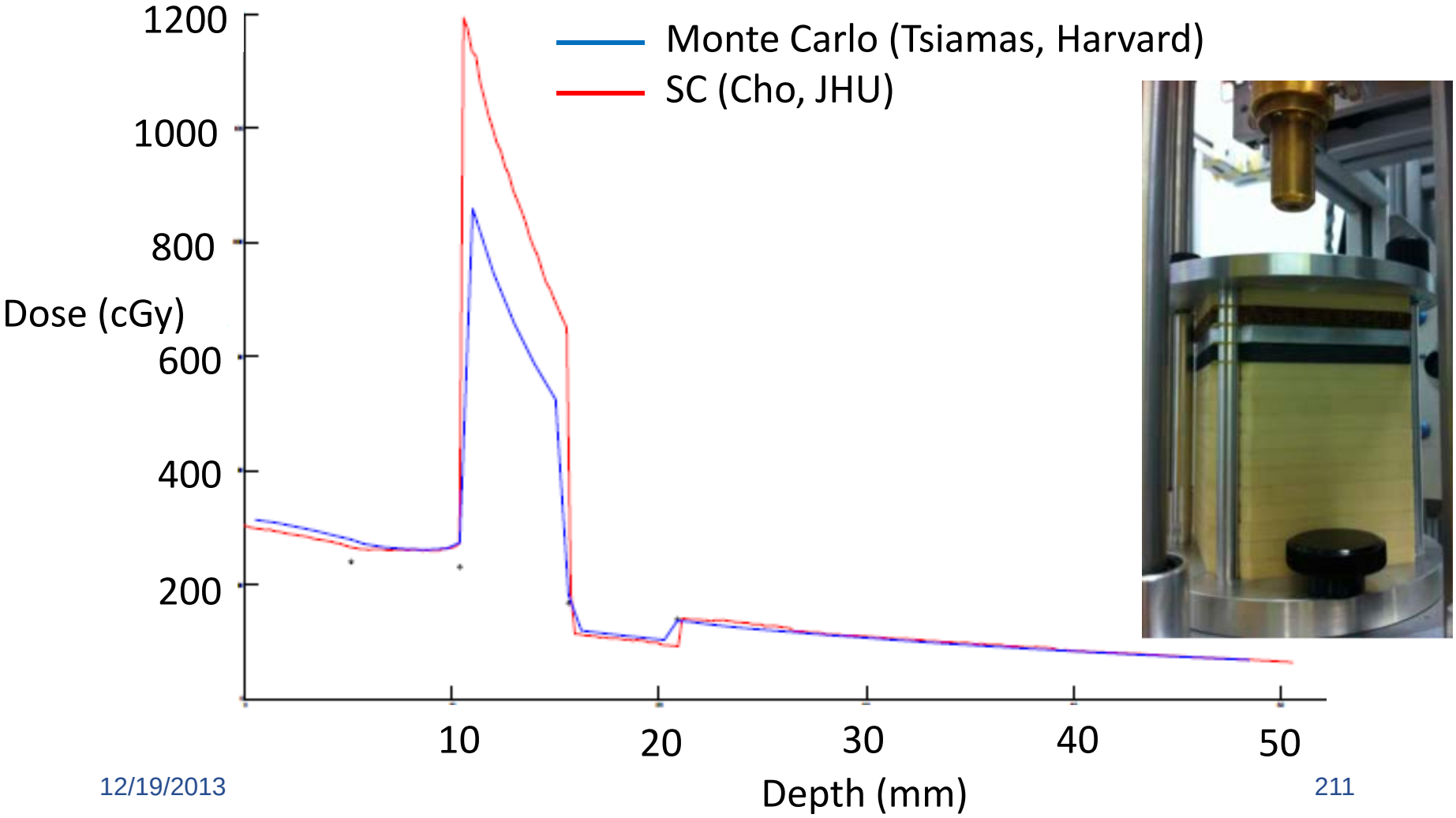

Comparison of SC with MC
Correcting for density scaling

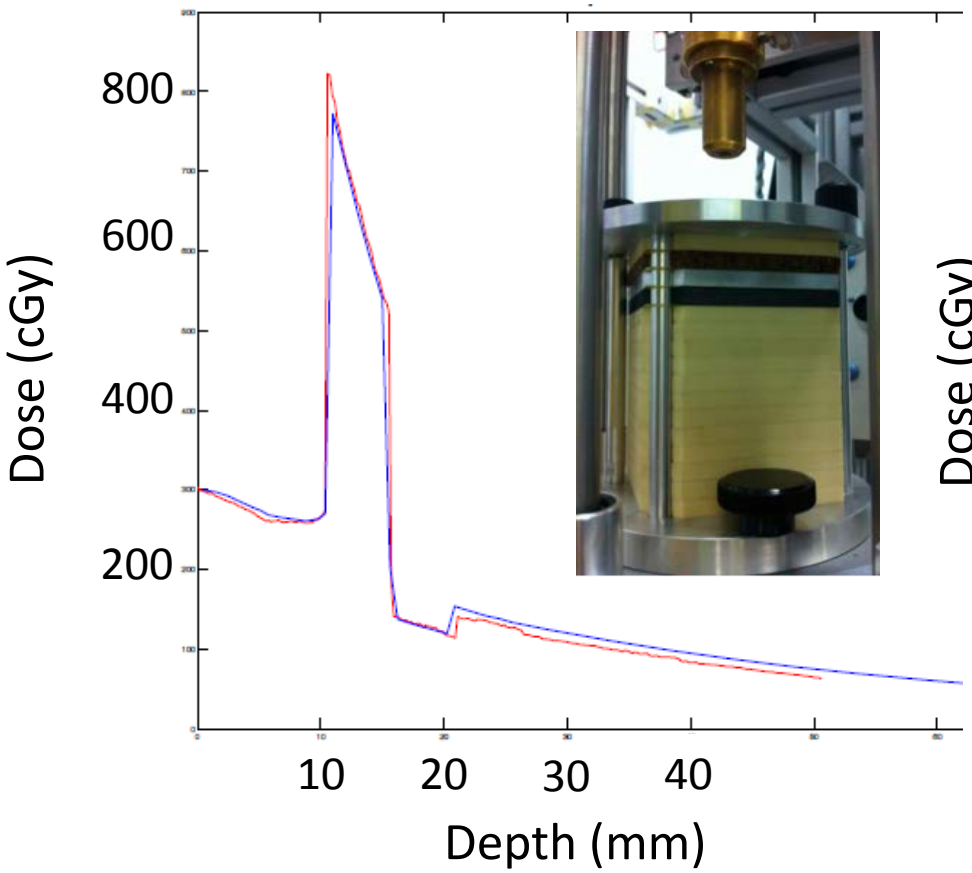

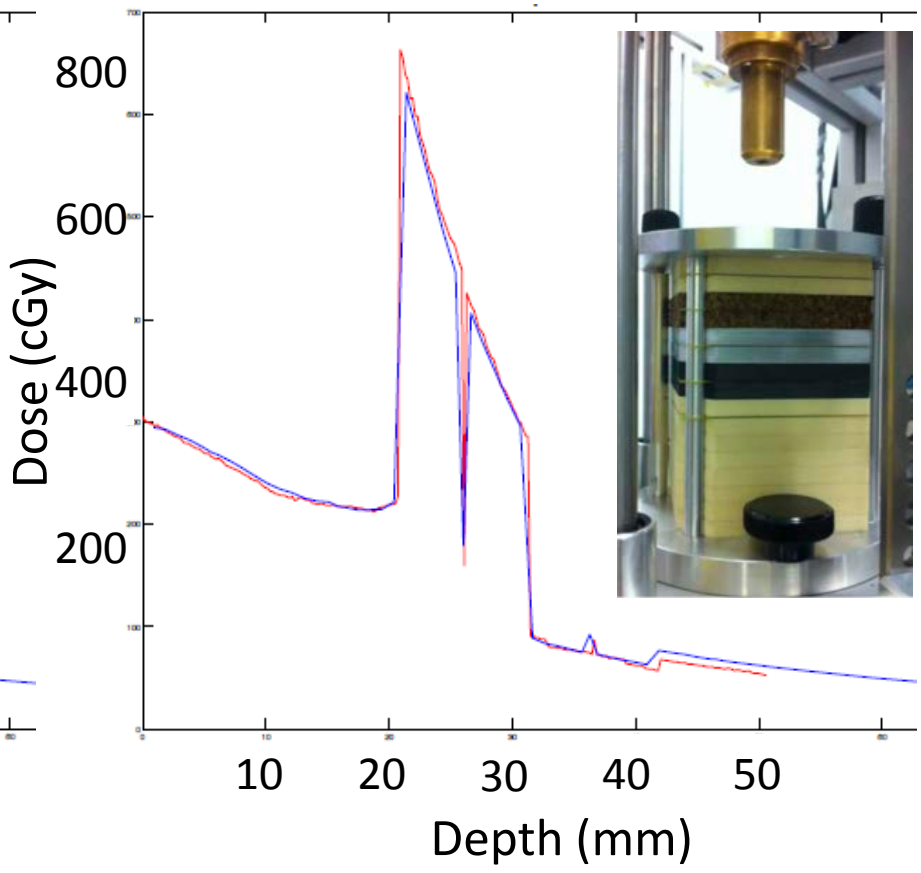

On-board BLI/BLT for Beam's Eye View Irradiation with the SARRP (R01 CA158100)

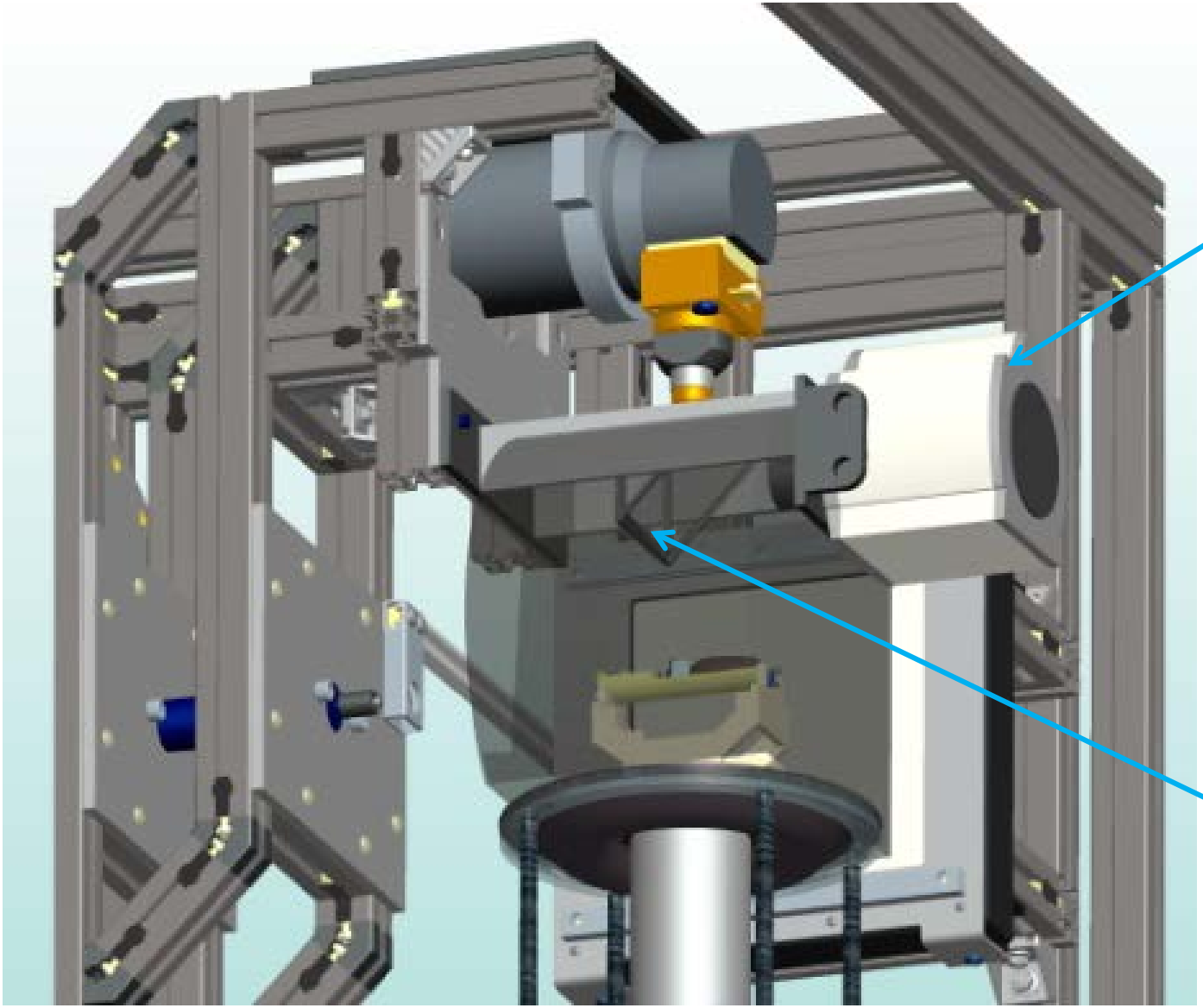

CBCT

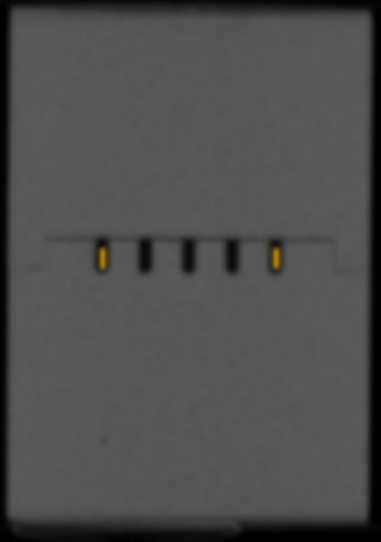

Coronal

Transverse

BLT

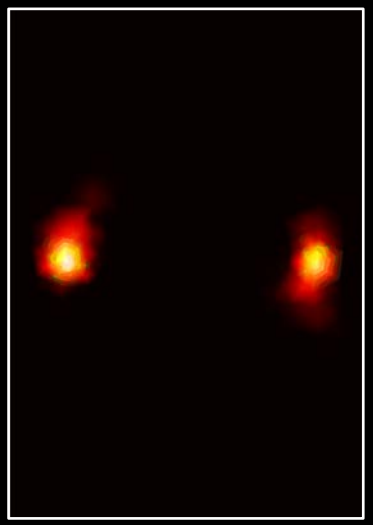

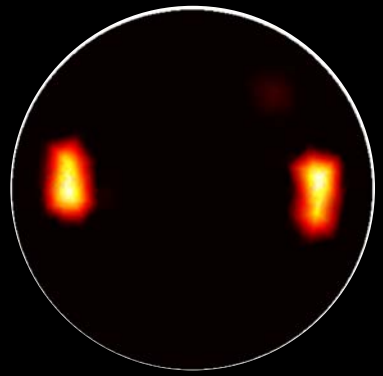

BLT Reconstructed with only one wavelength (630nm). accurate in vertical position, but 1-2mm error along axial direction. Multi-spectral recon would improve the accuracy.

Combining Stereotactic Radiation and Anti-PD1 Therapy in an Orthotopic Mouse Glioma Model (Zeng et al)

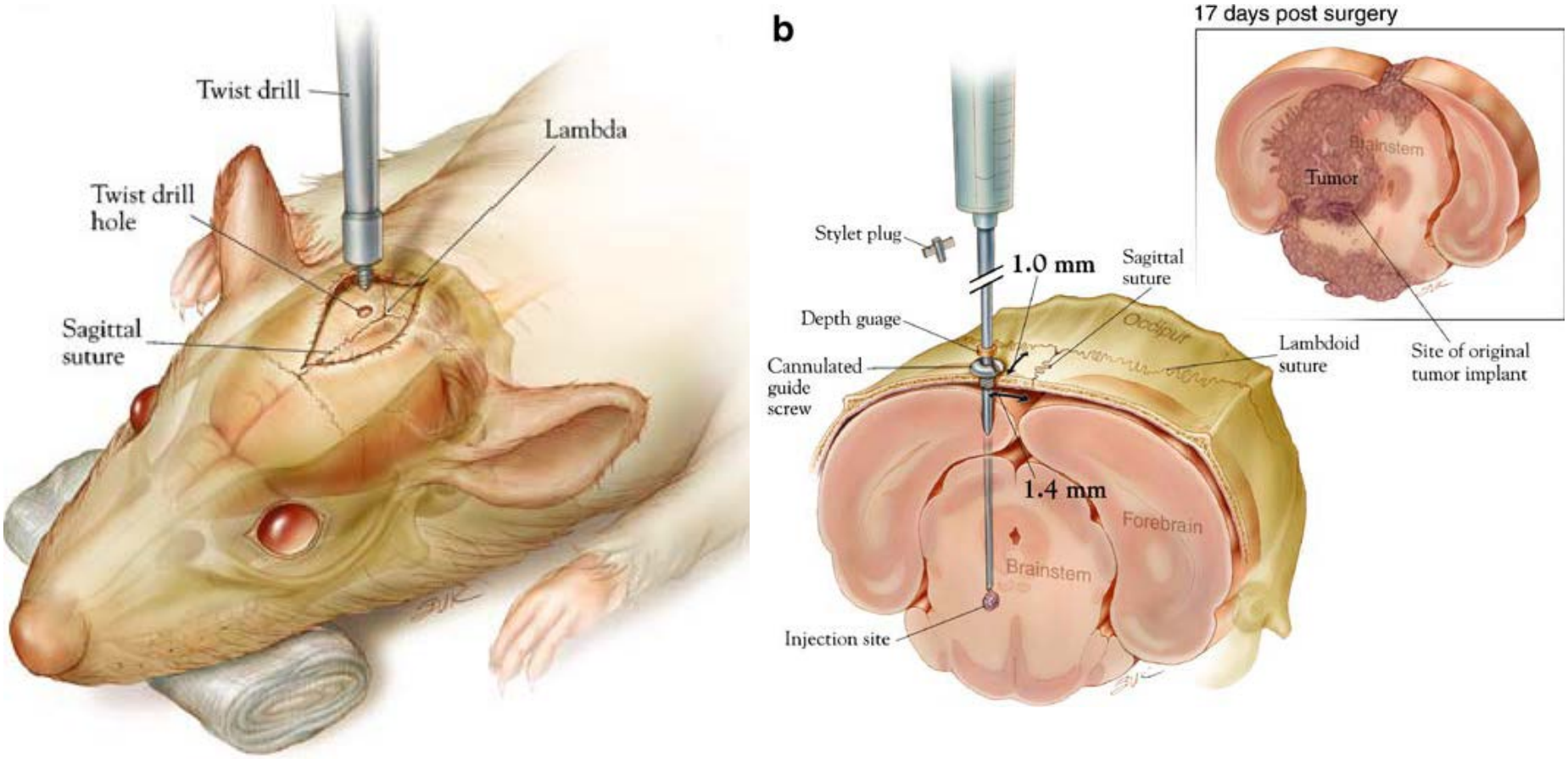

Experimental Design

Day	No Tx	RT only	PD-1 only	RT+PD-1
0	Tumor Implantation			
7	Bioluminescent Imaging			
10		Radiation	1st antibody dose	Radiation; 1st antibody dose
11				
12			2nd antibody dose	2nd antibody dose
13				
14			3rd antibody dose	3rd antibody dose
21	Bioluminescent Imaging			

Radiation = 10 Gy in 3 mm beam

Antibody = anti-PD-1 antibody, 200 µg/mouse

JOHNS HOPKINS MEDICINE

Survival Outcome

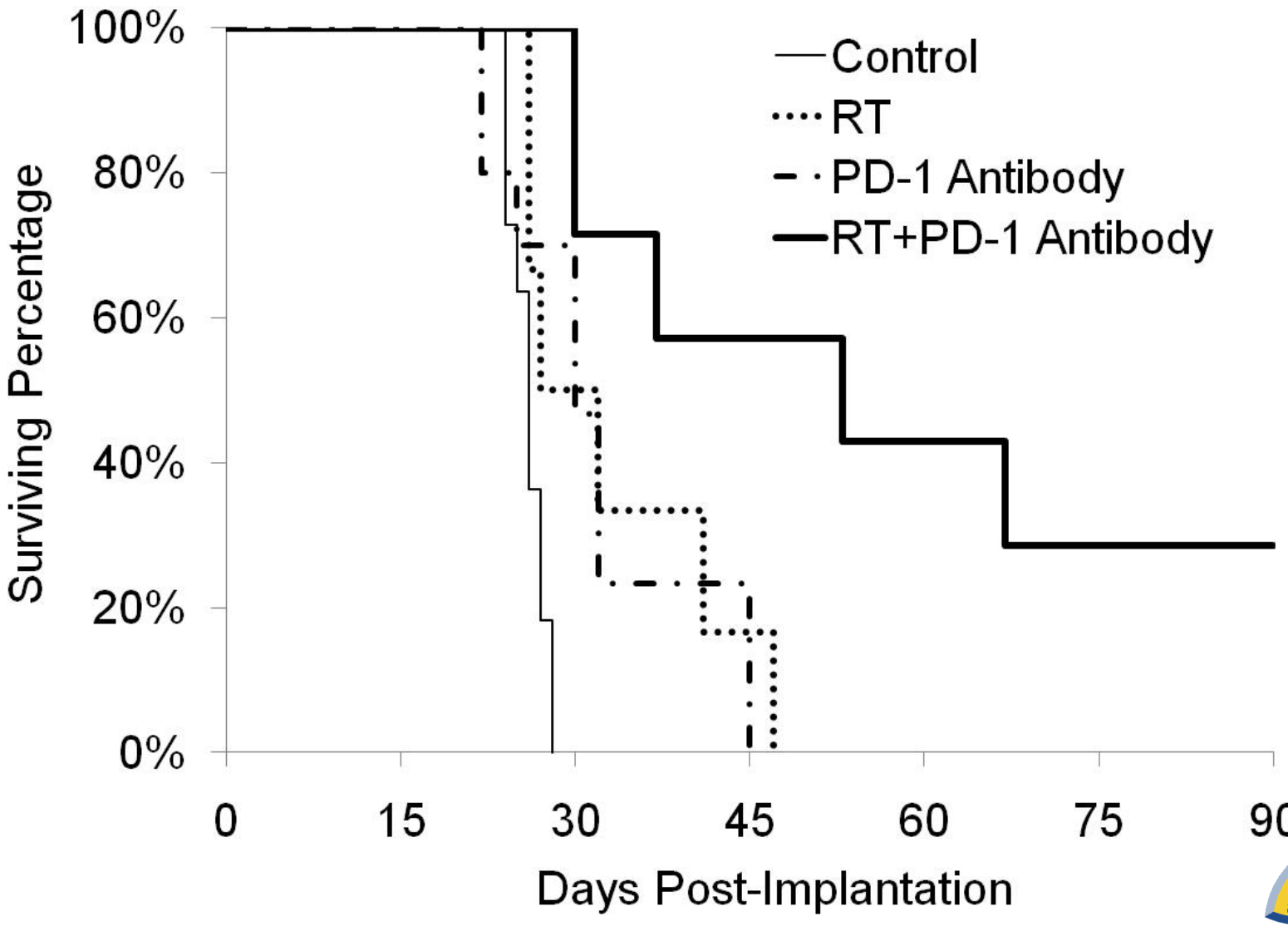

JOHNS HOPKINS
MEDICINE

Flank Re-challenge

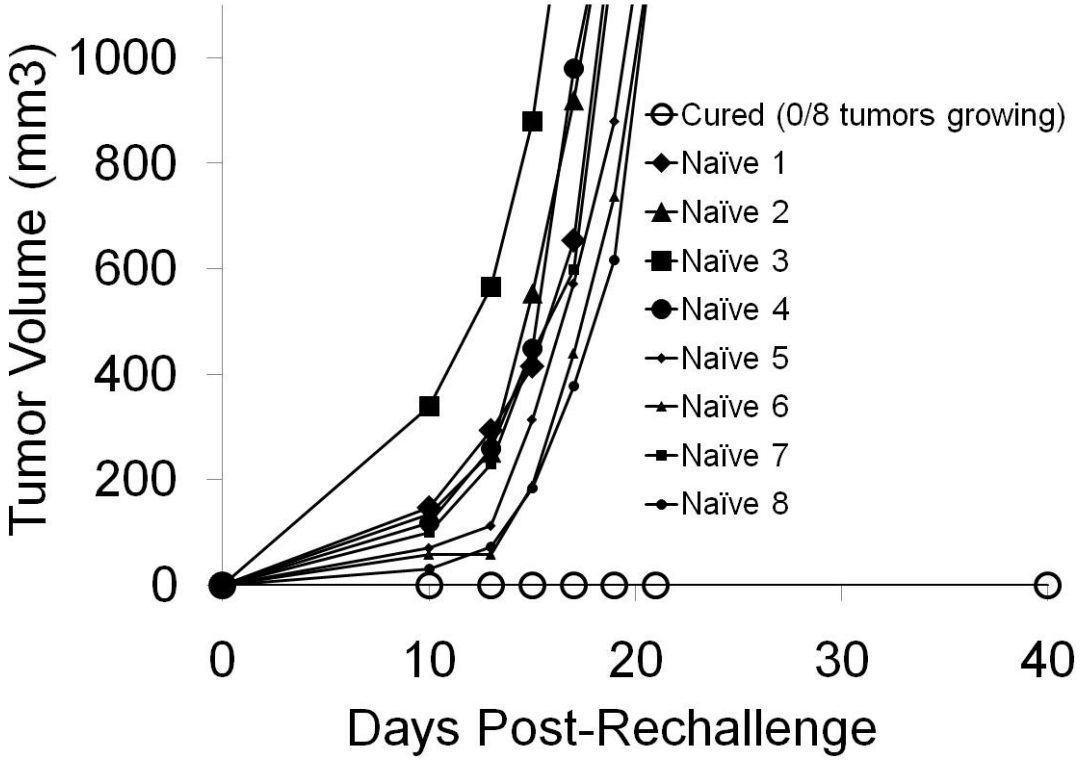

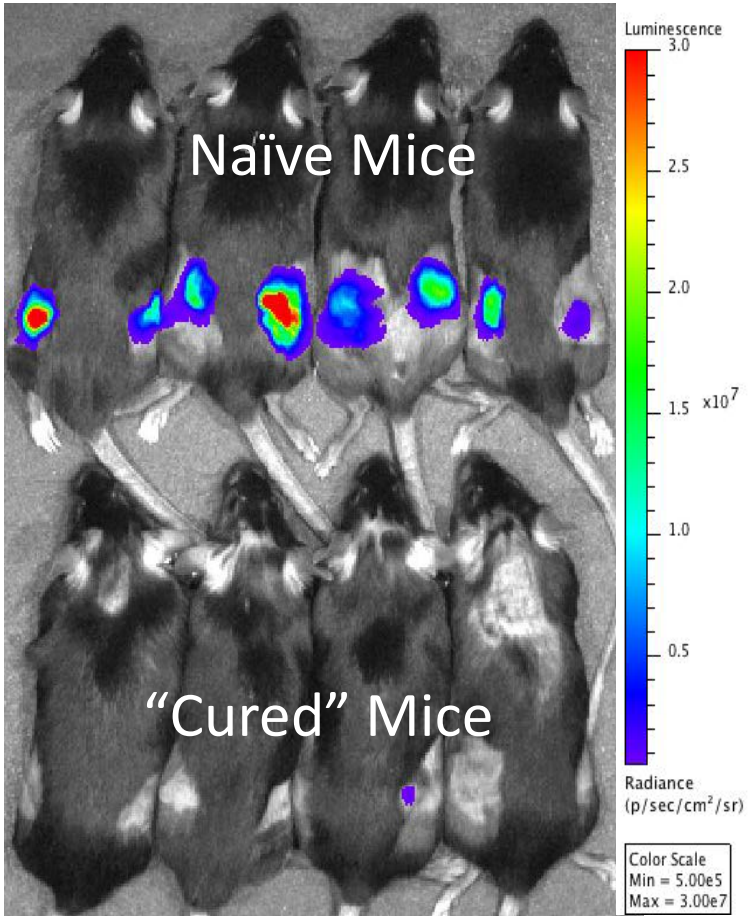

What do we do for the next 5 years?

- Medicine (and radiation oncology) is undergoing tremendous changes driven by technologies and information
- Treatment strategies will employ multiple therapeutic agents with radiation
- Personalized medicine will be based on genetics, treatment response, functional/anatomic ….
- Physics need to expand beyond technologies:
  - *Technology, Informatics, Biology,……*
  - *We must innovate*

4D MRI (JHU/Siemens)

- 4D CT is a 2 min snapshot, not often re-evaluated
- Long duration (15 – 30 min) MRI to represent treatment

4D MRI – Tracked Motion

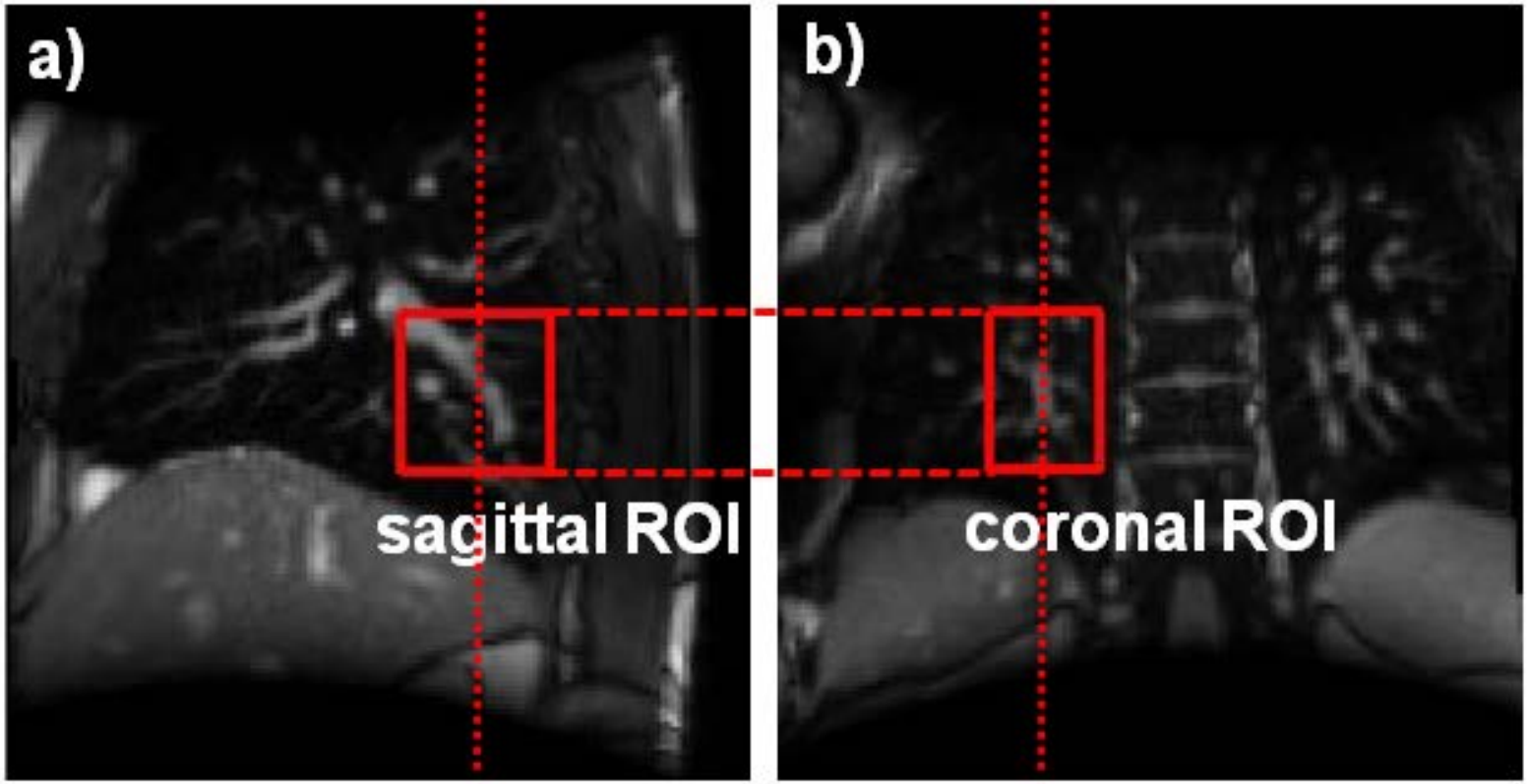

4D MRI – Characterization of Motion

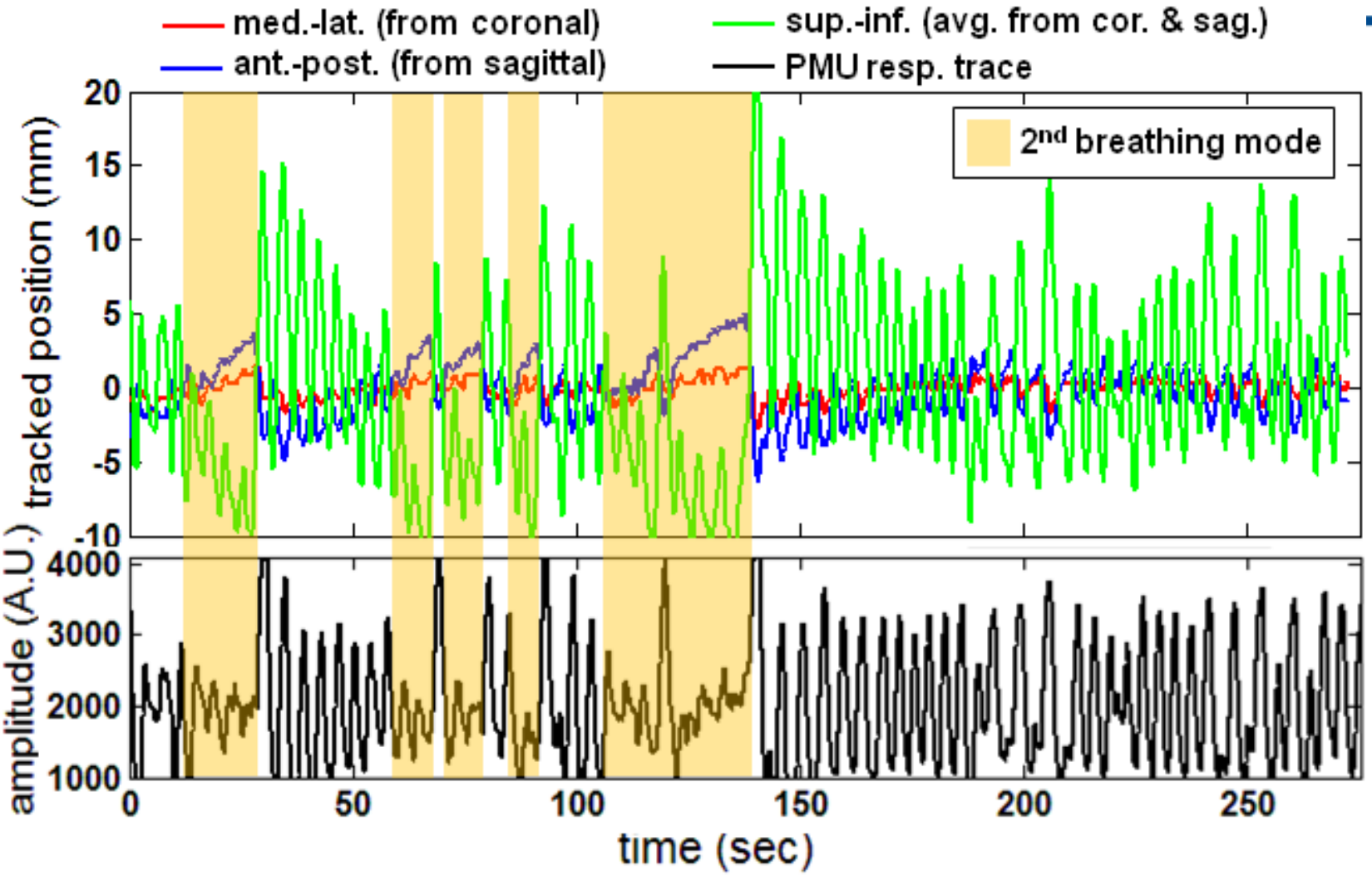

4D MRI – Characterization of Motion

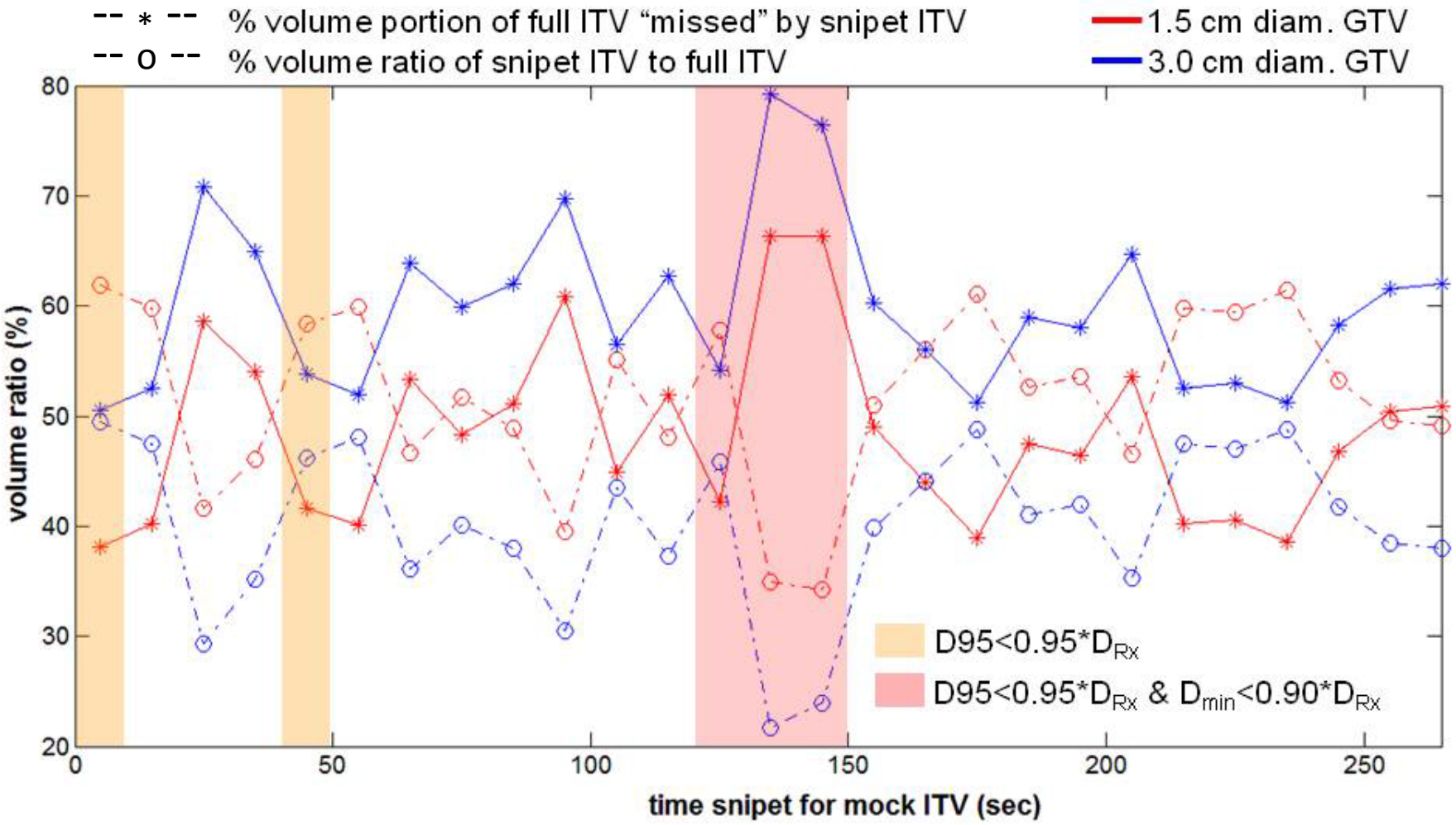

Motion Management: A case for Breath-hold

- Breath hold imaging is the gold standard
- *Breath-hold and gating are not mutually exclusive*
- Active Breathing Control for reproducible breath-hold
  - Integrate the ABC process to maximize compliance
  - Short, normal or deep inspiration BH (ABC/gating)
  - Gate the accelerator with the ABC device

Diagnosis vs Prescription

JOHNS HOPKINS MEDICINE

JOHNS HOPKINS MEDICINE

MOSAIQ Browser

an Oncospace project

Home | Patient Stats | Department Stats | Patient Records | Physician | Billing | External | Free Text Query

- Summary
- Toxicities
- Toxicity Progression
- Weekly Stats
- Patients and Zip Codes
- Offset Predictions
- Offset Trends
- Offset Raw Data
- Rx Frequency
- Rx Charting

185 Prostate: MN
186 Testis: MN
187 Penis & Male Genital Or
188 Bladder: MN
189 Kidney & Other Urinary (
190 Eye: MN
191 Brain: MN
192 Other parts Nervous Sys
193 Thyroid Gland: MN
194 Endocrine Glands & Stru
195 Other/Ill-Defined Sites: M

☑ Select morphology

Acute leukemia, NOS
Adenocarcinoma, metastatic, NOS
Adenocarcinoma, NOS
Adenoid cystic carcinoma
Adenosquamous carcinoma
Astrocytoma, anaplastic type (T-191.__)
Astrocytoma, NOS (T-191.__)
Carcinoma, metastatic, NOS
Carcinoma, NOS
Carcinomatosis
Carcinosarcoma, NOS

◉ Order by fraction, dose ○ Order by dose, fraction ○ Order by frequency ○ Order by total dose

◉ Absolute value ○ Percent frequency

Include all

☐ Ignore fractions/doses used less than 1 times(s)

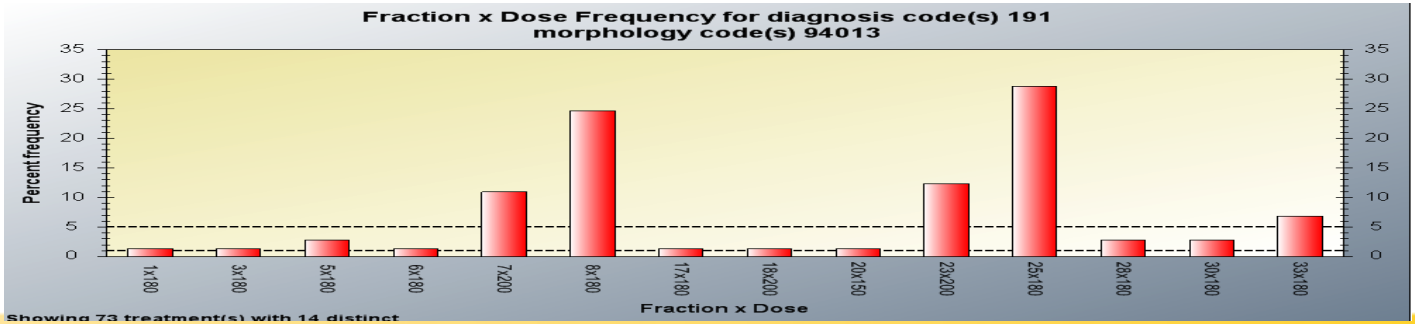

OncoSpace: Adapting the SkyServer Approach

JOHNS HOPKINS MEDICINE

- SDSS is a collaborative effort to map 25% of the sky
- SkyServer publishes data from the SDSS
- >> 100's of new discoveries in astrophysics
- Increased scale and scope for research

- Shared resources
  - Methodology
  - Software
  - Expertise
  - Experience
- New opportunities
  - Analysis
  - Visualization
  - User experience
- Skyserver.sdss.org

Alex Szalay PhD - JHU
Jim Gray PhD - Microsoft

CAMPS Officers

(January 1, 2013 - December 31, 2013)

President:	**Jun Deng**
President-elect:	**Holly M. Lincoln**
Secretary:	**Douglas Boccuzzi**
Treasurer:	**Bob Hoffman**
Board Member at large:	**Morgan Willard**
Board Representative:	**Gene Cardarelli**
Past President:	**David J. Carlson**

http://chapter.aapm.org/camps/index.htm

Acknowledgement

Platinum Sponsorship

Elekta

Gold Sponsorship

Bard Medical

Biocompatibles

BrainLAB

Landauer

MGS Research

Scandidos

Standard Imaging

Sun Nuclear

Velocity

David Brenner, Ph.D., D.S.

Higgins Professor of Radiation Biophysics
Director, Center for Radiobiological Research
Columbia University Medical Center

B.A., M.A., 1974, Oxford University
M.S., 1976, Medical College of St. Bartholomew's Hospital, University of London
Ph.D., 1979, University of Surrey

Academic Appointment

2008- Higgins Professor of Radiation Biophysics and Director, Center for Radiological Research, Columbia University Medical Center, Professor of Environmental Health Sciences.

1994- Professor of Radiation Oncology and Public Health, and Director, Radiological Research Accelerator Facility, Center for Radiological Research, Columbia University Medical Center.

1993-94 Tenured Associate Professor of Radiation Oncology and Public Health, Center for Radiological Research, College of Physicians & Surgeons of Columbia University.

1992-93 Associate Professor of Radiation Oncology (Tenure), Center for Radiological Research, College of Physicians & Surgeons of Columbia University.

1986-92 Assistant Professor of Radiation Oncology, College of Physicians & Surgeons of Columbia University

Career Achievement

- **Numerous awards**
  - Radiation Research Society Failla Gold Medal Award, 2011
  - University of California, Berkeley, Miller Professor, 2002
  - Honorary Degree (Doctor of Science), Oxford University, 1996
  - Oxford University Carter Physics Prize, 1974
- **Numerous grants from NIH, DOE, NASA and ACS**
- **Five patents**
- **Two books**
- **Over 270 peer-reviewed papers**

Research Focus

- Developing mechanistic models for the effects of ionizing radiation on living systems, both at the chromosomal and the animal (or human) levels

- Dividing his research time equally between the effects of high doses of ionizing radiation (relating to radiation therapy) and the effects of low doses of radiation (relating to medical, environmental and occupational exposures)

Yan Yu, PhD, MBA, FAAPM

Vice Chair and Professor
Director, Division of Medical Physics
Department of Radiation Oncology
Thomas Jefferson University

B.S., 1983, University of London
Ph.D., 1986, University College London
MBA, 1998, University of Rochester

Academic Appointment

2008-2010 Tenured Professor and Director of Medical Physics
Department of Radiation Oncology, Thomas Jefferson University

2006-2007 Tenure Track Professor and Asso. Dir. of Medical Physics
Department of Radiation Oncology, Thomas Jefferson University

2004-2006 Professor
Department of Radiation Oncology, University of Rochester

1999-2003 Associate Professor
Department of Radiation Oncology, University of Rochester

1994-1999 Assistant Professor
Department of Radiation Oncology, University of Rochester

Career Achievement

- **Numerous awards**
  - Fellow, AAPM, 2008
  - George Cassarett Excellence in Translational Research Award, University of Rochester, 1997 and 2004
  - IAU Travel Award, 1991
  - ORS Award, Science and Engineering Research Council, U.K., 1983 - 1986
  - SERC Scholarship, University of London, 1983 - 1986
- **Numerous grants from NIH, DOD, ACS and etc.**
- **Three patents**
- **Six book chapters**
- **Over 130 peer-reviewed papers**

Research Interest

- Stereotactic and IMRT treatment optimization using computational intelligence techniques
- Robotic assisted platform for radiation delivery, motion tracking
- Intraoperative dynamic dosimetry for prostate brachytherapy
- Optimization of needle-based, Image-guided intervention, including biopsy and therapy
- High intensity focused ultrasound for ablative therapy
- Animal models of tissue oxygenation, tumor vasculature and normalization
- Microbeam RT: from cells to small animals

John Wong, Ph.D.

Professor and Director of Medical Physics
Department of Radiation Oncology and Molecular Radiation Sciences
Johns Hopkins University School of Medicine

B.A., 1974, University of Toronto
M.S., 1977, University of Toronto
Ph.D., 1982, University of Toronto

Academic Appointment

1982-1992
Assistant to Associate Professor of Radiation Physics
Mallinckrodt Institute of Radiology
Washington University, St. Louis

1992-2004
Director, Clinical Physics
Department of Radiation Oncology
William Beaumont Hospital

Associate Professor to Professor of Medical Biophysics
Oakland University

2004-present
Professor, Director, Division of Medical Physics
Department of Radiation Oncology and Molecular Radiation Sciences
Johns Hopkins University School of Medicine

Career Achievement

- **Numerous awards**
  - 2001 George Eddelstyn Medal, Royal College of Radiology, UK
  - 2002 5th Nagalingam Suntharalingam Lecturer, Thomas Jefferson University, Philadelphia
  - 2003 1st James A. Purdy Lecturer, Wash. University, St. Louis
  - 2003 Lawrence Lanzl Award Lecture, AAPM Midwest Chapter, Loyola University, Chicago
  - 2004 Fellow of AAPM
  - 2010 Collins Lecturer, Radiation Oncology, MGH, Boston
- **Numerous grants from NIH, DOD and industry etc.**
- **Five patents**
- **12 graduate students, 19 residents and fellows**
- **Over 130 peer-reviewed papers, 16 book chapters**
- **Over 60 invited talks**

Research Interests

- Real-time quality assurance measurements in RT
- Integrated 3D X-Ray/ultrasound guided radiation therapy of soft tissue targets
- An integrated x-ray/optical tomography system for preclinical radiation research
- Informatics infrastructure for data sharing and decision support
- Small Animal Radiation Research Platform (SARRP) for pre-clinical research